WWU
MÜNSTER

A Laboratory Manual of Kidney Perfusion Techniques

Hans-Joachim Schurek

In collaboration with Klaus Hinrich Neumann, Frank Schweda and Jan Czogalla

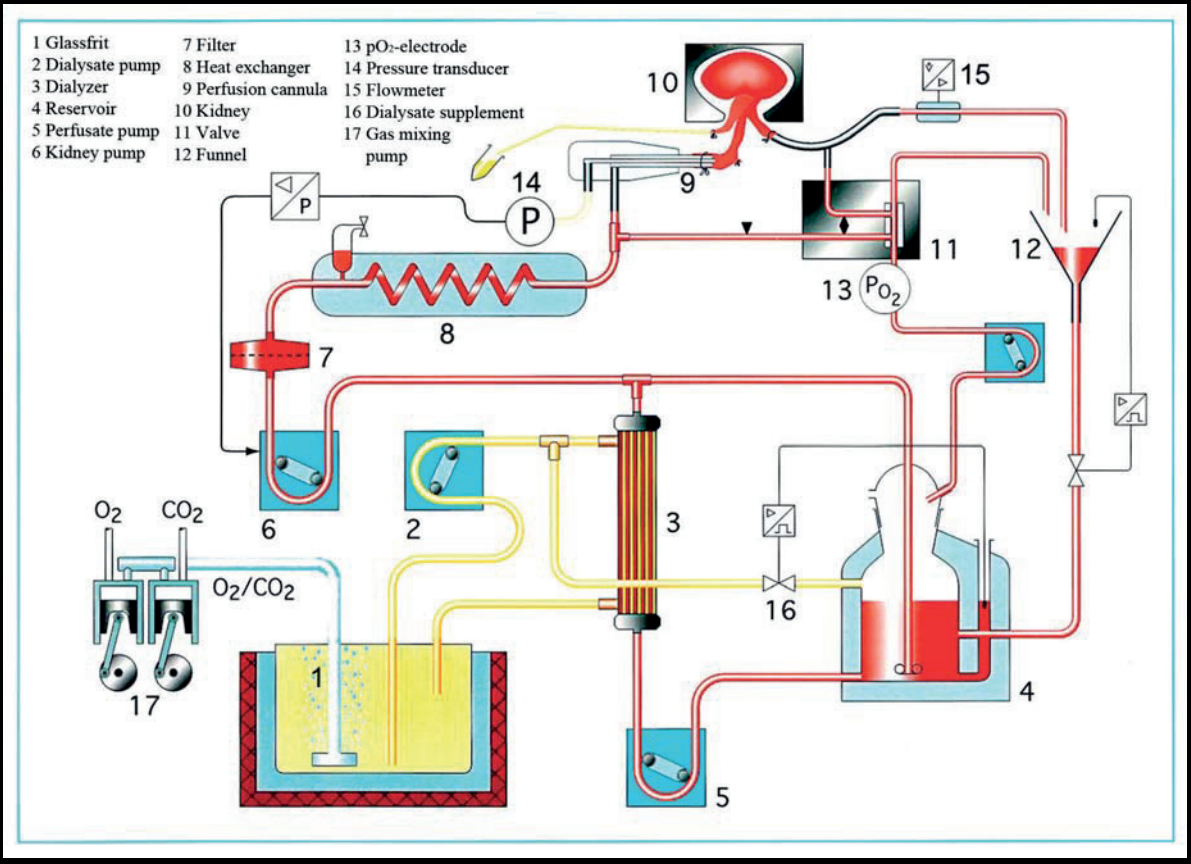

Hans-Joachim Schurek

A Laboratory Manual of Kidney Perfusion Techniques

WWU
MÜNSTER

Wissenschaftliche Schriften der WWU Münster

Reihe V

Band 6

MV WISSENSCHAFT

Hans-Joachim Schurek

A Laboratory Manual of Kidney Perfusion Techniques

In collaboration with Klaus Hinrich Neumann, Frank Schweda and Jan Czogalla

MV WISSENSCHAFT

Wissenschaftliche Schriften der WWU Münster
herausgegeben von der Universitäts- und Landesbibliothek Münster
http://www.ulb.uni-muenster.de

Bibliografische Information der Deutschen Nationalbibliothek:
Die Deutsche Nationalbibliothek verzeichnet diese Publikation in der Deutschen Nationalbibliografie; detaillierte bibliografische Daten sind im Internet über http://dnb.d-nb.de abrufbar.

Dieses Buch steht gleichzeitig in einer elektronischen Version über den Publikations- und Archivierungsserver der WWU Münster zur Verfügung.
http://www.ulb.uni-muenster.de/wissenschaftliche-schriften

Hans-Joachim Schurek
„A Laboratory Manual of Kidney Perfusion Techniques“
Wissenschaftliche Schriften der WWU Münster, Reihe V, Band 6

ISBN 978-3-8405-0154-8 (Druckausgabe)
URN urn:nbn:de:hbz:6-22259740573 (elektronische Version)

direkt zur Online-Version:

Satz: Hans-Joachim Schurek
Titelbild: Jörg Dieter Biela, *Experimentelle Nephrologie*, Medizinische Hochschule Hannover
Umschlag: readbox unipress

Dedicated to Marianne

Acknowledgement

I owe particular debts of gratitude to the following individuals.

To my mentor and faithful supporter Prof. Klaus Hierholzer (1929-2007), I owe my original acceptance as a member of his team in the newly established Department of Clinical Physiology at the former *Klinikum Steglitz* of the Freie Universität Berlin in 1969. He was endowed with an infectious enthusiasm for research and supported me even after I switched to internal medicine, allowing me to continue working in his laboratory until I moved to Hannover in 1975. My long-time colleague Prof. Hilmar Stolte, who sadly passed away in August 2015, gave me my first professional position in 1975 at the Medical School in Hannover, where he provided a laboratory workplace at very short notice, and in later years I could always depend on his advice and his backing. I also thank the Directors of the Clinic, Prof. Jan Brod and his successor Prof. Karl-Martin Koch, for their support and encouragement. I am especially indebted to the latter for seconding my application for sabbatical leave in 1988, when Prof. Christian Bauer invited me to work as a guest in the Department of Physiology at the Irchel/Zurich (Switzerland). Here I was able to build up an experimental system for kidney perfusion in which to study the synthesis of erythropoietin, together with Drs. Holger Scholz, Armin Kurtz and Kai-Uwe Eckardt.

I am very grateful to my friend and colleague Klaus Hinrich Neumann for many stimulating discussions, for his unstinting work on all micropuncture projects on the IPRK in Hannover, and not least for his contribution to this manual. Thanks also to my colleague Frank Schweda for contributing a chapter to this manual (IPMK) and the practical contribution of Jan Czogalla. Joerg Dieter Biela has served as a consultant and active designer of technical equipment for me for decades, and his early developed IT skills have also been of great help.

Thanks to Paul Hardy from Düsseldorf. He recently kindly agreed to edit my and our English translation of the text into a readable form, and I am enormously grateful to him.

Thanks to Brian D. Ross (Altadena CA, USA, formerly Oxford) for his advice and for permitting me to use illustrations from his 1972 Laboratory Manual.

I also thank Börje Haraldsson of the University of Gothenburg for letting me use a Figure from his 2008 review and to the American Physiological Society for permission to use four illustrations from its publications. Thanks to Springer Science Publishing for their prompt reply concerning the use of older pictorial material. In contrast, attempts to obtain permission to re-use material published by Clarendon Press (Oxford) from anonymous copyright licensing agencies were extremely trying and ultimately ended in failure.

Thanks to Dr. Kerstin Schnurr from the MedInnovation GmbH in Berlin-Adlershof for giving me the opportunity to characterize our BSA preparations with the new ESR-based functional test, which was developed by her firm in Berlin (Chap. 9.8).

My special thanks also goes to the “Deutsche Forschungsgemeinschaft” for their longstanding support during the years 1974 to 1992 and last but not least to the Else-Kroener-Fresenius-Foundation, which has funded a joint scientific project with Eberhard Schlatter and Bayram Edemir over the past several years.

Preface

The decision to write the present work was prompted by the example of the laboratory manual entitled “Perfusion Techniques in Biochemistry”, written by Brian D. Ross and published by Clarendon Press, Oxford 1972. His book presents an excellent overview of organ perfusion techniques. Chapter 3 deals with techniques of liver perfusion, which was the pacemaker in the field those days, especially after Leon L. Miller had established the isolated perfused rat liver as a model, which he used to demonstrate the synthesis of serum proteins (other than immunoglobulins) by the isolated liver. Chapter 4 is devoted to the kidney and extends over 36 pages. Studies carried out in the Laboratory of Sir Hans Adolf Krebs demonstrated that the metabolic activity of the perfused kidney was higher than that seen in tissue slices, largely due to the dominant influence of ion transport upon energy metabolism in the organ. We and others later showed that certain metabolic substrates have a significant effect on ion transport in the kidney.

I worked on kidney perfusion over a period of 20 years, and struggled with its many problems. In the early period (1969-1975) I benefited from the enthusiastic encouragement of Klaus Hierholzer, the first director of the then new Institute of Clinical Physiology in Berlin, where I continued to work part time in parallel with my clinical education in Berlin until 1975. Hilmar Stolte greatly facilitated my start in Hannover and he provided a laboratory workplace in his Experimental Nephrology Unit. It was a period in which I learnt a lot. My thesis in Tübingen dealt with liver perfusion, my postdoctoral thesis at the Medical School in Hannover was devoted to kidney perfusion. My contacts with international colleagues and members of the scientific community in Berlin, as well as in Hannover, were very stimulating. In Hannover, I enjoyed the support of Jens Bahlmann, who gave me access to his collection of reprints relating to kidney perfusion. During this period, Jan Brod and later on Karl Martin Koch headed the Department of Nephrology within the Center for Internal Medicine.

In 1988, I took sabbatical leave to work in Christian Bauer´s group at the Department of Physiology in Zürich on the synthesis of erythropoietin in the isolated perfused rat kidney. The Institute’s workshops were extraordinarily helpful in establishing the experimental setup, and I benefitted from a stimulating group of younger colleagues, including Armin Kurtz, Kai-Uwe Eckhardt and Holger Scholz.

After my retirement from clinical work, I was pleased to be able to avail of a guest position at the University Hospital of Münster and – with the support of Eberhard Schlatter and Giuliano Ciarimboli - I was able to set up a kidney perfusion system and resume experimental work. This led me to reflect on the experimental expertise I had acquired and to collect material that might be helpful to those beginning to work in the field of kidney perfusion. The Deutsche Forschungsgemeinschaft supported this work for years, bridging support was provided by the Ministry for Arts and Science of Lower Saxony, and in later years the Else Kroener-Fresenius Foundation supported the group.

This laboratory manual does *not* aim to provide a comprehensive treatment of developments in the area of organ perfusion. Instead, the present work discusses a very subjective selection of topics to help readers to choose the most appropriate model for a

given problem by describing the strengths and limitations of each of the available options. The Laboratory Manual by Brian D. Ross mentioned above is still worth reading. I am grateful for the contribution of my friend Klaus Hinrich Neumann about technical niceties of tubular micropuncture in the isolated kidney and of Frank Schweda on the isolated perfused mouse kidney, who have now brought the kidney perfusion tradition that began with my sabbatical leave in Zurich to Regensburg.

The material for this handbook and all the results cited are the fruit of my collaborations with many doctoral candidates and the stimulating scientific environment we created together. I will always remember the valuable assistance of Charlotte Mueller-Suur over the many years of my stay in Berlin. The exchange of ideas and views with the scientific community drawn to the *Institut für Klinische Physiologie* under the directorship of Klaus Hierholzer - with Eberhard Aulbert, Claus Behn, Petra Brandt, J.P. Brecht, Hans Ebel, Michael Fromm, Hans-Ulrich Gutsche, Ulrich Hegel, Roland Kirsten, Helge Lohfert, Roland Mueller-Suur and Michael Wiederholt - was a formative and enriching experience. Ingrid Krause became my first doctoral candidate, and I helped to supervise the work of Petra Brandt and Helge Lohfert.

While on a visit to the laboratory in Berlin, Hilmar Stolte encouraged me to come to Hannover, and there he gave me exactly the support I needed. I will never forget Iris Kilian for her skillful and sure hand in preparatory work generally, in the isolation of kidneys, in analytical work and especially in micro-analytical methods. Very special thanks are due to my longstanding technician and engineer, illustrator and friend Jörg-Dieter Biela, who gave me invaluable support in preparing Figures and in the development of the technical equipment. My first doctoral candidate in Hannover was Eberhard Schlatter, who was followed by Werner Meier, Eveline Assel and Christel Sonnenburg (co-supervised). She in turn was followed by Andreas Wiemeyer and Janosz Panzer (co-supervised), Josef Schlarmann, Horst Pagel and Christian Kellner (co-supervised), Gisela Wruck and Wulf-Peter Jesinghaus, Michael Hartwig, Hermann Thole, Harald Flohr, Harald Bertram and Uwe Jost (a particularly committed and valuable coworker), Mathias Bruno Zeh, Oliver Walter Johns and last but not least Giuliano Ciarimboli. Jeanette Alt won the respect of all as laboratory supervisor, and a large measure of the credit for the consistently high quality of the analytical work done in Hilmar Stolte´s group in Experimental Nephrology must go to her.

In summer 2006, Eberhard Schlatter arranged a meeting with former doctoral fellows, and encouraged and invited me to set up a new research group in Muenster. I accepted the invitation, which enabled me to supervise the doctoral work of Jens Klokkers, Christina Koeppen and Viktor Repp. In collaboration with Bayram Edemir and Eberhard Schlatter, a research proposal was submitted and accepted, and over a period of three years, we succeeded in throwing new light on the inability of the cell free perfused kidney to concentrate urine. In Münster, I have had support of two technicians, first Rita Schroeter and then Antje Stoeber, and I would like to thank both of them for their invaluable contributions – and for agreeing to work for an old-timer like me/for someone who is as long in the tooth as I am.

Hans-Joachim Schurek Lingen, Münster, 2017

Table of Contents

Preface

Table of Contents **V-VIII**

Introduction **1**

1. Overview of experimental models of the kidney **5**

1.1. Historical aspects of the perfusion of isolated kidneys 5

1.2. Oxygen supply – a critical parameter 7

2. General principles of kidney perfusion **8**

2.1. Single-pass (once-through) perfusion 9

2.2. Recirculation 9

2.3. Recirculation and regeneration of the perfusate by dialysis 11

2.4. Reperfusion of an anatomically perfusion-fixed kidney as a model 11

3. Advantages and general limitations of in-vitro perfusion of the mammalian kidney **12**

3.1. Flow-constant versus pressure-constant perfusion 18

3.2. Concentrating and diluting capacity 18

3.3. The permeability of albumin in the IPRK and the “repaired defect” hypothesis 21

4. Perfusion techniques **27**

4.1. Perfusion medium 27

4.1.1. Salt solutions 27

4.1.2. Addition of substrates 27

4.1.3. Preparation of perfusate and dialysate 30

4.1.4. Albumin stock solution 31

4.1.5. Other colloid additives 31

4.1.6. Semisynthetic perfusate with oxygen carriers 33

4.2. Perfusion drive systems, measurement of flow and pressure 37

4.2.1. Hydrostatic pressure 37

4.2.2. Gas pressure 38

4.2.3. Flow measurement, peristaltic pumps. Flow constant or pressure constant perfusion 39

4.2.4. Other techniques of flow measurement 40

4.3. Temperature control 41

4.3.1. Temperature controlled cabinet 41

4.3.2. Temperature control by water jacketing 44

4.4. Aeration 44
4.4.1. Aeration via a glass frit 44
4.4.2. Glass oxygenators in recirculation technique 45
4.4.3. Membrane oxygenators used in the recirculation technique 48
4.4.4. Capillary oxygenator 51
4.4.5. The dialyzer as a “kidney lung” (dialung) 52
4.5. Filtering 54
4.5.1. Filtration of the perfusate 54
4.5.2. In-line filtration 55
4.6. Cannulation 57
4.6.1. Arterial access to the kidney, perfusion cannulas 57
4.6.2. Venous Cannulation 60
4.6.3. Ureteral catheter 61

5. Material for the perfusion apparatus 66
5.1. Single-pass System 66
5.2. Recirculation system 76
5.3. Recirculation mode with dialyzer for aeration and regeneration 78
5.4. Reperfusion after anatomical fixation 80

6. Sterilization and disinfection procedures 83
6.1. Disinfection bath 84
6.2. Thermal disinfection 84
6.3. Sterilization by ethylene oxide 84
6.4. On sterility of the perfusate 84

7. Anesthesia 86

8. Surgical techniques and connection procedure 86
8.1. Selection of surgical instruments 86
8.2. Surgical technique and connection procedures 87

9. Measurements: Parameters and methods 99
9.1. Temperature 99
9.2. Perfusion flow rate 100
9.3. Oxygen consumption 102
9.4. Urinary flow rate, urinary flow blockage 102
9.5. Glomerular filtration rate (GFR) and its measurement 103
9.5.1. Inulin, polyfructosan, sinistrin 103
9.5.2. Creatinine 103
9.5.3. Other markers for determination of GFR 104

9.6. Electrolytes Na, K, Ca, Cl, HCO_3 104
9.7. Osmolality and colloid-osmotic pressure 106
9.8. Colloids, substrates incl. amino acids, protein and glucose 109
9.8.1. Albumin 109
9.8.2. Other colloids 110
9.8.3. Metabolic substrates 112

10. Kidney perfusion: comparison of results 114
10.1. Single pass perfusion and recirculation with dialysis 114
10.1.1. Perfusion flow rate, urine flow rate, GFR and filtration fraction in relation to albumin concentration 115
10.1.2. Kidney weight – a problematic reference parameter 120
10.1.3. Autoregulation of renal perfusion flow rate 122
10.1.4. Fractional sodium reabsorption and absolute transport rate TNa 125
10.1.5. Glucose reabsorption 127
10.1.6. Potassium secretion 128
10.1.7. Efficiency of sodium transport in relation to oxygen consumed 132
10.2. Recirculation perfusion. Perfusion experiments on the endocrine function of the kidney 133
10.3. Recirculation with regeneration of the perfusate by dialysis 137
10.4. The anatomically fixed kidney as a tool for analyzing the glomerular filter 138
10.4.1. Perfusion fixation of the isolated kidney for reperfusion 138
10.4.2. Fixation solution for reperfusion experiments 140

11. Tabellarium and abbreviations for the tables 141

12. Annex 150
12.1. Biochemical studies on the energy metabolism of the IPRK 150
12.2. Morphological studies of the IPRK, perfused either cell-free or with erythrocyte-containing medium 153
12.3. Hypothesis to account for oxygen deficiency in the cell-free perfused kidney 167
12.4. Overview of the contributions of our group to the four different techniques of renal perfusion 177

Klaus Hinrich Neumann, Göttingen

13. Special aspects of micropuncture experiments on the IPRK 180
13.1. Studies on the isolated perfused rat kidneys 180
13.2. Glomerular morphometry 184

Frank Schweda, Regensburg

14. The isolated perfused mouse kidney **187**

14.1. Perfusion techniques 187

14.2. Perfusion medium 189

14.3. Perfusion apparatus 190

14.4. Surgical preparation and cannulation of the renal artery 193

Ad 14.2 Appendix 195

Sheep erythrocytes as O_2 carriers during perfusion of the isolated mouse kidney. Contributed by **Jan Czogalla, Zurich,** Institute of Anatomy, University of Zurich, Switzerland

15. Technical appendix and image collection of the IPRK **197**

16. Appendix on the history of renal perfusion 1849–1908 **208**

17. References **212**

Introduction

A search for the term “kidney perfusion“ in the US National Library of Medicine´s database PubMed in Jan 2017 turned up a total of 14071 citations, “isolated perfused kidney” found 3422, and “isolated perfused rat kidney” (IPRK) 2213 entries. Some of these do not match the search profile, and mostly they are singular results. Very few publications deal with the methodology of perfusion, its background, possibilities, capabilities and limitations (162-164, 186, 223, 224), or with the choice of the most appropriate model for a specific question (246). An organ such as the kidney naturally functions best in a healthy organism. Once a kidney has been removed from its normal context, it is crucial to find the optimal compromise between the demands of the problem at issue and the experimental model to be adopted. An isolated kidney is, in effect, a “dying kidney”, although it may continue to function for between 1 and 4 hours, depending on one´s definition of normal. This of course holds to an even greater extent for fractionated experimental models, such as tissue slices, cell suspensions, isolated cell organelles (e.g., mitochondria, cell membranes) and for the tissue cultures used as standard models in molecular biology. The basic reason for the progressive deterioration in function can be found in the stresses set up by the transition from perfusion by whole blood to the use of a more or less artificial perfusing medium. As Mephisto remarks in Goethe´s drama “Faust”, Studierzimmer II: “Blut ist ein ganz besondrer Saft”: “blood is a quite special juice”. Indeed, blood is a “liquid organ”, a highly complex cocktail that is steadily being reconditioned by the actions of other organs, and this complexity explains why all efforts to maintain kidney function in isolation are ultimately doomed to failure. If we want to approach its fantastic properties, then we should leave an organ as the kidney within the body. Whether or not circulating micro-RNAs play any role in regulating kidney physiology only time can tell (296c).

One vital but strangely neglected function of the blood in this context is its role in the maintenance of the integrity of the endothelium (166, 231), which no artificial perfusate so far developed can fully provide. Indeed, if this issue is the key to long-term viability of the isolated organ, it deserves to be analyzed in much greater detail, in particular with respect to the preservation of the endothelial glycocalyx (97, 204, 208) of glomerular and tubular capillaries.

The following Figure provides a summary of the historical development of experimental models for the study of kidney function, most of which derive from in-vivo studies on experimental animals. To eliminate the impact of extrarenal factors, biochemists went on to develop in-vitro techniques based on the use of tissue slices of parenchymal organs like the liver and the kidney. These advances led to the discovery of a plethora of metabolic pathways, such as the Krebs cycle and the urea cycle, enzymes such as oxygenases, and much else. Initially, studies on respiration were carried out with the aid of simple manometric methods, exemplified by the Warburg apparatus (124). Indeed, from our present-day perspective, it is quite astonishing to recall how many seminal discoveries in biochemistry were made with the manometric techniques pioneered by Otto Warburg. Equally fascinating are the contributions to a better understanding of kidney function made by the clearance techniques, hemodynamic studies and especially the classical micropuncture methods developed by physiologists. Ussing in Copenhagen studied the function of epithelial ion transport in frog skin and toad bladder, and the double-chamber he developed was

a milestone in the history of transport physiology (149, 299). This technology made it possible, for the first time, to measure voltage-driven trans-epithelial sodium transport. When a countervailing electrical potential was applied, the current in the external circuit was equivalent in magnitude to the flow of ions transported across the membrane, quasi a short-circuit current. This breakthrough sparked the development of a set of tools for physiological studies on transporting epithelia, such as that of kidney tubuli, leading to measurement of the electric potential, to intracellular recordings, and the use of ion selective electrodes etc. These tools enabled researchers to characterize the different segments of the tubular epithelia in a nephron both in vivo and in vitro using isolated perfused tubules in their native state, as well as the influence of hormones and pharmaceuticals such as diuretics. Another milestone was the invention of the patch-clamp technique by Sakmann and Neher, which generated a wealth of new insights (179, 180) by permitting functional analyses of membrane patches containing a single ion channel. This in turn led to the functional and genetic definition of individual channelopathies. Light microscopy, and more especially electron microscopy, provided fascinating visual images that reconciled ultrastructural morphology with functional findings. These advances gave pharmacologists unprecedented opportunities to study diverse aspects of drug actions and test new drugs in vitro. Comparison of results obtained in the isolated perfused liver with those from simple experimental models such as tissue slices made the disadvantages of the latter clear, and resulted in more precise analyses of metabolic pathways. Tubular ion transport in isolated perfused kidneys was found to require much higher levels of oxygen consumption than those observed in tissue slices, which support only a basal level of metabolism. In this sense the isolated perfused kidney takes an intermediate position between the unperturbed organ and the tissue slice in the canon of experimental models.

In the meantime, research in nephrology has progressed to the molecular dimension, with the adoption of molecular biological and genetic methods. The ability to knockout genes in experimental animals or conversely to activate genes by knock-in techniques has opened up many new avenues to an understanding of mechanisms of pathogenesis and the biotechnological manufacture of new drugs, such as the synthesis of human erythropoietin in ovarian cell cultures of hamsters.

Investigations of cell culture systems have become so dominant today that they now significantly shape modern nephrological research. It is now possible, for instance, to identify and express specific ion and water channels in the cell membrane. Moreover, knowledge of their molecular structures, functions and localization in the membrane continues to accumulate. Fascinating new insights into connecting bridges between cells (so-called tight and leaky junctions) have emerged. What is true for ion and water channels applies equally to the characterization of transport molecules, ion pumps and signaling cascades that surpass the highest standards of control engineering. Many orphan diseases in clinical medicine have been dissected genetically and the mutations responsible for them are known, for example, the different types of Bartter syndrome, Gitelman syndrome, Fanconi syndrome and renal diabetes insipidus. And given the complexity of renal function, it is astounding that such a simple tool as a dialysis membrane suffices to detoxify the blood of a uremic patient.

As a young specialist in internal medicine, I treated many patients with acute renal insufficiency in the ICU of the Medizinische Hochschule Hannover. I was once interrupted by a visit from a well-known biochemist (Theodor Bücher) from Munich, who was interested in the technique of dialysis as it was practiced in those days. What surprised him most was the fact that, apart from physiological salts, the only metabolic substrate added to the dialysate was glucose. In his view, not to include the whole cocktail of substances found in normal blood was tantamount to a crime. However, I was able to reassure him by pointing out that only 5% of the circulating blood passes through the dialyzer membrane at any one time and that the organism is well able to cope with such small losses. Nevertheless, we nephrologists are all too well aware of the drawbacks of dialysis, in which essential substances are lost and physiological functions are irrevocably degraded. These deficits explain why renal transplantation remains the replacement of choice in the long-term.

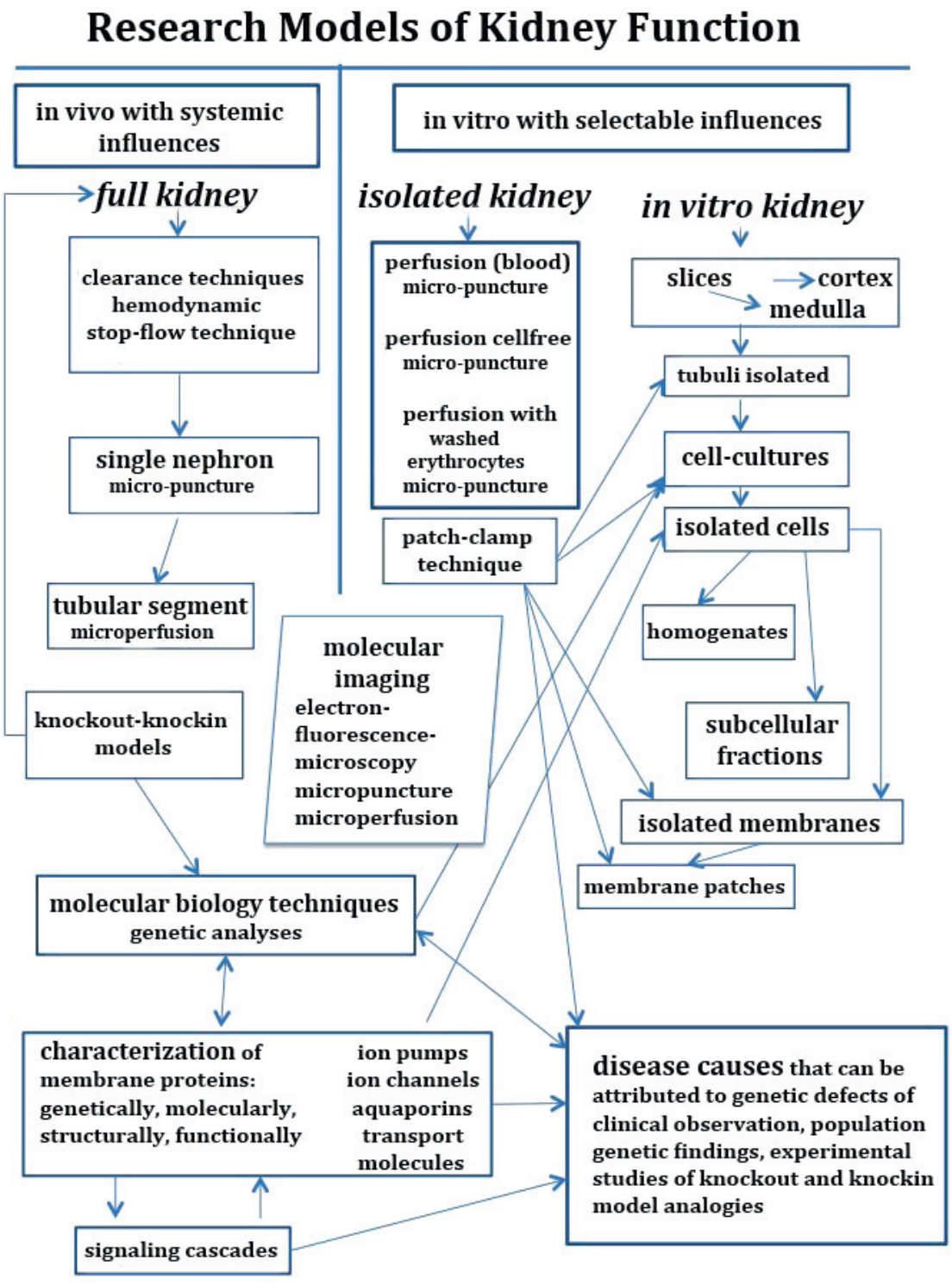
Research Models of Kidney Function
in vivo with systemic influences
in vitro with selectable influences
full kidney
isolated kidney
in vitro kidney
clearance techniques
hemodynamic
stop-flow technique
single nephron
micro-puncture
tubular segment
microperfusion
knockout-knockin models
perfusion (blood)
micro-puncture
perfusion cellfree
micro-puncture
perfusion with washed erythrocytes
micro-puncture
patch-clamp technique
molecular imaging
electron-
fluorescence-
microscopy
micropuncture
microperfusion
slices
cortex
medulla
tubuli isolated
cell-cultures
isolated cells
homogenates
subcellular fractions
isolated membranes
membrane patches
molecular biology techniques
genetic analyses
characterization of membrane proteins:
genetically, molecularly, structurally, functionally
ion pumps
ion channels
aquaporins
transport molecules
signaling cascades
disease causes that can be attributed to genetic defects of clinical observation, population genetic findings, experimental studies of knockout and knockin model analogies

1. Overview of experimental models of the kidney

Chart 1

The scheme provides a historical overview of the development of experimental techniques in kidney research which have contributed to the present state of our knowledge of the organ´s function. The left side of the diagram focuses on studies of the kidney under in-vivo conditions, which provide information on renal function under almost normal conditions but have the disadvantage that systemic, extra-renal influences may adversely affect interpretation of the findings. The in-vitro techniques referred to cannot fully mimic normal renal function but are essential for the detailed analysis of cellular mechanisms. In particular, the development of the patch clamp technique, which allows for the electrophysiological investigation of single ion channels in membrane patches, has enabled molecular genetic characterization of so-called channelopathies. The isolated kidney represents an intermediate model: it excludes extrarenal influences, but it is in essence a dying organ, with limited function. This underlines the fact that the naturally functioning kidney in vivo is a highly efficient organ that regulates salt and water balance and acid-base balance, and eliminates waste products. It is also the target and the site of synthesis of hormones and metabolic substrates. The kidney acts on many other metabolic control circuits and allows us to adapt to life in multiple habitats.

1.1. Historical aspects of the perfusion of isolated kidneys

According to C. Jacobj (115), the earliest studies of isolated and artificially perfused kidneys are those reported by Carl Eduard Loebell in his 1849 doctoral dissertation in Marburg (153) and by Ernst Bidder in 1862 in his thesis submitted to the Imperial University of Dorpat (29), now Tartu in Estonia. Whereas Loebell´s thesis is written in Latin, which was still the language of science in his day, Bidder wrote his thesis in German, the new language of science those days. Bunge and Schmiedeberg subsequently demonstrated the synthesis of hippuric acid (47) in the isolated dog kidney in 1876. However, the techniques used in these investigations differed fundamentally from organ perfusion in its modern sense.

In order to track down the site of hippuric acid synthesis, Bunge and Schmiedeberg first performed extensive preliminary experiments on frogs, and ultimately identified the kidney as the organ responsible for production of the compound. They then proceeded to remove the kidneys from a dog and, in the decisive experiment, they cannulated the vessels with glass tubes, and added as precursors benzoic acid and glycine to the defibrinated and filtered blood. The blood was then passed through the kidney via the glass cannulas under gravity from a carboy placed at a height of 1,75m. The detection of hippuric acid in the outflowing blood, within the kidney and in the urine confirmed their hypothesis that the substance was synthesized by the kidney. They referred to their experiments as “Durchleitungsversuche”, or transit tests. These studies were carried out in the Institute of Experimental Pharmacology at the University of Strasbourg, and led to the development of the remarkable perfusion apparatus designed by Jacobj.

Carl Jacobj provided the first detailed description of the equipment in 1890 in a paper entitled “Apparat zur Durchblutung isolirter überlebender Organe”, which was published in the Archiv für experimentelle Pathologie und Pharmakologie (Vol 26) (see Figure 16.0.1./ 16.0.2 in the Appendix) (115). In this paper, Jacobj pointed out that Carl Ludwig and his

coworkers in Leipzig had pioneered methods for the artificial perfusion of organs. The laboratory manual published by B.D. Ross includes a historical timetable (taken from a paper published in German by K. Skutul in 1908 of the Pharmacological Institute of the University of Kiev), which provides an overview of the chronology of the technical developments in the field (224, 277), s. Appendix to Chapter 16.

A serious and perennial problem of these early studies, carried out with whole blood, was an unexplained vasoconstriction of the kidney. Descriptions of the first experimental systems always include the observation that, prior to its passage through the kidney, the arterial blood was bright red, while the blood leaving the kidney was dark blue, indicating that the rate of perfusion was extremely low. Alphonse Nizet, who had significant experimental expertise himself, described this phenomenon in detail in his review of 1975 (186). Empirically, the addition of a functional lung in the extracorporeal circuit was shown to resolve the problem (14, 102, 103, 298). This led to the view that a vasoconstricting factor was eliminated by the lung and to the idea that deposition of destabilized lipoproteins in the kidney contributed to perfusion resistance by fat embolism (24). Nizet was convinced that erythrocytes are the source of this vasoconstrictor, which they released into the surrounding plasma, once they are outside of the vascular tree. This factor was also detectable in the aqueous hemofiltrate of hemodialysis patients (which also comes into contact with foreign surfaces during extracorporeal circulation!), and we were able to neutralize it by addition of verapamil to the perfusion solution (233, 234). For patients on dialysis (exposure to an extracorporeal circuit) it is not a problem, because they can inactivate it in their lungs. Indeed, Nizet reported that the isolated kidney itself is able to neutralize the vasoconstrictive principle if freshly collected, unstirred donor blood is used, together with a mild method of oxygenation (e.g., via a membrane oxygenator) and recirculation volumes of less than 15 times the weight of the kidney (186, 187, 189), and if the initial vasoconstriction is (optionally) suppressed pharmacologically. In a dog kidney perfused with whole blood (240) - a system that fulfilled all the criteria listed by Nizet - Schnermann et al. successfully demonstrated by micropuncture a feedback control of glomerular filtration rate. My colleagues and I were unable to detect such a feedback in the isolated, cell-free perfused rat kidney (unpublished results of Hans-Ulrich Gutsche and Reinhard Brunkhorst in my laboratory in Hannover, June 1979), see also Fig. 12.3.7.

Vasoconstriction was not the primary reason for the introduction of cell-free perfusion solutions (with or without the addition of thoroughly washed erythrocytes) as a semi-synthetic medium – an approach which was first used by Schimassek in the isolated rat liver (232). Nevertheless, this procedure has had a positive effect on the maintenance of the isolated kidney. Historically, 1959 was a milestone, as Ch. Weiss published results (307) obtained with an isolated perfused rat kidney. Using a cell-free perfusate, he showed that the autoregulation of blood flow is detectable even in the absence of red cells. This refuted the then prevailing hypothesis proposed by Pappenheimer and Kinter, which postulated that autoregulation of flow in the kidney was the result of so-called *plasma skimming* (123, 195). Up to this time, only larger mammals like the dog (186), the pig and the rabbit had been used as donors of experimentally isolated perfused kidneys. Ongoing miniaturization of analytical techniques then enabled researchers to use kidneys obtained from small mammals. Cell-free perfusion required the provision of sufficient dissolved oxygen to keep the organ alive, so the perfusate was either gassed with pure oxygen without bicarbonate, or gassed with 95% oxygen and 5% CO_2 in the presence of bicarbonate as a buffer system. In renal perfusion, sodium bicarbonate has the advantage of facilitating trans-tubular

sodium-transport, unlike phosphate-based buffer systems without bicarbonate. One reason for this is that bicarbonate reabsorption enables the maintenance of a trans-epithelial chloride gradient (183), which itself serves as a driving force for the NaCl reabsorption – although this remains controversial (28).

1.2. Oxygen supply – a critical parameter

Perfusion without oxygen carriers (e.g. erythrocytes) is prone to cause tissue damage due to oxygen deficiency owing to the specific anatomy of renal vessels, especially in areas with a high susceptibility, such as S_3-segments (proximal tubule) and in particular the medullary part of the thick ascending limb of Henle´s loop (7, 63). Here in the outer medulla, oxygen supply is at the brink of deficiency (259, 260, 263). Morphologist Manjeri Venkatachalam was the first to point to the particular vulnerability of the S_3 segments of the proximal tubules to oxygen deficit, as they are localized within the interbundle area (300). Physiologist Christoph Weiss had shown earlier on that the oxygen consumption in the IPRK continues to rise in parallel with the perfusion flow rate, and interpreted this as an indication of inadequate oxygen supply (142, 306), while Dume, and Koch et al., speculated about a possible diffusion shunt for oxygen in 1966 (67).

If it is mandatory to prevent oxygen deficiency, oxygen carriers (e.g. red cells) must be added (70). It is enough to add 5% of the volume as red cells if the solution is gassed with 95% O_2 and 5% CO_2 (263). It is essential to wash erythrocytes several times (bovine, porcine, human or sheep) and thus to dilute the vasoconstrictive principle. Using whole blood as an admixture results in immediate vasoconstriction, even when blood has been drawn gently and carefully (s. above). This can be prevented only by blockade of α-receptors (186, 187, 189) or by calcium-channel blockers such as verapamil (253, 254). It is better to avoid this by using washed red blood cells. H. Schimassek first introduced the use of bovine erythrocytes for the perfusion of the isolated rat liver (232) because they were regarded as particularly stable. Interspecific differences in erythrocyte sizes (between rat, human, bovine) are of no practical consequence (209). The use of other oxygen carriers, such as fluorocarbon preparations (82) and ultrapure solutions of modified and polymerized hemoglobin has been discussed. However, there has been no real breakthrough in this area, despite multiple experiments over many years (personal communication W. Pfaller concerning stroma-free hemoglobin) (15, 16, 144, 147, 310, 311), though Baines has expressed a more optimistic view (15, 16). And work in this field continues (148)*.

Whether a relative deficiency of oxygen radical scavengers may contribute to functional defects of the IPRK is discussed in literature, i.e. to explain the enhanced glomerular leakiness for albumin (295) .

*There is an interesting new way – not yet used in the IPRK - to enhance oxygen capacity by using the extracellular macro-hemoglobin of the marine annelid worm Arenicola marina. This path has been developed by the French biologist Dr. Franck Zal and his company´s name is Hemarina. One may expect that this macro-hemoglobin will not be filtered at the glomerular capillaries and its large size may not significantly contribute to the colloid-osmotic pressure (296b).

2. General principles of kidney perfusion

Attempts to perfuse the mammalian kidney with freshly drawn whole blood have regularly failed, as discussed by Alphonse Nizet (186). Efforts to do so result in immediate vasoconstriction – even when the blood is drawn with extreme care, and regardless of whether defibrinated (103) or heparinized (46) blood is used. This phenomenon spurred the development of perfusion media composed of repeatedly washed erythrocytes and colloidal salt solutions (232). Perfusion without oxygen carriers like erythrocytes, even when the perfusate is gassed at high oxygen pressure, tends to result in tissue damage due to oxygen deficiency owing to the specific nature of the anatomy of renal vessels, especially in regions such as S_3-segments (proximal tubule) and the medullary section of the thick ascending limb of Henle´s loop. This susceptibility arises from the special architecture of the renal vessels in the cortex and medulla. The tight contact between arteries and veins facilitates the shunt-diffusion of blood gases (134, 260, 263), especially when erythrocytes are omitted (263). Colloid-free perfusion media lead to a significant increase in the kidney volume, equivalent to a 30 to 50% increase in the initial weight, and the urinary volume reaches 50% of the glomerular filtration rate (251); see Chapter 10.

There are four basic types of perfusion technique (Variant 1 - 4), whose advantages and drawbacks are discussed in detail below:

2.1. Single-pass (once through) perfusion (4, 234, 246, 251, 256, 257, 307)

2.2. Recirculation (13, 32, 35, 58, 185, 186, 205, 223, 237, 293)

2.3. Recirculation and regeneration of the perfusate by dialysis (20, 169, 246, 251)

2.4. Reperfusion of an anatomically perfusion-fixed kidney.

We established this last variant as a model with which to analyze the physical properties of the glomerular filtration apparatus without having to perform laborious micropuncture experiments (50-53, 78, 266, 317).

The choice of procedure largely depends on the experimental question at hand. In the single pass perfusion technique (variant 1) the use of bovine serum albumin would be too expensive, except when using a mouse kidney. Variant 2 requires the smallest amount of albumin perfusate (60 to 100ml) and has become the most widely used technique. Variant 3 requires a somewhat larger volume of perfusate as it makes use of a “dialung” or kidney-lung” (dialyzer). Sterile filtration and/or online filtration (when recirculation is used) is/are equally important in all cases. In the first three methods, oxygen deficiency will arise in the absence of oxygen carriers (e.g., washed red cells), especially in the outer medulla and in the medullary rays of the renal cortex. In the following section, I discuss each of these methods in turn.

2.1. Single-pass perfusion (Variant 1)

Oxygenation of the perfusate is carried out by aerating through sintered glass. This is possible when gelatin-based colloids (Haemaccel), hydroxyethyl-starch (HAES), dextran or pluronic (84) are used, but results in extreme foaming with BSA, which may also promote denaturation of the protein. We have used a combined system of recirculation, which is readily convertible to the single pass mode to enable analysis of metabolism and clearance of uremic middle molecules (233, 234). A membrane oxygenator is used to equilibrate the albumin-containing perfusate. Smyth et al. used a single-pass system with albumin either alone (280) or combined with Ficoll (279) and equilibrated the perfusate at a high flow-rate (2 L gas/min) by means of a capillary dialyzer. These authors provided no information on fluid loss by the hollow fibers. The dialyzer and other parts of the system were immersed in a water bath. This is critical for hygienic reasons. This has been practiced historically in peritoneal dialysis of man, but was later abandoned due to problems with contamination and replaced by dry temperature conditioning. It is better to use water bath jacketed glass coils upstream and downstream of the dialyzer.

Perfusion without colloids is possible, but requires a different procedure compared to an isolated Langendorff preparation of a rat heart (66); it is essential to decapsulate the kidney and not to use ureteral catheters made of PE/PP10, which are too narrow. Cortell (59) points out that PE10 ureteral catheters are particularly unsuitable for the use especially at high diuresis rates (see Fig. 4.7.1.), as in the case of colloid-free perfusate (250, 251). A major advantage of the single pass mode is the constant supply of substrates, such as arginine as a constant source of NO, which is otherwise rapidly depleted in a pure recirculation system especially at small volumes, if it is not replaced continuously (206, 207). If erythrocytes are added, an artificial lung, such as a glass-bulb (film-) oxygenator, membrane oxygenator or a dialyzer (dialung) as in mode 3, must be used for oxygenation where the aerated dialysate is used to equilibrate and regenerate the perfusate. In addition, the effects of the infusion/omission of peptide hormones such as arginine-vasopressin (by proportional infusion or withdrawal of hormones) can be analyzed more easily (305) than when Variant 2 is used.

2.2. Recirculation (Variant 2)

Variant 2 is the technique of choice if one is interested in following cumulative biochemical or pharmacological effects over time. Examples include the study of metabolic processes such as gluconeogenesis, the elimination or breakdown of drugs or the impact of hormones (23, 32, 58, 107, 108, 162, 164, 177, 185, 223, 225, 227, 237, 294). Membrane- or glass-bulb oxygenators were initially used as artificial lungs, but nowadays special capillary dialyzers are preferred. Functionally the best colloid is albumin - bovine serum albumin (BSA) has the lowest viscosity at a given colloid osmotic pressure (COP), and therefore provides the highest perfusion flow rates at any defined perfusion pressure. Compared to other colloids albumin has a well-defined molecular weight. Bowman and Maack have best exploited the advantages of the recirculation method, as their apparatus is easy to set up and the functional results are comparable to those achieved with the method established by the Oxford Group of BD Ross and his followers. Urine was mostly reinfused, except in the case of clearance studies, and the withdrawal of perfusate and urine must be compen-

sated for if the recirculating volume is very small. Pegg, however, has rightly pointed out that the urine contains particles that can block capillaries and enhance resistance to flow (196). Within 30 min after initiation of cell-free perfusion, detached fragments of tubular epithelia appear in the urine sediment (218), and this desquamation process has been verified by morphological studies (7, 263), thus confirming Pegg´s observations. These findings led to the inclusion of a filter between the perfusion pump and the kidney, which also removes particulates originating from the surgical procedure used to isolate the kidney from the animal.

The recirculation mode is particularly suitable for biochemical and pharmacological studies because it facilitates the analysis of cumulative effects. Authors differ on whether BSA can be used in form of the crude Cohn faction V (23, 33, 162, 163) or should be defatted and dialyzed before use (55, 57). The former group finds the albumin-bound substances present in the Cohn V fraction useful, while the other group prefers tighter control over the composition of the perfusion medium. Moreover, the latter approach is generally thought to provide better functional stability of the preparation, as becomes apparent from continuous monitoring of multiple parameters such as flow, pressure, pO_2 and temperature. Indeed, it was the observation of a rapidly evolving acidosis in the isolated rat liver – perhaps due to the HCO_3 consumption for urea synthesis and/or a lactic acidosis due to hypoxia – in small volumes of perfusate that led to the first use of dialysis (20).

Fig. 2.1.: ***Urinary sediment from an IPRK perfused with washed human erythrocytes.*** The micrograph shows several human erythrocytes, one cell ghost and a larger tubular cell, which may be big enough to clog capillaries within the vascular bed.

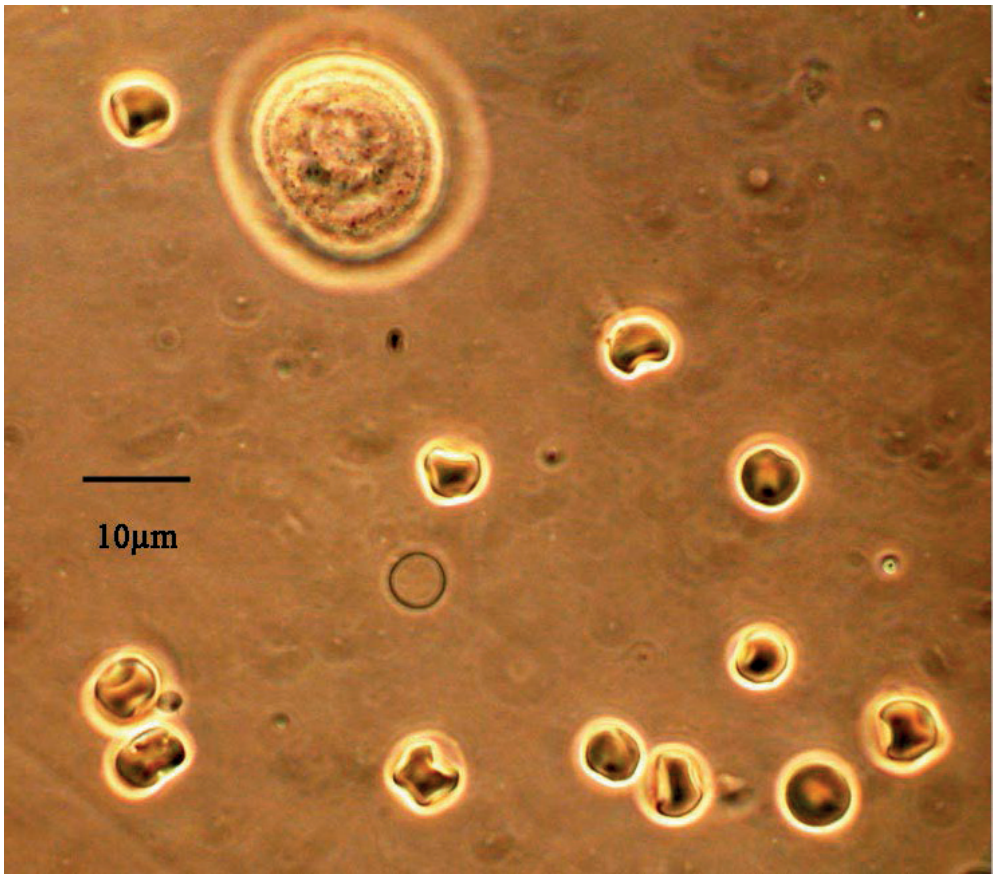

2.3. Recirculation & regeneration of perfusate by dialysis (Var. 3)

This technique combines the advantages of the single-pass perfusion and recirculation modes, and my colleagues and I have used it particularly for physiological studies. In this case, the dialyzer also serves as the oxygenator, as the dialysate is aerated continuously via sintered glass frits in the mode of the single-pass perfusion. Cumulative effects reflected in changing concentrations of small metabolites, as seen in a pure recirculation system, are avoided. One disadvantage of this method is the greater technical effort required to compensate for the ultrafiltration implemented by the dialyzer. We used a level control of perfusate and automatic supply of dialysate that compensates for ultrafiltration and the removal of perfusate and urine samples. We routinely use a dialysate-to-perfusate ratio of ≥20, i.e., 200-250ml perfusate to 5000 ml of dialysate. This provides a quite stable composition of the perfusate as in a single pass perfusion mode and prevents the rapid loss of arginine as a source of nitric oxide (NO) (206, 207). Thus, the method is best suited for time-consuming micropuncture experiments (182, 184, 206, 207, 245, 248, 251, 266, 267, 291, 292). It also proved to be effective in other respects (106, 135, 136, 241, 242, 263, 267). So-called low-flux dialyzers with smaller pore size, which prevent the passage of albumin into the dialysate (unlike high-flux dialyzers which, however do not play a role *in vivo* due to the sealing capability of whole blood), are most appropriate in this context. Over the past 12 years, this technique has been applied to larger mammals like rabbits (3, 315), dogs (110) and pigs (89, 90). When Baumung and Peterlik (20) first used dialysis in liver perfusion they had to build their own dialyzer using cellophane tubes. But today´s mass produced dialyzers are affordable and durable, provided appropriate cleaning procedures are followed before reuse.

2.4. Reperfusion of an anatomically perfusion-fixed kidney (Var. 4)

By reperfusion of anatomically fixed kidneys, we were able to analyze the glomerular filter apparatus under conditions that are not applicable in vivo. For example, it was possible to analyze the permeability of albumin at acid pH near the protein´s isoelectric point or below, when the surface charge of albumin switches from negative to positive. The idea was triggered in response to the workload involved in the large numbers of micropuncture experiments required to analyze glomerular permeability for albumin in the isolated perfused rat kidney (245, 248, 266, 292). The electric charge within the glomerular filter apparatus is preserved even in the perfusion fixed kidney. Reale et al. demonstrated the conservation of negative charge at the glomerular capillary membrane histochemically after perfusion fixation using glutaraldehyde (210-215). The aim was to obtain a preparation where GFR is high enough and identical to the urinary output. Therefore, we perfused kidneys for 15min at 100mmHg (effective perfusion pressure) with the addition of verapamil (4.4 µmole/l); beginning 2 min before fixation we increased the perfusion pressure to 150mmHg and maintained it at that level during the fixation period. The fixation solution was a 1.25% glutaraldehyde, phosphate-buffered salt solution at pH 7.1 with 6% HAES as a colloid. Why the colloid additive? Our first fixation done without colloid but under normothermia, revealed that the abrupt drop in the colloid-osmotic pressure to zero leads to a drastic increase of the perfusion resistance, thereby delaying and hampering the fixation. The addition of HAES (hydroxyethyl starch) improved fixation quality significantly and thus allowed us to establish this model (s.a. the morphological study: (263)).

The kidneys were stored together with their double-barreled aortic cannula at 4°C in a special designed custom-built acrylic glass box, until used for reperfusion days or even weeks later, s.a. Fig 5.4.1.- 5.4.4. (50-53, 78, 266, 317).

3. Advantages and general limitations of in-vitro perfusion of the mammalian kidney

Blood perfused organs in vivo are usually exposed to an oxygen pressure that barely exceeds 100mmHg. Hemoglobin, the oxygen-transporting pigment of erythrocytes is fully saturated at 100mmHg and the mechanisms that dispose of reactive oxygen species are designed to cope with this oxygen pressure (191). Conversely, the organism has strategies that help prevent or adapt to short- and long-term oxygen deficiency. The pressure amplitude of oxygen in vivo is below 100mmHg; in vitro it is higher when a partial pressure of 95% of oxygen is used for equilibration. The demonstration of a preglomerular arteriovenous shuntdiffusion leads to the assumption that peaks are smoothened so as to mitigate oxygen intoxication (72, 185, 260). If a kidney is subjected to cell-free perfusion in vitro, an adequate oxygen supply can be provided (within limits), if the perfusate is saturated with 95-100% oxygen, but this leads to much higher amplitudes of the oxygen pressure than are attained in vivo. This is the only way to supply enough oxygen to the organ in dissolved form. An organ like the kidney is pervaded by a complex network of blood vessels, such as countercurrent exchanger within its vascular tree in cortex and medulla. There are areas which are particularly prone to injury owing to oxygen deficiency, despite the high level of oxygen in the venous perfusate. After a short period of time one can find morphological defects in S_3-segments of the proximal tubule and the TAL-segments, which are distant from the vascular bundles of vasa recta (7, 263). The reason for the much higher depletion of oxygen in this area compared to the whole kidney is that the blood supply derived from the renal medulla is already low in oxygen, which has been extracted by shunt-diffusion in advance before. The addition of 5-10% of washed erythrocytes are sufficient to prevent these lesions at short term (hours, when equilibrated with 95% O_2) (263). Whereas in vivo the whole kidney takes up only 8% of the oxygen supplied, in the cell-free perfused kidney at high partial pressure this figure reaches 50%. Furthermore, in the outer medulla, the oxygen extraction level in vivo is much higher - reaching approximately 80%. What then can be expected in vitro, even though a cell-free perfusate provides for significantly higher medullary perfusion than is attainable in vivo? Brezis derived the in vivo 80% oxygen extraction ratio based on the calculations of Julius J. Cohen (39, 56), so one can assume that oxygen deficiency is inevitable in vitro. Another feature of cell-free perfusion is that amplitude differences in pCO_2 and pH between arterial and venous perfusate are considerably higher than in vivo, although they are significantly dampened if erythrocytes are present, due to their high transport capacity for CO_2/HCO_3 and the presence of carbonic anhydrase, plus the buffering capacity of hemoglobin and plasma proteins. This difference relative to the in vivo situation will at least result in a disruption of homeostasis, although the functional significance of this perturbation remains to be clarified.

Under in vivo conditions, there is a significant increase in the colloid osmotic pressure COP along the filtering glomerular capillaries (Fig. 3.0.1). In vitro the perfusion rate is higher by a factor 4-15 (depending on the colloid) compared with the flow of plasma in vivo at a

comparable GFR. This means that there is little increase in COP along the capillaries and, unlike the case in vivo, at a starting COP of around 20mmHg there is no significant change within the post capillary vascular bed, as it occurs in vivo, which is important for the uptake of the reabsorbate (88, 312). This partly explains why the fractional sodium reabsorption and the reabsorption of fluid do not attain in vivo values. If, however, a higher concentration of albumin is used, mimicking the protein concentration expected in the postglomerular vascular bed surrounding early proximal tubules, the fractional sodium reabsorption is higher, but the GFR does not reach in vivo values nor the values seen in experiments with 5g% albumin (34, 152, 251). At all events, the choice of a high COP for perfusion (7-7.5g % albumin) and acceptance of a reduced GFR is a good compromise with respect to maintaining the stability of the preparation and is especially suitable for the recirculation mode. To compare the reabsorption capacity at a comparable GFR we used verapamil at a high COP (albumin >7,5g %) to dilate the vas afferens and thus the GFR could be enhanced to the level of an albumin 6g % experiment. This shows that the absolute (T_{Na}) and the fractional sodium reabsorption is comparable at a high or normal COP. A high fractional sodium reabsorption can be reached in vitro only with reduced GFR, providing further evidence that the model does not reach the in vivo levels of efficiency and performance (see Tab. 11.1.1., Fig. 10.1.12, Fig. 10.1.19) (251). These deficits may be attributable to the fact that the in vivo oxygen supply is optimized and to the differences concerning the endothelial surface layer (204).

What might account for the striking difference between the plasma flow in vivo and in vitro perfusion rate? It is in part due to the viscosity of the cell-free albumin solution, which is significantly lower than that of blood plasma or any other plasma substitute. The other major contributory factor is the lack of vasoactive hormones - catecholamines, angiotensin II or its precursor angiotensin I, which is produced by the action of renin on angiotensinogen - and it affects the perfusion of the kidney cortex as well as the medulla. Perfusion of the renal medulla in vivo is facilitated by a reduced dynamic hematocrit (318) and regulated by hormones such as arginine vasopressin (AVP) (319) and a complex variety of other factors (68) which may not play any significant role in the IPRK.

The most effective and complex vasoactive hormone in the kidney seems to be the endothelin system (126). The latter has consequences for the concentrating ability of the IPRK. The high rate of perfusion of the medulla precludes the preservation and build-up of steep osmotic gradients between renal cortex and medulla. This, however, does not mean that the antidiuretic hormone AVP has no effect. Measured as free water reabsorption, it is possible to demonstrate the effect of AVP upon the incorporation of AQP2 into the luminal membrane of the collecting duct both physiologically and by fluorescence-labeled antibodies (Fig. 3.2.).

Definitions of Osmotic Clearance, Free Water Clearance and Free Water Reabsorption:

$$\textbf{Osmotic Clearance: } C_{osmol} = U_{osmol}/P_{osmol} \cdot \dot{V}$$

The **Free Water Clearance** C_{H_2O} is calculated as follows: urine time volume and osmotic clearance

$$C_{H_2O} = \dot{V} - C_{osmol}$$

the **Free Water Reabsorption** T_{H_2O} is calculated as follows: osmotic clearance and urine time volume

$$T_{H_2O} = C_{osmol} - \dot{V}$$

As shown below and in the chapter "Comparison of Results" the differences between the in vivo kidney and the isolated perfused kidney with respect to concentrating and diluting capacity result from the high perfusion rates within the renal medulla that accompany cell free perfusion, which are incompatible with the build-up of an appreciable concentration gradient. By adding washed erythrocytes, U/P_{osmol} gradients of at least a factor of 4 can be achieved, as Lieberthal showed in 1987 (145, 146). The fact that the capacity to concentrate and dilute urine is available, but cannot be realized due to the lack of the concentration gradient between cortex and medulla, is not reflected in terms of free water reabsorption or excretion. What might be the reason for the discrepancy between the concentrating capacity of the in-vivo kidney of the rat - which may reach a U/P_{osmol} quotient of 10 - and the preparation of Lieberthal, which manages a ratio of 3-4 with a hematocrit of 45% (with washed erythrocytes)? Most probably it is the difference of the rate of perfusion in the renal medulla, which is likely to be higher when a semisynthetic perfusate with albumin and washed erythrocytes is used instead of blood, which exhibits a much higher plasma viscosity. Fibrinogen, for instance, contributes with 0,3g/dl as much to viscosity as 4g/dl albumin. Of course, vasoactive factors, such as catecholamines, prostaglandins and peptide hormones like angiotensin, endothelin (126), ADH etc., certainly make a contribution also (68, 319). Within the inner stripe of the outer medulla, the concentration of the receptors for angiotensin II and prostaglandin E_2 are particularly high (38).

We still know very little about whether and how e.g. endothelin acts as a highly potent vasoconstrictor in the isolated kidney. In principle, the endothelium itself synthesizes and secretes endothelin. Natriuretic endothelin receptors are found in highest densities in the area of collecting ducts (126). To me it seems noteworthy that the constancy of flow in the isolated kidney is higher when the perfusate contains only the standard eight amino acids rather than all 20 amino acids. We have not studied this issue systematically, either with endothelin antagonists or with receptor antagonists.

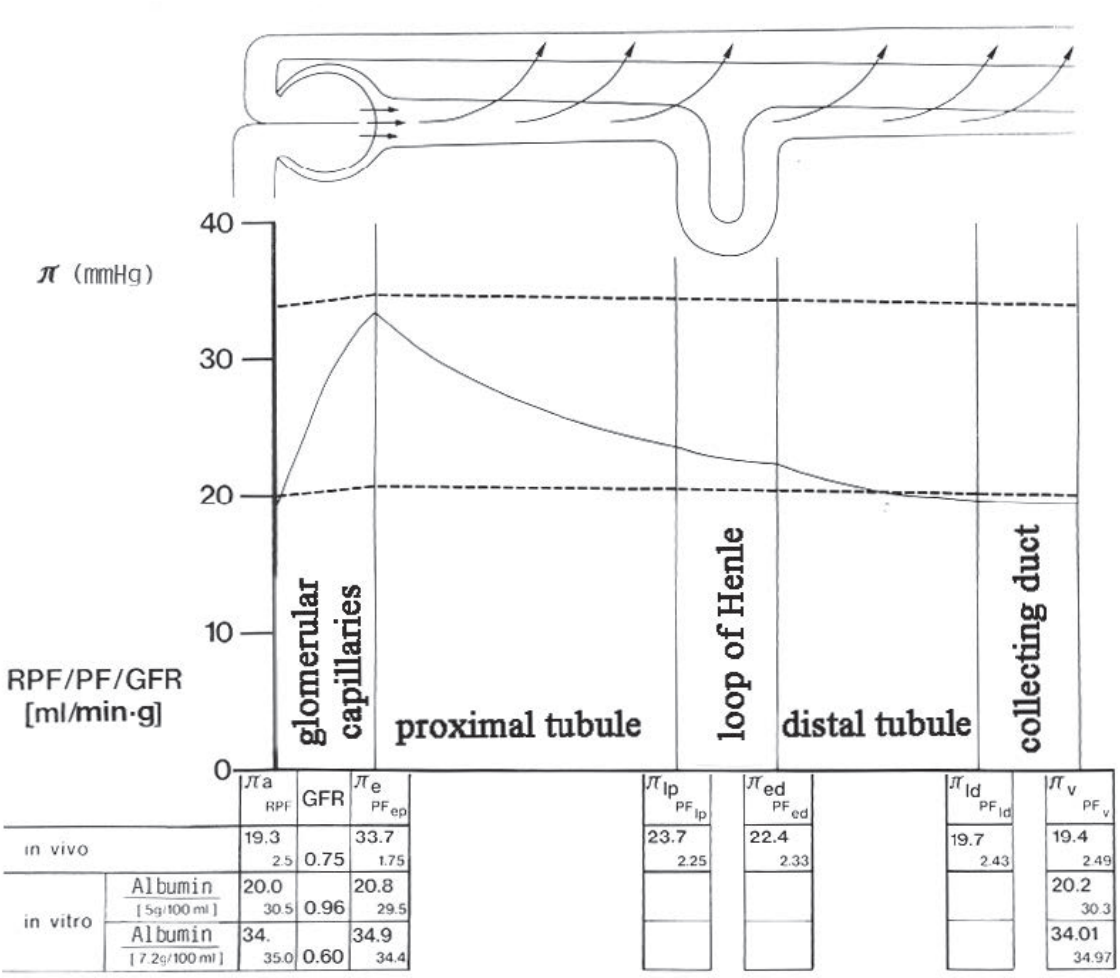

Fig. 3.0.1.: ***Idealized profile of the colloid-osmotic pressure COP along the nephron.*** Comparison of in-vivo results (solid line) with those for the cell free perfused isolated kidney using two different concentrations of albumin (5g and 7,2g/dl). Original drawings taken from (250) and based on published data (251).

Fig. 3.0.1 shows the marked differences between in-vivo and ex-vivo perfusion schematically represented by the course of the colloid osmotic pressure along the nephron. These differences first become manifest along the glomerular capillaries. In the rat, the COP increases sharply from 19.3 to 33.7mmHg at a filtration fraction of 30%, while in cell free ex-vivo perfusion the filtration fraction reaches less than 3%, whether perfusion is performed with a normal or enhanced BSA concentration. In the further course, the high postglomerular COP is more than sufficient to take up the reabsorbate from the proximal tubule in vivo. Cell-free in-vitro perfusion is unable to do so: the postglomerular COP is either too low - as in the case of “normal COP” of the perfusate with of 5g% albumin - or it is excessive at 7,2g% as specified in this scheme.

In Fig. 3.0.2, the schematic representation is limited to the change in pressure along the glomerular capillaries. Under in vivo conditions, there is a variable hydropenia, whereby filtration equilibrium is reached after only half of the capillary length, in the second variant at the end of the route. In comparison, the in-vitro situation is much simpler and there is no need for complicated calculations.

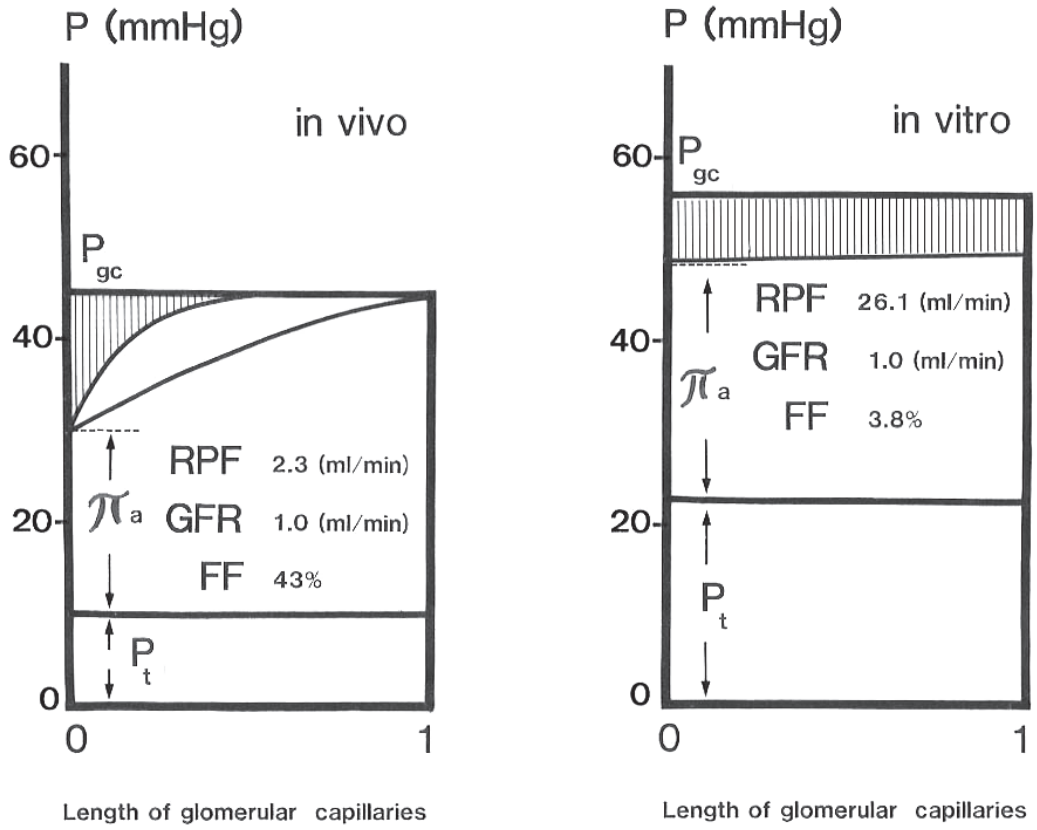

Fig. 3.0.2.: ***Relative contributions of the driving forces of filtration at the single-nephron level in vivo and in vitro.*** Only in the in-vivo case is equilibrium reached at normal or reduced extracellular space. In the in-vitro situation perfusion flow rates are ten times higher and the filtration fraction is an order of magnitude lower at comparable GFR. Accordingly, the COP changes dynamically along the capillaries in vivo, but not in the in-vitro perfused preparation. This difference makes the IPRK ideal for the analysis of glomerular filtration dynamics with the aid of the micropuncture technique (181, 182, 184, 267). P_t: tubular pressure, π_a: colloid-osmotic pressure, RPF: renal plasma flow or perfusion flow rate, FF: filtration-fraction.

Finally, Fig. 3.0.3 depicts the salient parameters in three dimensions along the glomerular capillary length with the effective filtration pressure **efp** on the ordinate, the capillary length on the abscissa and the plasma - or perfusate - flow rate $\dot{\mathbf{Q}}$ on the Z-axis. The conditions prevailing in-vitro are depicted in the foreground, with high perfusion flow rates at essentially constant **efp** along the capillary length. In the background we see characteristics of the in-vivo condition, with plasma flows in the 70-120nl/min range. Here too, a variant in which the filtration equilibrium is already attained after half the capillary length is shown, together with further unrealistic variants.

William J. Arendshorst from Chapel Hill has published a detailed discussion of issues relevant to filtration dynamics under in vivo conditions (9, 10).

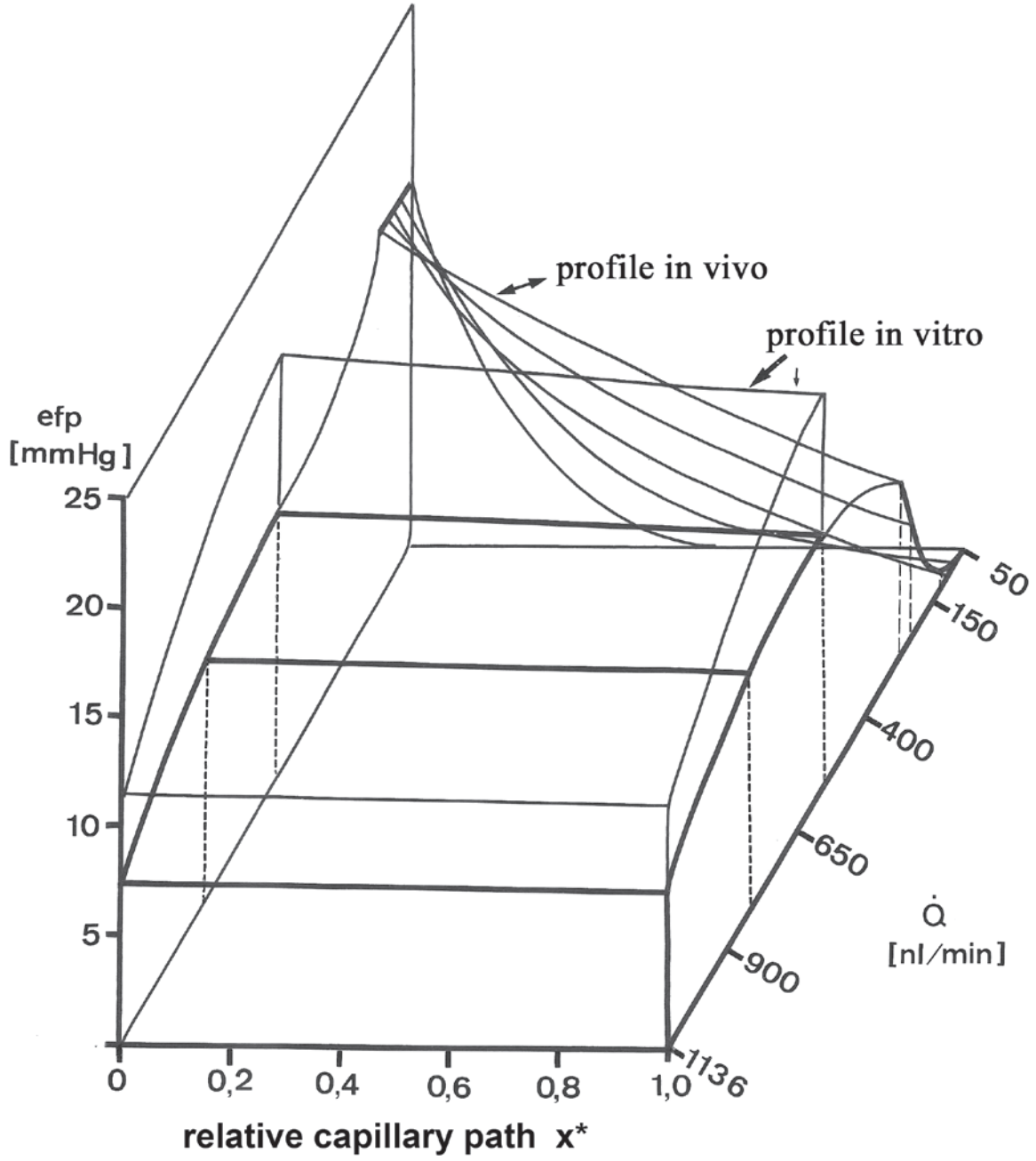

Fig. 3.0.3.: ***Effect of changes in glomerular plasma flow Q̇ (nl/min) on the efp profile along the length of the glomerular capillaries.*** The effective ultrafiltration pressure **efp** hardly changes along the capillary length in the IPRK, in contrast to the in-vivo situation, where very clear changes in plasma flow are observed. In vivo, the plasma flow Q̇ at the single nephron level in the rat ranges from 70 to a maximum of 120nl/min. In vitro, however, the perfusion flow rate is around 10 times higher (Z-axis), so that the tenfold lower filtration fraction implies that the entire filtration area is fully available even under physiologically very simple conditions. Filtration equilibrium is not reached by the end of the glomerular capillaries e.g. as observed in hydropenia in vivo; see also Fig. 3.0.1., 3.0.2. The diagram is taken from our own work (250).

3.1. Flow-constant versus pressure-constant perfusion

For biochemical and pharmacological studies, the simpler flow-constant perfusion is often preferred and depending on the specific course of the perfusion resistance, increasing perfusion pressure will generally promote self-regulation. The higher albumin concentrations used, as well as in-line filtration, contribute to the stability of this preparation, as do the lower GFR at a high albumin concentration and the associated reduction of the workload (33).

Pressure-constant perfusion is the preferred variant for use in the analysis of hemodynamics or hydrodynamics of the tubular system. For this purpose, it is, however, necessary to use a more sophisticated apparatus for pressure measurement within a double-barreled cannula and to provide for feedback regulation of the peristaltic pump and a damping of pulsatility by means of a surge tank and (optionally) electronic damping. A stable preparation is a prerequisite for micropuncture experiments and therefore we preferred to use the third perfusion mode (recirculation plus dialysis) for this purpose. We used a substrate-enriched Krebs-Henseleit BSA solution with or without 5% erythrocytes, which is constantly regenerated and gassed over a larger volume of dialysate, essentially employing the dialyzer as “dialung or kidney-lung”. This permitted experiments to be carried out under adequately stable conditions for periods of 2-3 hours (181, 182, 184, 251, 267).

3.2. Concentrating and diluting capacity

Whereas rat kidneys can concentrate urine by factor 4-10 relative to blood, this is not feasible by cell-free perfusion of the kidney, even when high doses of antidiuretic hormone (arginine-vasopressin) or (1-deamino)-D-Arg-vasopressin (dDAVP) have been used. This is largely due to relatively high in-vitro perfusion rate of the renal medulla. The in-vivo rate is much lower owing to the presence of erythrocytes, which have to negotiate the long vasa recta and also retard the flow rate because of the multiple branching, thus enabling the build-up of steep osmotic gradients. Another crucial factor may be the uptake of urea by transport proteins in the medullary collecting duct and in the cell membranes of erythrocytes, which probably contribute to the high accumulation of urea in the renal medulla. Erythrocytes can quickly take up urea via these transport proteins in a position-dependent manner and rapidly deliver it to the medulla (121, 228-230, 297). Since the discovery of urea transporters in individual sections of the loop of Henle (178, 229), the passive model of urine concentration propagated by Kokko and Rector (127) is no longer tenable.

Thick ascending limbs known to be the core (or motor) of the concentrating mechanism are thought to suffer from oxygen deficiency especially in the interbundle region under cell free perfusion. These TAL-segments are found in cortical and mid-cortical nephrons, whereas TAL-segments of juxtamedullary nephrons surround vascular bundles directly and thus benefit from a radial oxygen diffusion and, if necessary, can increase their GFR accordingly. It should be noted that even those S_3-segments of the proximal tubule, which lie in the interbundle area next to the affected TAL´s are damaged too (263).

In terms of the attainable level of free water reabsorption or free water clearance, no significant differences from the in vivo situation are observed in the steady state phase during the first hour (publication in preparation). This argues that the function of the collecting ducts (CD) remains intact during this time. Fluorescence-labeled antibodies have

revealed the insertion of AQP2 into the luminal membrane of the collecting duct under AVP administration and its relocalization into the cytoplasm after AVP withdrawal (125, 262). Within 10 mins after starting single pass perfusion without AVP, osmolality of urine drops below the osmolality of the perfusate and the excretion of free water begins. Addition of AVP results very quickly (within 10 min) in a rebound in osmolality and Fig. 2c demonstrates that, at higher doses of the hormone, AQP2 is incorporated not only into the luminal membrane but also into basolateral membranes. The latter was detectable under in-vivo conditions only after considerable effort and required the use of additional stimuli, such as long-term treatment with aldosterone (64). Baines and Ross have pointed out that non-oxidative metabolism of glucose plays an essential role in modulating the dilution capacity of the urine by the collecting ducts (17), a view discussed by Julius J. Cohen earlier on (54). Lieberthal et al. demonstrated the dominant role of erythrocytes in enabling a high concentrating ability in the isolated perfused kidney, when they added increasing amounts of washed bovine red cells up to 45% hematocrit (145, 146). Nonetheless, the highest concentration of urine attained in their experiments required blocking of prostaglandin synthesis in the presence of dDAVP, and amounted to 1200mosmol/l - not the 3000mosmol/l seen in antidiuresis in vivo.

The isolated kidney perfused by a cell-free medium can reach a U/P_{osmol} of 0.5-0.6 as a minimum equivalent to a Uosmol of approximately 160mosmol/kg H_2O. By addition of arginine-vasopressin (AVP) or desmopressin (dDAVP) a U/P_{osmol} of 1.1 – 1.2 can be reached, while adding erythrocytes has a much greater effect, as discussed above. Specifically, it depends whether AVP is administered from the beginning of perfusion and subsequently withdrawn, or withdrawn immediately after the start of perfusion. We have studied these issues over the last few years and the data are being prepared for publication (262).

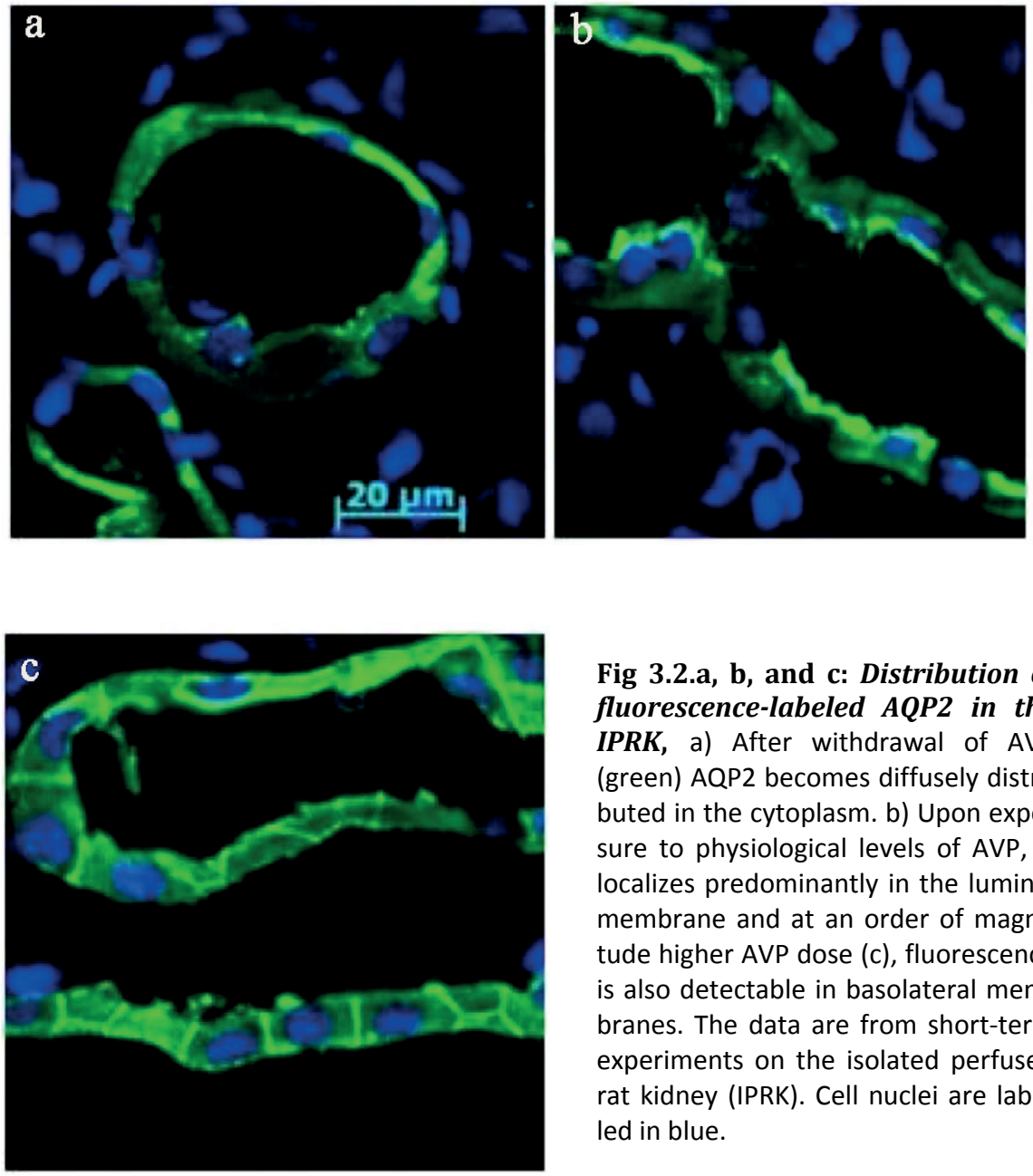

Fig 3.2.a, b, and c: ***Distribution of fluorescence-labeled AQP2 in the IPRK,*** a) After withdrawal of AVP (green) AQP2 becomes diffusely distributed in the cytoplasm. b) Upon exposure to physiological levels of AVP, it localizes predominantly in the luminal membrane and at an order of magnitude higher AVP dose (c), fluorescence is also detectable in basolateral membranes. The data are from short-term experiments on the isolated perfused rat kidney (IPRK). Cell nuclei are labeled in blue.

These data were presented in 2011 at the 90th Congress of the "Deutsche Gesellschaft für Physiologie in Regensburg (262) and can be found in the PHD thesis of Jens Klokkers (125), doctorate to Dr. rer. nat. in the year 2010 in the Department of Biology at the Mathematics and Natural Sciences Faculty of the University of Münster.

3.3. The permeability of albumin in the IPRK and the "repaired defect" hypothesis

In the initial experiments on the isolated rat kidney, carried out by Brian D. Ross and his group, they found an increased excretion of protein in the urine of the kidneys perfused with BSA, with levels of 3-5,3mg protein/ml urine at a quite low GFR of 150µl/min·g kidney (wet weight), measured as clearance of creatinine (185). They went on to state that "proteinuria was somewhat high, but this is of limited significance since the rat kidney in vivo excretes injected bovine albumin" (150, 151). We have worked intensively on these issues (194, 244, 245, 248, 252, 266, 291, 292). The following figures illustrate our principle findings, which led to the "repaired defect" hypothesis (244).

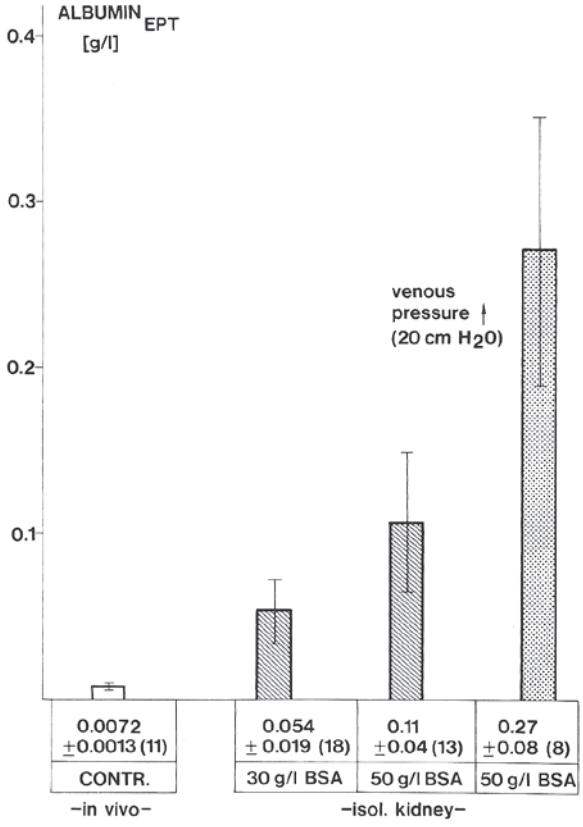

Fig. 3.3.1.: ***Albumin levels at the early proximal tubule in vivo and in vitro.*** Fluid was withdrawn from early proximal tubuli by micropuncture. Albumin levels in nl samples were estimated by staining and densitometric analysis of band areas after ultramicroscale-discelectrophoresis in microcaps (Joyce-Loebl two-beam microdensitometer). Control values were obtained from rat kidneys exposed in vivo during Inactin anesthesia. In-vitro values were measured in the isolated kidney perfused with two different concentrations of albumin (3 g% & 5 g%). The column on the right demonstrates a further increase of the albumin concentration in the early proximal tubuli, after the pressure of the venous outflow had been increased to 20cm H_2O.
$Albumin_{EPT}$ = early proximal tubule.

Michael Weiner pointed to the fact that BSA is not identical to rat albumin. This certainly holds for the number of negative charges, while the size and shape of these molecules are nearly identical (247). According to Peters, the BSA molecule carries 17 negative charges compared to 12 in rat albumin (203). If negative charges hinder glomerular passage, as one would expect, rat albumin should have an easier passage under in vitro conditions than BSA. Thus, the effect tends to be underestimated. Another factor is that albumin acts as a transport molecule for lipids and water-soluble substrates, and exists in differently charged states in vivo which may not be directly comparable to those of the molecules as used in vitro. We have not performed a rigorous delipidation of albumin with activated carbon but subjected the protein to intensive dialysis. Aliquots were then stored at -20°C until use. Recently a functional test for albumin has been developed (s. chapter 9.8.).

In order to determine the precise timepoint of the increase in proteinuria during the in-vivo to in-vitro transition, we first measured the protein levels in urine collected from the animal´s metabolic cage. The second sample was obtained during anesthesia as ureteral urine from the kidney that was subsequently perfused. Immediately prior to the transition period, the urinary flow rate was increased by mannitol. Fig. 3.3.1 is modified, and is derived from the work of Horst Pagel in our laboratory in Hanover.

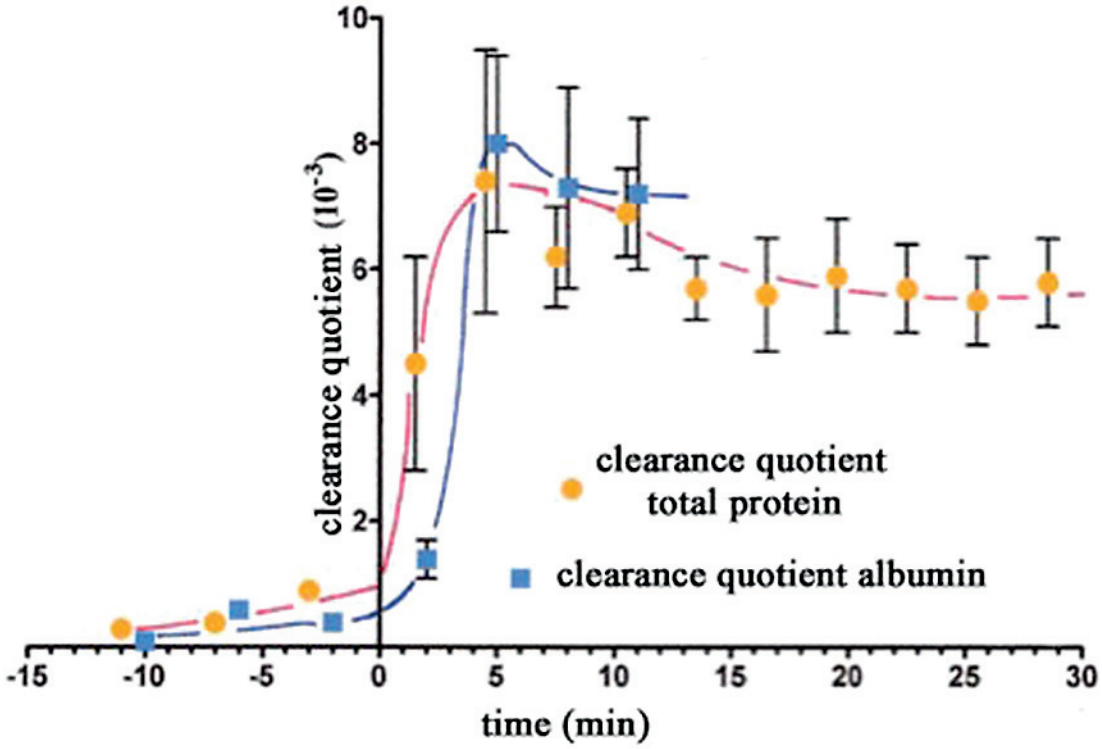

Fig. 3.3.2.: ***Clearance-quotient for protein/albumin during the transition period from in-vivo to in-vitro conditions.*** The initial values on the negative timescale were obtained from urine samples taken from the animal´s metabolic cage. The following values before zero time are for samples obtained during barbiturate anesthesia, and the values just before the transition were obtained following mannitol diuresis to raise the urine volume sufficiently to enable an early data recording after the transition to in-vitro perfusion (modified from Pagel (193, 194)). The clearance-quotient for total protein is higher than that for albumin in the early in-vitro phase. Shortly thereafter it equalizes, when the washout period ends and the albumin in the perfusate is the only remaining colloid.

The addition of 5% erythrocytes from the beginning reduces the clearance ratio for albumin by half, and this value remains stable over the further course of the experiment. In contrast, the clearance ratio continues to rise with time in the absence of erythrocytes. Swanson has shown, that even after later addition of red cells prevents any further increase in the clearance ratio (293). Hence, the question is how to explain this phenomenon. The study of this issue has led me to the hypothesis that in-vitro perfusion with cell free media unmasks membrane defects that facilitate the passage of albumin. The larger defects can be blocked by the passage of erythrocytes, while the smaller ones support the high residual excretion of albumin (244).

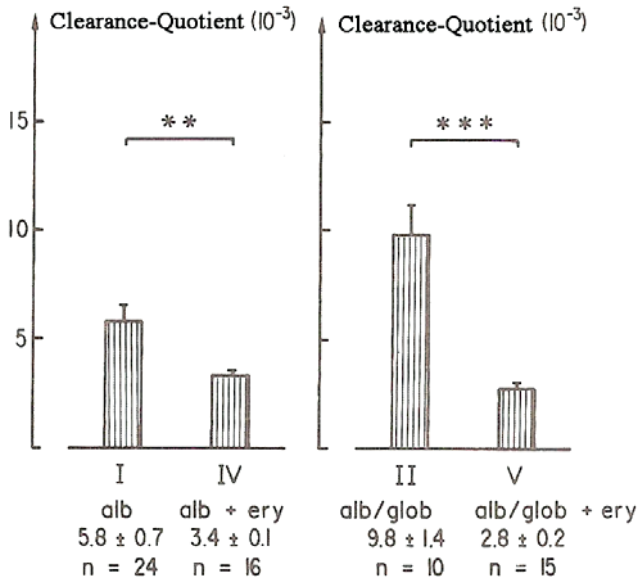

Fig. 3.3.3.: ***Clearance ratio for albumin in the IPRK without and with addition of red cells.*** Significant reduction of the clearance ratio at a comparable GFR, (group I and IV). The difference is even more apparent in the collective with albumin and addition of globulin (group II and V) (193, 194).

The following figure comes from the study by Swanson (293) and is reproduced by permission of the APS.

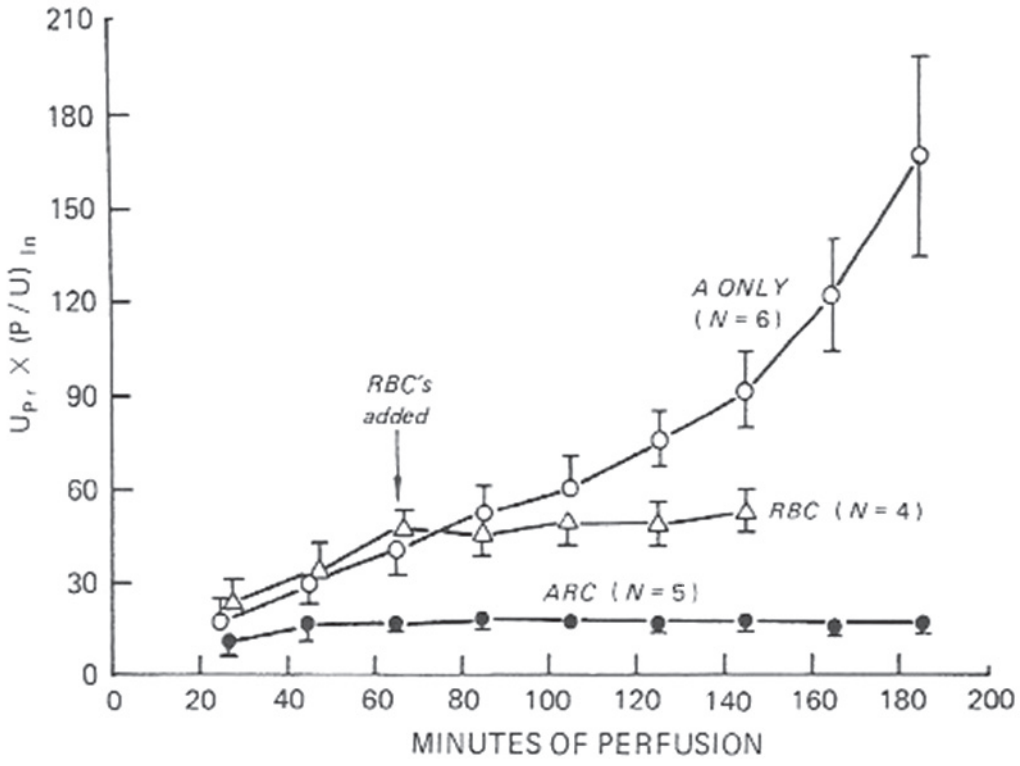

Fig. 3.3.4.: ***Calculated concentration of albumin in the ultrafiltrate in three study groups.***

1. Perfusate with albumin and red cells (ARC)
2. Time-delayed addition of red blood cells (RBC) and
3. Albumin solution without red blood cells (A only)

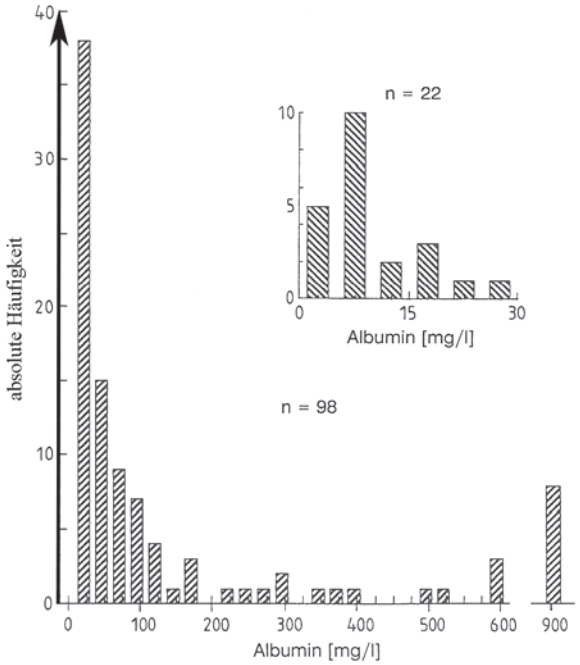

Only with a larger number of micropuncture samples (n = 98) did it become clear that a skewed frequency distribution exists. Many findings were in the range of in vivo values, but approximately 16% of the samples lay in a significantly higher range. This supports the assumption that only this small fraction of glomeruli exhibit significant leaks or defects, which are unmasked under the conditions imposed by cell-free perfusion, but are sealed by erythrocytes. In order to obtain valid data, micropuncture samples from early proximal tubules were collected under pressure control using the "Berlin" system of a microperfusion pump combined with a miniature pressure measurement system (154), s.a. chapter 13.

Fig. 3.3.5.: ***Frequency distribution of the concentration of albumin in early proximal micropuncture samples.*** The small insert are normal findings from in vivo studies in rats (69). In 17 of 22 samples values were below 1.5 mg%; in the other 5, levels of up to 3 mg% were recorded. Under the influence of angiotensin infusion, a rightward shift of the frequency distribution occurs, as it exists on the isolated perfused kidney without any infusion.

Infusion of angiotensin II into the IRPK does not increase the level of proteinuria (296). This could be a basis for the understanding of functional proteinuria during exercise, orthostasis, fever and congestive heart failure, all of which can be assigned to the so-called non-selective type of proteinuria and can be blocked by ACE inhibitors (30, 104, 248, 249, 258, 266).

Is there a correlation between proteinuria and erythrocytes in the IPRK?

The "repaired defects" hypothesis, first formulated in 1986 based on the observation that cell free perfusion with BSA as a colloid immediately leads to bleaching of the kidney. However, microscopic examination revealed the presence of hematuria in the urine sediment for up to 60 minutes after the start of the perfusion. The decrease in the red cell number followed an exponential course (244). If red cells were added to a level of 5%, the hematuria leveled off at approximately 100 red cells/min during the second hour of perfusion – a factor of 100 higher than that seen in in-vivo studies of urine collected in the metabolic cage. Viktor Repp supplemented these test series in his thesis work (218) and demonstrated, that perfusion in the single-pass mode without a colloid led to even faster excretion of red blood cells compared to perfusions with BSA, presumably due to the higher glomerular filtration and urinary flow rates. If one calculates the total number of excreted erythrocytes, one gets a figure of $0.5\text{-}1.0 \cdot 10^6$ cells that find their way via the glomerular capillaries into the final urine (calculated from the area under the curve). Converted to 30.000 glomeruli per single kidney, this amounts to 17 to 34 red blood cells

per glomerulus that escape through the endothelium of glomerular capillaries via transient defects that are otherwise occluded by erythrocytes. What they left behind is the higher albumin permeability with BSA in the perfusate, which in turn can be reduced by adding sealing erythrocytes (see Figs. 3.3.3. and 3.3.4.). The remaining level of proteinuria is still much higher than in vivo. The added erythrocytes therefore occlude only larger defects (≥ 200nm). Under in vivo conditions, whole blood can seal defects in a variety of ways. Cellular elements, such as erythrocytes and leucocytes, can plug larger leaks, and are supplemented by platelets in combination with clotting factors, proteins like orosomucoid and the so-called "sieve plugs", which correspond to a functional lining of the fenestrations of the endothelium of the glomerular capillaries by glycocalyx. These "sieve plugs" are no longer discernible following conventional perfusion fixation and can be detected only with special procedures. They can also be disturbed functionally by hemodynamic perturbations such as the infusion of angiotensin II. This could explain many forms of functional proteinuria as well as forms of permanent or functional hematuria (glomerulopathy of thin basement membrane, higher basic hematuria in children relative to adults – due to a thinner basal membrane). Functional proteinurias induced by fever, orthostasis, load, stress or angiotensin II, are unselective proteinurias, and thus based on larger defects as they are needed for the passage of albumin. Experiments with dextrans of varying size have shown that there is a shift toward permeability to the larger dextran molecules upon infusion of angiotensin II (31).

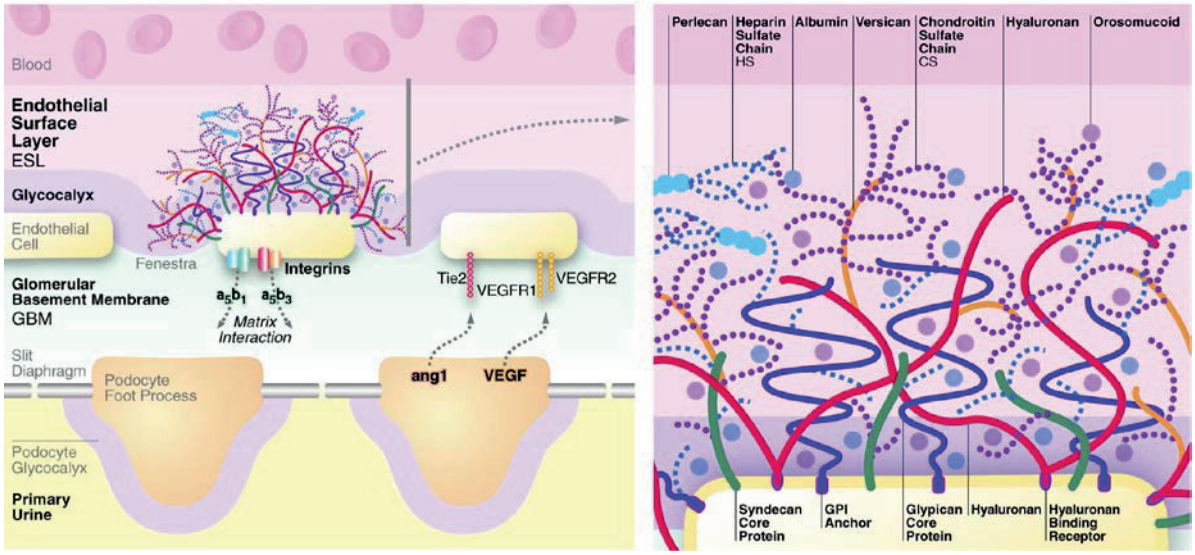

Fig.: 3.3.6.: ***Schematic representation of the "sieve plugs" from a review by Boerje Haraldsson*** (97)**.** The function of orosomucoid was discovered by chance in studies with a preparation of human albumin, which was contaminated with orosomucoid (98). Reproduced by permission of the author and APS.

Shedding of the glycocalyx of the endothelial cells of capillaries is a functional and reversible mechanism, induced by hemodynamic stress or other procedures, that has been discussed in a number of studies and reviews (85, 97, 166, 170, 204, 208, 217, 231, 301, 302). An intact glycocalyx and the integrity of its functional surface layer seem to be essential for the physiological barrier function of the vascular endothelium of capillaries, and are even more important for glomerular capillaries due to their higher endoluminal perfusion pressure.

IPRK-based studies of the importance of negative charge on the glomerular basement membrane.

The sieving characteristics for macromolecules in the IPRK undergo dynamic alterations, which differs significantly from the in vivo conditions. To grasp the significance of the negative charges on the penetration of negatively charged macromolecules we have used different perfusion techniques. Use of the polycation protamine chloride to neutralize negative charges leads to a strong vasoconstriction, which can be abrogated by verapamil. Whereas the baseline permeability for albumin in the IPRK is higher than that in vivo by factor 10-20, addition of protamine chloride causes a progressive further increase to 100 times that observed in vivo (11, 12, 284, 285). When we repeated this study in the reperfused, anatomically fixed kidney, we saw only a slight increase in permeability. The complexing polycation causes no significant ultrastructural changes in the glomerular capillary wall once the collagen scaffold of the GBM has been crosslinked by fixing. Without this crosslinking, negative charges can be clustered by the polycation, leaving large uncharged regions between them (78). Using this model of the fixed and reperfused kidney, we were able to study perfusate with BSA at different pHs or perfusate supplemented with a chemically cationized albumin (317). The latter increased the permeability by a factor of 2, while reducing the pH from 7.4 to 4.0 did so by a factor of 8. In the same study several different size classes of dextran were used, and protamine was found to increase permeability for the T110 molecular weight class alone -- by a factor of 2.5 (317). We published further findings using this model in the years 1999-2003 (50-53) to demonstrate the potency of such an experimental model.

The data given by Swanson (293) regarding the increase of the clearance ratio for albumin over time when a cell-free perfusate is used and a stable situation by added red cells are qualitatively equivalent to our own experiences. This relates to the addition of 5% red cells. Thus, the otherwise morphologically detectable damage to TAL-segments and proximal S_3 tubules is missing. Viktor Repp demonstrated in his thesis (218) that, during cell-free perfusion, epithelial cells or fragments of them could be detected in the sediment of the urine as early as 30 min after the start of perfusion. This is a reflection of hypoxic cell damage and the addition of red cells suppresses these defects. The minimum level of supplementation with red cell addition required to suppress cell damage is not yet known. We have never used less than 5%; however, it is conceivable that 2% is sufficient (see contribution of Frank Schweda chapter 14). At 5% red cells, the combination of reduced oxygen capacity and presumably much higher flow rates in the renal medulla may be sufficient to prevent hypoxic damage. An interesting contribution from the Oxford group demonstrated the high susceptibility of the proximal tubule to oxygen deficiency, when hypoxia is limited to prevent TAL-damage (70), see also Chapter 12.3.

Whereas Boyce and Holdsworth (36) stated: “the demonstration that the glomerular filter in the IPK has a normal negative charge barrier indicates that the increased protein excretion in IPK systems cannot be attributed to abnormalities of this component of the filtration barrier”, another Australian group (295) discussed a relative deficiency of oxygen radical scavengers. Addition of mannitol, superoxide dismutase, catalase and a pretreatment of the donor animal with allopurinol prevented the increase of the clearance-ratio for albumin as it was shown by Swanson only by the addition of red cells (scavenger function?), comparable to our own experience.

4. Perfusion techniques

4.1. Perfusion medium

4.1.1. Salt solutions

The most common basic salt solution now used in kidney perfusion is the Krebs-Henseleit type. Other formulations (Tyrode or Ringer solution and their variants) are solely of historical interest in this context; in particular, phosphate buffer has been entirely replaced by bicarbonate buffers, which require continuous input of 5-6% CO_2. Table 1 gives the composition of the original Krebs-Henseleit, together with the substrate-enriched variant that we use.

Table 4.1: ***Compositions of the original Krebs-Henseleit salt solution and two modified versions (mmol/l).*** *The concentration of chloride, but not that of sodium, is reduced when substrates are added. Calcium concentrations are given as total calcium and as ionized Ca^{++}. Measured levels of ionized calcium are usually lower than theoretically expected. When perfusate is dialyzed continuously, [Ca^{++}] remains stable at a low level, even when the albumin concentration increases (depending on dialysis conditions, see Fig. 9.6.1.).

Composition	NaCl	Na^+	Cl*	K(Cl)	$Ca(Cl_2)/Ca^{2+}$	$MgSO_4$	$Mg(Cl_2)$	$NaHCO_3$	HCO_3	NaH_2PO_4	KH_2PO_4	glucose	urea
Krebs-Henseleit	118			4.7	2.52	1.64		24.88			1.18	5.55	
Modified		140	109	5	2.0 / 0.9		1		25-27	0.72		8.4	6
Substrate-enriched		140	105*	5	2.5/0.9		1 (0,8)		25-27	0.72		8.4	6

4.1.2. Addition of substrates

The addition of various metabolic substrates/intermediates of glycolysis or the Krebs cycle, of long- or short-chain fatty acids (such as butyrate) and amino acids enhances rates of tubular transport and increases oxygen consumption. Moreover, it functionally stabilizes the preparation, and this observation has led to the use of various substrate mixtures as supplements (25, 71, 256, 257, 264).

Table 4.2: ***Substrate additives.*** Recipe 1 (R1) has been used since 1972, and was first described in 1975 (257). Note that the glucose level was raised to 8,4mmol/l. R2 has been used since 1985 (263), α-ketoglutarate and malate since 1986 (242), butyrate is used when required (246).

R1	*Glucose*	*Pyruvate*	*Lactate*	*Glutamate*	*Oxaloacetate*
mmol/l	*8.4*	*2*	*2*	*2*	*1*

R2	*Glucose*	*Pyruvate*	*Lactate*	*Glutamate**	*Oxaloacetate*	*Ketoglutarate*	*Malate*	*Butyrate*	*Cystein*	*Glutathione*	*Carnitine*
mmol/l	*8.4*	*0.3-2*	*2*	*1.6*	*1*	*1*	*1*	*1*	*0.5*	*0.5*	*0.1*

*Halve of the glutamate is contained in the amino acid mixture. Pyruvate, glutamate and butyrate are added as sodium salts. Lactic, oxaloacetic, ketoglutaric and malic acids are added in their acidic forms, and upon dissociation the protons are exchanged for cations from sodium bicarbonate, thereby producing a high initial pCO_2 in the dialysate (see preparation of perfusate).

Table 4.3.: ***Supplementation with amino acids.*** A 10% amino acid solution (Aminoplasmal AS10; Braun, Melsungen Germany) is added to a final concentration of 0.05-0.1% (0.5-1ml in 100ml basic solution). In earlier experiments we added only eight amino acids (251) first used by DeMello and Maack (63) in 1976. Then in 1982 the Epstein group published their results with the full spectrum of amino acids (71).

Recipe 1 is from Bowman and Maack (1972) with 6 amino acids (35).
Recipe 2 is from DeMello and Maack (1976) with eight amino acids, which we also followed (63, 250, 251).
Recipe 3 with all 20 amino acids was recommended by Epstein in 1982 (71).
Recipe 4 is a modified version of R3, which we have used since 1982 (243, 263). The small amounts of citrate and acetate result from the use of the Genius System for batch preparation of the basic solution, which we adopted in 2007 (see 4.1.3.: Preparation of perfusate).

R1

amino acids	Met	Arg	Ala	Gly	Asp	Ser
mmol/l	0.5	1	2	2	3	2

R2

amino acids	Ile			Met					Arg		Ala	Gly	Asp		Pro	Ser
mmol/l	1			0.5					1		2	2	3		2	2

R3

amino acids	Ile	Leu	Lys	Met	Phe	Thr	Trp	Val	Arg	His	Ala	Gly	Asp	Glu	Pro	Ser	Tyr	Cys	Gln	Asn
mmol/l	0.3	0.4	1	0.33	0.32	0.24	0.07	0.33	0.5	0.24	2	2.3	0.2	0.5	0.31	1	0.2	0.5	2	0.2

R4

amino acids	Ile	Leu	Lys	Met	Phe	Thr	Trp	Val	Arg	His	Ala	Gly	Asp	Glu	Pro	Ser	Tyr
mmol/l	0.38	0.68	0.67	0.3	0.28	0.35	0.08	0.53	0.66	0.2	1.18	1.6	0.42	0.49	0.48	0.22	0.02

other substrates	citrate	acetate
	0.05	0.66

*For the production of the basic electrolyte solution, we used the Genius System for the first time in 2007; thereby it came to the addition of citrate and acetate at a low concentration.

Glutamate, cysteine and glycine are precursors of glutathione, and their inclusion helps to maintain the starting level of reduced glutathione. However, only the addition of the full spectrum of physiological amino acids results in an overall improvement of functional parameters (71), albeit at the price of a reduction in glomerular filtration rate.

Special note: The recipe successfully employed in our experiments during the years 1975 – 1982/85 (see below) was based on the use of a batch of BSA obtained from Reheis/Armour in USA, sterile water supplied by the hospital's pharmacy, and the sterile concentrated salt solutions used in intensive-care units (ICUs). This was supplemented with the eight amino acids used by Thomas Maack's group (63), a mixture of substrates (glucose, oxaloacetic acid, pyruvate, lactate and glutamate) that was first used during my time in Berlin (prior to 1975) (257), and an amount of calcium calculated to be equivalent to a level of 1.25 mmol/l in the dialysate (see below). All tools and containers used during the preparation of the solution, such as pipettes and glass vessels, had previously been sterilized by dry heat. The tubing of the perfusion apparatus was sterilized with ethylene oxide and stored in sealed bags of paper/transparency foil. Metal and glass parts were sterilized by dry heat. This careful attention to detail paid off, and was essential for maintaining the stability of the preparation during the time-consuming micropuncture experiments (181, 182, 184, 245, 250, 252, 266, 267, 290-292).

Composition of the perfusate during the period 1975-1982

A. Dialysate for the preparation of the BSA stock solution (BSA powder was dissolved in dialysate, then dialyzed against it, and stored as 10% BSA in 100-ml aliquots)

Na	140	mmol/l	Cl	123	mmol/l
K	5	mmol/l	HCO_3	25	mmol/l
Ca	1.25	mmol/l	HPO_4	0.72	mmol/l
Mg	0.6	mmol/l	Neomycin-sulfate	10	mg/l

B. Solutions for the perfusion & dialysis of the perfusate (final concentration)

Perfusate (100-250ml)			**Dialysate (2000-5000ml)**	
Na	140	mmol/l	140	mmol/l
K	5	mmol/l	5	mmol/l
Ca	2.5*	mmol/l	1.25*	mmol/l
Mg	1	mmol/l	0,6	mmol/l
Cl	104	mmol/l	104	mmol/l
HCO_3	25	mmol/l	25	mmol/l
HPO_4	0.72	mmol/l	0.72	mmol/l
Urea	6	mmol/l	6	mmol/l
Glucose	8.3	mmol/l	8.3	mmol/l
Na-oxaloacetate	1	mmol/l	1	mmol/l
Na-pyruvate	2	mmol/l	2	mmol/l
Na-L-lactate	2	mmol/l	2	mmol/l
Na-glutamate	2	mmol/l	2	mmol/l
Methionine	0.5	mmol/l	0.5	mmol/l
Alanine	2	mmol/l	2	mmol/l
Serine	2	mmol/l	2	mmol/l
Glycine	2	mmol/l	2	mmol/l
Arginine	1	mmol/l	1	mmol/l
Proline	2	mmol/l	2	mmol/l
Isoleucine	1	mmol/l	1	mmol/l
Aspartic acid	3	mmol/l	3	mmol/l

*The free calcium concentration in the dialysate was constant, whereas the total calcium concentration in the perfusate varies with albumin concentration and reaches a minimum of 1.25mmol/l in the albumin-free perfusate. The measured concentration of ionized calcium (Ca^{++}) was 0.2-0.3mmol/l lower than that calculated on the basis of the added calcium salt. Chapter 9 describes the methods of measurement, and demonstrates the relationship between albumin and calcium under continuous dialysis (to regenerate the perfusate), which differs from the expected behavior (see Fig. 9.6.1.). The theoretically calculated concentration of calcium is also lower when measured in the dialysate with the appropriate ion-selective electrode (Radiometer ABL 505) at pH 7.4, as we recently (2014) ascertained. We used albumin at concentrations of between 2.5 and 7g/dl (and at 10g/dl in the non-filtering kidney variant). Differences in Na-concentration between perfusate and dialysate are due to the albumin concentration (which determines the volume of the protein-free distribution space).

4.1.3. Preparation of perfusate and dialysate

The solutions are made up by mixing prepared stock solutions or ampoules of sterile concentrates (clinical preparations) with sterile distilled water. When phosphate is added prior to aeration with CO_2 (which lowers the pH), it should be added last – slowly, under constant stirring, and at its final dilution. Development of opalescence signals the precipitation of calcium phosphate crystals, in which case the solution must be discarded.

For preparation of the large quantities (5-10 liters) needed for the single-pass variant 1 or recirculation with regeneration by dialysis, we prefer the following approach: If the neighboring clinic has a Genius dialysis system (FMC), we prepare the salt solution for the perfusate in 90-l batches. Under aeration of the prepared batch with sterile (filtered) compressed air (supplied by a small compressor with a silicone adapter), we fill aliquots of 5 or 10 liters into gas-tight glass bottles containing neomycin (50 or 100mg neomycin, freshly prepared in 1 or 2ml). Afterwards the glass containers are stored at 6°C in a refrigerator. The dry salt component is e.g. DS135/35 (135 Na, 35 mmol HCO_3) and a liquid component HC 42 (4 mmol KCl, 1.25mmol $CaCl_2$, and 0.5mmol $MgCl_2$). During preparation of the batch, small amounts of acid (HCl, citric acid and acetic acid) introduced in the liquid component lead to the release of CO_2 from the HCO_3, and the pH falls below 7.0. Under these circumstances, the phosphate-free solution is stable for weeks and months. On the day of use, we enrich and acidify this basic solution by substrates as lactic, malic, oxaloacetic and α-ketoglutaric acids (further raising pCO_2). Addition of magnesium chloride increases its concentration from 0.5 to 0.8 mmol, and potassium added e.g. as K-lactate (+1 mmol/l) brings its level to 5 mmol/l. Supplementation with glucose raises its molarity from 5.5 to 8.4 mmol/l. Then amino acids are added following the recipes given above together with e.g. AVP/dDAVP. Finally, phosphate is added at a low pH before sterile filtration under compressed air (2 bar). Even after that, the pCO_2 remains high and equilibration is necessary to bring its down to the range of 40mmHg. We use a gas-mixing pump (Gigamax, Fa. Wösthoff Messtechnik GmbH, Bochum, FRG) to equilibrate the perfusate initially with pure oxygen, thereafter with 95% O_2 and 5% CO_2, sometimes 94% and 6%. The use of an interposed filter (e.g. from a transfusion tube system) to trap residual droplets of mineral oil emanating from the pump has proven to be effective and useful. Under these conditions, the measured HCO_3 is in the range of 25-27mmol/l (reduced from 35mmol by the addition of substrates as sodium salts, resp. acids). For sterile filtration we use filtered air compressed to 2 bar, a pressure vessel of 10 liters capacity (stainless steel, Sartorius, Göttingen, FRG) and a membrane filter with a diameter of 142mm (cellulose acetate membrane, pore size 0.2µm), with or without an attachment for a 2 Liter container. For the single-pass mode, the standard system is adequate. For variants 2 and 3 the attachment is recommended. For use in mode 3 the dialysate is first passed from the 10 liter pressure vessel via the attached 2 liter overhead attachment. This approach is necessary because a residual volume of approximately 200 ml remains at the base of the 10-liter pressure vessel in which, a volume inadequate for the albumin perfusate (see Figs. 4.5.1., 4.5.2.). This residue can either be discarded or filled into the overhead attachment using a funnel, and filtered. Thereafter the empty 2-liter overhead is filled with the albumin perfusate and directly connected to the pressure source (see fig. 4.5.2.).

4.1.4. Albumin stock solution

For mode 2 or 3 experiments, albumin is prepared as a 10% stock solution by stirring 1 kg of albumin (BSA) powder into 10 liters of dialysis fluid until fully dissolved (1 g albumin (BSA) powder in 10 ml dialysis fluid). This solution is further purified by dialysis (at constant volume) in a cooling chamber. We used a commercial low-flux dialyzer against 10-liter of dialysate for 6 to 8 hours, changing the dialysate every 2-4 hours. The purpose of this step is to remove/dilute out small albumin-bound substances, thereby contributing to a higher degree of standardization. Aliquots (100ml) of the purified solution are stored frozen at minus 20°C. Some authors, such as Bowman, Maack and Bekersky, prefer to retain these substances as metabolic fuels, and often dispense with the dialysis step (23, 33, 162, 163). In studies of fatty acid metabolism, removal of albumin-bound lipids by passage through activated charcoal has proved to be essential (57). In the case of mode 2 recirculation, we prepare an aliquot of diluent containing all additives (metabolic substrates, amino acids etc.) which is combined with the albumin stock solution before sterile filtration. For mode 3, it is sufficient to mix the albumin stock with dialysate on final dilution and equilibrate the perfusate by dialysis. At a proportion of perfusate to dialysate of 1:20, dilution of the substrates is negligible, although one may adjust the additives to the final concentrations appropriate for perfusate and dialysate. In our early days, we used cellophane dialysis tubing (cuprophan) when preparing the albumin stock solution and dialyzed in a large beaker with a magnetic stirrer.

4.1.5. Other colloid additives

To keep costs down, colloids other than albumin, such as gelatin derivatives (Haemaccel®, Gelifundol®), dextran, hydroxyethyl starch, Pluronic F108 or Ficoll 70, have been used for the single-pass mode. These colloids allow for aeration of the solution via a glass frit, which is not possible with albumin owing to foaming (although – undeterred -- Smyth has apparently used a dialyzer to aerate his albumin solution (280), as there was no mention of ultrafiltration in the paper). At comparable colloid osmotic pressure, albumin has the lowest viscosity (172) and enables the highest rates of perfusion and oxygenation to be achieved, while the GFR is higher than that attainable with other colloids at similar COP.

Table 4.4.: Overview of common colloids

*Employed as the sole colloid or in combination with BSA
[e.g. BSA/Ficoll as used by Smyth (278)]

Brand name	Short name	Chemical	Manufacturer
Haemaccel®	Polygelin	gelatin, cross-linked	Delta Select
Dextran	Polysacharose		Pharmacia
Ficoll®, Histopaque®, Polysucrose	Copolymer	sacharose-epichlorhydrin-copolymer	GE Healthcare
Haes-steril®	HAES	hydroxy-ethyl-starch	Fresenius Kabi
Pluronic F108	PEG-PPG-PEG	polyethylenglycol-polypropylenglycol-polyethylenglycol	BASF, Sigma Wyandotte MI USA

The commercially produced colloids are not as homogeneous and their molecular weights not as sharply defined as that of albumin. Low and medium molecular-weight fractions of e.g. gelatin preparations are partly filtered and concentrated by absorption of fluid in the tubules during perfusion, which leads to a significant increase in viscosity in the distal tubule (verified by intratubular pressure measurements, unpublished). This in turn reduces GFR and may become functionally relevant when these substances are used as the sole colloid (257). Absorption of filtered colloids leads to changes (vacuolation) in the proximal tubule (266). Vacuolation occurs to a limited extent also with albumin (BSA), which is progressively filtered by a factor of 10-20 in the isolated kidney compared to the in-vivo conditions (244, 245, 248, 266, 291, 292). Brink (Nijmegen, Netherlands) measured the fractional clearance of Pluronic F108 in relation to the GFR and showed that the sieving coefficient increased to 0.58 at a low GFR, and was still raised considerably, at 0.33, when the GFR was normal at 1 ml/min (43). This corresponds to a significant amount of filtered colloid. Thus, urine viscosity increases by reabsorption of sodium and water, and thereby disturbs the hydrodynamics in the tubular system. One result is the regularly observed fall in GFR (<0.5 ml/min g kidney).

In the pure recirculation mode, the volume necessary to fill the system depends on the type of oxygenator used and the volume of preperfusion solution required until the recirculation is closed. A minimal recirculation volume of 40 to 80 ml is needed (19, 35) when a glass oxygenator is used, for example. Note that arginine - as a source of NO - is very rapidly depleted, causing increased resistance to perfusion. This problem is less pronounced with larger volumes or when higher concentrations of albumin (>7g/dl) are used, and can be avoided by continuous regeneration of the perfusate by dialysis (mode 3). In any case, the preperfusion phase in the recirculation mode has mostly been driven by gravity (162, 163). In mode 3 we used 250-ml volumes of albumin perfusate (BSA 5g/dl) and 5000 ml of dialysate. In the single-pass mode, the initial perfusion reduces the amount of perfusate to approximately 200 ml before the recirculation circuit is closed (e.g. 8 ml/min for 6 min, see Methods). The initial perfusion rate used is 8-10 ml/min in constant-flow mode, after that in constant-pressure mode at closed circuit.

The dialysate is aerated via a glass frit; the dialyzer simultaneously serves as an oxygenator to equilibrate the perfusate (dialung). This method was first described for the perfusion of the isolated rat liver (20); Abraham (2) pointed out that Mayes & Felts independently described this 1966 (169). One should use only low flux dialyzers. High flux dialyzers exhibit a much higher albumin permeability. In dialysis patients, this does not matter, since the use of whole blood ensures that molecules the size of albumin are retained. During our early years in Hannover, we used the capillary-plate dialyzer (Hoeltzenbein) from Travenol, switching later to the cross flow dialyzer Secon 101 produced in Göttingen. In the 6 years up to 2014 we used the low-flux Polysulfon hollow-fiber dialyzer F4 from FMC (Fresenius Medical Care) and then turned to its successor model FX5. The filling volume of the F4 model was 50ml at 0.8m²; the FX5 model offers 54ml at 1m² surface. Dialyzers with less surface and filling volume are welcome, but may be more expensive.

4.1.6. Semisynthetic perfusate with oxygen carriers

In order to avoid oxygen deficiency during the perfusion of isolated kidneys, it is vital to add oxygen carriers. The reason why the kidneys of warm-blooded animals are so sensitive to oxygen deficiency lies in the nature of their vascular architecture, especially in the outer medulla. This is very different from e.g. the Langendorff heart preparation, which functions reasonably well even without colloids or oxygen carriers (66). On the one hand, the shunt diffusion of solutes, but also of blood gases, within the vascular bundles of the outer medulla between ascending and descending vasa recta permits the build-up of osmotic gradients between cortex and medulla. On the other hand, this leads to low oxygen pressure in the renal medulla and to trapping of CO_2, a long known phenomenon. What was less clear is that shunt diffusion of blood gases also plays an important role in the renal cortex - especially between arteria and vena interlobularis, which represents the largest contact area between arteries and veins in the renal vasculature (190, 259-261). This fact no doubt favored the localization of erythropoietin synthesis in the renal cortex in the course of evolution, for reductions in oxygen pressure and capacity can be monitored quite efficiently there (128, 129, 134, 139) - in an organ whose metabolism quantitatively reflects the activity of the whole organism.

To improve the function of isolated kidneys of warm-blooded animals various options have been evaluated, including the use of the following oxygen carriers:

4.1.6.1. **Perfluorocarbon preparations** have a high solubility and capacity for blood gases (82); problems arise in the production of homogeneous particle sizes and emulsification of microspheres.

4.1.6.2. **Stroma-free cross-linked hemoglobin preparations** (16, 144, 148, 310, 311) and Hemarin M101 macro-hemoglobin of a marine invertebrate – Arenicola marina (296b)

4.1.6.3. **Washed bovine or human erythrocytes** (145, 232, 263)

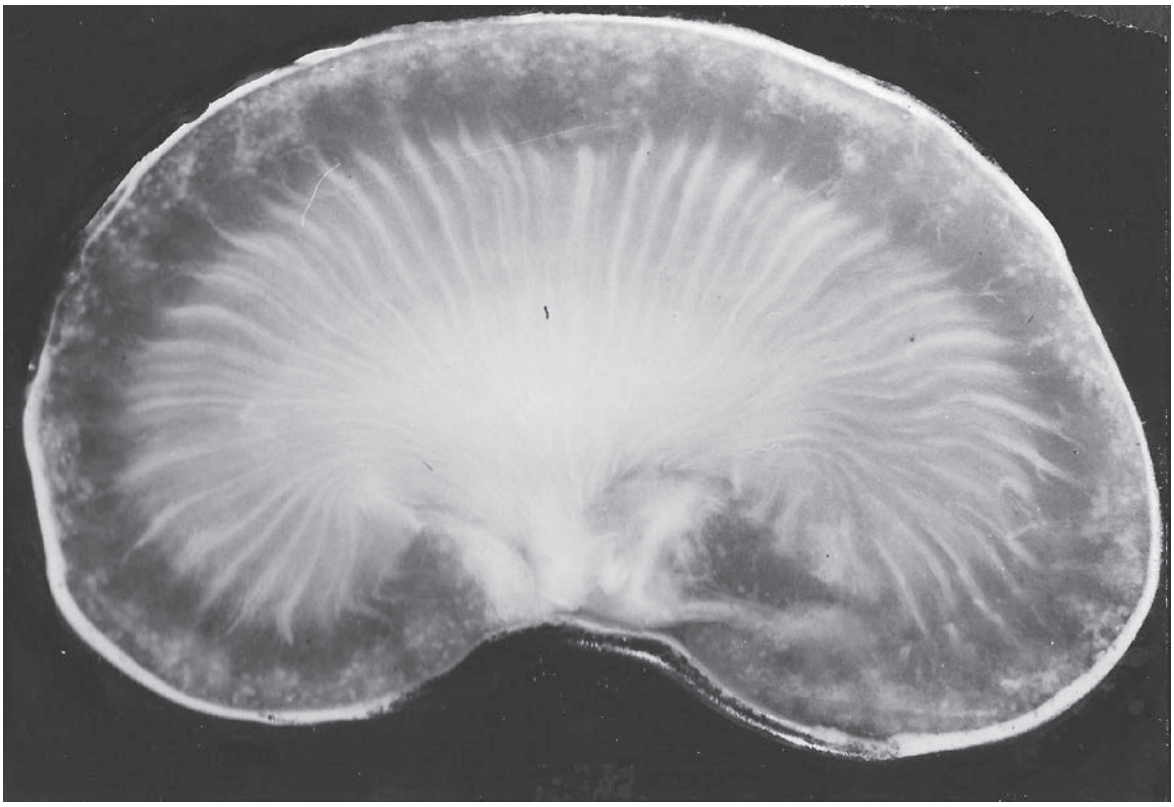

Fig. 4.1.1.: ***Sagittal section of a rat kidney after perfusion with ultrasonically emulsified perfluorocarbon as perfusate.*** Labelling of the vascular tree with an inhomogeneous microsphere preparation (white). This was an early and unsuccessful attempt to exploit the high solubility of oxygen in perfluorocarbons (Berlin 1973). The problem was a rapid increase in resistance with decrease in perfusion flow rate. Franke has published data obtained with a different emulsifying technique (82) that uses high pressures and may yield more homogeneous microspheres, but this procedure has not found general acceptance.

The high hopes placed in emulsified perfluorocarbon microspheres and preparations of hemoglobin have not been realized (16, 82, 144, 147, 148, 283, 310, 311), and washed erythrocytes remain the oxygen carrier of choice. If a mixture of 95% oxygen and 5% CO_2 is used for equilibration, the addition of 5(10) % red blood cells is sufficient to prevent oxygen deficiency at high perfusion rates. This type of semi-synthetic perfusate was introduced by H. Schimassek for perfusion of the isolated rat liver (232). In the isolated perfused rat kidney, the addition of 5-10% washed red cells (bovine or human) suppresses morphological signs of oxygen deficiency that otherwise appear in the area of S_3-segments of the proximal tubule and thick ascending limb (TAL) segments of Henle´s loop (263, 300), but does not provide the degree of functional stability seen in the in-vivo kidney.

The functional stability of the IPRK is crucial. When 5g% albumin (BSA) is used at a colloid osmotic pressure (COP) below 20mmHg and a perfusion pressure of 100mmHg, the GFR is as high as it is in vivo at 1ml/min per g kidney. Nevertheless, the functional stability of the preparation, measured in terms of the fractional Na reabsorption, progressively declines. When the albumin concentration is increased to 7g % - comparable to levels in the postglomerular capillaries of proximal tubules in vivo – the fractional Na-reabsorption is essentially unchanged, but the GFR falls by 50%. Thus the stability of one parameter may actually mask a loss of function (163). This finding also raises the basic question of why the

isolated perfused kidney fails to exhibit the functional stability of the in-vivo organ, even under supposedly optimized conditions. But it must be borne in mind that the in vivo conditions are far more complex and optimized in all respects (thanks to homeostasis, interactions with other organs, the highly complex perfusate cocktail provided by whole blood, “blood as a very peculiar liquid”, Goethe, Faust I, Studierzimmer II). The fact is that the isolated perfused kidney is a simplified model, and one must accept its intrinsic limitations.

Why should erythrocytes be washed?

The use of whole blood (with an anticoagulant such as heparin) for extracorporeal perfusion of the kidney leads to a drastic rise in perfusion resistance (46, 103, 186, 188). At constant pressure, perfusion comes to a virtual standstill due to vasoconstriction. The factor responsible is present in plasma, is released -- as Nizet surmised -- by the erythrocytes, and can be antagonized by α-blockers or the calcium antagonist Verapamil®. The use of Verapamil enabled us to analyze the clearance of uremic middle molecules from the hemofiltrate of uremic dialysis patients. The vasoconstrictive factor is also present in uremic hemofiltrate (233, 234), and is perhaps released when blood comes into contact with artificial surfaces.

Therefore, it is advisable to use a semi-synthetic perfusate made up of washed erythrocytes and an Albumin-Krebs-Henseleit solution. After centrifugation, removal of the buffy-coat and blood plasma and three to five subsequent washes suffice to remove the factor, eliminating the risk of vasoconstriction. As wash solution, we use the final dialysate.

Bovine erythrocytes are considered quite stable, but it is not always easy to obtain fresh preparations. We and others have also used human erythrocytes, which are comparable in size (7-8 µm diameter) to rat erythrocytes (7.4µm, (209)). A volume of 50 to 100ml whole blood drawn by addition of 5000 U of heparin is enough for two experiments when a recirculation volume of 200-250ml is required. Human red cells from expired blood bags have successfully been used for (rat) liver perfusion, but for renal perfusion, the inevitable hemolysis is a complicating factor. It is known (173, 316) that α-tocopherol prevents hemolysis, but we ourselves have no personal experience with tocopherol, and whether it works for expired blood has not been studied. Nevertheless, experiments with expired blood have been carried out in larger animals, such as dogs (186, 188, 240) using α-adrenergic blocking, for example. In 1987, Lieberthal described the use of bovine erythrocytes, which he washed and prepared by a very complex process under sterile conditions. The results, however, showed that the effort was worthwhile, as Lieberthal was able to demonstrate the importance of the erythrocytes in the establishment of concentration gradients between the renal cortex and medulla. The maximum osmotic gradient (U/P_{osmol}) attained in cell-free perfusions in the presence of antidiuretic hormone (AVP, ADH) was 1.2. Addition of the washed red cells to a hematocrit up to 45 % raised the U/P quotient to 3-4, though the maximum quotient of 4 was reached only under the influence of prostaglandin synthesis inhibitors (145, 146). In antidiuresis the rat kidney can reach a quotient of 10 in vivo, which corresponds to an osmolality of urine as high as 3000 mosmol/kg H_2O.

Preparation of bovine erythrocytes (after Wilfred Lieberthal, (145, 146)).

The jugular vein of live cows was the source of bovine blood, which was drawn into the sterile bags used by blood banks, prefilled with sodium citrate and dextrose (Fenwall Labs., Travenol). The erythrocytes were processed within three days, and plasma, leucocytes and thrombocytes were separated off using sterile techniques (centrifugation at 3500g for 10 min). The remaining cells were then passed through a filter (Pall) to remove residual leukocytes and platelets. The red cells were washed in a blood cell processor (IBM, model 2991) with a solution containing 0.9% NaCl, 0.2 % glucose and 40mg of inorganic phosphate adjusted to pH 7.0. Every batch of erythrocytes was washed five times with 200ml of this solution. Finally, cells were resuspended in the same solution filled into sterile bags and stored at 4°C for maximum of 2 weeks. Tests revealed that leukocyte count had been reduced by 97.8% and platelets by 97.6%. Immediately prior to use in experiments, an adequate volume of erythrocytes was removed (under sterile conditions), washed 3 times (removing the supernatant (buffy coat) each time), and then brought to a hematocrit of 45% with the albumin solution.

Critical comment: While I have great admiration for the persistence and rigor shown by Wilfred Lieberthal in his approach to the preparation of bovine erythrocytes, I would argue that he should have used a Krebs-Henseleit bicarbonate solution for the final wash of all. During pretreatment with NaCl, the red cells lose bicarbonate and accumulate chloride (235). Subsequent mixing with the Albumin-Krebs-Henseleit (AKH) solution causes them to exchange their excess chloride for bicarbonate from the AKH solution, which in turn implies that the latter now contains correspondingly less $NaHCO_3$. Our mode 3 recirculation with dialysis against a large volume avoids this problem. Otherwise, the time-consuming procedures used by Lieberthal are worthwhile, but they require appropriate resources and facilities offered by a blood bank with a blood cell processor for animal raw material.

Extra note

Dr. Jan Czogalla of Zurich has meanwhile located a source of fresh and defibrinated sheep blood in England. For details, see more at the end of the contribution of Frank Schweda, Chapter 14.

4.2. Perfusion drive systems, measurement of flow and pressure

4.2.1. Hydrostatic pressure

The simplest drive system utilizes the difference in height between the perfusion reservoir and the kidney. Gas pressure also provides a driving force in the case of single-pass perfusion, where the gas mixture is discharged through a water column or a regulated valve.

In the recirculation system, a roller pump is used to raise the pressure of the perfusate to the desired level. Fig 4.2.1 shows a system used by Brian D. Ross in the laboratory of Sir Hans-Adolf Krebs in which the oxygenator is accommodated in a tower placed on top of the temperature-controlled cabinet (185). Here, flow rate is measured either by the injection of gas bubbles and observation of their passage through a calibrated glass tube (see Fig. 4.3.3.) or monitored with a rotameter (where the motions of a float of known density within a tapered tube reflect the flow rate).

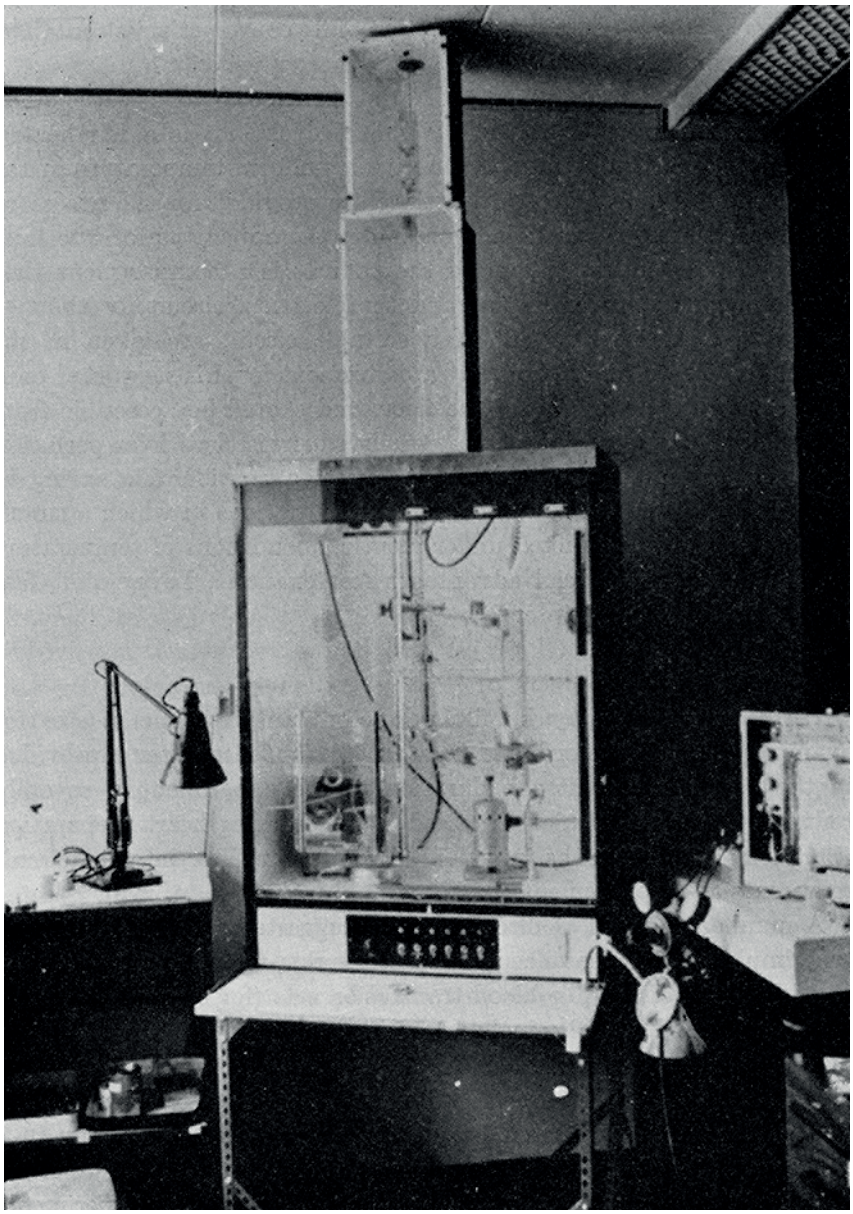

Fig 4.2.1: ***Perfusion cabinet for the IPRK.*** The photograph is taken from the laboratory manual by Brian Ross (224). The cabinet is extended in height especially for kidney perfusion. For the isolated rat liver, which is usually perfused via the vena portae at a significantly lower pressure, the tower is dispensable. (reproduced with the author´s permission).

4.2.2. Gas pressure

The gas pressures required in the single-pass mode can be achieved with much less effort. The gas mixture (95% O_2, 5% CO_2) for oxygenation is injected at positive pressure via a glass frit into a closed glass container (e.g. a Woulff bottle) and discharged via a water column into a 2-m tall glass riser, allowing (within limits) a constant perfusion pressure to be maintained. In this arrangement, the perfusion pressure measured at the entrance to the perfusion cannula depends somewhat on the resistance of the perfusion cannula. One can use either a premixed gas ("Carbogen": 95% O_2 and 5% CO_2) supplied by a pressurized cylinder via a pressure reducer, or a gas mixing pump (fig. 4.1.3.). The gas used should be filtered and humidified.

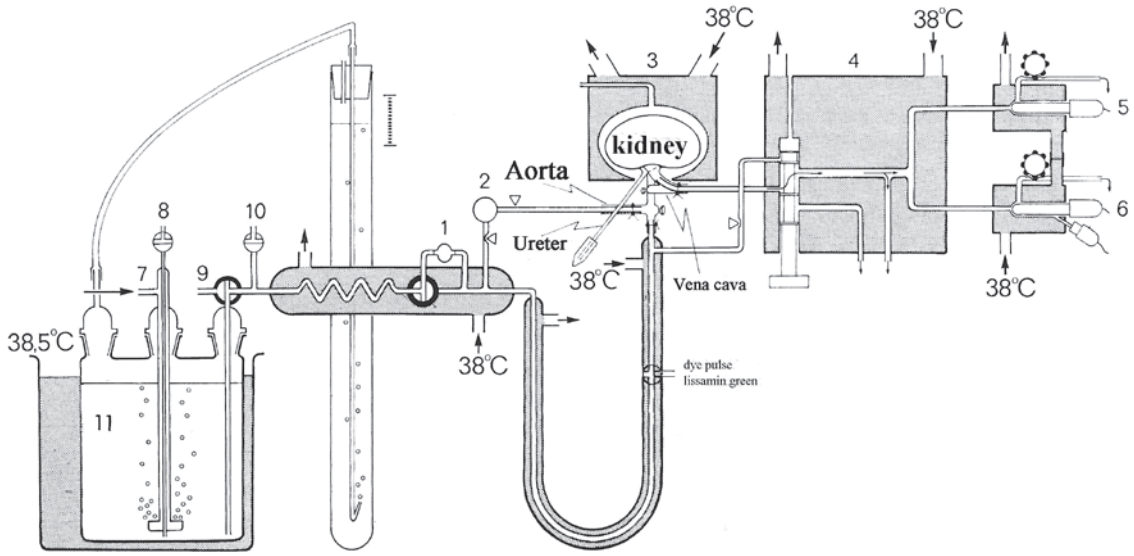

Fig. 4.2.2.: ***Schematic diagram of a perfusion apparatus rigged for the "single pass mode"*** (256, 257)**.** All components that are kept at a constant temperature are *hatched*. 1. Electromagnetic flow sensor; nowadays ultrasound-based sensors are available (see Chapt. 9.2.). 2. Pressure transducer. 3. Kidney in tray. 4. Switching block. 5. O_2-electrode. 6. CO_2-electrode. 7. Gas inlet (warmed and humidified). 8. Sampling port. 9. Connection to an alternative perfusate. 10. Air trap, 11. Reservoir (Woulff bottle). In this case, the perfusion cannula is fixed in the mesenteric artery and the pressure-measuring cannula is in the distal aorta. In those days, the flow rate was measured with an electromagnetic flow sensor (via the voltage induced by the ion current in the AC field). The gas outlet through a water column builds up the perfusion pressure.

Pressure measurement: In the early days we used pressure transducers (strain gauges) from Statham Instruments Inc. (now Gulton-Statham, Rochester, USA), which were very expensive. Now we make use of the "single-use pressure transducers" employed in ICUs (intensive care units) with integrated preamplifier and calibration button. These are relatively cheap and robust, and re-use is common under laboratory conditions.

4.2.3. Flow measurement, peristaltic pumps. Flow constant or pressure constant perfusion

The use of a peristaltic pump provides more options for all perfusion variants (single-pass perfusion, recirculation and recirculation combined with dialysis). The simplest method, constant-flow perfusion, allows one to investigate the effect of vasoactive substances by recording the perfusion pressure. In this case, all other aspects of the physiological function of the organ are of secondary interest. Constant-pressure perfusion is technically complex, but more appropriate for the kidney. Ideally, the perfusion pressure is measured directly before the kidney. This can be done either as shown in Fig. 4.2.2., with the perfusion cannula placed in the mesenteric artery while the perfusion pressure is measured in the distal aorta (257), or by using a double-barreled cannula inserted into the distal aorta until just before the renal artery junction, in which case the pressure signal comes via the inner cannula of the double-barreled cannula (Fig. 4.2.2, 4.2.3 and 4.6.3-4.6.6 (251, 253, 254)). The pressure signal can either be passively recorded, or it may additionally be used to electronically control the pump for constant-pressure perfusion (161, 251). Pressure pulsations created by the peristaltic pump may be preferred (186) or can be compensated for by a buffering chamber (*Windkessel*) and/or electronically attenuated (RC attenuators). In older publications one sometimes comes across 2-valve pumps (see Jacobj (115) or Leon L. Miller (174)) which produce systemic pressure pulses, but also cause less hemolysis when blood or washed erythrocytes are used. Whether pulsatile perfusion is beneficial or not is still a matter of debate.

If the pump generates an analog signal that reflects its rotation speed (tachogenerator feedback), the rate of pump revolution can be recorded as the perfusion rate by means of a chart recorder as well as the pressure signal (repeater). The first apparatus of this type we used was developed by Joachim Lutz (159, 161) and manufactured by Apparatebau E. Jandke in Würzburg, Germany. In principle, analog-to-digital conversion can be used and data can be recorded by PC. However, we prefer analog recording on a multi-channel recorder (Rikadenki, Tokyo, Japan; Linseis, Selb, Germany). Recording of flow rates via the analog signal from the pump requires that no leakage occurs between perfusion cannula and renal artery. This can be evaluated at the point of venous outflow (gauging by ml) or from any difference between the calculated and the measured level of oxygen consumption. The device currently used to control the peristaltic pump is shown in Figs. 5.1.05 and 5.1.06. My coworker Jörg-Dieter Biela developed the apparatus in his own workshop. Fig. 4.2.3 shows the modification of the apparatus, with peristaltic pump and feedback control via the output signal from the pressure transducer for constant-pressure operation. In this mode, it is easy to demonstrate the autoregulation of renal perfusion by pressure changes of 20mmHg via a step switch. In addition, constant-flow operation is possible with analog recording of flow and pressure. For measurement of arterial pO_2, the bypass is opened by pushing the slide in the valve block (top right), while the extra flow is restricted by a preconstriction. Thanks to feedback control, the extra flow is detected and the pressure remains constant. In constant-pressure mode, protection against overshooting is no trivial matter. Electronics and hydraulics need to be well matched. In particular one should avoid small air bubbles in the hard-hose lead to the pressure transducer. The in-line filter must be well vented. In addition, the volume of the buffering chamber (Windkessel) can be critical. If it is removed from the circuit (clamped off), one can generate pulse amplitudes of

20mmHg or more. The best option would be to combine a two valve artificial ventricle (see Miller Fig. 4.3.1) with flow measurement by ultrasound.

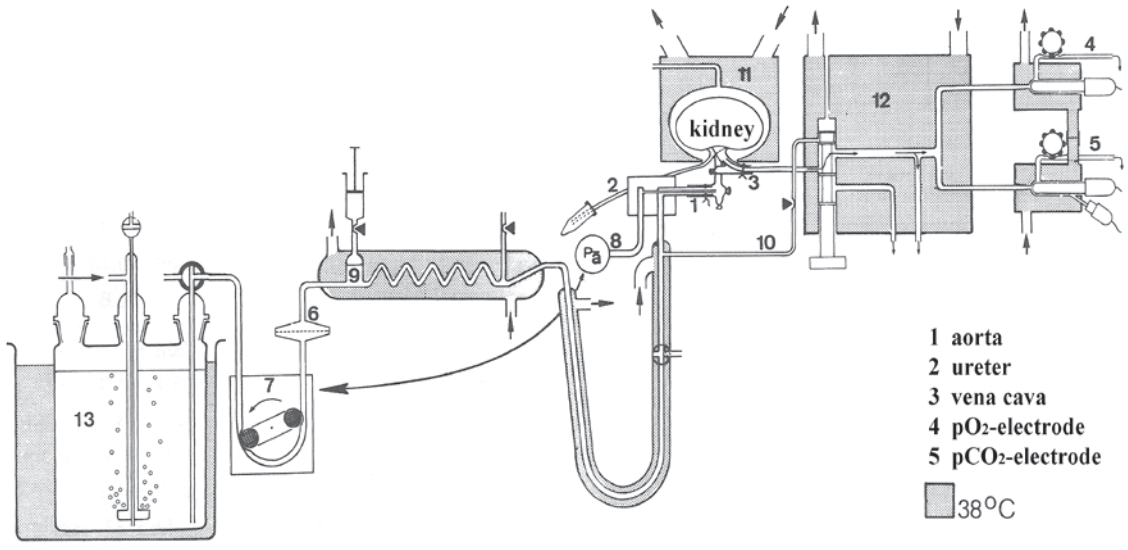

Fig. 4.2.3.: ***Schematic diagram of the perfusion apparatus with a peristaltic pump*** (246, 254)**.** 1. Double-barreled cannula inserted in the aorta. 2. Ureteral catheter. 3. Vena cava. 4./5. pO_2 and pCO_2-electrode. 6. Inline filter (8µm). 7. Servo-controlled peristaltic pump, feedback regulated by the pressure signal from 8. 8. Pressure transducer, connected to the inner barrel of the double-barreled cannula. 9. Pressure buffer. 10. Bypass for arterial gas measurement, 11. Kidney tray. 12. Valve block. 13. Reservoir (2 or 5 liters). The flow rate was recorded continuously based on the tachogenerator feedback from the peristaltic pump (preamplifier) (Rikadenki, Tokyo, Japan; Linseis, Selb, Germany).

4.2.4. Other techniques of flow measurement

In addition to the rotameter with its visual readout, flow rates can be measured electromagnetically and by means of ultrasound. In fact, the Transonic T106 flowmeter with cannulating flow probe SN22 (Transonic, Ithaca, NY, USA) allows one to use the ultrasonic transit-time method on cell-free media. Thus, one can also register the flow continuously, as with the technique in which the feedback signal is derived from the tachogenerator of the perfusion pump; however, in this case application to constant-pressure perfusion requires a preamplifier.

4.3. Temperature control

4.3.1. Temperature controlled cabinet with a perspex sliding front door

This type of temperature control became standard for biochemical and pharmacological studies of the isolated perfused rat liver (174, 232). As the rat liver is normally perfused via vena portae only for simplification, a low perfusion pressure suffices. The system used for rat liver perfusion designed by Miller and his first publication on the synthesis of plasma proteins by the liver was a milestone (174). The renal perfusion system used by the Oxford research group led by Brian D. Ross was adapted to provide the higher perfusion pressure by constructing a tower on top of the cabinet to enable the glass oxygenator to be placed in an elevated position, and was used for metabolic studies (185).

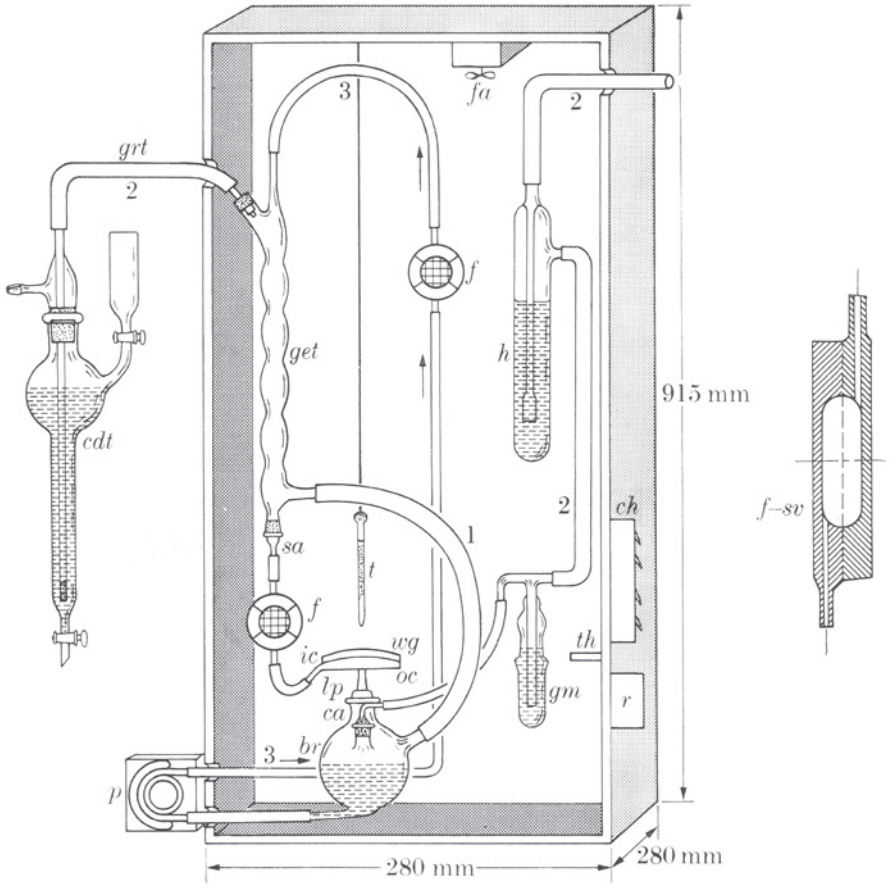

Fig. 4.3.1.: ***Perfusion Apparatus manufactured by Metalloglass Inc. based on Miller´s design for the rat liver*** **(174). Air circulation within the cabinet is driven by a fan (fa), while** a thermostat (th) and electric heating coils (ch) attached to the housing control the temperature. Note the two built-in filters (*f*) in the circuit (shown in detail in side view on the right). The filter membrane used was made of white silk (100-150 mesh/inch). The other labeled components are: 1. Overflow with gas inlet to the glass oxygenator (get), 2. Gas inlet, humidifier (h), gas pressure measurement (gm), 3. Output of perfusate from the pump (p) via the filter (f) to the oxygenator (get), straight adapter (sa), second filter (f), inflow cannula (ic), watch glass (wg), outflow cannula (oc), liver platform (lp), thermostat (th), relay (r), gas return tube (grt), carbon dioxide trap (cdt). In the original, as shown in the next figure, a two-valve pump was used instead of a peristaltic pump.

The major disadvantage of the cabinet with a sliding door is the fact that the door must be opened every time an intervention is necessary. The pump used in Miller's original paper (174) was a two-valved, so-called Bluemle pump - a type which Jacobj had already employed in his apparatus in the year 1890 (115), though his was driven by a water-powered motor (Figs. 16.0.2, 16.0.3). Later on, this sort of pump was used to minimize levels of hemolysis when necessary (76).

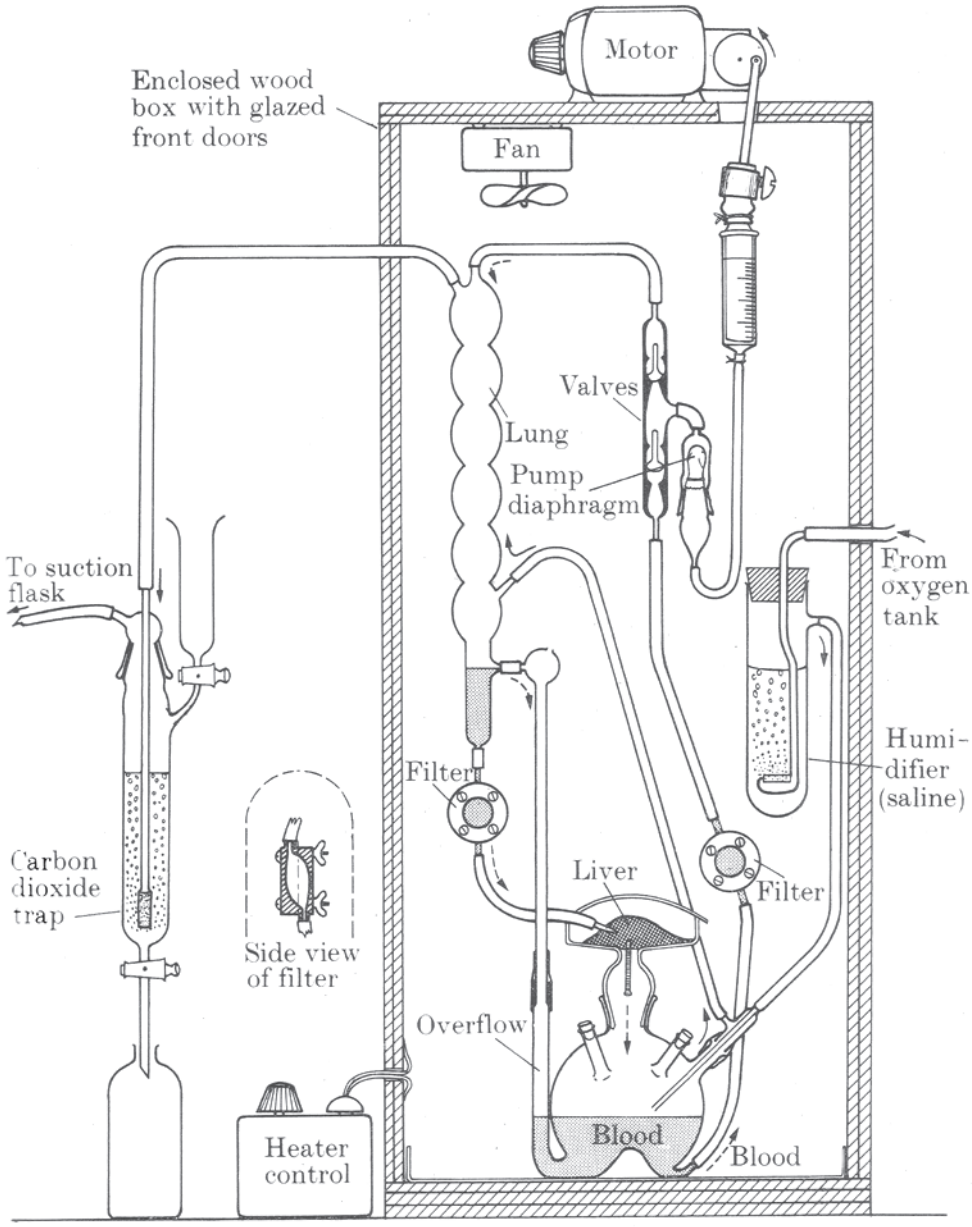

Fig. 4.3.2.: ***Schematic representation of the original perfusion apparatus developed by Miller*** (174). Two-valve pump with eccentric rotor, connecting rod and a modified syringe (for volume displacement), which was connected to the valve chamber by a diaphragm. In this version, blood is drawn from the reservoir via a filter; the filter was no doubt later switched from the pre- to the post-pump position, as implemented in the modified version marketed by Metalloglass. When blood or purified erythrocytes are added to the perfusate, a two-valved pump causes a lower rate of hemolysis than a peristaltic pump.

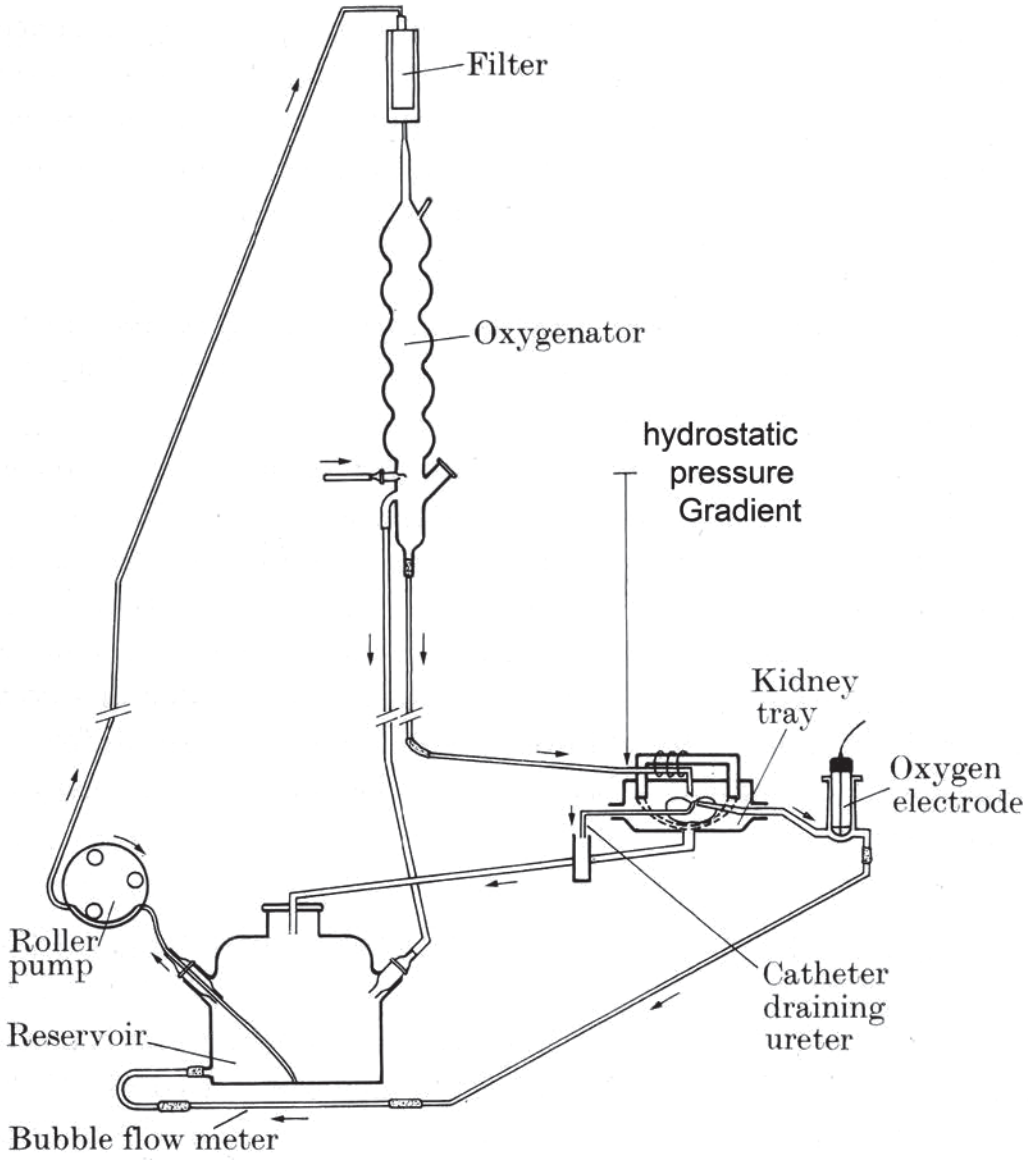

Fig. 4.3.3.: ***Schematic diagram of the perfusion circuit used by the Oxford Group*** (185, 224). The cabinet is omitted. The glass oxygenator was positioned high above the kidney to achieve a hydrostatic pressure of 120cm H_2O (see Fig. 4.2.1.). The organ was placed on a suspended nylon mesh and hung on the glass cannula (see Fig. 4.6.2.). The venous outflow was directed to an oxygen electrode and a 2-ml graduated pipette was used as a bubble flowmeter. The pump flow rate in the oxygenator circuit was set to a higher value than that in the perfusion circuit to improve the oxygenation of the perfusate. Modified from Brian D. Ross (224), reproduced with the author´s permission.

For details of the glass cannula used for perfusion of the kidney, see Figs. 4.6.1 and 4.6.2; for the complete apparatus including the cabinet, see Fig. 4.2.1. A temperature-controlled fan is also integrated, as shown in the previous diagrams of the Miller apparatus.

4.3.2. Temperature control by water jacketing

Physiological experiments designed to analyze the clearance of molecules and involving micropuncture of tubuli require easy access to the kidney. Therefore, water-jacketing is now used for temperature control in parts of the circuit, such as the reservoir, oxygenator, glass tubes and double-barreled hoses. This principle is used for all four modes of perfusion from single-pass to recirculation techniques. For single-pass perfusion, we immersed the reservoir in a circulating water bath equipped with a thermostat for temperature control. An aliquot of the warm water was used to preheat the equilibrating gas mixture. Smaller thermostats are used to monitor the rest of the route to the kidney preparation, i.e. the glass tubes and hoses leading to the kidney and those in the recirculation systems, the jacketed oxygenator and/or the reservoir, which is also water-jacketed. The kidney itself is placed in a tray made of stainless steel with temperature control by circulating water. Based on our experience, polypropylene couplings of the type used in compressed-air technology from Colder Products Company (St. Paul, MN. USA) connecting tubes and circulators have proved themselves in these roles. The couplings are available with and without a check valve, which opens after connection. With a connected counterpart, one can rinse and remove them easily. The use of water-bath disinfectants is recommended.

4.4. Aeration

4.4.1. Aeration via a glass frit

The simplest way to aerate the perfusate is via sintered glass frits in the single pass perfusion mode. In order to prevent evaporation losses, the gas mixture should be humidified. We pass the dry gas mixture through an air filter (e.g. 0,2µm, Midisart 2000, Sartorius Stedim, Göttingen, Germany) in a closed bottle of sterile water with a glass frit, the moistened gas is then dried slightly over a jacketed glass coil to prevent moisture from entering the perfusate. From the perfusate reservoir, the gas flows either directly (if a perfusion pump is used) or via a pressurizing water column to set up the perfusion pressure (see Fig. 4.2.2.). One can also use the latter method to enhance the oxygen pressure in the perfusate. We use a gas-mixing pump, initially fed with 100% O_2 to decrease the pCO_2 to 40mmHg and then with 95% O_2 and 5% CO_2, also 94/6% in case of need. Small droplets of mineral oil that might be emitted by the pump are trapped by a transfusion filter, preventing contamination of the dialysate or perfusate. To avoid foaming, perfusate with albumin as the colloid must be aerated indirectly, via an oxygenator or dialyzer. Foaming may cause denaturation of albumin. In Hannover up until about 1990, we scanned the level of the venous effluent capacitatively and returned it via a tube valve, almost free of foam, to the lower reservoir. To simplify the procedure we later returned it via a wide-lumen silicon tube, which may represent a backward step. We plan an analysis of this problem.

4.4.2. Glass oxygenators in recirculation technique

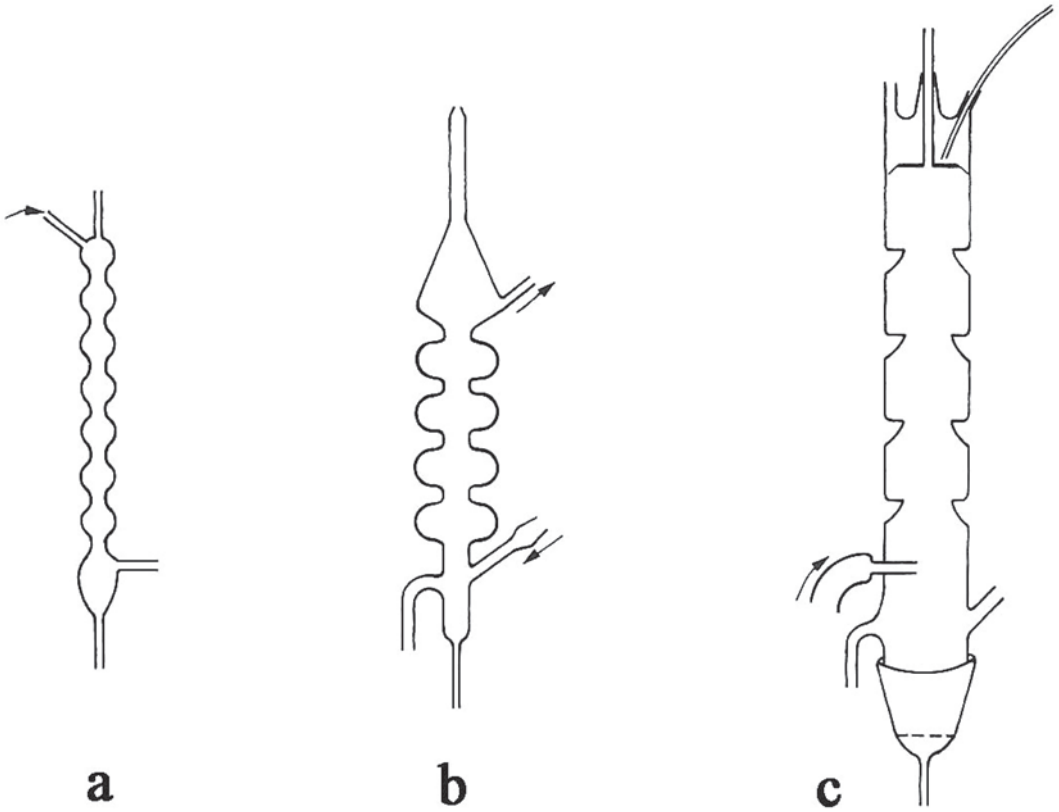

Fig. 4.4.01.: ***Types of multibulb glass oxygenators after B.D. Ross*** (224). Leon L. Miller used Type a (174) see also Fig. 4.3.2. Hems in Oxford designed Type b with precisely calibrated dimensions (shown in Fig. 4.4.02). Type c uses a rotating disc to stir the medium; Nizet used a modified version of this type for the perfusion of isolated dog kidneys (186). With a little more effort, the glass oxygenator can be water-jacketed for temperature control; this principle was first described by Staib in 1968 (286). Bowman and Maack also used water-jacketing in their oxygenator (34, 35) and incorporated the reservoir for the perfusate at the bottom (see Fig. 5.2.1.). Reproduced with the author's permission.

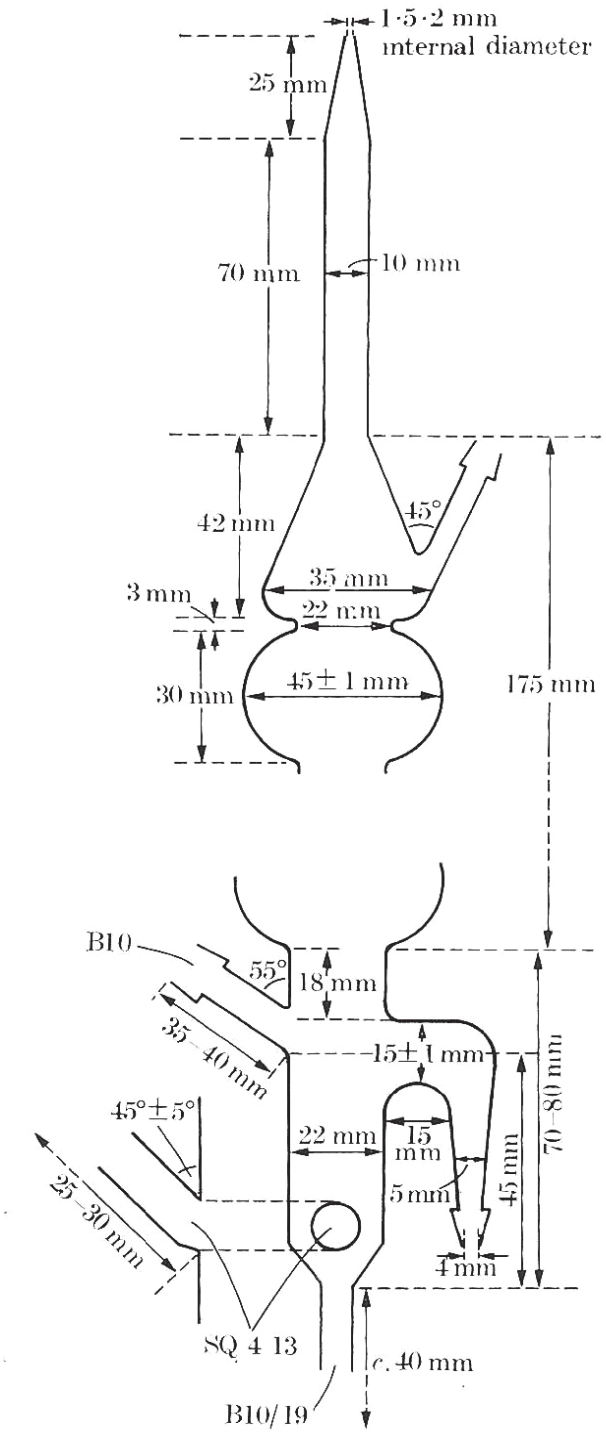

Fig. 4.4.02.: ***Details of the construction of the Hems oxygenator.*** One special feature is the upper part of the inflow section, which is designed as a conical entry bulb so that the thickness of the liquid film is reduced in two steps, thereby wetting the entire circumference. The device has 4 to 5 bulbs (105, 224). The measurements shown are external dimensions; the wall thickness is 2mm. The original glass tube was a heavyweight borosilicate glass of 22mm outer diameter. The lower part is designed to prevent frothing. The level of the overflow and gas inlet is critical in this respect. Reproduced with the author's permission (224).

The water jacketing of a glass oxygenator was first described by Staib (286), according to B.D. Ross (224).

The following Figures show a glass oxygenator of our own design from the workshop in Hannover, with water-jacketing. This type would benefit from a conical entry bulb like that specified by Hems. Inlet and outlet for gases were each located in the middle of a bulb and directed downwards to prevent frothing.

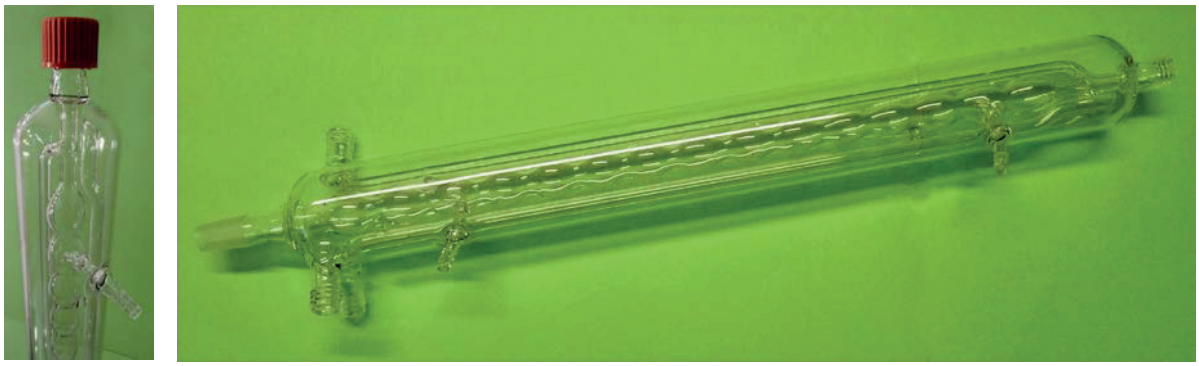

Fig. 4.4.03.: ***Jacketed glass oxygenator.*** The two screw connections on the left are in- and outlet for 38°C water, the two gas connections are on the front of the tube as shown, (on the left the inlet, on the right the outlet). On top and to the left side is the screw connection to the perfusion inflow; on the top right is the vent and the bulbous structure that facilitates wetting.

Fig. 4.4.04.: ***Glass oxygenator with associated reservoir.*** Both are jacketed for temperature control by means of a circulatory thermostat. On the left is an interrupted overflow outlet to which a valve can be attached to regulate the input of compressed air, on the right there is shown an uninterrupted overflow from the oxygenator to the reservoir (design by Schurek, unpublished).

Fig. 4.4.05.: ***Reservoir attached to the oxygenator.*** The reservoir has two water bath connections sealed with screw caps. On the left is the connection to the base of the inner vessel, on the right, the connection to the venous effluent from the kidney, which should ideally be located higher up (see Fig. 5.3.2 for an improved version).

4.4.3. Membrane oxygenators used in the recirculation technique

Various types of membrane oxygenators have been described in the literature. At first, membrane oxygenators were not commercially available, so different laboratories developed several simple prototypes, such as tubing oxygenators, flat membrane oxygenators and capillary oxygenators. Four variants are shown here, the latter two of which (Figs. 4.4.07, 4.4.08) we have used extensively.

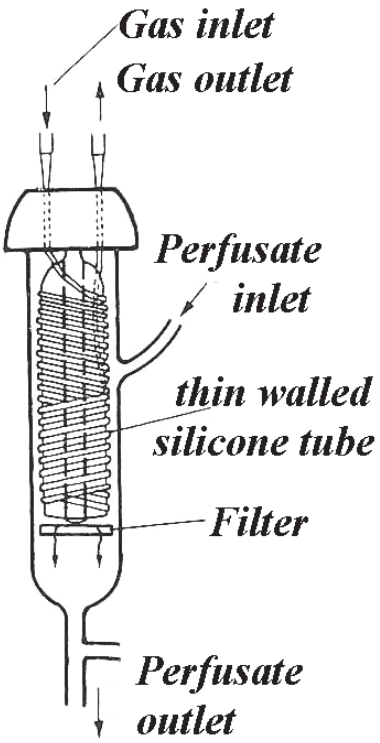

Fig. 4.4.06.: ***The silicone tube oxygenator after Folkman*** (79). The gas enters the tube which is wound around a glass rod, and is in direct contact with the perfusate, which is introduced via the side inlet. A glass frit at the bottom serves as a filter. The thin-walled silicone tube is not particularly robust and exhibits a pressure-dependent change in volume, and diffusion capacity is limited to small flow rates. Modified after Folkman.

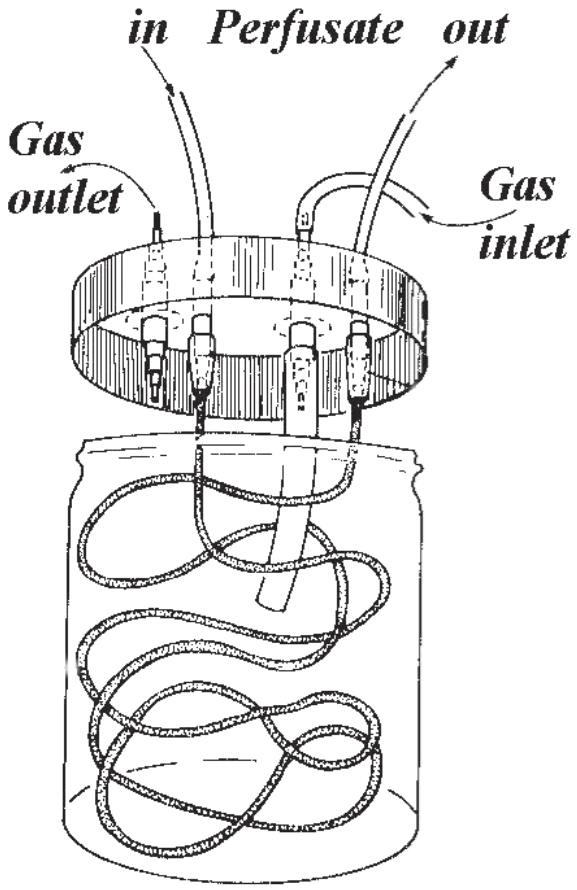

Fig. 4.4.07.: ***The silicone tube oxygenator after Hamilton*** (96). The perfusate passes through a 5-meter silicone tube with the following specifications: inner diameter 1.47mm, wall thickness 0.25mm. The tube (which is used only once) is inserted, loosely coiled, into a sample vessel (e.g. a mustard jar!) with a volume of about 500ml, and attached to appropriate connectors inserted in holes cut in the lid. Note that the gas inlet and outlet are far apart. The wall thickness used is a compromise, and was chosen to reduce the risk of buckling. In tests of effectiveness, a 12g rat liver was perfused with washed rat erythrocytes at flow rates of 10ml/min. Adequate oxygenation could be achieved at a hematocrit of 22% and a (gas) flow rate of 1.5 liters/min. A filling volume of 8-10ml for the silicone tubing is optimal. The oxygenator is equipped with only a single outlet directly to the liver, which is sufficient in one passage to provide oxygen and the pressure required for perfusion via the portal vein.

The Hamilton oxygenator is suitable for the perfusion of a mouse kidney, provided a separate oxygenator circuit is set up to achieve the higher perfusion pressure necessary. For the perfusion of a rat kidney, even higher perfusion flow rates are necessary (15-45ml/min) and higher levels of oxygen uptake in the oxygenator circuit are required relative to the amount of perfusate supplied to the kidney. In addition, the dimensions of

the tube may need alteration. The main advantages of the Hamilton design are its simple construction, ease of use (no cleaning!) and low cost compared to the exorbitant prices charged for commercially available systems. A year earlier, Felts and Wayne had described a tube oxygenator (74) which was equipped with three parallel silicone tubes with thicker walls, which can withstand the arterial pressures encountered in the perfusion system of Mayes and Felts. These authors perfused the hepatic artery and portal vein separately (169).

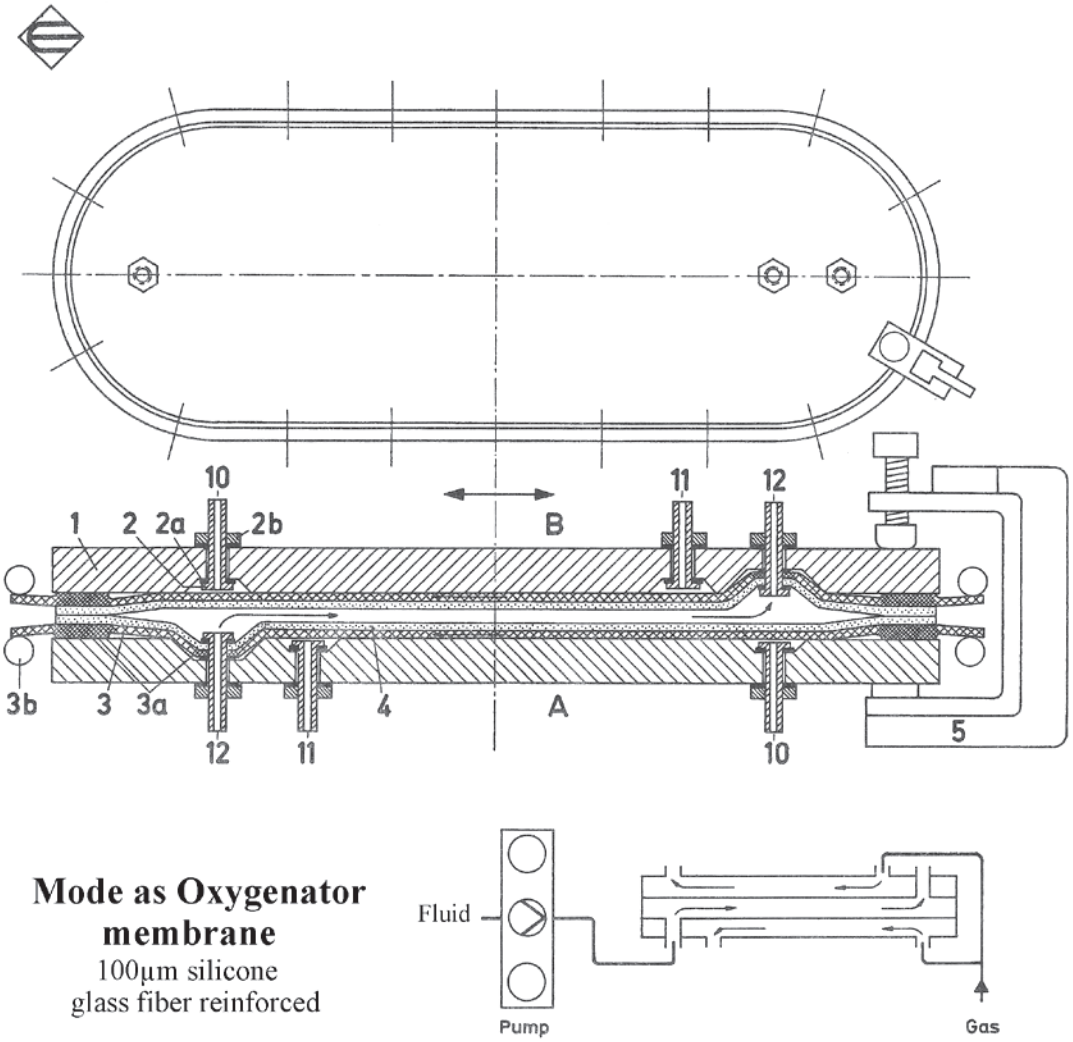

Fig. 4.4.08.: ***Membrane oxygenator after Röskenbleck & Niesel*** (221). This system, originally used as a thin-film dialyzer, was later also used as oxygenator, having been equipped for this purpose with a fiber glass-reinforced silicone membrane (Detakta, Hamburg, Germany), which was originally intended for use as an electrical insulator. In all, 18 clamps are used to hold the outer glass slabs in place. Problems with the flow at the inlet and outlet (discharge block) led to search for an alternative solution (see Fig. 4.4.09). Eschweiler (Kiel, Germany) also supplied this type of membrane oxygenator, originally for use as a thin-film dialyzer.

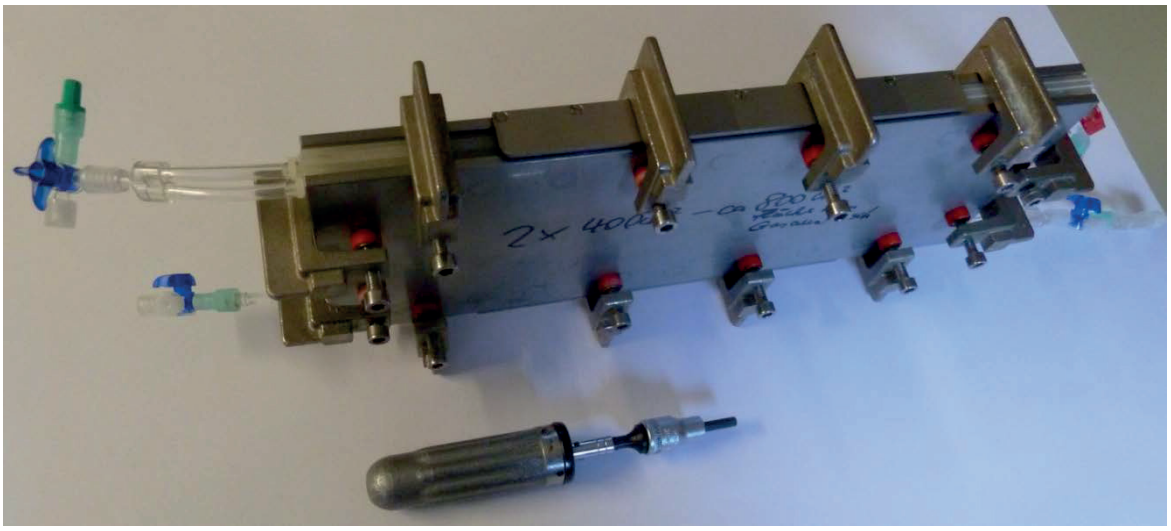

Fig. 4.4.09.: ***Membrane oxygenator after Röskenbleck, modified after Schurek*** (unpublished). The grooved inner plates are from a RP6 dialyzer, formerly manufactured by Rhone-Poulenc (Hospal); the inner frame is covered by two layers of fiber glass-reinforced silicone membrane (Detakta, Hamburg, Germany) which form the interior compartment for the perfusate. A set of 18 clamps ensures that the outer stainless steel plates are tightly appressed to the grooved inner plates (torque wrench in the foreground). The gas flows between silicone membrane and grooved plate on both sides in countercurrent to the perfusate. The effective area for gas exchange is 2x400cm²; the filling volume with tube connections is 10-20ml, and can be reduced by using thinner sealing material and by counter-pressure (gas side).

4.4.4. Capillary oxygenator

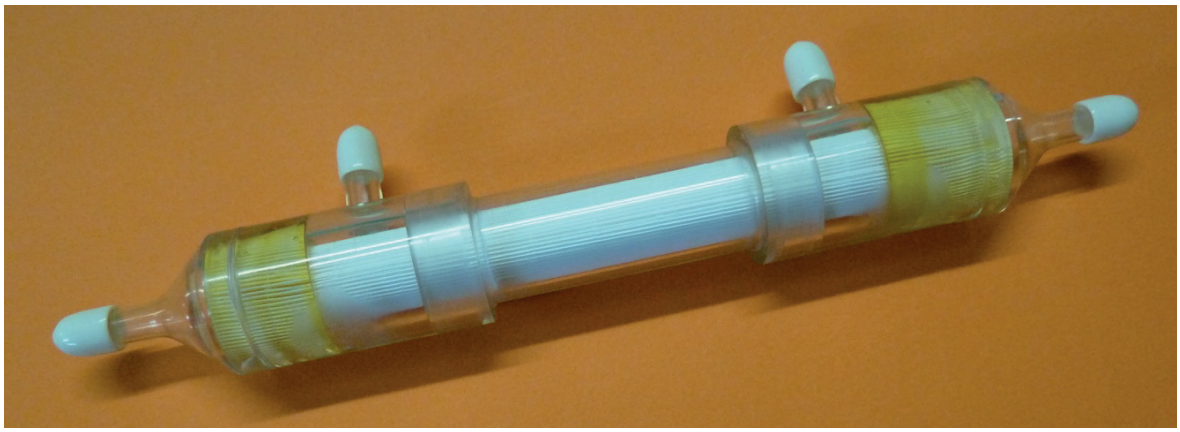

Fig. 4.4.10.: ***Capillary oxygenator.*** As an alternative to the relatively large membrane oxygenator, Dr. Rintelen from the Enka company (now Membrana, 3M, Wuppertal, Germany) supplied us some time ago with an oxygenator made of test modules consisting of a bundle of polypropylen capillaries embedded in polyurethan with end caps for the perfusate and lateral connectors for gas inlet and gas outlet.

After its first use, a cleaning procedure involving the use of formalin resulted in damage (bubble-like protuberances) to some of the capillaries. We subsequently cleaned the unit by rinsing with NaCl solution and demineralized water and then drying it. Since this

oxygenator is permeable to water vapor, dry gases should not be used. Each module contained 570 hollow fibers (lumen 280 µm, wall thickness 50 µm, 10 cm effective length) with a total surface area of 500 cm², and had an optimal filling volume of 6.2 ml including connecting caps. The efficiency approached that of the membrane oxygenator (Fig. 4.4.09).

4.4.5. The dialyzer as a "kidney lung"

The first dialyzer we used as a combined oxygenator/dialyzer was the capillary plate dialyzer, which was designed by Dr. Josef Hoeltzenbein in Münster (Germany), and manufactured and sold by Travenol (251). This type of dialyzer was ideal due to its small filling volume of approx. 65ml, the restricted ultrafiltration rate and a surface area of 0.92m² (Type M1000). The perfusate is in contact with the capillary exchange surface over a distance of only 6 cm, but this is enough for adequate oxygenation because of the better blood-film geometry (see Fig. 4.4.11 for a comparison between hollow fibers and capillary film). The dialysate distributes in diagonal countercurrent to the perfusate. We later switched to the Polysulfon low-flux capillary fiber dialyzer F4HPS from FMC (Fresenius Medical Care, Bad Homburg, Germany) because no plate dialyzer of comparable size (filling volume 51ml, surface area 0,8m²) is now on the market. Indeed the F4HPS itself has meanwhile been superseded by the type FX5 (54ml, 1m²). So-called high-flux dialyzers are not recommended because of their higher permeability; on the one hand, they have a higher ultrafiltration rate and, on the other, a higher permeability for albumin. The latter soon disappears under laboratory conditions if whole blood is used, i.e. the dialyzer attains its final, stable permeability only after being exposed to whole blood (219), probably because the larger pores are sealed by material present in whole blood. This phenomenon is also observed in the glomerular capillaries of the kidney (244, 245, 248-250, 266). This example underlines the fact that not every type of dialyzer is suitable and that the permeability for albumin should be low. The Polysulfon dialyzer F4HPS was used repeatedly, thoroughly rinsed after use and stored with a filling of 3% formalin solution. Before reuse, the unit was intensively rinsed and dried in a stream of filtered compressed air. In addition, the dialyzer type FX5 prevents loss of albumin and incorporates a modified Polysulfon membrane (Helixone®).

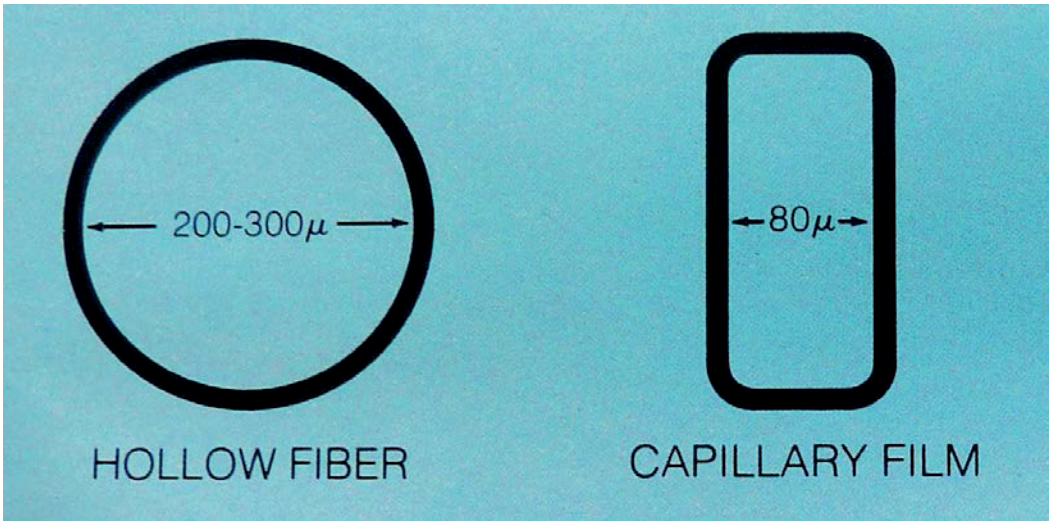

Fig. 4.4.11.: ***Comparison of the geometry of a hollow capillary fiber with that of the capillary film of a Hoeltzenbein dialyzer.*** Note that diffusion distances are shorter in the latter.

Fig. 4.4.12.: *Hoeltzenbein-dialyzer (HD™ Capillary Film Dialyzer)*. Historical model M1000, once produced in Belgium by Travenol Laboratories Inc. The inlet for blood/ perfusate is on the front, the outlet on the rear face. Dialysate enters and exits via the Hansen couplings on the bottom and top, respectively. The surface area of the dialyzer membrane was 0.92 m^2, the filling volume 65ml and the ultrafiltration coefficient was low. Dialysate flow was driven by a centrifugal pump at low pressure (Type 1022 Eheim GmbH, Delzisau, Germany), see Chapter 5.3.

The use of capillary dialyzers as oxygenator, - gas instead of dialysis fluid

Smyth described a single-pass system that used a capillary dialyzer as an oxygenator (279, 280), with a gas mixture of 95% O_2 and 5% CO_2 flowing through the dialysis compartment external to the capillaries (2 liters/min). He used a dialyzer from Dow Cordis (C-DAK 135sce). The letters SCE stand for saponified cellulose ester fibers, which are not as hydrophobic as modern synthetic fibers like Polysulfon. Hence, the more modern synthetic fibers available today may be more appropriate for this purpose. Dialyzers that are clinically used in pediatric wards offer less filling volume and surface area, but I prefer low-flux dialyzers. To prevent ultrafiltration of water from the perfusate, gas should emerge from the dialyzer against a higher than atmospheric pressure, e.g. into a water column of a defined height.

Up to now we have used dialyzers as oxygenators only in our mode 3, where the perfusate was equilibrated and reconditioned by the dialysate. Systematic studies of the use of dialyzers as oxygenator with gas flow instead of dialysate are pending.

4.5. Filtering

4.5.1. Filtration of the perfusate

The aim here is the sterile filtration of the final perfusion solution immediately before addition to the perfusion apparatus. Fig. 4.5.1 demonstrates our set-up.

Fig. 4.5.1.: ***Filtration-assembly 1.*** On the right is the 10 liter stainless-steel container. Filtration is driven by compressed (2 bar) and filtered air, which is passed through the sterilizing filter, and goes from there via a silicone tube directly into the glass reservoir (dialysate). Immediately in front of it is the 2 liter filter attachment (filling port above), which is routinely used for filtration of albumin solution in step 2. But since the large 10-liter container cannot be emptied completely, the 2-l vessel filter attachment can also be used to sterilize the ≈ 200ml that remains, leaving only minimal amounts of residue in the filter (Sartorius, Göttingen, Germany).

Fig. 4.5.2.: ***Filtration-assembly 2.*** The filtration attachment, mounted for filtration of 5 or 10liters of dialysate (Step1). In the second step, 200-ml volume remaining is optionally filled into the filter attachment via a funnel on top and filtered also. In the third step, compressed air is connected directly to the side connector of the 2-liter filter attachment, and the perfusate (albumin solution or other colloids) is filled in and filtered into a sterile glass bottle.

After albumin filtration, the outlet and tap must be cleaned very thoroughly, as surface residues of dried albumin can cause problems (position behind the filter).

4.5.2. In-line filtration

For renal perfusion, in-line filtration has proven to be especially suitable for the recirculation mode (174, 227). During the isolation of the kidney, small particles may be detached, which then invade the arterial vascular bed and block capillaries. Experience has shown that GFR in the recirculation mode is more stable with in-line filtration than without a filter. Here, for cell-free perfusates a pore size of between 8 and 14µm is selected. Specifically, we use a filter with a diameter of 42mm; the filter housing is made of stainless steel and was obtained from Sartorius (Göttingen, Germany). When washed red blood cells are used, the filter should be removed, placed in a bypass or covered with a polyester mesh (Leon L. Miller used white silk with a mesh count of 100-150/inch (174) when blood was the perfusate). Sterilization conditions for the filter membrane depend on the material used. Cellulose acetate, but not cellulose nitrate* or polyesther mesh, can be sterilized by dry heat at 132°C (oven). Zoltan Endre in Oxford used two different filters when using added red cells one from Pall (Pall Corp. Port Washington, NY, USA) and a transfusion filter from Fenwal (20-40µm) (Fenwal Inc. Lake Zurich, Il., USA) (70). If urine is returned to the perfusate (in pure recirculation mode or when cell-free perfusate is used), which may be admissible for small recirculation volumes, one runs the risk of loading cellular debris into the perfusate. Within about 30 min the first cellular debris (218) appear in the urine sediment (which forms as a consequence of the relative lack of oxygen; see the first fig. 2.1), and may block capillaries and reduce both perfusion flow and the glomerular filtration rate.

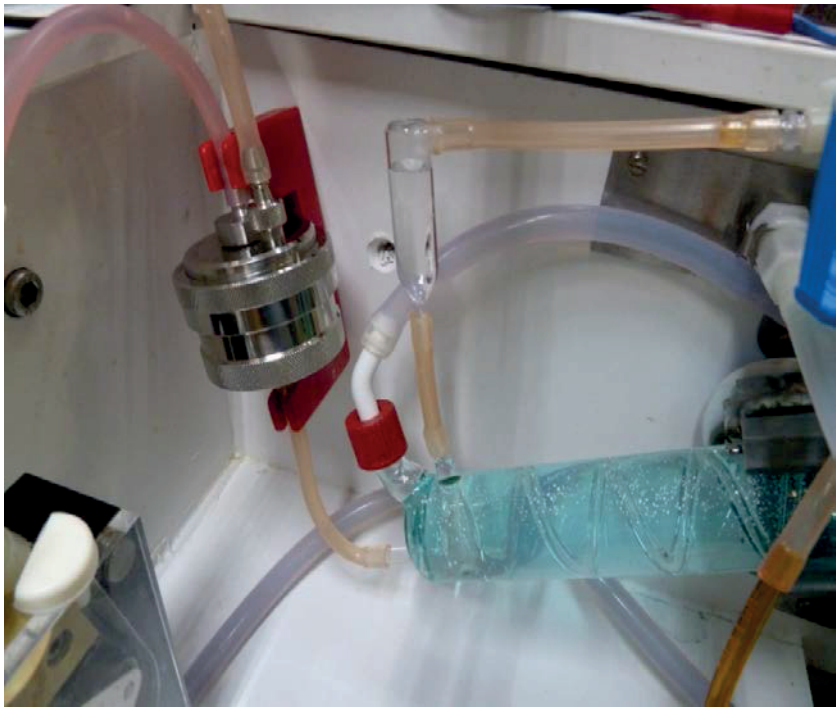

Fig. 4.5.3.: ***In-line filter.*** The cellulose nitrate filter (42mm diameter, pores 8µm; Sartorius, Göttingen, Germany) on the left is inserted between the perfusion pump and the glass heating coil with pressure buffer (Windkessel) and bubble trap. A screw-vent connection can be seen at the front end of the filter. To vent the lower chamber, rotation of the filter is necessary during the preparation.

*__Note:__ Sterilization of cellulose nitrate filters by exposure to dry heat at 132°C (in direct contravention of the recommendations of the manufacturer) alters the pore size, causing the filter to clog up within a short time.

Pegg has pointed out that, in his experience, only the use of “0.2 micron filters” provided the stability of flow rate required for perfusion of isolated perfused rabbit kidneys! (Sterility problem?). In addition, a reinfusion of urine is associated with the risk that particles in the urine (tubular cell aggregates etc.) will enter the renal capillary bed and contribute to an increase in perfusion resistance (196-200). Our own observations show (218) that during cell-free perfusion cellular debris appears in the urine sediment within about 30 min after the start of perfusion; this phenomenon is not observed when the perfusate contains added erythrocytes. There is also a report (263) which describes the morphological damage that occurs in P_3 proximal tubular segments and TAL segments during cell-free perfusion. An additional way to maintain stable flow rate in pure recirculation and constant-pressure perfusion is to add verapamil, a calcium-channel blocker (99). This, however, leads to the loss of all autoregulation of the perfusion rate (see Fig.10.1.10).

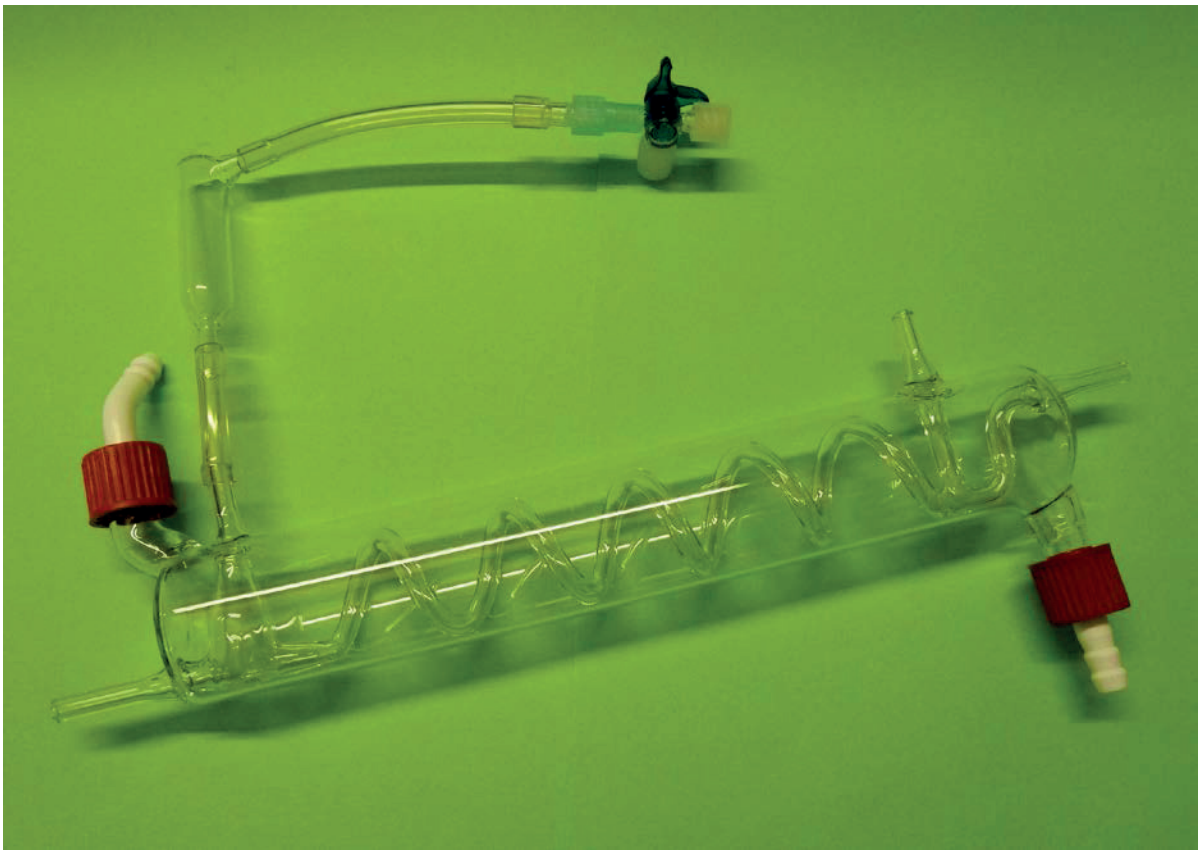

Fig. 4.5.4.: ***Temperature controlled glass coil with buffering chamber (Windkessel), bubble trap,*** and return connection. Perfusate flows from left to right. The volume of the buffering chamber visible at the left end can be changed by adding an extension on top, as shown (s.a. Fig. 4.5.3.). On the right is a T-outlet that provides for the return of medium to the reservoir prior to the start of perfusion, which avoids “no flow” areas. Dimensions: overall length: 295mm, o.d. of glass tube 38mm, glass coil o.d. 6mm, i.d. 2.5mm. Glass screw thread standard GL 14 for water circulation thermostat.

4.6. Cannulation

4.6.1. Arterial access to the kidney, perfusion cannulas

The original technique used by Weiss (307) was to intubate the right renal artery via the aorta (not via mesenteric artery, which is not shown in the original sketch). The arterial cannula was slipped into the renal artery through intubation of the distal aorta. The vena cava was intubated by a cannula with lateral perforations from caudal (L4) and ligated on the cranial side (L6).

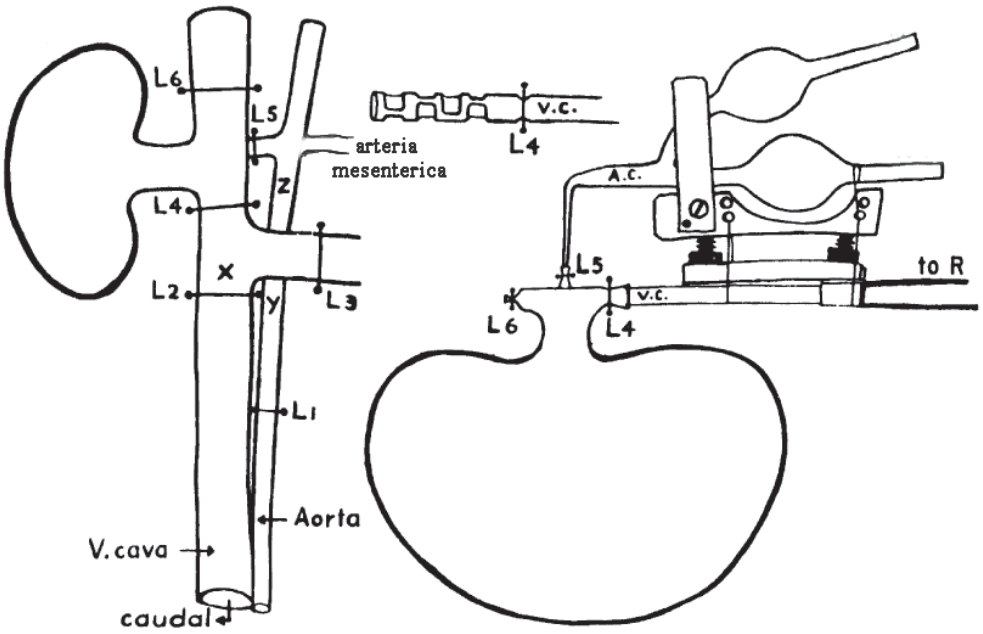

Fig. 4.6.1: ***Modified original sketch of the cannulation technique used by Weiss*** (307). Schematic diagram of the surgical field showing ligation points. The pressure measurement was performed just before the narrow end of the cannula. The sketch is modified and based on the original publication by Weiss, in which the mesenteric artery (along which later on the cannula was inserted into the renal artery) was not shown. Reproduced by permission of the APS.

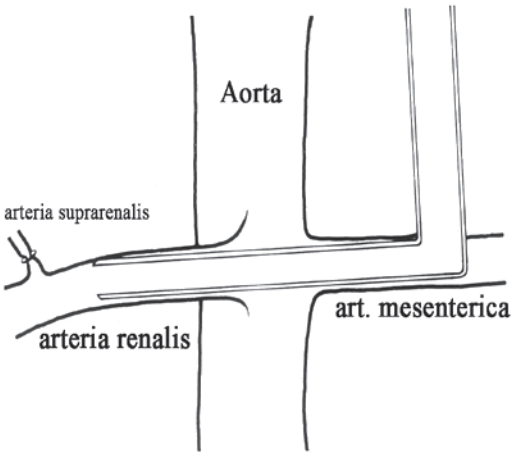

Fig. 4.6.2.: ***Technique for cannulation of the right renal artery with a glass cannula via mesenteric artery.*** This approach ideally requires that both vessels branch off at the same level (185), which is not always the case. The Figure is modified from the version in the handbook by Brian D. Ross (224). The dimensions of the glass cannula is 3.5mm (o.d.) and 2mm (i.d.), tapering to 1.3mm o.d. and 1mm i.d. at the tip, which permit intubation of the mesenteric artery of rats weighing 350 to 400g. Reproduced by permission of the author.

To measure the effective perfusion pressure, we modified this technique in 1971 - perfusing via a cannula inserted in the mesenteric artery and measuring the perfusion pressure via the distal aorta (251, 256). Later on, we used this arrangement for constant-pressure perfusion with feedback control of the perfusion pump. We then went on to develop the double-barreled cannula, with which only the distal aorta was intubated (253, 254). Unaware of this technique, which was described in 1975 and 1976, 6 years later Loutzenhiser et al. (157) referred to the errors associated with indirect pressure measurement prior to the stenosis of the cannula.

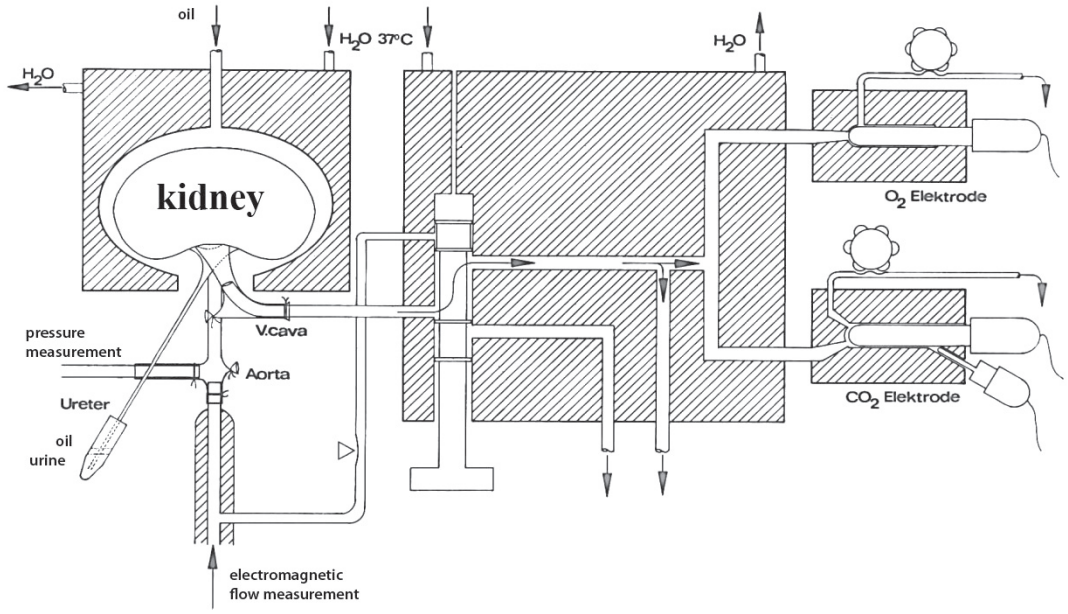

Fig. 4.6.3.: ***Schematic diagram of the set-up used by Schurek 1969-1975*** (256, 257). The cannula for perfusion is positioned in the mesenteric artery, the cannula for pressure sensing in the aorta. The venous cannula is mounted on the valve block on the right and is introduced from the cranial end into the vena cava inferior and ligated. By moving the piston in the valve block, the preconstricted arterial bypass is opened to the gas electrodes and the venous channel is now bypassed. The gas electrodes are always open to the atmosphere at one end, in order to avoid pressure fluctuations on their membranes. ***Note that the valve block was used only in the single pass mode.*** The current standard technique uses a double-barreled cannula inserted via the aorta from caudal end and was developed later (253, 254). This requires ligation of the suprarenal artery and smaller side branches of the aorta between the cannula and the right renal artery. Oil was introduced into the system only in connection with micro-puncture experiments in the single pass mode, and the urine receptacle was covered with a layer of oil only if volumes of urine were very low (rare). For the more recent system with valve block, see Figs. 8.2.10 - 8.2.12.

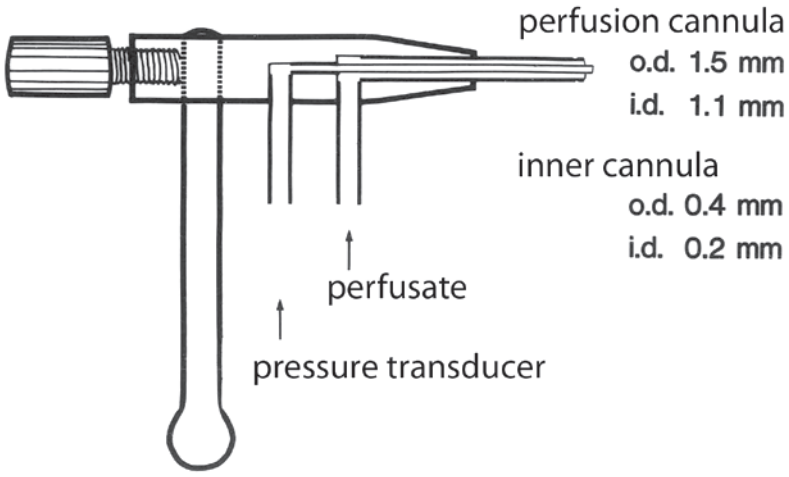

Fig. 4.6.4.: ***Schematic diagram of the standard cannula used in the aortic position since 1974.*** The double-barreled cannula has a circumferential groove at the front which serves to anchor the binding thread. The ball-lock pin fits into a magnetic recess in the block to facilitate cannulation of the aorta (253, 254). First description 1975.
o.d., outer diameter;
i.d., inner diameter.

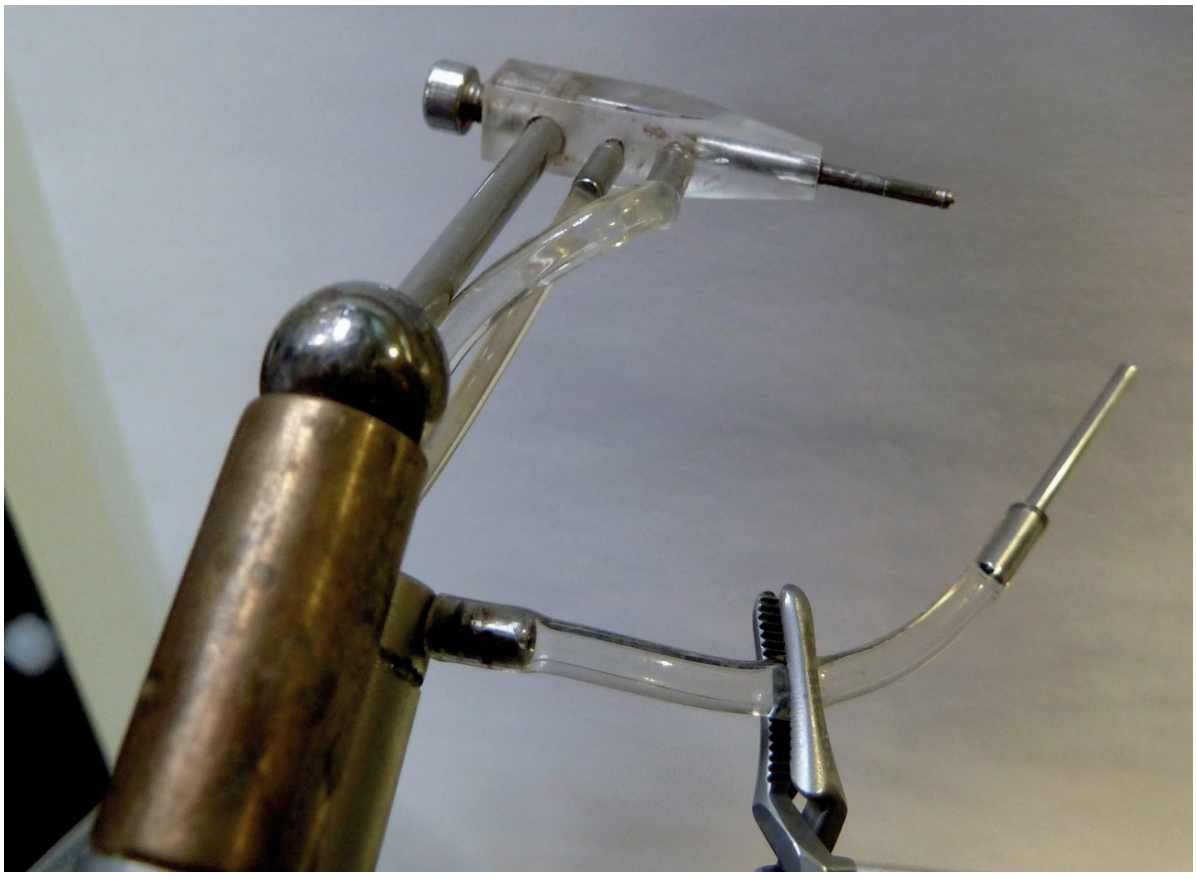

Fig. 4.6.5.: ***Detailed view of the aortic cannula.*** The cannula is mounted via a magnetic ball-and-socket joint (IBS Magnet, Berlin, Germany). The left port connects the inner cannula with the pressure transducer. The arterial bypass is clamped off with an alligator clip, which is opened for arterial pO_2-measurements. The small protruding inner cannula serves as a pioneer for the intubation of the aorta. The stainless steel needles are firmly affixed to the acrylic block.

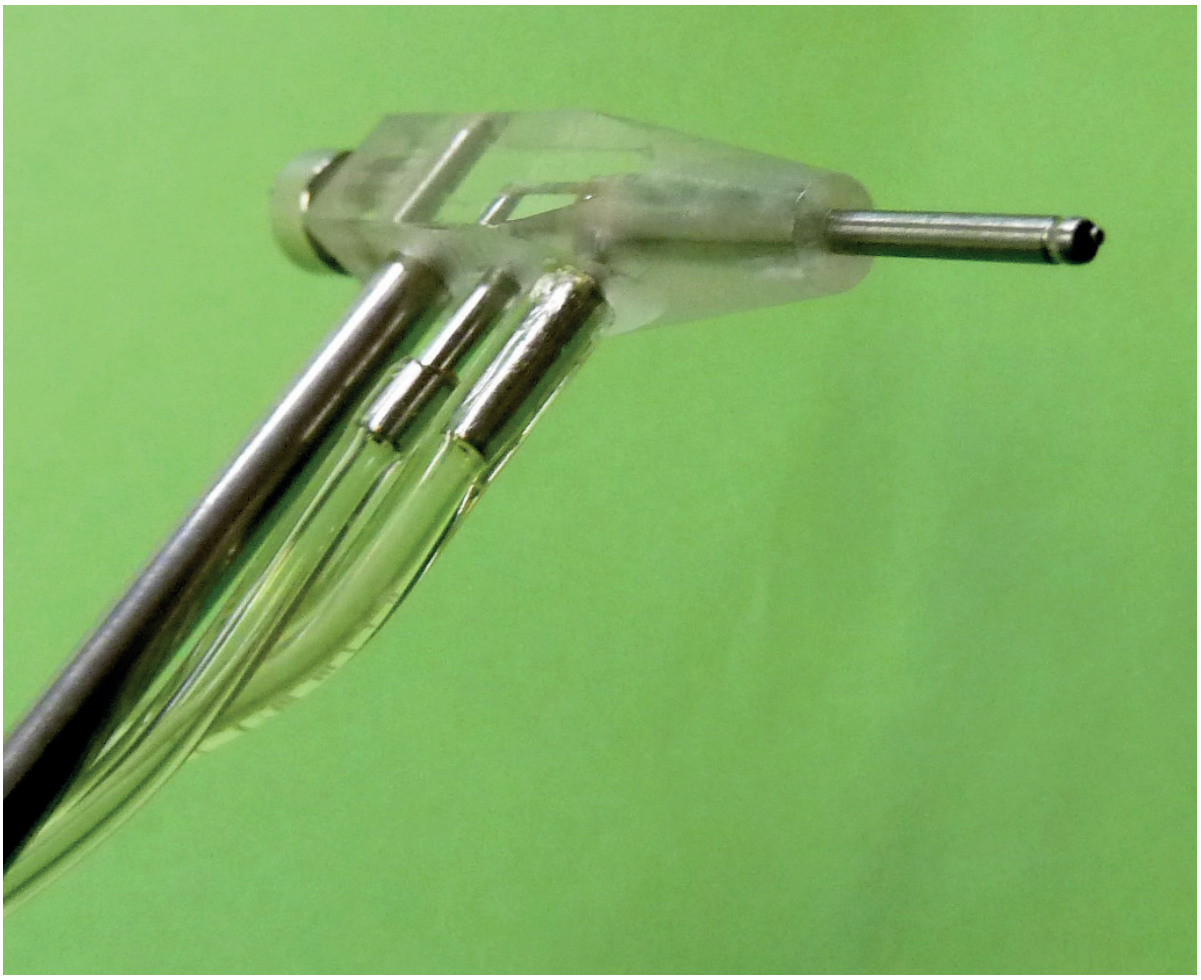

Fig. 4.6.6.: ***Detailed view showing the inner cannula.*** The protruding inner cannula seen on the right extends all the way back to the angled connection that links it to the pressure transducer. The circulating perfusate is sealed off from contact with the pressure channel.

4.6.2. Venous Cannulation

Many authors avoid the venous cannulation altogether, and view it skeptically (162, 163). However, it is necessary for the measurement of oxygen consumption, and our procedure allows it to be done without difficulty. After renal perfusion has been established and flow rate and perfusion pressure is being continuously recorded by a chart recorder, we ligate the vena cava and can intubate it quite easily. The venous cannula can be pivoted near the venous opening and one can draw the vein over the cannula with two fine watchmaker's tweezers and fix it. Then the open distal end of the vena cava can be closed with a ligature. In each phase, one can read on the continuous flow recording whether an obstruction arises etc. Fig. 4.6.3 shows the set-up we used until about 1975. For the technique used later on, see Figs. 8.2.04 and 8.2.11 and the last model in 8.2.12.

Fig 4.6.7.: ***Venous cannula with swivel.*** The vertical T-outlet of the venous cannula serves as a fulcrum and allows one to swivel it into the open cranial end of the vena cava. After fixing the cannula with the ligature, the distal end of the vena cava is also ligated. The effluent flows into the funnel below the kidney tray; on the right is a Luer-connector for venous sampling via a syringe. The outer diameter of the cannula is 3.2mm. The thin portion of the T-outlet is connected to the Tygon tubing for the pO_2-pressure measurement. For further details, see the Technical Appendix.

4.6.3. Ureteral catheter

It is crucial to select the proper ureteral catheter. In 1972 Cortell had pointed out (59) that the PE10 tube commonly used in rats with e.g. 50-100mm length is inadequate at higher urine flow rates, especially when low-molecular-weight fractions of colloids are filtered and enhance the viscosity of the urine. Two studies (34, 152) describe the phenomenon of "erratic behavior" of GFR in the IPRK at low colloid-osmotic pressure, i.e., a drop in the GFR instead of the expected increase. When the "appropriate" catheter is used, the GFR increases as the colloid-osmotic pressure falls, as one would expect on the basis of Starling´s concept (287). For perfusion with ***colloid-free media***, it is necessary to remove the kidney capsule in order to avoid compression in the vascular tree and the tubules due to interstitial swelling. Under these conditions, the proximal tubular pressure reaches 50mmHg without decapsulation at a GFR of approximately 0.5ml/min·g kidney; with decapsulation the corresponding values are 30mmHg and 1.2-1.6ml/min·g kidney under otherwise comparable conditions (i.e. an effective arterial pressure of 90mmHg, see Fig. 4.7.1). A critical point is a bleeding into an already cannulated ureter, especially at low urine flow rates and because the obstruction may be discovered late. With a continuous recording of the perfusion flow rate, such a blockage may become apparent earlier (by flow depression). The tip of the ureteral catheter should not be thrust to the renal pelvis, as this can easily lead to hemorrhage. One way to reduce complications is to intubate the ureter with a bubble-free prefilled catheter. Some authors administer mannitol i.v. and intubate the expanded ureter under osmotic diuresis.

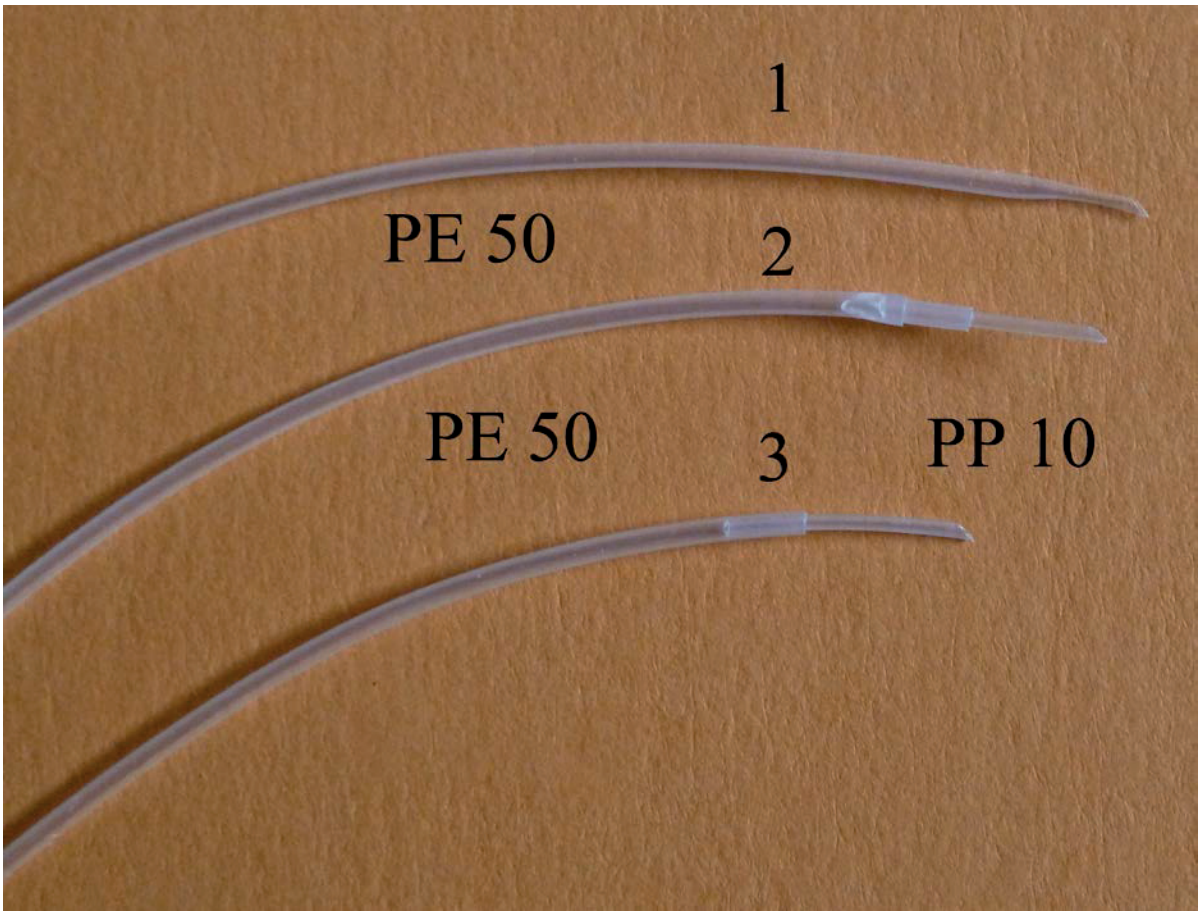

Fig. 4.6.8.: ***Front end of the ureteral catheter.*** 1. PE50 tubing, drawn out after heating to taper it. Note the considerably thinner wall and the taper. 2, 3. PE50 joined to PP10 with (2) or without (3) a spacer. The catheter is tied in front and secured with the ureter ligation thread. In the early years, we also tapered glass cannulas, extended with PE50 (s.a. Fig. 4.7.0).

If the upper third of the ureter is intubated with a “dry” catheter, after the initial filling of the tip, one can observe that the urine front proceeds with each contraction of the ureter/kidney pelvis. This is somewhat dependent on the state of diuresis. To stimulate urinary flow some authors use mannitol or furosemide. Avoid the entry of air bubbles into a prefilled ureteral catheter.

Hydrodynamics in the Nephron and the Colloid-Osmotic Pressure (COP)

In the early days we calculated the colloid-osmotic pressure using the formula of Landis and Pappenheimer (140) for albumin. These values are slightly higher than measured later on with a 20000 Dalton membrane (Osmomat 050, Fa. Gonotec, Berlin, Germany), see Chapter 9.7. Landis and Pappenheimer proposed the following empirical formula for colloid osmotic pressure due to albumin: $2.8c + 0.18c^2 + 0.0012c^3$, where c is the concentration of albumin in g/dl.

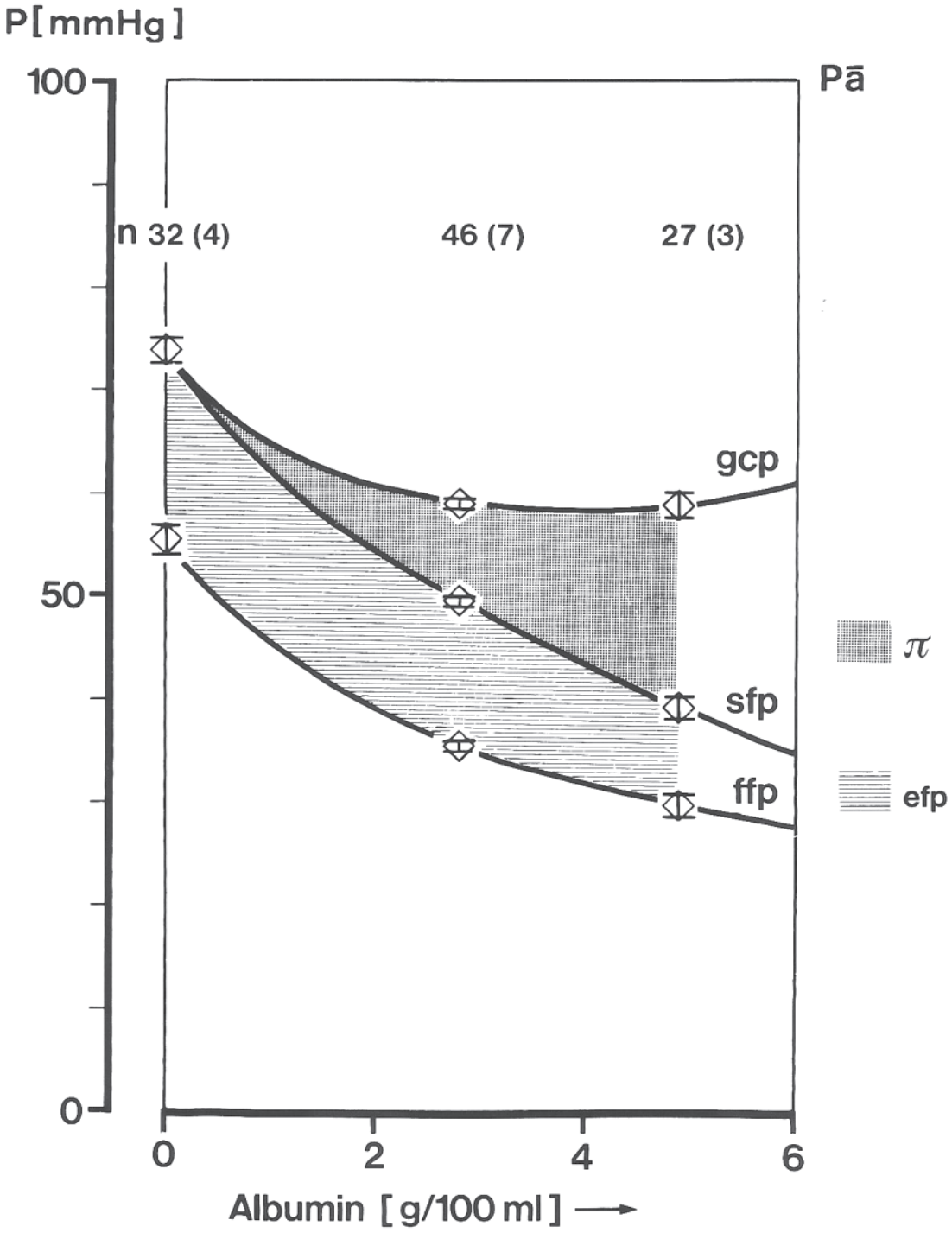

Fig. 4.6.9.: ***Pressure conditions in the glomerulus.*** Hydrodynamics of superficial nephrons plotted against the albumin concentration in the perfusate. Tubular free-flow pressure (ffp) and stop-flow pressure (sfp) are measured in the same early proximal tubule (250). We calculated the glomerular capillary pressure from sfp and the calculated colloid-osmotic pressure (mean±SEM). Tubular pressures were measured by two different methods (141, 154) first by Gerd Schwietzer with the Landis technique (0% BSA) (141), and by Klaus Hinrich Neumann with the Berlin technique (154) (BSA=>2g %). See also results, Chapter 11.

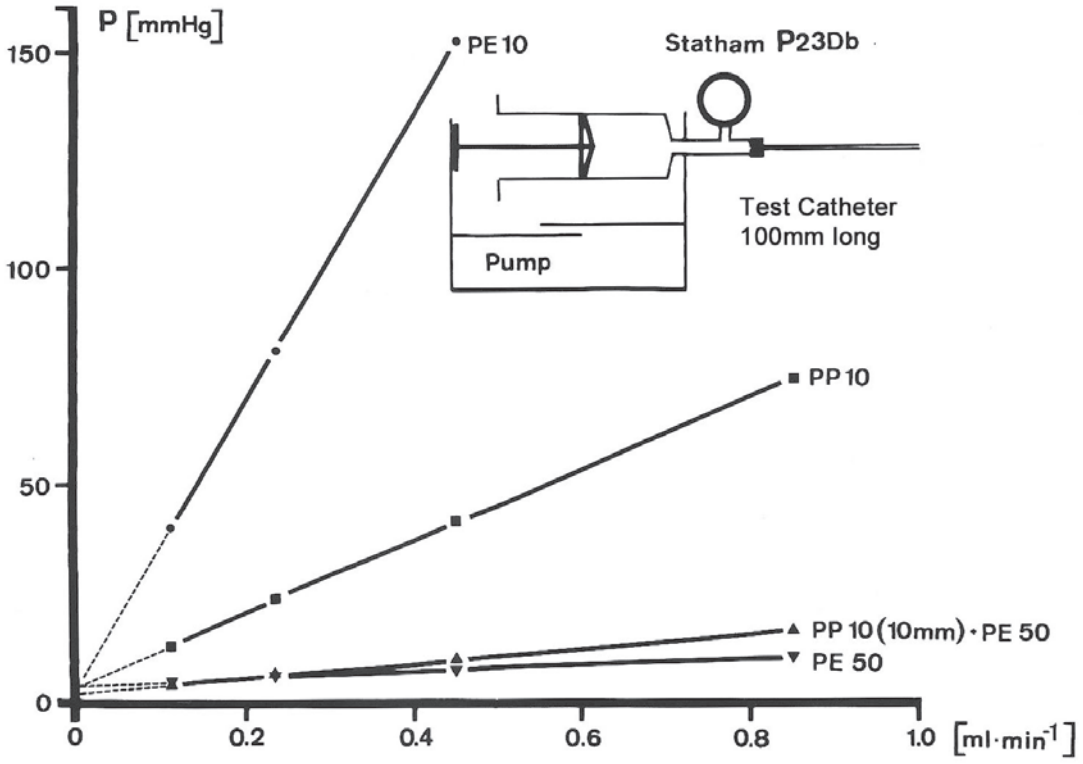

Fig. 4.7.0.: ***Characteristics of ureter catheters.*** The diagram provides an overview of catheter characteristics, which were investigated systematically using 0.9% NaCl-solution. The flow-dependent increase in pressure in various plastic tubes that are used as ureteral catheters serves as a measure of flow resistance. The PE10 catheter was the cause of the artefactual "erratic behavior" of GFR referred to above. As a standard catheter, we used either a combination of a short length of PP10 inserted in PE50 or PE50 with a glass tip. The thin PP10 catheter was shorter than 10mm (PP = polypropylene, PE = polyethylene). The Figure is from the 1981 Habilitation (250).

We have used as standard catheter the combination PP10 short/PE50 longer or PE20 short/PE50 longer or a glass tip and PE50 (same pressure profile). The thin PP10 catheter at the tip was less than 10mm long (PP = polypropylen, PE = polyethylene). The Fig. is from the habilitation thesis of 1981 (250). The PE10 tube has an i.d. of 0.011 inches and an o.d. of 0.024 (i.e., 0.28mm i.d. and 0.61mm o.d.). The corresponding values for PE50 are 0,023 and 0,038 inch (0.58mm and 0.97mm). The PE50 thermally on PP10 level and thus get an optimal ureteral catheter. Even better may be a rounded glass tip attached to PE50.

Importance of the kidney capsule for the perfusion without colloids

In single pass mode, the kidney capsule should be removed on the ventral side before the start of perfusion when a colloid-free perfusate is used. The capsule facing the hilum is raised a little with fine watchmaker's tweezers, and can then be easily cut away. In the rat kidney, there are no significant vascular connections to the capsule, unlike the case e.g. with the kidney of the cat (as venous drainage through the capsule). Fig. 4.7.1 demonstrates the impact of the presence of an intact capsule upon GFR and the hydrostatic pressure

measured in early proximal tubules (so far unpublished); a first notice was given by Fülgraff (84b) in micropuncture experiments in vivo (furosemide diuresis). A prerequisite for the high GFR is a free urinary outflow (i.e. ureteral catheter with a sufficient bore (i.d)). Two papers in which a PE10 tube was used as a ureteral catheter reported a low GFR and referred to it as the "erratic behavior" of GFR (34, 152). This is incompatible with Starling´s concept (287) and has been shown to be an artifact* (245, 250, 251). The micropuncture data have been obtained by the Landis technique** (141) together with Gerd Schwietzer and by the technique from our Berlin laboratory*** (154) together with Klaus Hinrich Neumann.

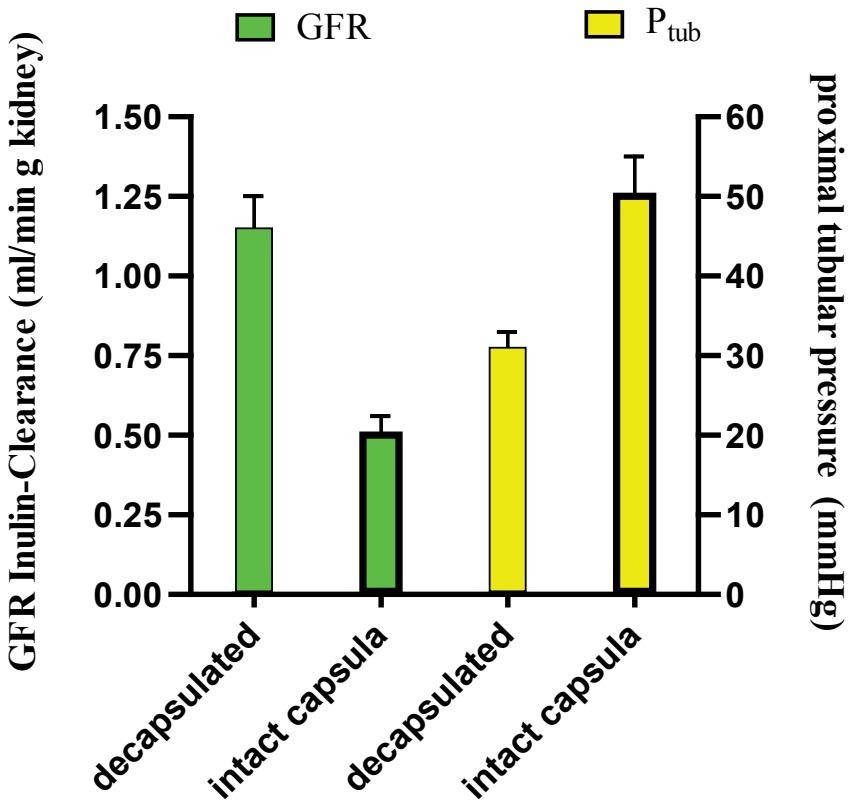

Fig. 4.7.1.: ***Isolated perfused kidney, single pass, colloid-free perfusate.*** The impact of decapsulation on colloid-free perfusion emerges from these data. The increased tubular pressure observed when the capsule is left intact limits the GFR; detaching the capsule causes the tubular pressure to fall and increases GFR. In our 1981 publication (251), decapsulation was not used systematically. This practice was prompted by the above findings and has been followed since then, with the result that initial perfusion rate and GFR are significantly higher (unpublished findings). For colloid-free perfusion, an effective perfusion pressure of 90mmHg is adequate (with colloid 100mmHg).

* In vivo a ureter with peristalsis wins out over a PE10 catheter, as urine is actively propulsed in the former.

** Dr. Gerd Schwietzer performed the micropuncture experiments in the Hannover laboratory using the Landis technique (unpublished). At that time he was Prof. Karl-Heinz Gertz´s assistant at the Institute of Physiology (Hannover Medical School).

*** Dr. Klaus Hinrich Neumann performed the micropuncture experiments in the Hannover Laboratory using the Berlin system of pressure measurement, see Chapter 13.0.

5. Material for the perfusion apparatus

5.1. Single-pass System

We designed the perfusion apparatus in such a way that the different perfusion techniques (single-pass mode, pure recirculation and recirculation with dialysis) can be carried out without major modifications. A thermostatic trough with immersion thermostat and circulation pump was large enough for both the 5-liter dialysate reservoir as well as providing for gas humidification. A ground-glass stopper attached to a plunger inserted in a 500-ml Erlenmeyer flask was used as a glass frit to humidify the gas, which passes into a water bath-jacketed glass coil. In order to avoid the ingress of condensation, a second water bath jacketed glass coil was inserted downstream as an added drying measure. A glass riser (3-4cm in diameter, 200cm high) for the effluent gas was optionally incorporated to increase its partial pressure, which is adjusted by altering the immersion depth of the pipe (tube) in the water column; this can also be used as a hydrostatic pressure drive (s.a. fig. 4.2.2.). A typical gas mixture of 95% O_2 and 5% CO_2 does not result in the **theoretical pO_2** of e.g. 760mmHg - 47mmHg water vapor pressure = 713mmHg x 0.95 **= 677mmHg**, but to pressures of 450-600mmHg, depending on conditions, including the perfusion flow rate and the rate of (unavoidable) diffusion of oxygen from tubes.

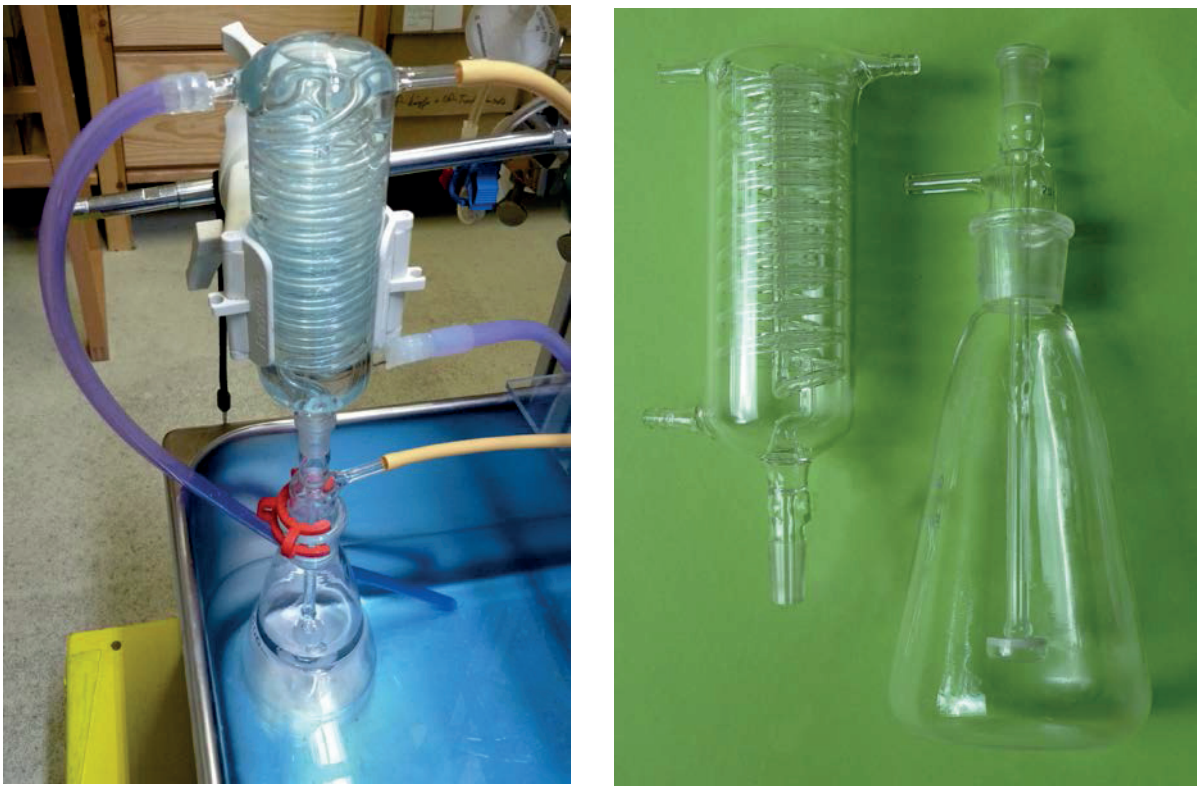

Fig. 5.1.01.: ***Control of temperature and gas humidification.*** A glass frit attached to a plunger is inserted into an Erlenmeyer flask filled with distilled water and moistens the gas, which is warmed up by passage through the water bath jacketed glass coil. In order to avoid percolation of condensation into the perfusate, a second water bath-jacketed glass coil is used to slightly dry the gas before it flows into the dialysate or to the membrane oxygenator.

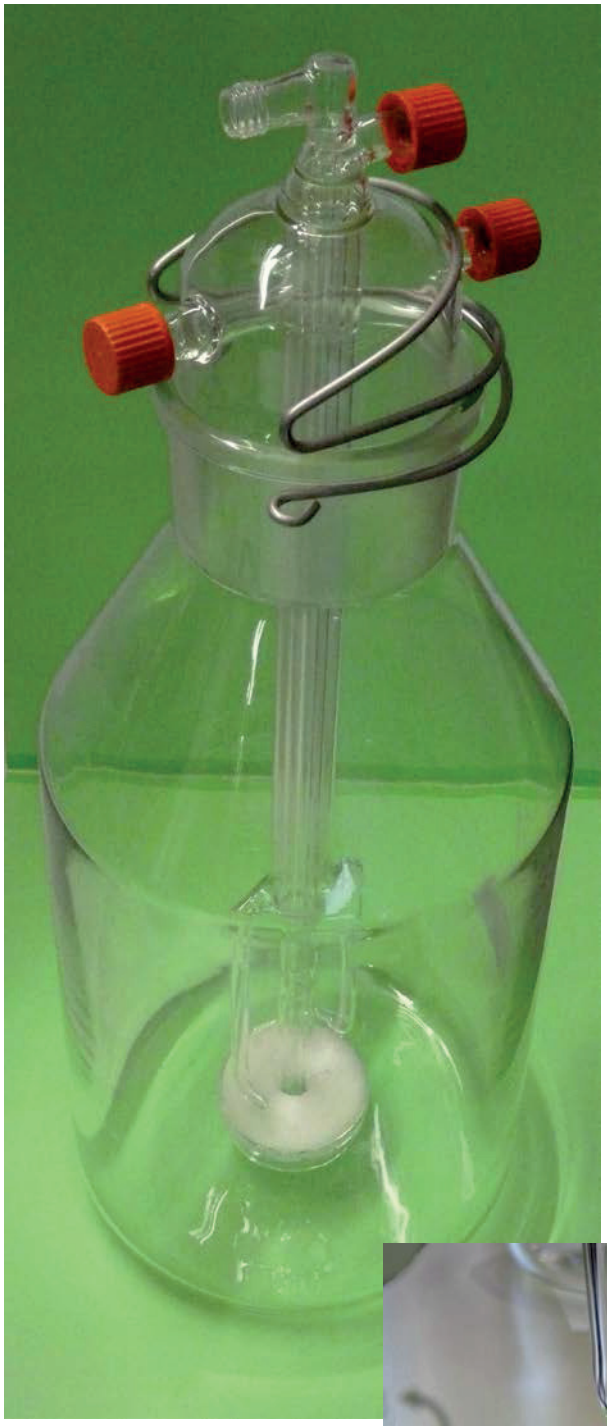

Fig. 5.1.02.: ***5-liter wide-mouth bottle with ground-glass frit (size NS86/55) attached to a plunger with four ports.*** Triple-dip tube: Narrow central tube with an opening just above the bottom of the bottle (top left port- without screw-cap). Above the central tube is the next gas inlet tube, which in an upwardly open glass frit opens at the bottom (upper port on the right). Above the third wide glass tube, which has two lateral outlets directed downward for recycling of the medium – lower port on the left – and a further lower port for venting on the right. The glass tubes that are bent over the glass frit cause rotation of the medium to facilitate mixing (a magnetic stirrer that fits in the space between the glass frit and the bottom of the bottle can also be used for this purpose). The system is suitable for the single pass-mode as well as the recirculation mode with dialysis (Glass-workshop MH-Hannover modified in Münster).

The inset shows details of the mixing nozzles for the recirculating dialysate positioned directly above the frit.

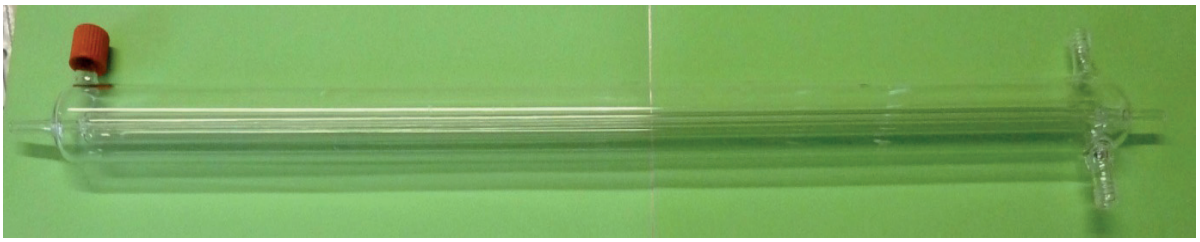

Fig. 5.1.03.: ***Temperature controlled bridge towards the recirculation pump*** versus perfusion pump, inlet and outlet ports for the circulating water are on the right, and on the left is the venting port. An additional middle glass tube allows the inlet and outlet for the circulation thermostat on one side only (the right). Overall length: 725mm, outer glass tube diameter 38mm, inner tube: o.d. 6mm, i.d. 2.5mm.

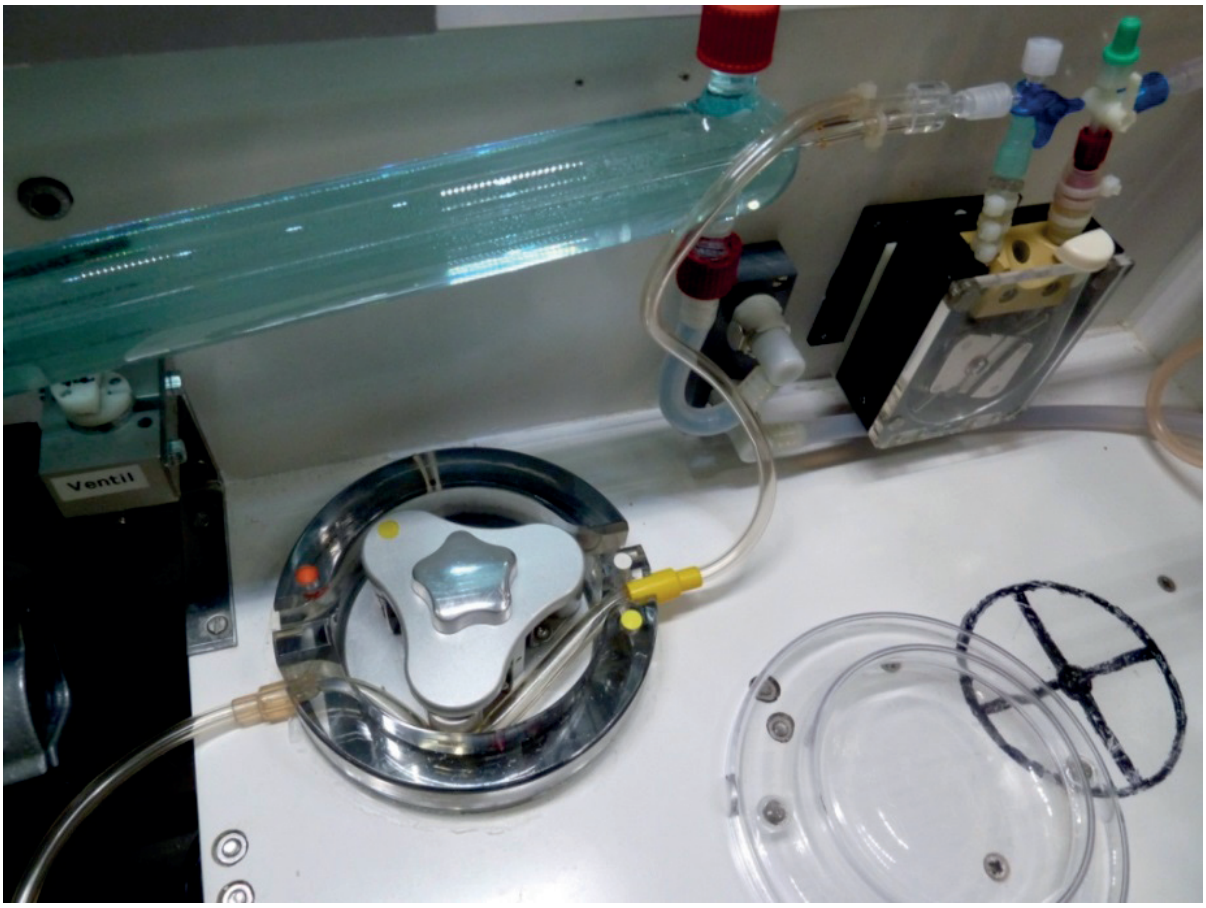

Fig. 5.1.04.: ***Recirculation pump*** (also usable in single pass mode, reducing stagnant liquid columns, and providing an additional stirring effect in the reservoir). On the right is the perfusion pump that supplies the kidney. The pump provides tachogenerator feedback (speed sensor) as an analog output so that the rotation rate (which is documented by a chart recorder) serves as a proxy for the flow rate. Since this signal is also used for feedback control, a booster amplifier is required to drive the recorder. The recirculation pump (dialyzer) is operated with two pump hoses in mode 3, one for the dialysate, the other for the perfusate. The flow rates (proportion) can be set differently by appropriate selection of tubing with the same wall thickness but different inner diameters.

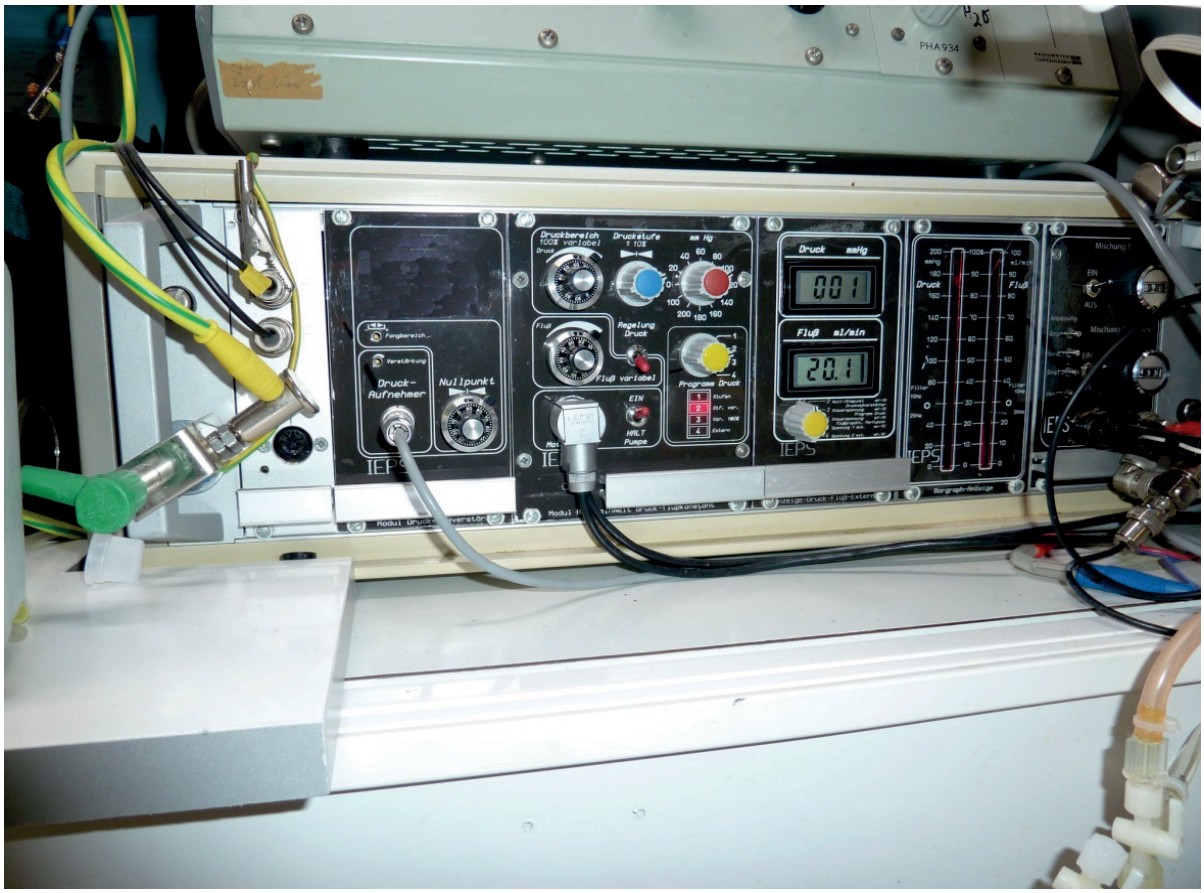

Fig. 5.1.05.: ***Control unit for the perfusion pump for use in constant-flow or constant-pressure mode.*** The slots on the left send analog data on pressure and flow to the chart recorder, the next slot to the right serves for the zero calibration of the pressure transducer. The third slot is the connection to the roller pump. We use the tachogenerator (speed sensor) signal from the roller pump to regulate the constant pressure mode and to deliver the analog data on the flow rate to the chart recorder. Here, the pressure can be changed in steps of e.g. 20mmHg or continuously, or the pumping mode can be switched to constant flow perfusion. The following two modules are indicators for flow and pressure. The first of these slots provides a digital display of pressure and flow. The second slot displays pressure and flow rates without damping on the vertical LEDs, providing visual readout of pulse rate and amplitude.

Steady-state infusion of hormones or pharmaceuticals

Joachim Lutz in Würzburg developed a system that allows the tachogenerator feedback signal from the perfusion pump (after appropriate amplification) to drive an infusion pump that responds proportionately to the flow (160). If a vasoactive substance is infused and the flow rate decreases, the rate of infusion of the substance is proportionately reduced. Thus the final concentration in the perfusate remains the same, and a steady state is easily achieved. We have implemented the system in our control unit (s. fig. 5.1.0.6).

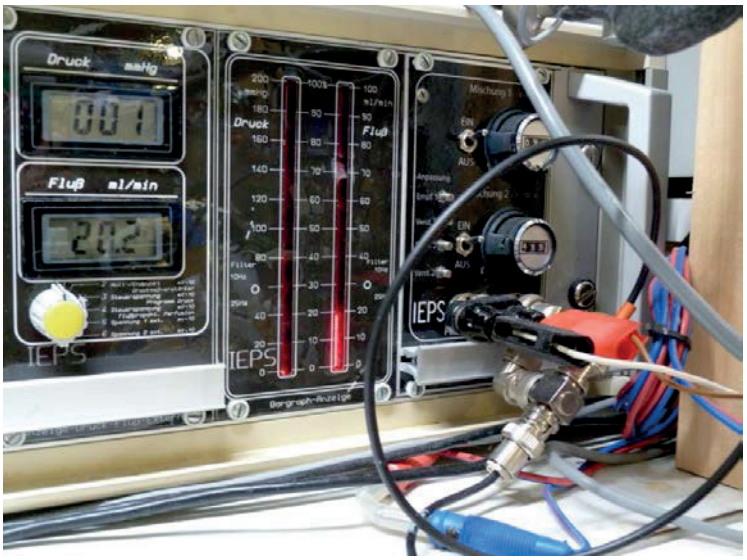

Fig. 5.1.06.: ***Detailed image to top.*** The unit on the right includes the circuitry that drives two infusion pumps proportionately to the perfusion rate. This enables the concentration of infused vasoactive hormones, for example, to be held constant during pressure-constant operation at varying flow rate. This has been used, inter alia, in collaboration with my colleague Armin Kurtz, and in the studies of the effect of angiotensin II done with Hermann Thole (136, 296).

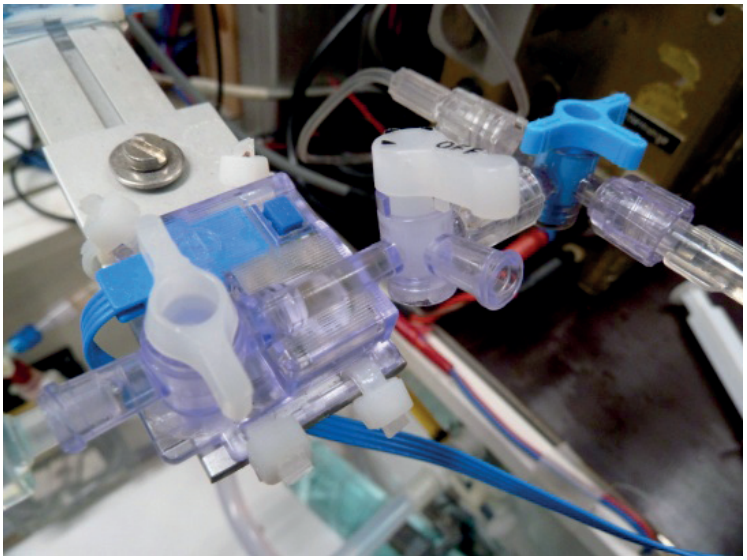

Fig. 5.1.07.: ***Pressure transducer with preamplifier and manual calibration*.***
This disposable system, developed for ICU´s, is also suitable for continuous use in clinical research laboratories.

*The small blue rectangle is the calibration button for
100 mmHg.

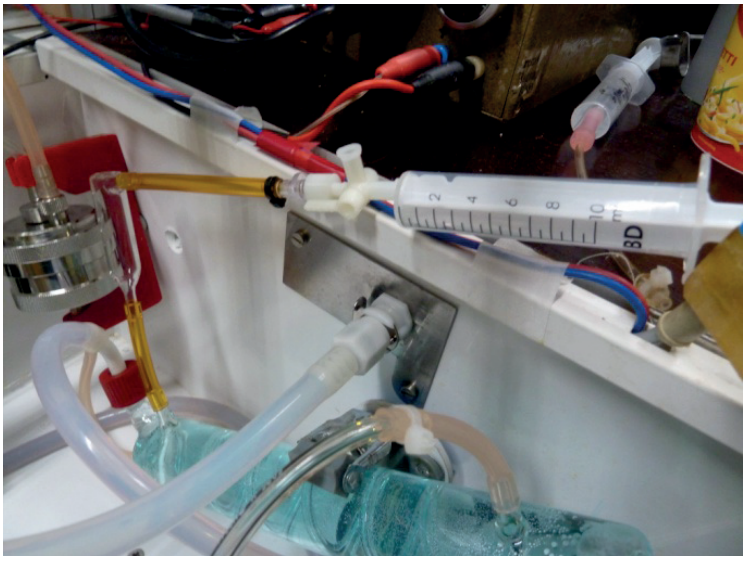

Fig. 5.1.08.: ***In-line filter.*** (s.a. fig. 5.1.10, membranes with 8-12µm pore size). Optional in the single pass mode, essential for the recirculation mode, but not suitable for situations in which red cells are used. For this last case, Endre has reported the successful use of Pall/ Fenwall (20-40µm) transfusion filters (70). Leon L. Miller used white silk with a mesh size of 100-150/inch for the perfusion of the isolated liver (174).

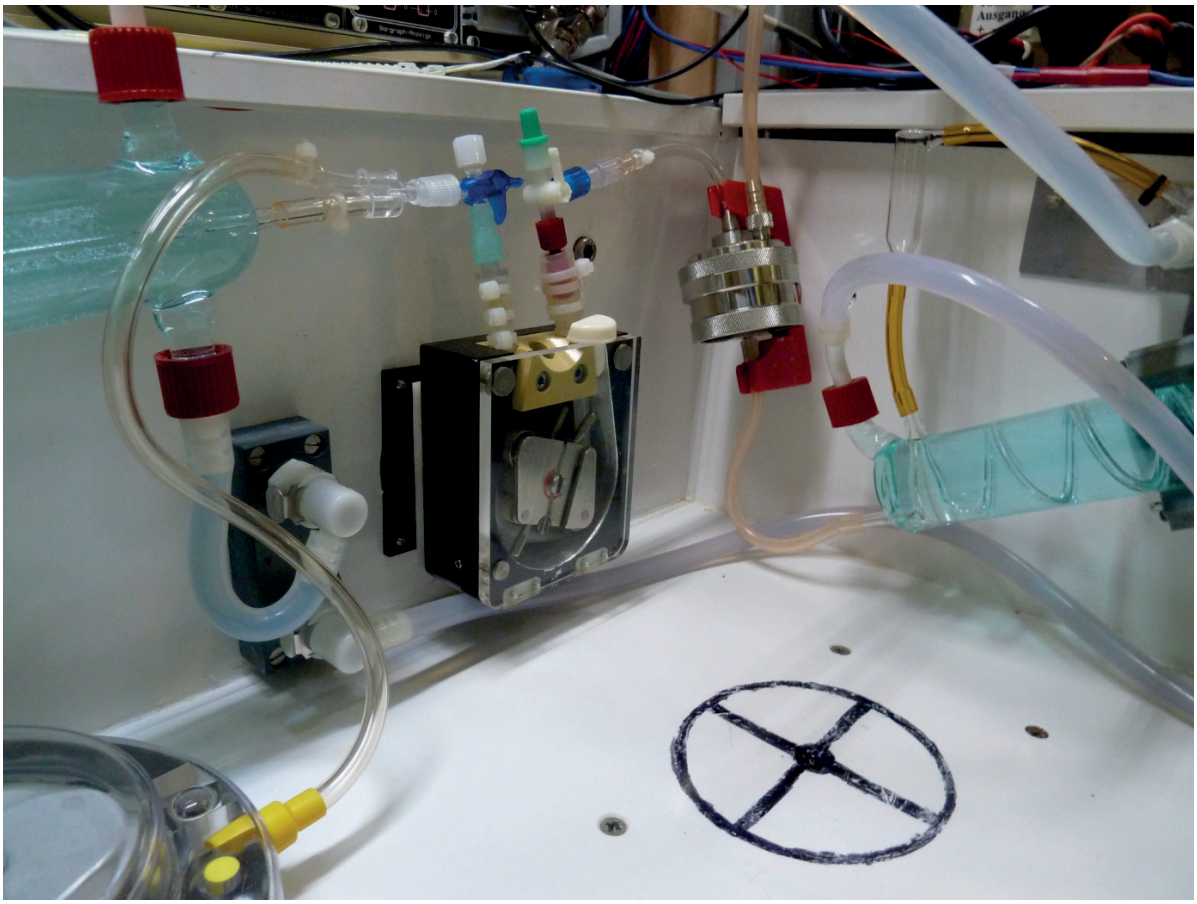

Fig. 5.1.09.: ***A close-up view of the components below the level of the perfusion stage*** (right). A magnetic stirrer is placed below the cross; when recirculation is used, the cross marks the position of the temperature controlled reservoir for the perfusate which is stirred with a magnetic rod. We use polypropylen-couplings employed in compressed air technologies (Colder Products Company, St. Paul, MN. USA) to connect tubes, both in the perfusion circuit and in the circulation system used to maintain system temperature. These are available with and without check valves.

Fig. 5.1.10.: ***Windkessel-extension***. The pressure buffer can be varied in height or fully clamped off, e.g. to achieve a pulsatility of flow and pressure. On the left is an in-line filter with a vent port (Sartorius, Göttingen, Germany).

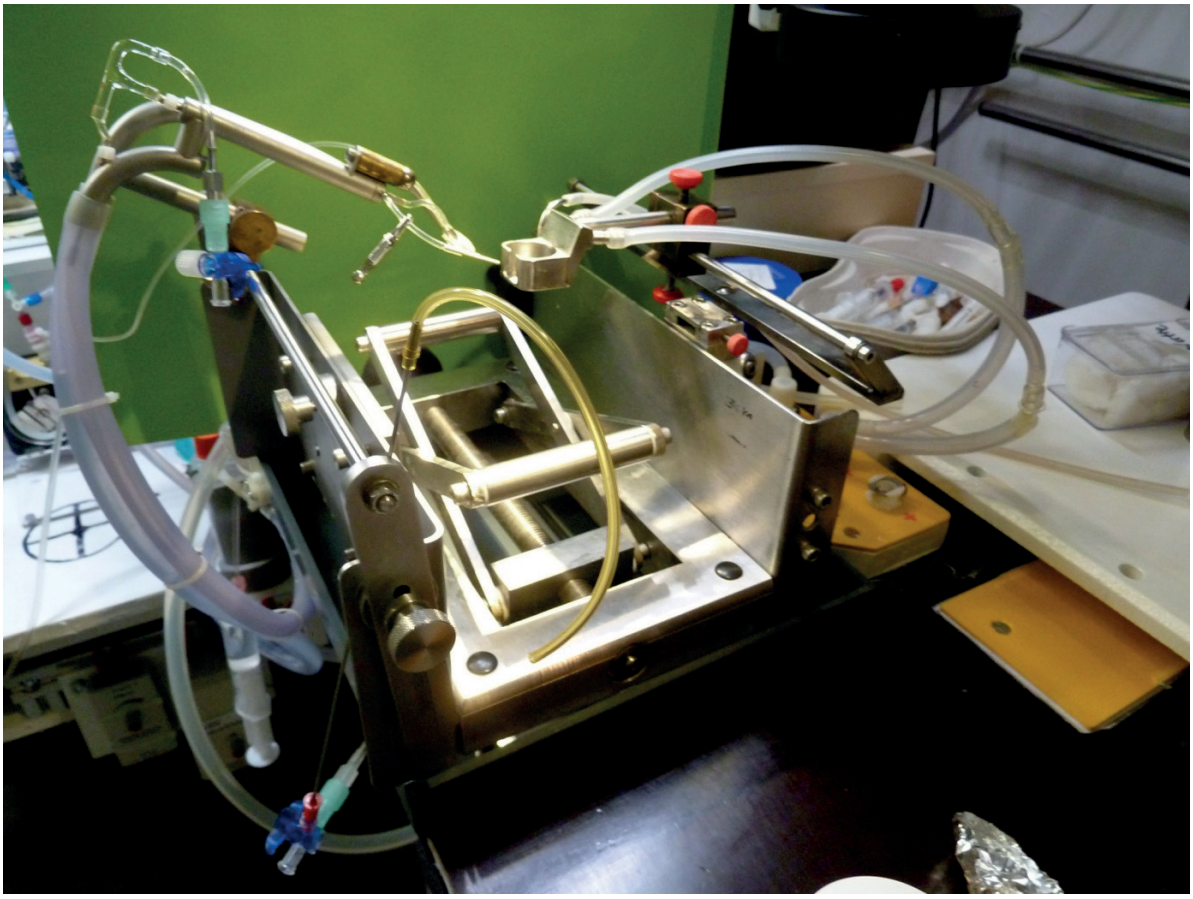

Fig. 5.1.11.: ***Perfusion platform (robust version for micropuncture experiments).*** The platform is placed in a drip tray, and equipped with mounting brackets for the kidney tray. Below and in front of the kidney tray is the aperture for insertion of the collecting funnel and opposite it is the mounting bracket for the perfusion cannula, (the perfusion "gun"). After the start of perfusion we lower the scissor lift on which the operation table rests, the remaining connections to the animal are severed and the temperature-controlled table is removed together with the donor animal.

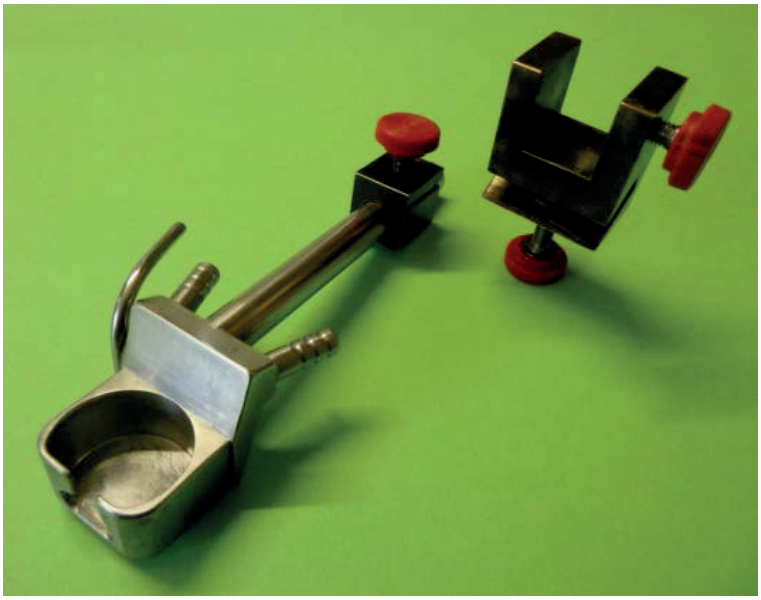

Fig. 5.1.12.: ***Water bath heated kidney tray made of stainless steel.*** The insert holder permits loading from above, so that the kidney can be placed in the kidney tray with the renal hilum projecting from the opening in the front wall. The tray on the left has a suction tube laser-welded to the sidewall. For details and dimension, see Fig. 15.0.8 at the Appendix.

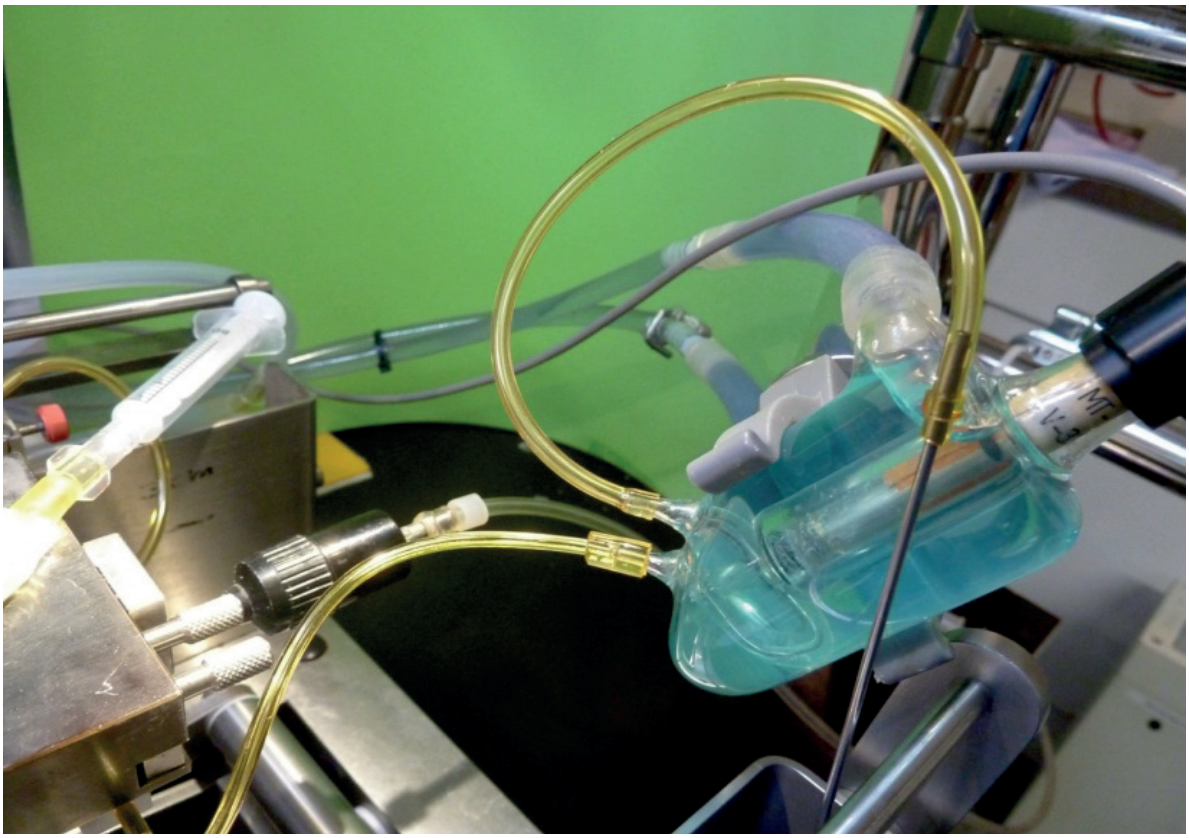

Fig. 5.1.13.: ***Constant-temperature flow cell for the oxygen electrode.*** A small roller pump drives the aliquot used for the measurement through the flow cell at a rate of 3-4 ml/min. The venous pO_2 is monitored continuously, arterial pO_2 is measured intermittently. In the single pass mode the fluid is discarded, otherwise it is recirculated. The connection upstream of the flow cell is open to the atmosphere. For arterial measurements, the valve bar is displaced electro-pneumatically and opens the preconstricted arterial bypass. Under constant-pressure perfusion the flow rate increases to the same extent as in the bypass. For micropuncture experiments the flow cell was rearranged backwards. The electro-pneumatic actuator allows vibration-free switching from venous monitoring to short periods of arterial measurement even during micropuncture.

Fig. 5.1.14.: ***Small roller pump.*** This is used to supply the flow cell (at 3 - 4ml/min) during pO_2-measurement.

Setup for the calibration of the oxygen macro electrode

Fig. 5.1.15.: ***Calibration of the O_2-electrode.*** The sketch on the right is the original drawing of the mixing chamber used for blood gas equilibration in an Astrup pH-meter, which we repurposed for calibration of the O_2-electrode. Below left is a schematic depiction of the double-walled glass cylinders used for equilibration of O_2 and N_2. The glass (circulation thermostat) chambers are connected in series; the cylinders vent via the connections on the top, as shown on the left below. In the coils the gases absorb moisture and flow into the mixing chamber shown above, and from there via a four-way valve to the O_2-electrode. The Astrup design provided an optimal solution to the problem of saturating the gases. The dry gas flows into the cylinder from below, rises in the lower small tube, is deflected and emerges from the aperture at the bottom into the aqueous phase in the form of small gas bubbles that rise to the surface, emerging from the water and then pass, warmed and moisture, via the inner double-lumen connecting tube into the mixing chamber. The outer tube transports the temperature controlled circulating water. Replicating these glass parts is a challenge for every glassblower. A zero calibration of the O_2-electrode can also be achieved with a thiosulfate solution.
($Na_2S_2O_3$).

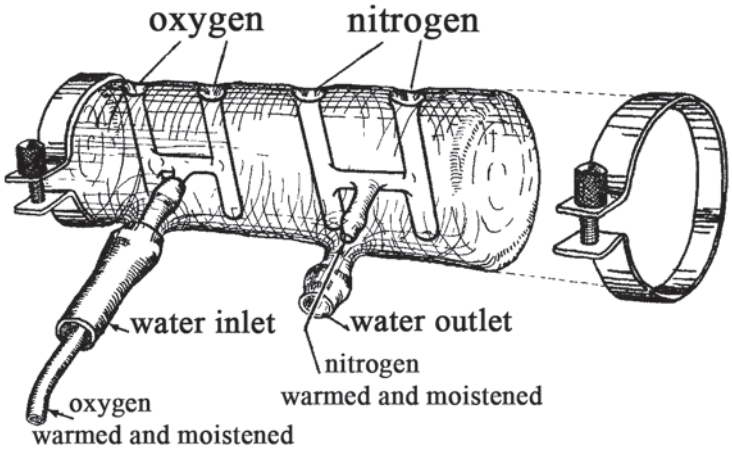

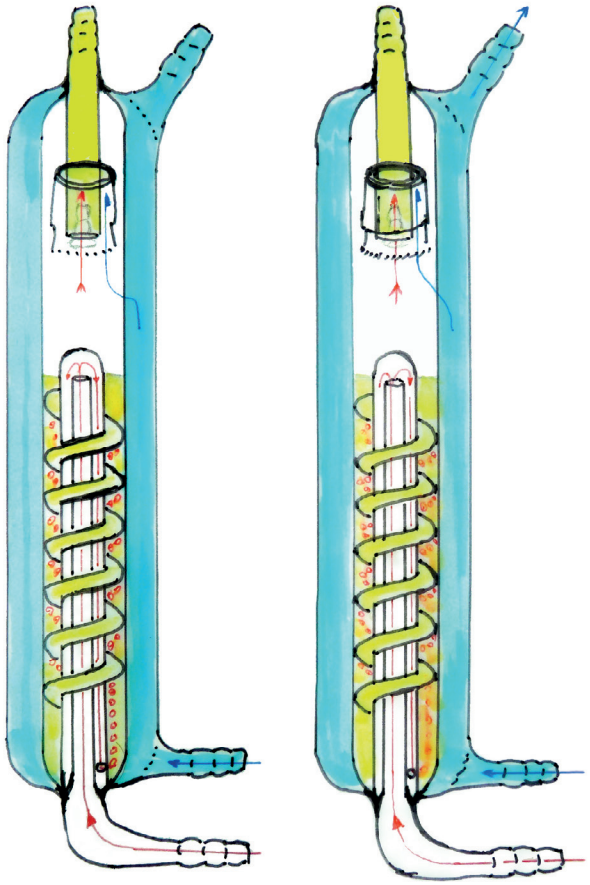

Fig. 5.1.16.: ***Effluent reservoir with inlet tube.*** On the left the perfusion pump, the in-line filter and the jacketed glass coil. The (bronze-colored) feedback-controlled infusion pump is mounted on top. On the bottom left are control modules for the magnetic stirrer that mixes perfusate with the test infusion and for the peristaltic pump for the gas pressure measurement (pO_2).

5.2. Recirculation system

The different systems available are adapted to specific requirements. Thus, the system favored by Maack for hormone studies is well established, but the version shown in Figure 5.2.1 is not suitable for use under the well-controlled conditions necessary for micropuncture studies, and was later modified accordingly (63).

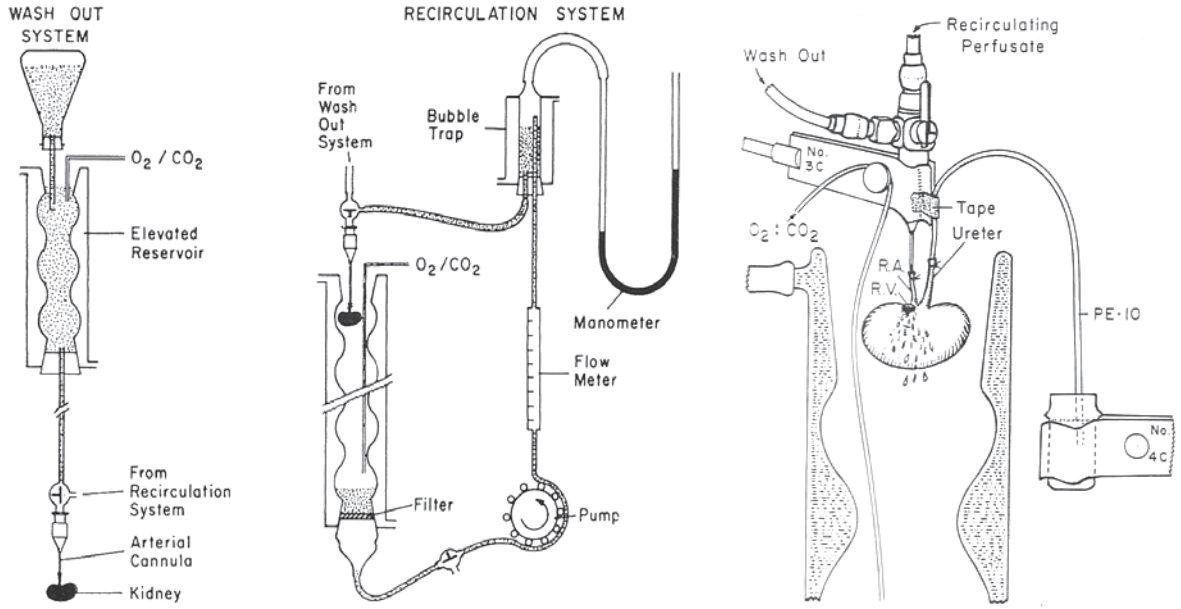

Fig 5.2.1.: ***Recirculation system used by Maack and Bowman.*** This demonstrates Thomas Maack´s preferred - and in his opinion very simple - IPRK system, which was described in a paper from 1972 (35) and whose advantages and limitations were later discussed in detail (162, 163). (Copyright permission APS). The detailed modified figure on the right is from a later work of Bowman (33).

Maack asserts that a trained experimenter should be able to connect his system to the "wash out" bottle within 10-minutes! After washing, the recirculation circuit is closed and the kidney is suspended in the constant-temperature oxygenator. He registered pressure and flow rate visually, and took samples via the four-way valve upstream and downstream of the kidney. Oxygenator and reservoir form a unit. The original recirculation apparatus used by the Oxford Group (described in chapter 4 (Fig. 4.3.3)) has a separate reservoir.

The apparatus we used is shown schematically in Fig. 5.2.2. Unlike the single-pass system, this requires a perfusate reservoir, which is placed on a magnetic stirrer. Fig. 5.2.2 shows the variant we last used, jacketed for water circulation and with a filling volume of 150-200ml. When erythrocytes are used at a volume fraction of 5-10%, a magnetic stirrer prevents sedimentation of the cells. The recirculation pump drives the perfusate at a flow rate of 100ml/min (up to 200ml/min with cell free medium) via the membrane oxygenator. The aliquot for the kidney preparation (20-40ml/min) is diverted from the perfusion line and pumped via an obligatory filter to the kidney; for cell-free perfusate 8-12µm filter porosity is sufficient, otherwise larger pores are needed, i.e. a polyester mesh or white silk as used by Leon L. Miller (174) or without a filter.

This apparatus enables perfusion in either flow- or pressure-constant mode. The perfusion pressure is measured at the tip of the double-barreled cannula and recorded as an analog signal, and the flow rate is measured via the tachogenerator feedback (speed sensor) from the perfusion pump **5**. The degree of functional stability provided by the recirculation system is less than that attainable when the perfusate is regenerated by dialysis (see also Table 10.1., Chapter 10.2).

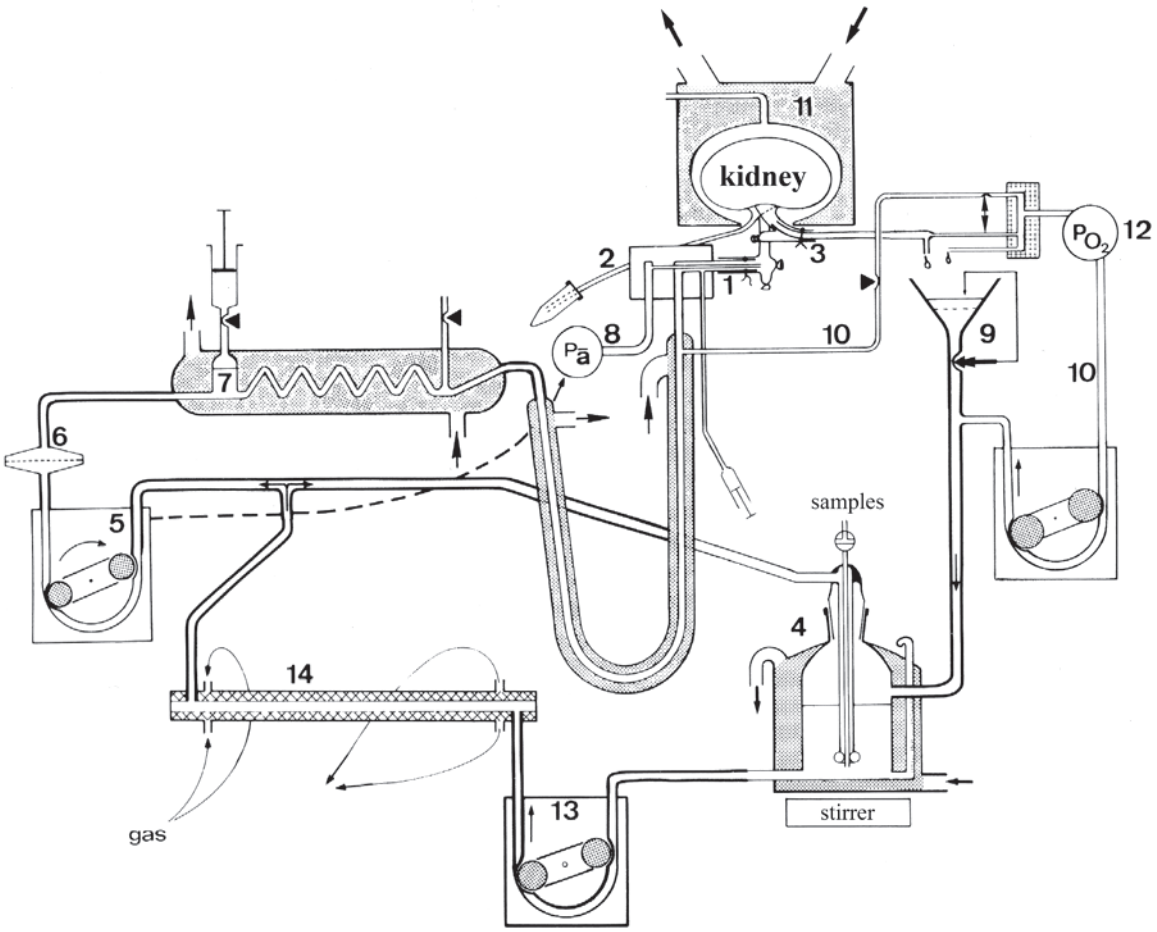

Fig. 5.2.2.: ***Schematic diagram of the basic recirculation unit*** (246). 1. Double-barreled cannula, shown here with a third port (e.g. for injection of a Lissamine Green bolus to estimate tubular passage times), 2. Ureter catheter. 3. Venous cannula, which protrudes through the vena cava into the renal vein. 4. Jacketed reservoir, connected to a temperature controlled water bath. 5. Feedback regulated peristaltic pump with a tachogenerator feedback for analog recording of the flow rate, 6. In-line filter, 8-µm porosity. 7. Adjustable buffering chamber (*Windkessel*), variable volume. 8. Pressure transducer. Originally a Statham element was used, but this has been superseded by a disposable system with integrated amplifier and calibration button. 9. Collecting funnel with valve-controlled effluent recycling to reduce foaming. 10. Suction line for the pO_2-electrode; venous pO_2 can be measured continuously and arterial pO_2 discontinuously via the arterial bypass (adjustable preconstricted bypass line). 11. Water-heated kidney tray. 12. pO_2-electrode in temperature-controlled glass cuvette. 13. Recirculation pump (pump rate >> pump 5). 14. Membrane oxygenator (see Figure 4.4.09.). I published this system in 1980 (246, 268).

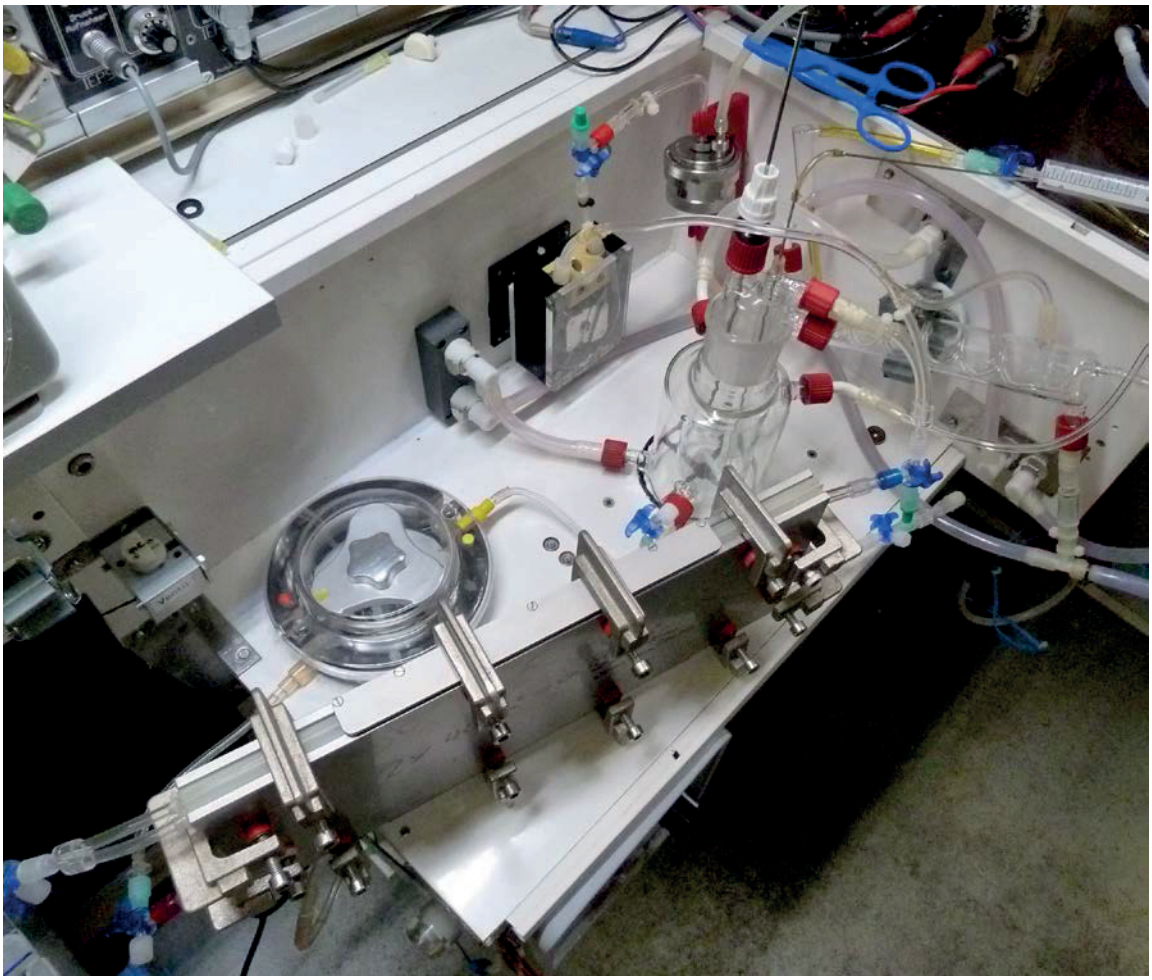

Fig. 5.2.3.: ***Photograph of the recirculation circuit with membrane oxygenator.*** The recirculation pump is positioned upstream of the membrane oxygenator, supplying the oxygenator with an increased circulation volume. Thus, the perfusion pump is always supplied with freshly equilibrated perfusate for the kidney. The jacketed reservoir is used in mode 2, as well as in mode 3 with dialysis. In mode 3 we use an adjustable measuring rod as one electrode, while a stainless steel tube which passes through a double-walled glass tube serves as the second. This latter tube returns the venous effluent (and the aliquot which is pumped through the oxygen electrode) and provides the contact with the perfusate surface necessary for the electronic level control, see Fig. 5.3.2.

5.3. Recirculation mode with dialyzer for gas equilibration and regeneration of the perfusate

In this mode, it is necessary to compensate for ultrafiltration by the dialyzer i.e. by an automatic recycling of dialysate into the perfusate. We prefer low flux dialyzers (i.e. Polysulfon F4/FX5 from FMC) for this purpose. This type of dialyzer can be used either to increase the albumin concentration or dilute it with dialysate. The easiest way is to use two electronic sensors, one adjustable in height in the reservoir. With a switching module, a hose valve (normally closed) is opened as soon as the level of the perfusate drops below that of the sensor dipping electrode, causing dialysate* to flow into the perfusate until the contact is closed again by the dipping electrode. The presence of surface foam, which

cannot be completely avoided with albumin as a colloid, also affects the operation of the sensor. The best way to prevent foam is to fill the dialyzer in the correct sequence, i.e. first filling the dialysate path (disconnected perfusate path) at a very low flow rate, then filling the perfusate path in counter-current mode (from the opposite direction, disconnecting the dialysate path), each outflow upwards directed (one switch between). Fig. 5.3.1 depicts the set up schematically.

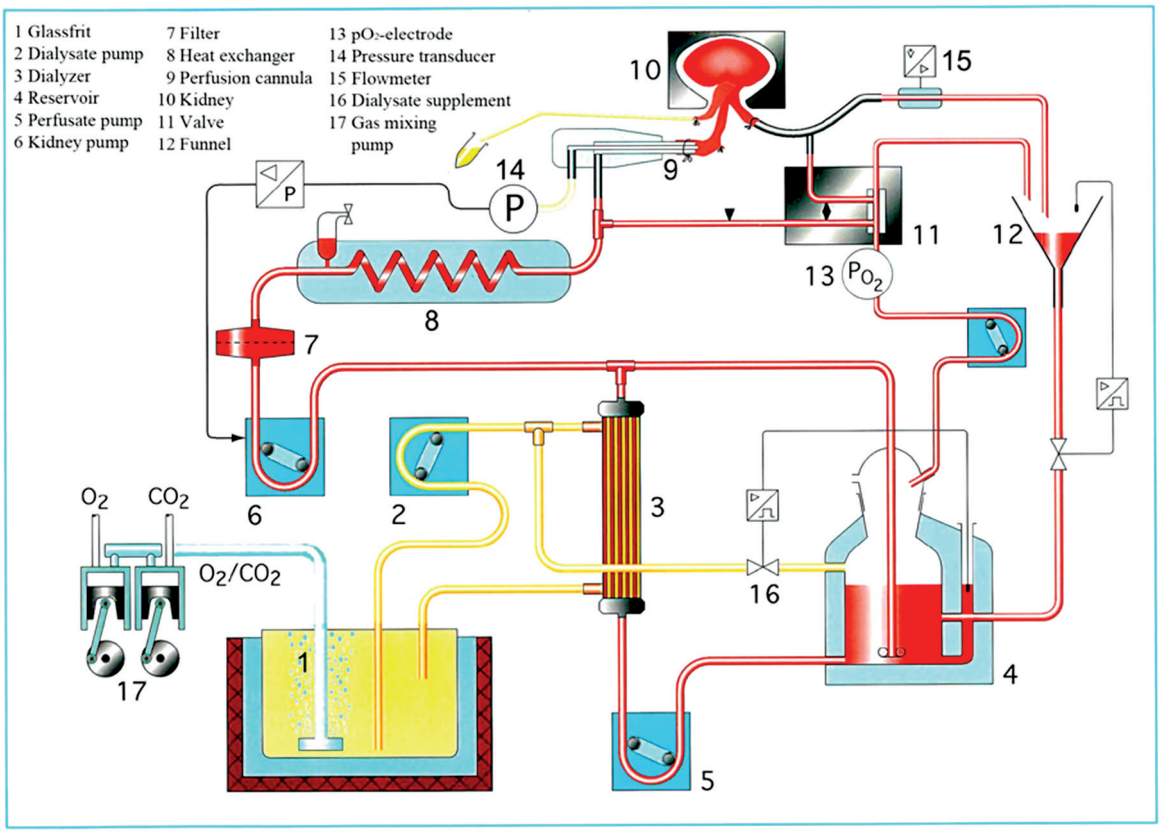

Fig. 5.3.1.: ***Recirculation mode using the dialyzer to oxygenate and regenerate the colloid-containing perfusate*** **(BSA)**. 1. Reservoir for dialysate (5-liter, see Fig. 5.1.02); the tubes to pump 2 and 5 can be driven by one pump head. Pump 6 is controlled by an analog feedback signal from the pressure transducer (14). Dialysate is reinfused via tube valve 16 to compensate for ultrafiltration by the dialyzer (3) (the sensor electrode in the reservoir itself is not shown). The effluent is returned via the collecting funnel (12), which is gravity-fed either through a wide-bore tube (our current practice) or via a valve to minimize foaming (as indicated in the scheme, and as previously practiced), but the latter may be not necessary. An electromagnetic flow probe (15) is optional. The system was first described in 1978 (245, 246, 250, 251). My coworker Jörg D. Biela created the above illustration (unpublished). In the early years in Hannover, a centrifugal pump (Eheim type 1022) was used, instead of the peristaltic pump (2), to drive the dialysate (about 360 ml/min). The magnetically coupled rotor was easy to clean. (251).

* The dialysate for refilling of the perfusate is diverted at a point upstream of the dialyzer, as a positive pressure is necessary for the correct operation of the magnetic tube valve.

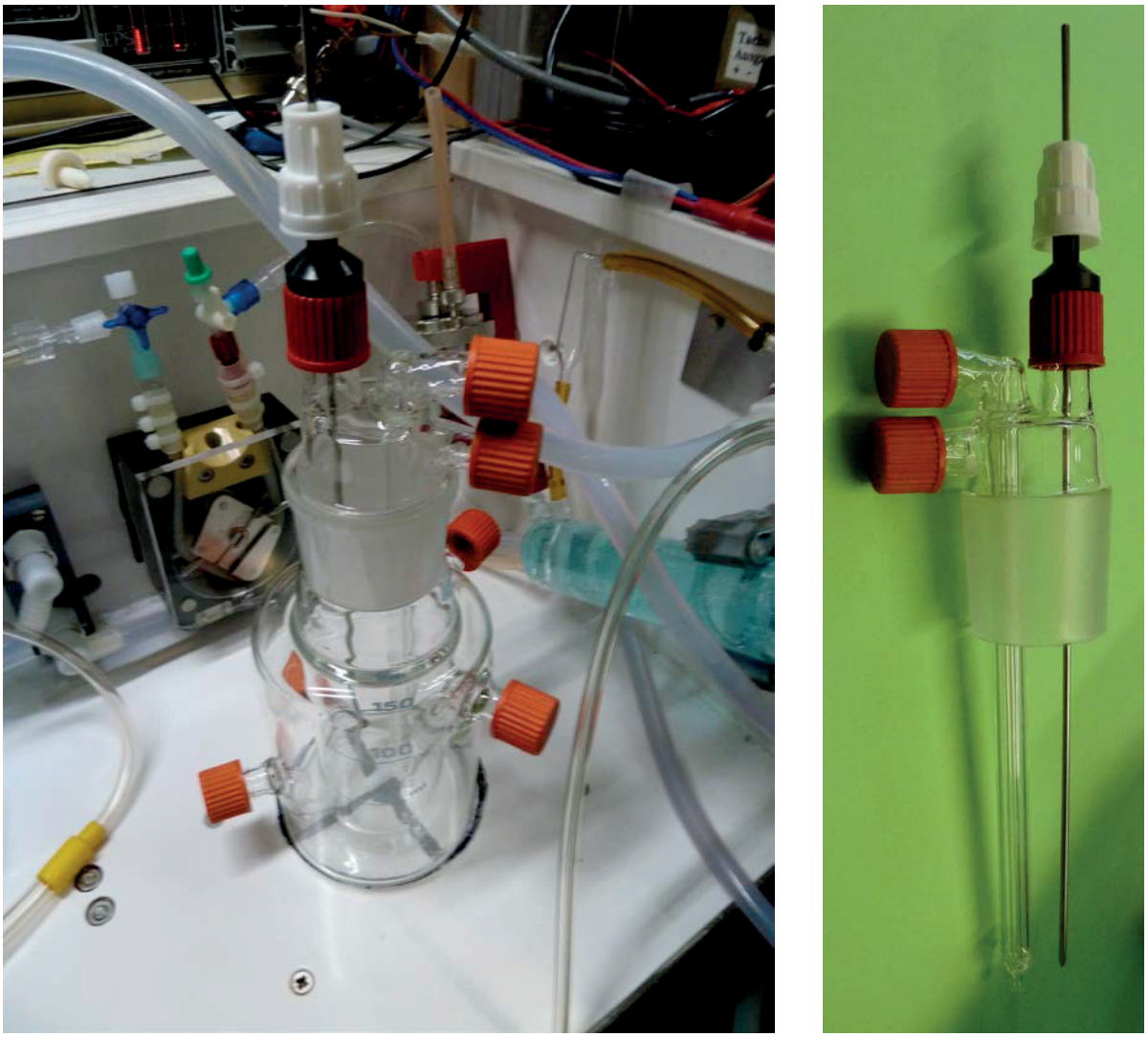

Fig. 5.3.2.: ***Jacketed reservoir with magnetic stirrer.*** The adjustable measuring rod and double-walled glass tube for the recycling of perfusion fluid are shown on the right. The aliquot for blood gas measurement is pumped via a separately inserted narrow stainless steel tube, which also makes contact with the perfusate and serves as the electronic level control, which is used for recirculation plus dialysis (see Fig. 5.2.3., which shows the steel tube in the inserted position).

5.4. Reperfusion after anatomical fixation

The method originated by chance when fixative leaked from the ureteral catheter during the fixation process. The complexity of micropuncture experiments, and the fact that the distribution of electric charge is preserved after fixation, prompted us to develop this reperfusion model. The technique used for the fixation and reperfusion has been described in detail in three doctoral theses and several publications (50-53, 78, 266, 317). The following Figures demonstrate the fixation set-up, the storage chamber for the fixed kidney including the perfusion cannula, the ureter catheter and the pressure-measuring line, as well as the set-up for reperfusing the kidney at normal temperature.

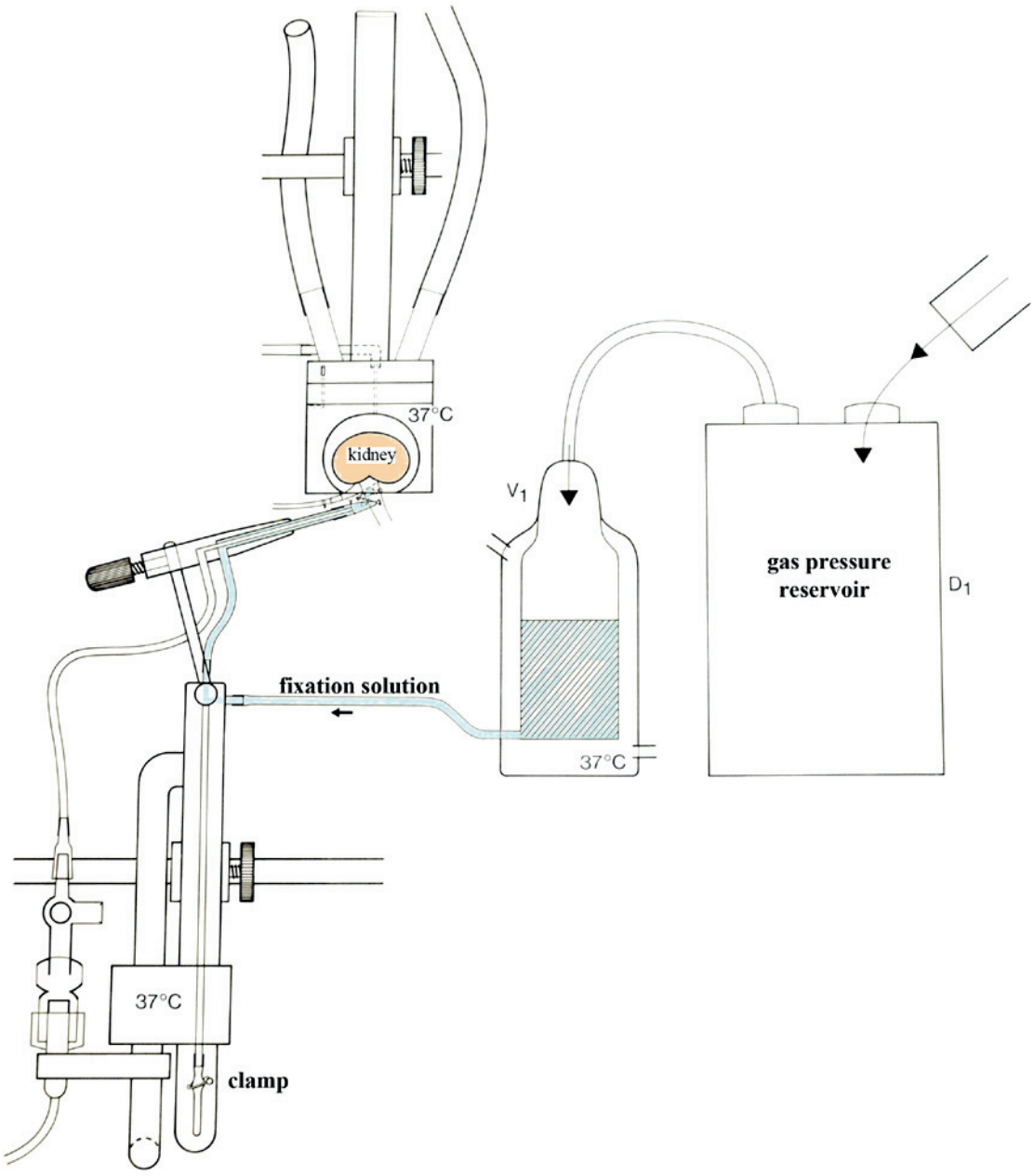

Fig. 5.4.1.: ***Set-up used for perfusion fixation.*** Fixation is carried out via the arterial bypass after blocking off the perfusate supply. A 1.25% solution of monomeric glutaraldehyde in PBS buffer with additional colloid (i.e. HAES 6 g%) is used, and a perfusate pressure of 150 mmHg has proven to be adequate when reperfusion is planned. Moreover, the addition of Verapamil shortly before the onset of fixation is important for sufficiently high filtration rates. The procedure was developed in 1985 and published later on (50, 53, 78, 266, 317).

For further details, see Chapter 10.4.

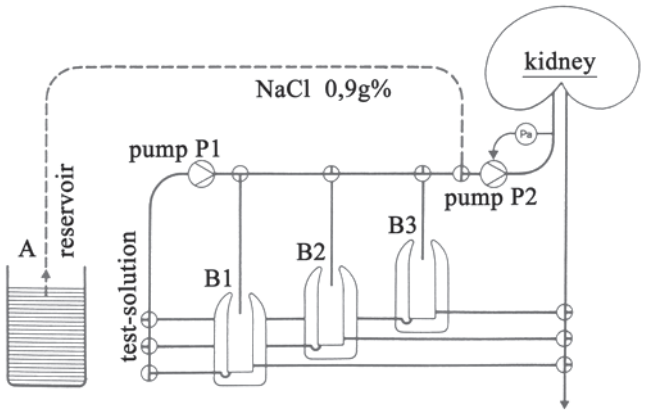

Fig. 5.4.2.: ***Schematic diagram of the reperfusion apparatus.*** A plexiglass box is used for storage of fixed kidneys at 4°C (see Fig. 5.4.4.). For reperfusion, the fixed kidney is flushed free of residual fixative with 0.9% NaCl-solution (37°C) at a pressure of 100mmHg. Thereafter, (see Fig. 5.4.3.) various test solutions can be used sequentially to determine glomerular permeability for macromolecules (50, 78, 266, 317).

Fig. 5.4.3.: ***Temperature-controlled triple chamber.*** This allows three different solution variants to be used sequentially for recirculation perfusion. Between changes, an aliquot is discarded in single-pass mode to avoid a contamination of the following solution. The upper ports are connected to the circulation thermostat. The three ports below connect the three chambers.

The next photo shows the storage box for the perfusion cannula, the kidney, the ureter catheter and for the pressure-measuring line plus three-way stopcock.

Fig. 5.4.4.: ***Storage box (cool box) for fixed kidneys.*** On the left is the open box, with perfusion cannula and pressure measuring line. Fixed kidneys (bathed in fixative) can also be stored in the box, which is then sealed with Scotch tape and kept at 4°C until use, days or weeks later.

6. Sterilization and disinfection procedures

All components of the perfusion apparatus that come into contact with perfusate or dialysate must be thoroughly rinsed, and disinfected or sterilized. In this respect, compromises should be avoided as far as possible, as our early experiences showed. Specifically, perfusate and dialysate must be sterilized by filtration through a 0.2 µm filter immediately after preparation, in accordance with the principles of clinical hygiene. In addition, in-line filters should be used to avoid contaminating the recirculating medium with tissue fragments inadvertently produced during the surgical procedures. Use of in-line filters is worthwhile even for single-pass perfusion, except when erythrocytes are added. In the latter case, large-pore filters (or none at all) may be used. Endre in Oxford used either of two different types of filters when red cells were added, one from Pall and a transfusion filter made by Fenwall (20-40µm) (70), Leon L. Miller used white silk of 100-150 standard mesh (174). In retrospect, our most stable preparations were those that were done in the Medical University in Hannover. When gas sterilization with ethylene oxide was still in routine use there, sets of tubing were tightly wrapped in paper/transparency foil for gas sterilization, stored until the gas had diffused away completely and then reused.

6.1. Disinfection bath

At the end of each experiment, tubing and plastic parts, such as three or four-way stopcocks, are rinsed with tap water or deionized water, and immersed within a disinfection bath (10-30 liter volume, Bode Chemie, Hamburg, Germany). We have successfully used both sodium hypochlorite (Milton®) and Clearsurf® (quaternary ammonium compounds, Fresenius Medical Care) for this purpose. The plastic material is soaked overnight, rinsed with deionized water on the following day, and dried in a drying cabinet at 52°C. Longer lengths of tubing may be ventilated with filtered compressed air and dried again.

6.2. Thermal disinfection

Glass and metal parts can also be treated in the disinfection bath, or are rinsed thoroughly after the experiment and then heat-treated in a drying cabinet at 132°C. In addition, plastic screw-caps used for glass connections can be disinfected in this manner, provided they can withstand the high temperature (see instructions by the manufacturer). To avoid the risk of microbial contamination from the water baths, the use of commercial additives is obligatory. Clouding of glass parts can usually be remedied with 50% citric acid; if this fails, a bath in chromosulfuric acid (available in any glass-blower´s workshop) can solve the problem.

6.3. Sterilization by ethylene oxide

When gas sterilization with ethylene oxide was still possible at the Medical University in Hannover, sets of tubing were tightly wrapped in paper/transparency foil for gas sterilization, stored to allow the gas to diffuse away completely and then reused. After the switch to physical plasma for clinical sterilization in Münster, this was no longer practical.

6.4. On sterility of the perfusate

Fig. 6.1.1 illustrates what happened when we used what was then the standard approach for the preparation of perfusate (i.e., without any sterilization). The plot clearly shows why we decided to use sterile perfusion solutions instead! The Haemaccel-based solution was prepared on the day of the experiment by mixing the dry powder with stock solutions of electrolytes and metabolic substrates for use in the single-pass perfusion mode. Note the drastic rise in perfusion resistance when the same batch of perfusate was used in subsequent experiments on the same day. This effect was eliminated only after the Haemaccel stock solution had been ***filtered and autoclaved***, then mixed with **sterile** electrolyte stock solutions and substrates and **filtered** again through an 0.2-µm membrane (257). When a high albumin concentration (e.g. 7g/dl) is used in the recirculation mode, this difficulty can be overridden by the extremely high flow rates under these conditions.

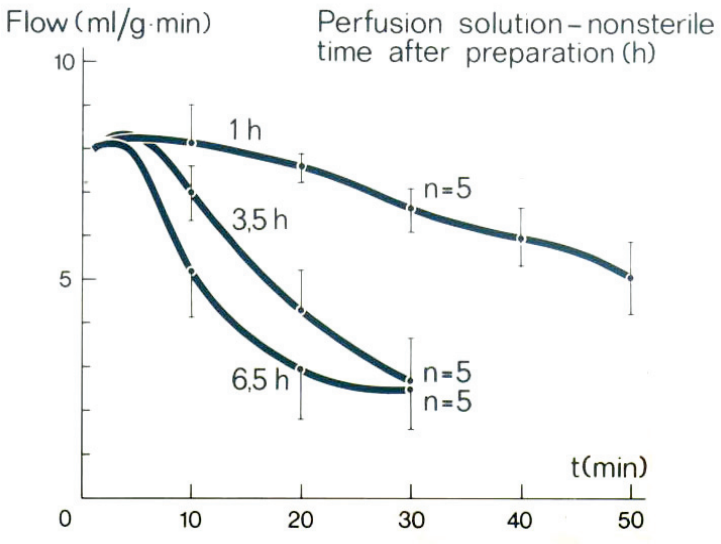

Fig. 6.4.1.: ***Time course of the flow rate in a single-pass perfusion with Haemaccel as colloid.*** The first perfusions began 1h after preparation of the solution. The subsequent ones were initiated on average 3,5h and 6,5h after perfusate preparation. Perfusion pressure was constant at 100mmHg (257).
Conclusion: The time-dependent increase in resistance correlates with the level of bacterial contamination.

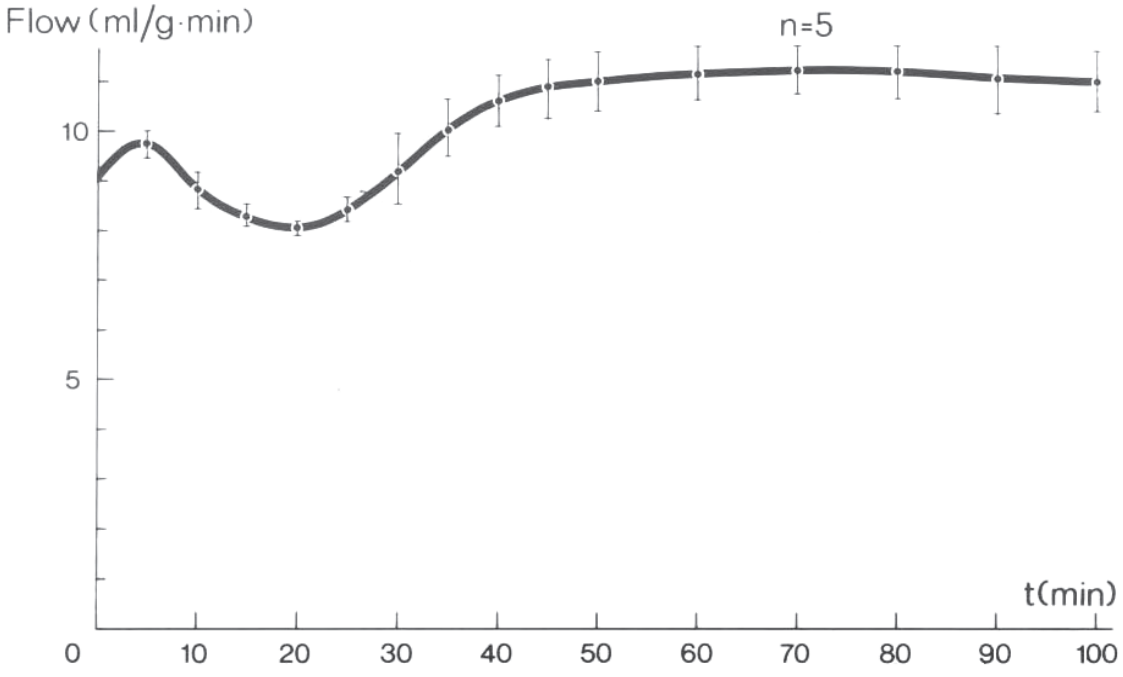

Fig. 6.4.2: ***Perfusion rate with sterile Haemaccel-solution***. In addition to sterilization of the perfusate itself, the perfusion lines were subjected to rigorous disinfection and sterilization. The fall in the flow rate at 20min is probably due to the filtration of low-molecular-weight fractions of filtered Haemaccel, which initially increases the viscosity of urine (257) at a time when the volume of filtrate is still low and the reabsorption capacity for sodium is still high.

When H.M. Brink in Nijmegen (Netherlands) used Pluronic F108 as the colloid (43), he too observed an increase in viscosity in the fluid in the tubules, based on measurements of this colloid in the urine.

7. Anesthesia

Anesthesia is commonly induced in the rat either with the barbiturate 5-ethyl-5 (1´-methylpropyl)-2-thiobarbituric acid (Inactin®) administered at 80-150mg/kg BW i.p., or with a 1:40 mixture of xylacine (2%) and ketamine (10%). Thiopental (Trapanal®) is a possible alternative. In anesthesia, one must avoid hypothermia. To do so, the animal should be placed on a heated table (>40°C) and the rectal temperature must be monitored.

Barbiturate anesthesia induces slight hypoxia, as revealed by a stimulation of erythropoietin synthesis (241, 242). Active ventilation with 25% oxygen inhibits this rise in the rate of EPO synthesis during the operation (242). Furthermore, the typical oscillation of nephron function disappears under the influence of barbiturate anesthesia, but is still detectable after light halothane anesthesia (143, 259). This type of anesthesia (halothane and its successor substances) is more complex to administer but easier to manage, and more supportive of renal function (119, 120). It is scarcely possible to quantify how many physiological investigations are carried out on small mammals in a state of hypothermia! Beginners will find anesthetization with Inactin easier, because the substance distributes into the fat stores, which then serve as a reservoir; in contrast, the combination xylacine/ketamine must be replenished frequently (by instillation into the peritoneum).

Anesthetization with gas-phase anesthetics such as halothane and its successors is more complex, but provides for better oxygenation (120, 143) and better renal function. Under these conditions, oscillations in nephron function persist, while they are suppressed by the barbiturate (117, 143, 259).

8. Surgical procedures and perfusion connections

8.1. Selection of surgical instruments

Here several variations are possible, depending on the manner of fixation on the operating table and the surgical technique chosen. The following Fig. shows the set of surgical instruments we currently use. The cork inserts lateral to the operating table (temperature-controlled by water-bath; see Fig. 8.2.01) can be used to secure abdominal-wall hooks.

Fig. 8.1.1.1.: ***Standard set of surgical instruments (above) and a cauterizing electrode.*** **Upper panel:** Impaled in the cork ring on the left is a selection of home-made stainless steel abdominal-wall hooks, together with two additional liver hooks. At the top are Sugi suction swabs and cotton buds for atraumatic dissection. On the right various forceps, including so-called watchmaker´s forceps (third pair from the right). On the extreme right are two differrent-sized Deschamps ligature needles (with eyelet for securing thread). Besides the cork ring are scissors. The small spring scissors in the center should be handled with care - it is essential for cutting the ureter, as well as the mesenteric artery or aorta, for intubation with catheters and cannula respectively. To the right is a small vascular clamp and a fixing clamp built by Martin Wensing in the research workshop in Münster that prevents the aortic cannula from slipping out if the ligature can be tightened only after the start of perfusion. **Lower panel:** Small, battery-powered cauterizing needle electrode (Erbe Elektromedizin GmbH, Tübingen, Germany).

8.2. Surgical technique and connection procedures

After induction of anesthesia, the animal (previously shaved on the ventral side) is placed on a temperature-controlled surgical or micro-puncture table. To maintain body temperature at 37°C (monitoring of rectal temperature is necessary), the table must be preheated to approximately 42-43°C. After opening of the abdominal cavity, a warm-water

pillow can be placed on the chest area, because in anesthesia, the body temperature can quickly drop below 35°C under anesthesia (feedback-regulated, electrically heated surgical tables are now available that monitor and maintain body temperature automatically). We have modified the surgical techniques of Weiss (307) and Bahlmann (13, 251, 253). The jugular vein can be initially intubated with PE10 tubing to compensate for fluid losses and for injection of heparin. Alternatively, heparin may be injected with a thin needle into a lobe of the liver immediately prior to the start of perfusion. After making a midline incision with scissors along the linea alba from the xiphoid process to the pubic symphysis, the gastric intestinal convolution is placed in a wet compress on the left and the abdominal cavity is exposed by securing the flaps of the abdominal wall with four appropriately positioned wall hooks (inserted into the lateral cork strips). To provide a better overall view, one may choose -- after thermal coagulation of the epigastric artery from inside the abdominal wall -- to resect the right abdominal wall transversely below the costal arch.

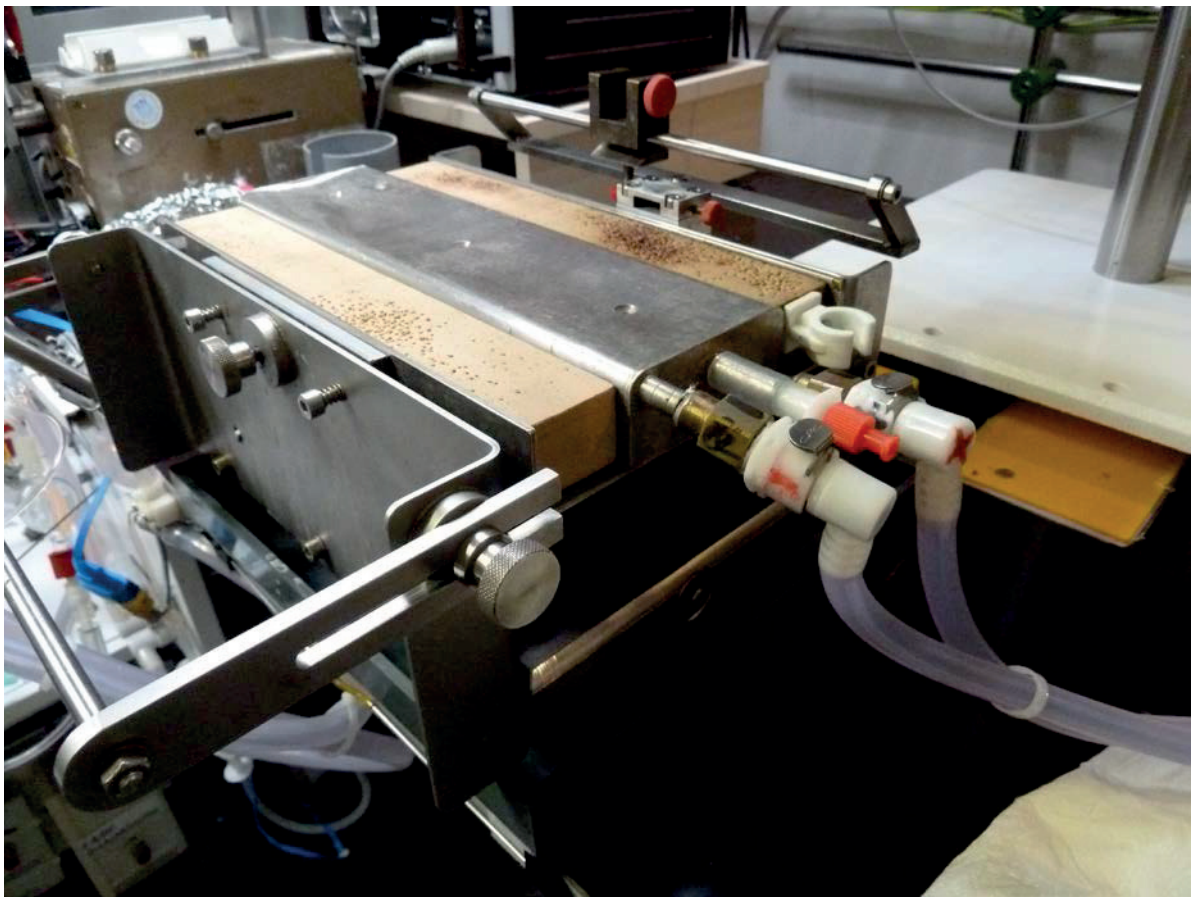

Fig. 8.2.01.: ***Small animal operating table.*** This is a robust version for micropuncture experiments. An insert for the operating table, heated by a circulation thermostat, enables it to be positioned and removed with the scissors lift. The mobile insert enables a second operation to be started at a second operating table while the perfusion set-up is being prepared (calibrated etc.) at the first station. For connection of water-jacket tubing see Fig. 5.1.09.

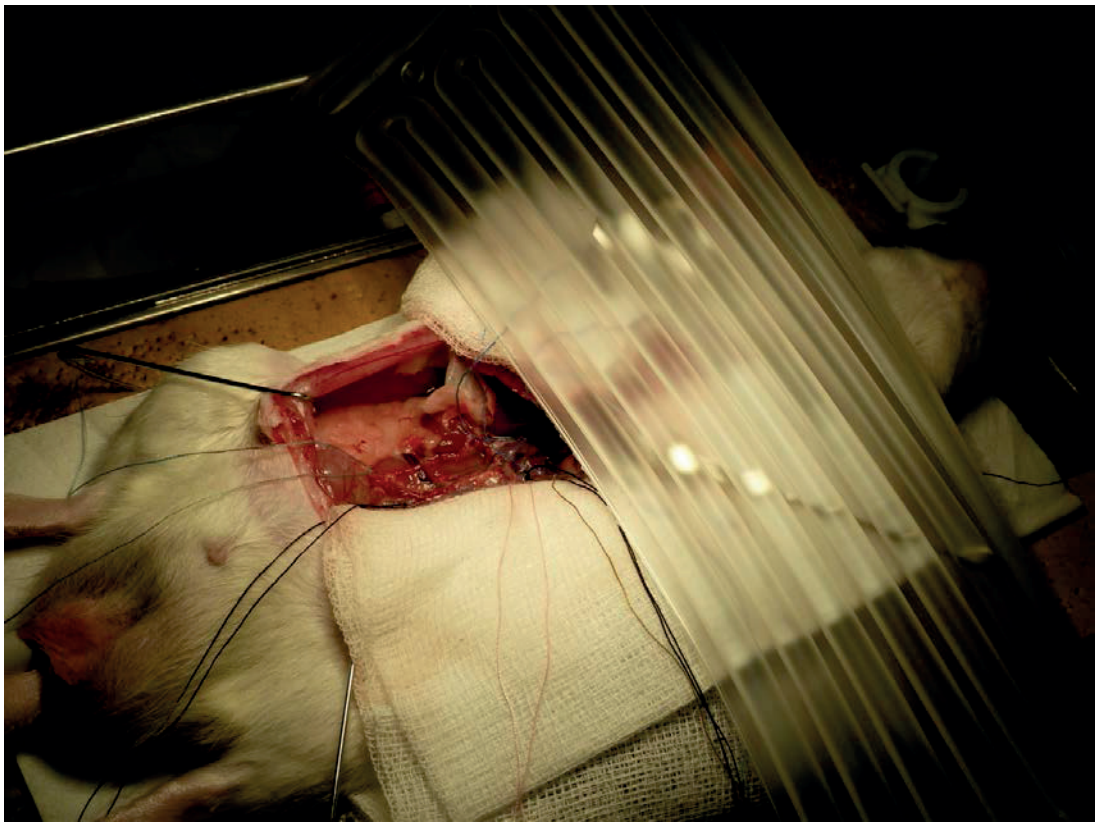

Fig. 8.2.02: ***Operating table and partial view of the viscera in the abdominal cavity.*** Operating table and view of the abdominal cavity, with the gastrointestinal convolution placed to the left and a water pillow on the chest wall to compensate for the heat loss. The right abdominal wall has not yet been resected.

To prepare the blood vessels for ligation, one should first proceed with blunt cotton buds to remove the thin peritoneum, and then extend using blunt tweezers. Figure 8.2.03 presents a simplified sketch of the disposition of the abdominal vessels. One can adopt either a fast or a meticulous strategy. The adrenal artery, which usually sprouts from the right renal artery, can be tied off directly. The remaining ligatures are first set in position only (for this purpose we use different colored polyester sewing thread, thickness Ne 40/2). The fat capsule is dissected away, leaving a rim of fat around the kidney to facilitate manipulation of the organ with forceps, and then the connection to the adrenal gland can be exposed with a pair of forceps and thermally cut. Here, a flat and broad liver hook provides a better overview. Before cannulating the ureter, first cut the surrounding fatty tissue away and remove the adventitia with its associated vessels where the incision is planned. Close off ligature 1 and tighten the ligature on the ureter slightly (e.g. using a small alligator clip or forceps). Cut the ureter halfway through at a point just below the level of the distal end of the kidney, widen the lumen with one jaw of a watchmaker´s forceps, intubate with the combined catheter (10mm PP10 cut obliquely and extended by insertion into PE50, or a glass-catheter with PE50 inserted) and secure it twice by ligature (PP10 and PE50) before setting the distal cut. The catheter tip in the ureter should not be

rotated or placed too close to the renal pelvis (and certainly not positioned within it). The right kidney can then be gently heaved in situ within the kidney tray. This is easier to do if the right abdominal wall is cut transversely after having first let the vasa epigastrica of the abdominal wall coagulate from the inside, cranial and caudal to the intended site of incision. Immediately before the final connection (prior to perfusion) the mesenteric artery as well as the left renal artery can be ligated off, following the injection of a small bolus of heparin (e.g. 50µl, 250U) i.v. or into a liver lobe (use a thin hypodermic needle). The distal aortic ligature can be tied off and the thread tightened (e.g. by the weight of an attached Halsted mosquito-clamp). After placing the vascular clip immediately distal to the origin of the right renal artery, the aorta can be cut in half. Under microscopic control, one can dilate the aorta at the point of incision with watchmaker´s forceps and intubate with the (previously flushed) double-barreled cannula. The small protruding inner cannula serves as a pioneer (the inner cannula is also flushed before via the pressure transducer). The cannula is advanced to the clip, mechanically fixed and then ligated. If the gap is too short, the cannula can be ligated after the start of perfusion, but in this case there is a risk that it may slip out of the aorta (s.a. Fig. 8.1.1.1; fixing clamp after Martin Wensing).

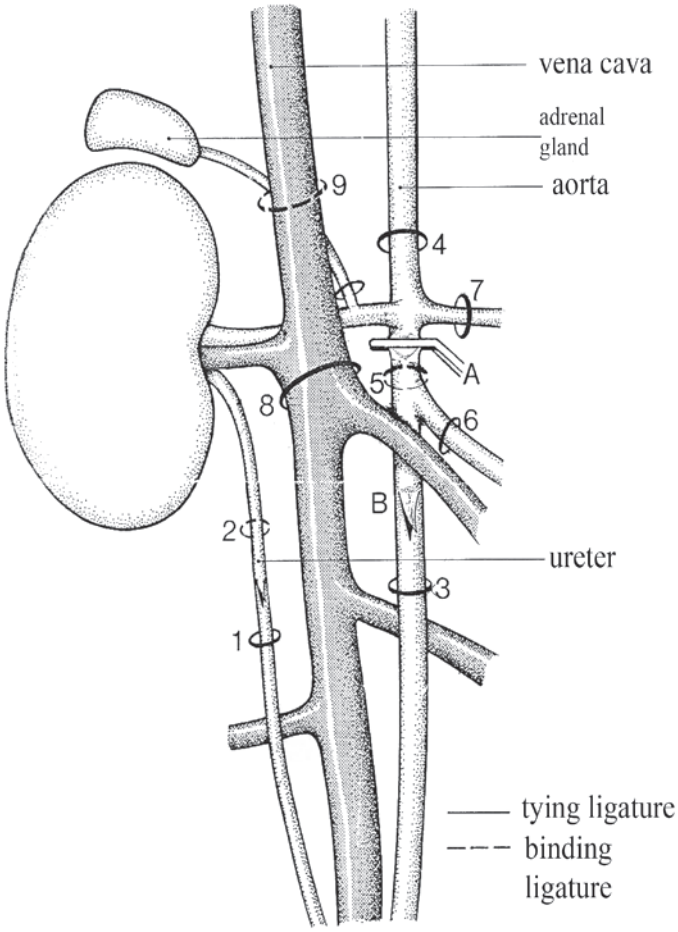

Fig. 8.2.03.: ***Overall disposition of the renal vasculature a er gross dissection.*** Modified after Ross (224). Tie-off ligatures are indicated by circles, connecting ligatures by broken circles. This scheme depicts our approach to cannulation of the distal aorta with a double-barreled cannula. Following the procedure of Bahlmann and Nishiitsutsuji-Uwo the renal artery was intubated via mesenteric artery, which is practical only when larger animals (>300 g) are used and requires “ideal” vascular anatomy (13, 185). The point of cannulation of the ureter lies closer to the distal end of the kidney, as shown in the schematic drawing. However, the catheter tip should not come into contact with the renal pelvis due to the risk of bleeding.

Then connect the suction tube to a suction pump (with collecting vessel or water aspirator). Tie-off the proximal aortic ligature, release the vascular clamp and begin perfusion, initially at constant flow (e.g. 8-10ml/min). Transect the aorta (including the associated sympathetic nerve on both sides) and the vena cava just below the liver, using active suction to clear the kidney tray of blood, which will otherwise obstruct your view. Lower the operating table together with the animal on the scissors lift. Disconnect the remaining connections until the kidney tray and perfusion cannula are free. The operating table is then pulled away with the animal, the kidney preparation is rinsed with warm saline to remove residual blood and the collecting funnel is swiveled or moved under the kidney tray. At this point, the recirculation circuit is closed and perfusion is continued in the pressure-constant mode. Mounted at the funnel is a metal catheter for intubation of the inferior vena cava, which is swung into position and fixed by ligature. The cava ligature is then closed distally.

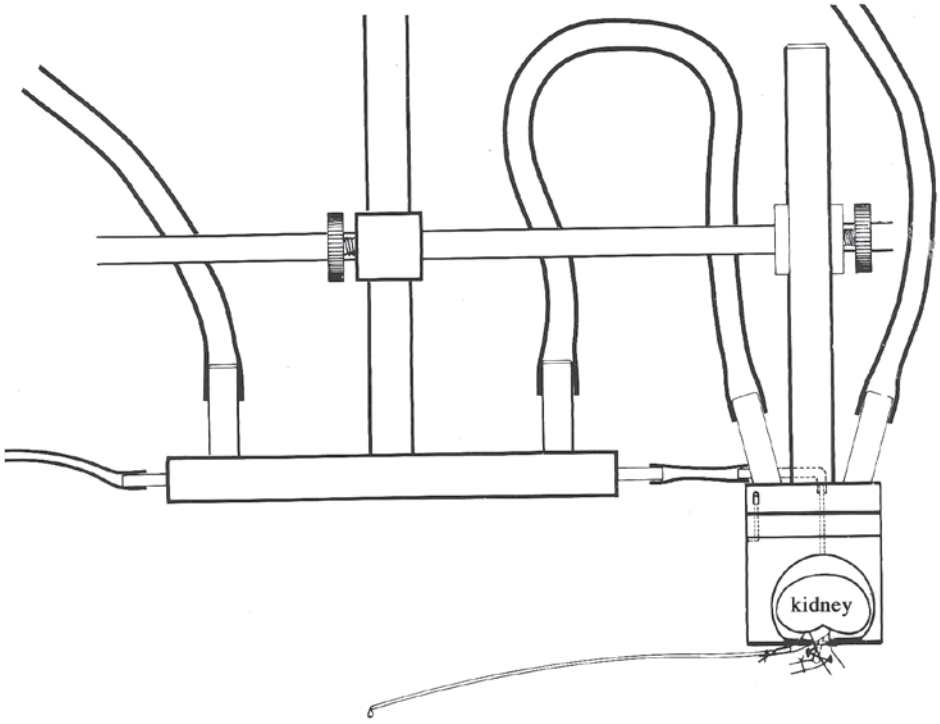

Fig. 8.2.04.: ***Position of the kidney in the tray.*** The kidney lies on the heated kidney tray (250). The warming block on the left is a relic of the time when, during single-pass perfusion, tubuli were micropunctured under an oil film, which was warmed up in this way.

The phenomenon of vasoconstriction after the start of kidney perfusion

Sympathetic nerve fibers/tracts run parallel to the aorta on both sides. If these nerves are not completely resected prior to the start of the perfusion, rapid and intense vasoconstriction may occur in parallel with the onset of gasping. Even short-term ischemia will ruin the kidney preparation. This was one of the lessons that taught us the meaning of “learning by doing” as we systematically “dissected” the problem.

The following Figure shows what happens, when the in-vivo circulation is switched to the in-vitro perfusion without first severing all links to the sympathetic nervous system.

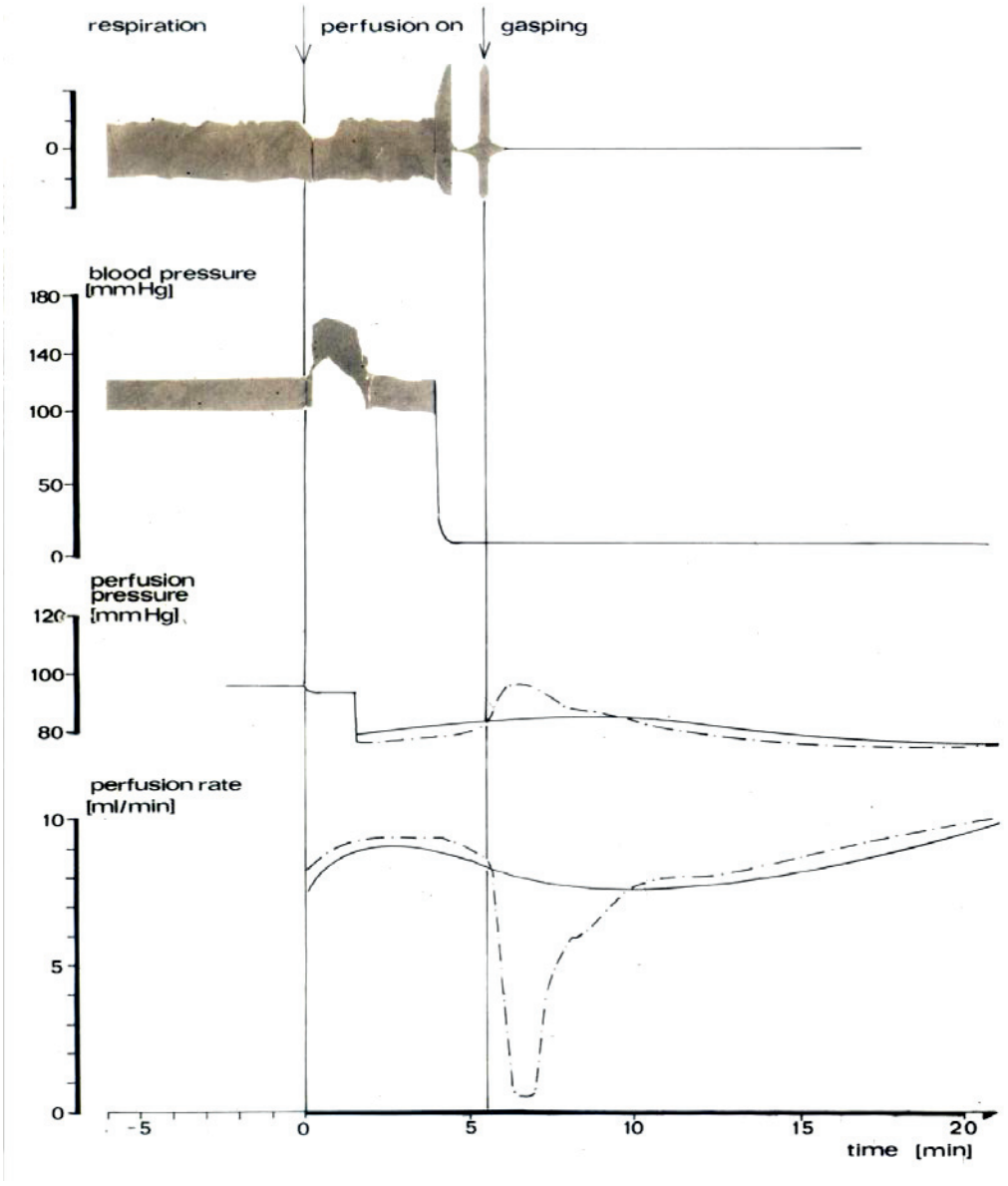

Fig. 8.2.05.: ***Historic record (1969) of sympathetically induced vasoconstriction in the transition phase from in-vivo to in-vitro circulation.*** Single-pass perfusion with Haemaccel-Krebs-Henseleit medium. Upper panels: Respiration (monitored via a thermosensor in the tracheotomy tube) and blood pressure (measured in the carotid artery). Lower panels: Perfusion pressure, i.e. gas pressure (see Fig. 4.1.3.) and electromagnetically registered flow rate (arterial inflow). With ligation of the aorta and initiation of in-situ perfusion, blood pressure rises and respiration amplitude falls. When the vena cava is resected and the aorta is then cut proximally, blood pressure falls precipitously. Two scenarios are shown for the period following the vertical arrow: The broken lines depicting perfusion pressure and flow demonstrates what ensues when resection of the aorta fails to sever the sympathetic nerves on both sides. The solid lines show the result when the nerves are successfully cut through (Institut for Clinical Physiology, Steglitz Hospital, FU Berlin (now Benjamin Franklin Campus), ca. 1969, unpublished).

Fig. 8.2.06.: ***The heated stainless-steel tray currently used for the right kidney.*** Note the lateral suction tube. The asymmetrical cutout in the front wall is designed to accommodate the ureter caudally. The tubing attached to the rear block feeds into a U-shaped channel. Also visible is the scissor lift for the operating table.

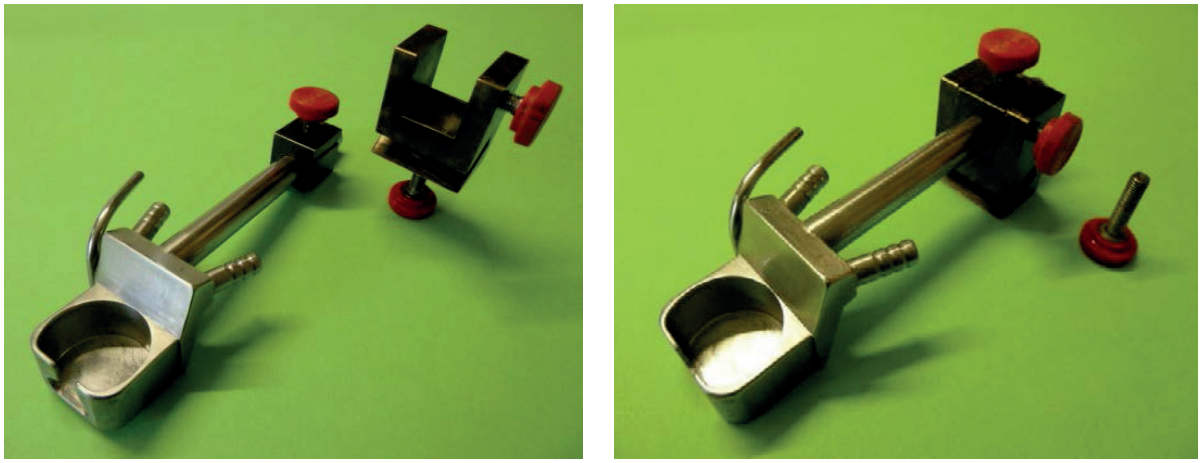

Fig. 8.2.07.: ***Detailed views of the mounting block for the kidney tray.*** The shaft attached to the kidney tray can be inserted into the rear bracket, enabling the kidney to be maneuvered obliquely into the tray from above. For details, see Chapter 15, Fig. 15.0.8 Appendix.

Fig. 8.2.08.: ***Frontal view of the double-barreled cannula.*** In the foreground is the double-barreled cannula with protruding inner barrel. Below it is the clamped tube for the arterial by-pass (pO_2-measurement), behind it the kidney tray connected to the water-bath, on the left the suction tube attached to the kidney tray. To the right of the kidney tray is the rectangular opening into which the arm of the effluent funnel is inserted and fixed.

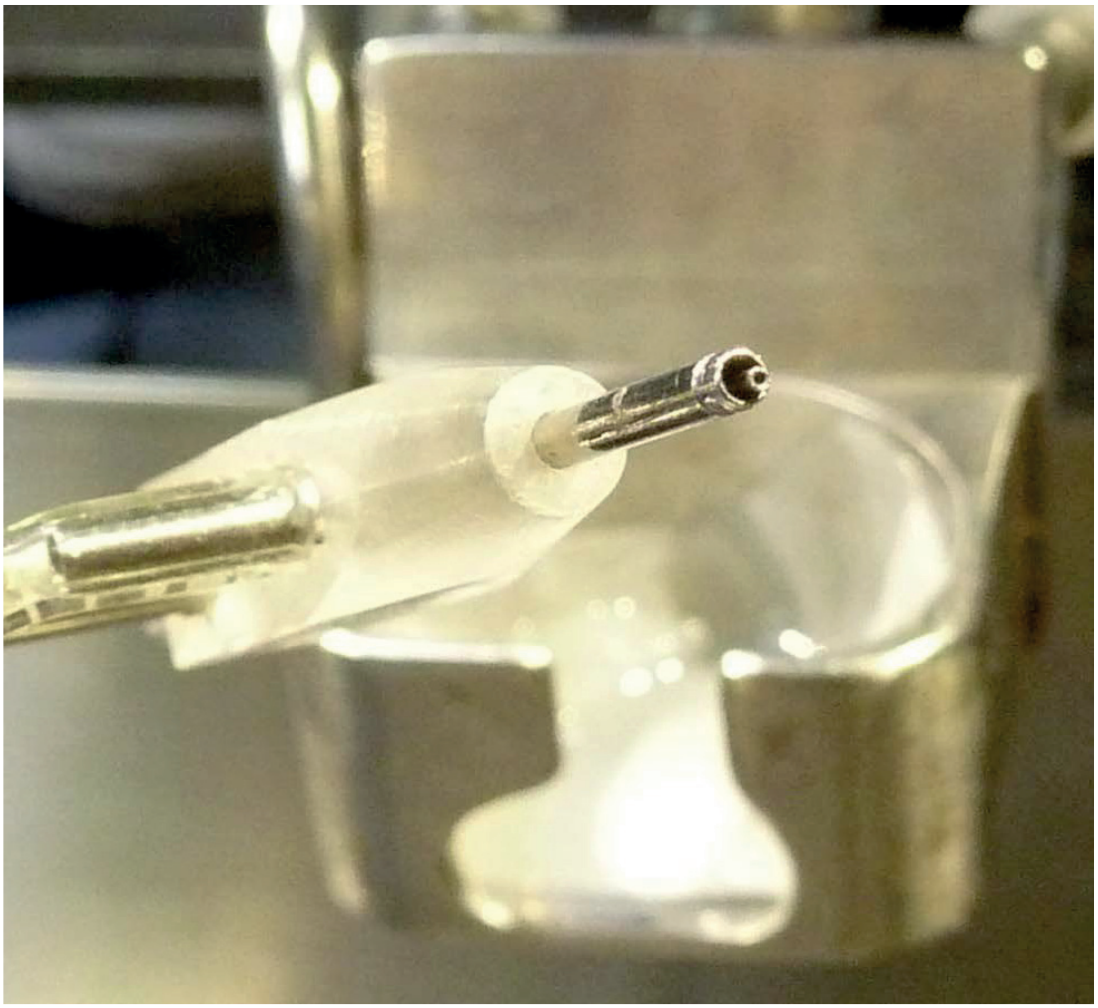

Fig. 8.2.09.: ***Detailed view of the double-barreled cannula***. Note the protruding inner (pressure-measuring) cannula, as well as the circumferential groove used to fix the binding ligature. The protruding inner cannula acts as a "pioneer" and facilitates intubation of the slit-cut aorta. For further details see Technical Appendix.

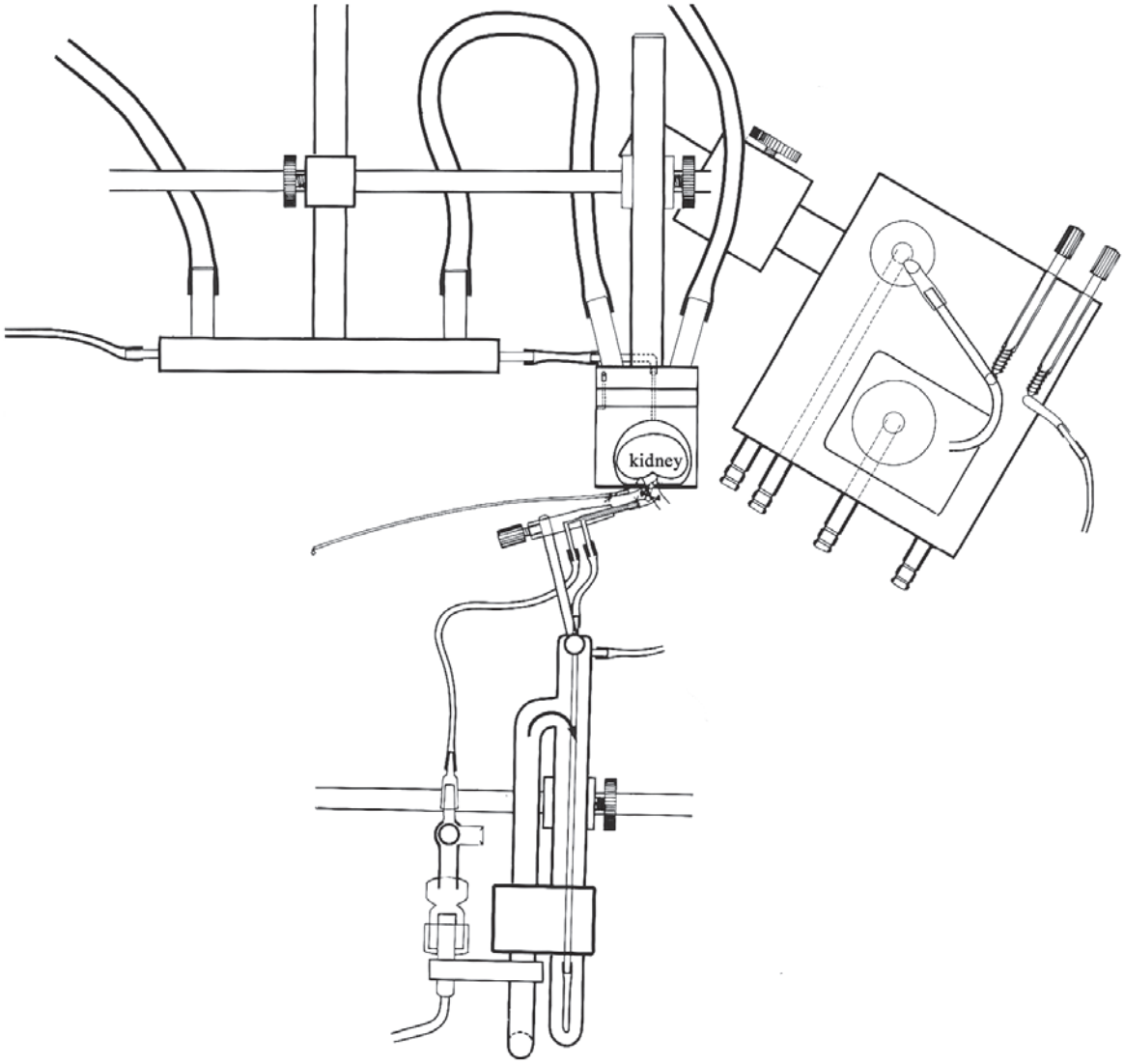

Fig. 8.2.10.: ***Schematic view of the set-up in Phase 1 after start of perfusion.*** The kidney is isolated and perfused in single-pass mode; the collecting funnel has been swiveled into position under the kidney tray (250). The holder can be rotated about a vertical axis. This type allows the effluent from the kidney to drain via the funnel directly below the kidney tray, separately from that from the cannulated vein. In single pass it is discarded, but it is returned to the reservoir in the recirculation mode. Separating the two discharges permits one to quantify any leakage that may occur. The block developed later has only one funnel. This block is only shifted laterally and no longer pivoted (251).

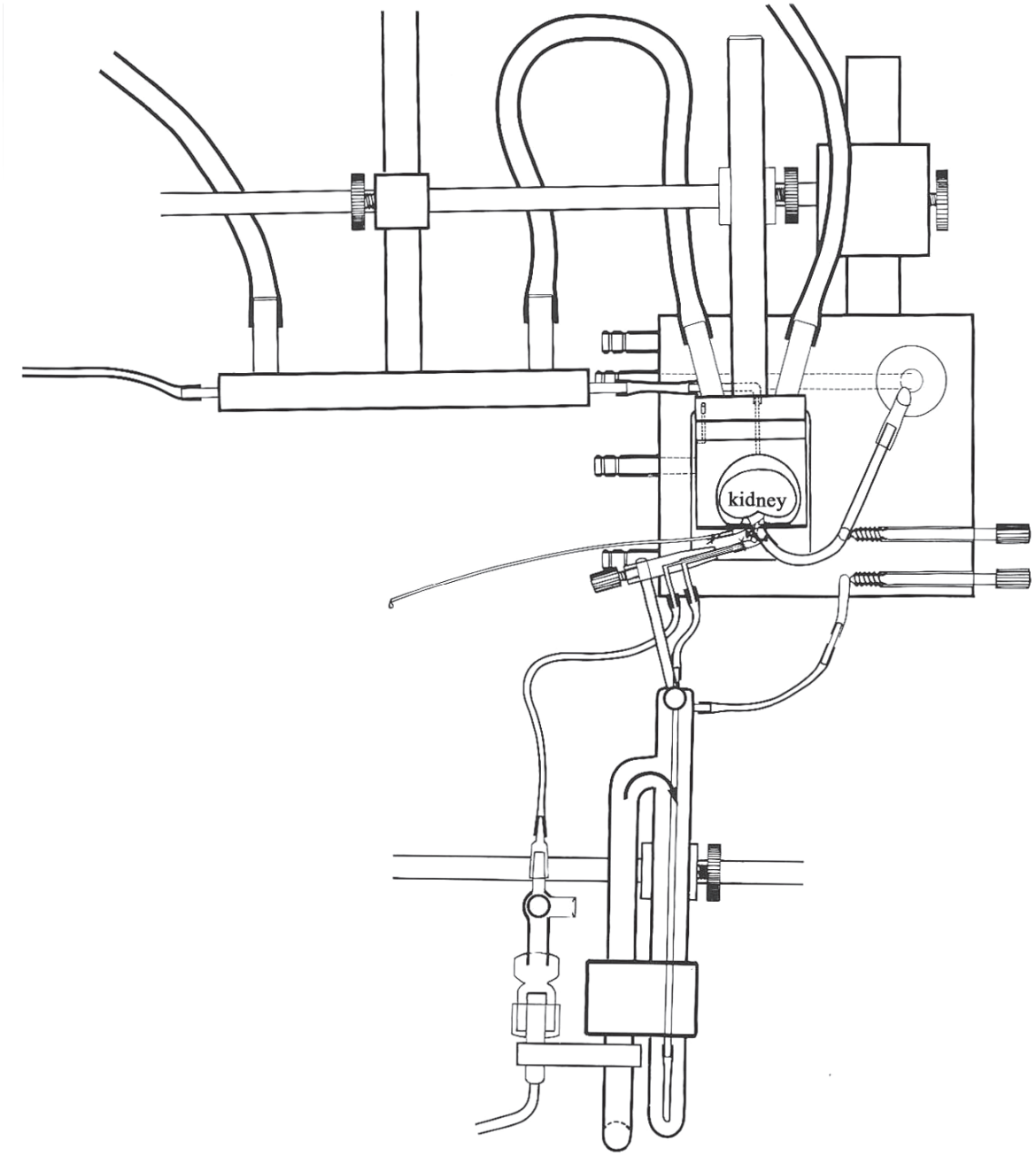

Fig. 8.2.11.: ***Schematic view of the set-up in Phase 2 after the start of perfusion.*** The collecting funnel is in position, the venous cannula is swung into the vena cava and fixed, and the distal ligature of the vena cava is closed, forcing the venous effluent to drain completely through the venous cannula. The fixation screw clamps the T-outlet, through which an aliquot tapped upstream of the pump can be pumped past the O_2-electrode (with an open overflow upstream of the pump) to measure venous pO_2. The arterial bypass can be alternately opened for measurement of arterial pO_2. For further details, see Technical Appendix.

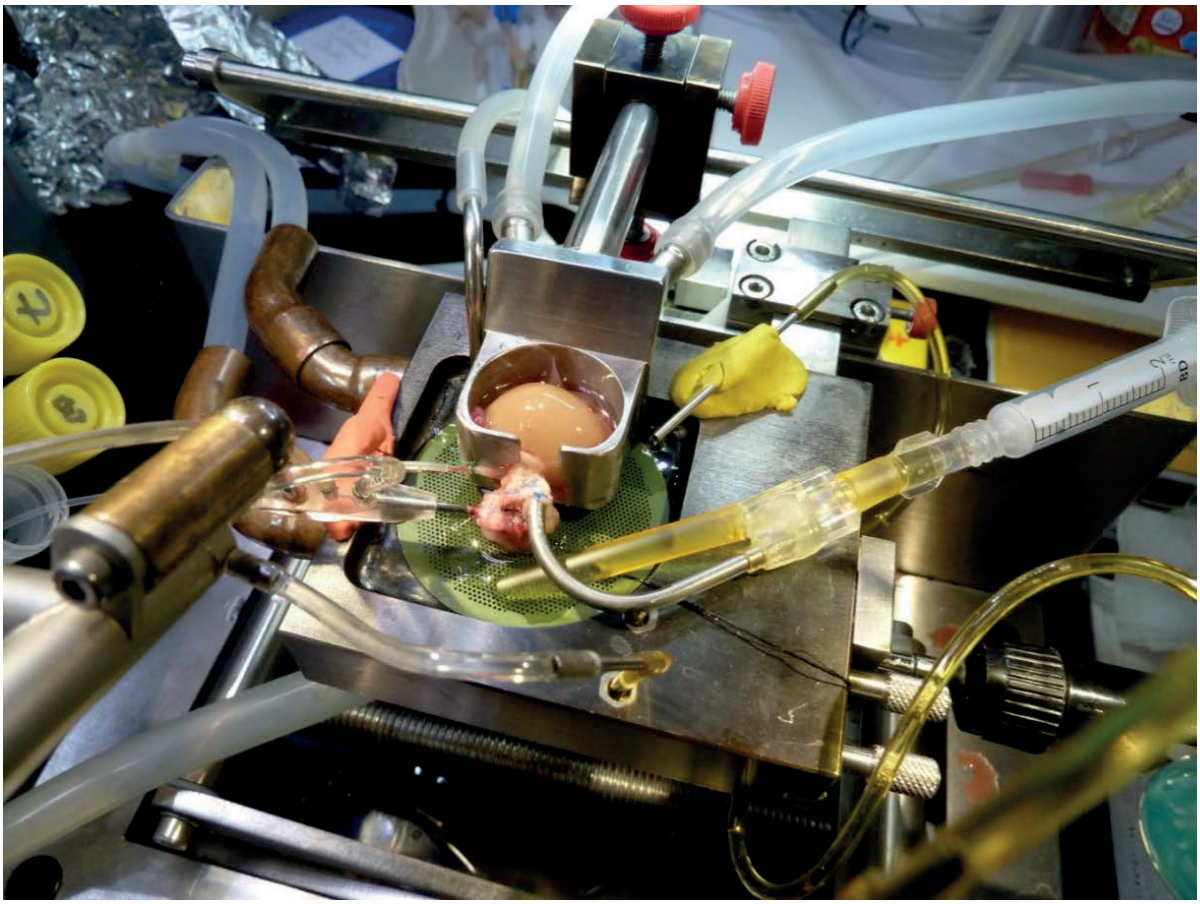

Fig. 8.2.12.: ***Perfusion with a cell-free medium.*** The kidney immediately takes on its intrinsic color. Compared to the collecting funnel shown schematically in Fig. 8.2.10/11, the simplified funnel in this picture is covered with a sieve plate from an online filter (collecting funnel made of stainless steel, Research Workshop, Münster University Hospital). Cannula within the aorta, the vena cava and the ureter catheter (fixed with red plasticine). The yellow plasticine surrounds a steel cannula, which connects the O_2-measuring cuvette to the atmosphere. On the right in the foreground is the arterial bypass for selective measurement of arterial pO_2. The knurled knobs to the right of the funnel-block serve to preconstrict and limit the flow through the arterial bypass, and fix the venous cannula to its downwardly branching T-piece. The venous cannula is connected to a Y-junction, one arm of which returns the venous effluent to the sieve plate, while the other provides a sampling site (Luer port) that can be used to deliver venous effluate to a blood gas monitor.

Blood gas measurements on cell-free media may result in incorrect analyses when aspirated with a syringe because of the relatively small amount of physically dissolved oxygen (gas) present compared with the total amount of gas in the whole blood. This is particularly true for arterial samples. Cheung has discussed this issue in connection with studies on the isolated perfused rat liver (49). Sampling at a freely draining outlet or the use of glass capillaries to which the sample adheres are preferred (see the arterial sample port in Fig. 8.2.13).

Fig. 8.2.13.: ***The holder for the perfusion cannula (the "perfusion gun").*** The "gun" is water-heated up to the magnetic ball-and-socket joint on which the aortic cannula is mounted. On the left arm, warm water flows via a silicon tube from below. In the right arm to which the cannula is attached, the inner steel pipe containing the perfusate is externally connected to a glass tube in F-form, which functions as a final bubble trap and allows one to take samples of arterial perfusate*. The draining tube contains the smaller Tygon tube that supplies the perfusate. Between experiments, perfusion cannula and inner tube are thoroughly rinsed and then filled with 3% formalin solution and stored until to the next experiment.

* Cheung discussed the analytical problem of measurement of pO_2 in cell-free media in connection with studies in the isolated perfused rat liver (49). In earlier days, glass syringes were used for this purpose with smooth-running pistons.

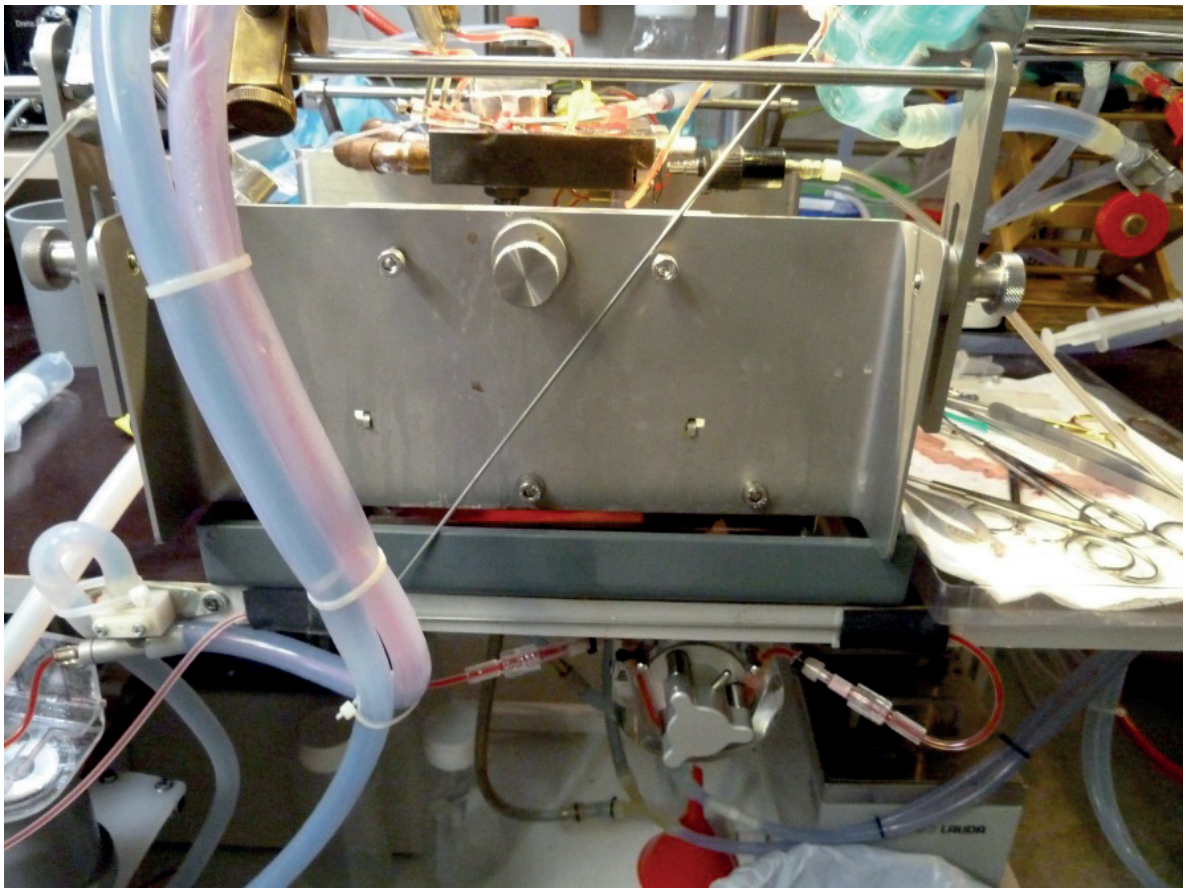

Fig. 8.2.14.: ***Perfusion gun connected to the circulation thermostat.*** Water-bath ports that heat the holder for the perfusion cannula. The inner tube (which is jacketed by the outlet tube) contains a perfusate with added erythrocytes. Below left are the tube that feeds in fresh perfusate and the one that drains the circulating water. Under the table is the peristaltic pump that drives the circuit of the water-heated flow cell of the oxygen electrode. The perfusion gun is movably mounted on the shaft above the operating table, and can be moved in all three directions and locked into position. This provides for optimal positioning and fixation of the aortic cannula.

9. Measurements: Parameters and methods

9.1. Temperature

Passive temperature control by means of an air-conditioning system in a closed cabinet has many disadvantages, aside from the inherently slow response of the medium. Thus, a micropuncture experiment would not be possible under such conditions. Although Bahlmann did indeed use such a cabinet, he positioned the perfused kidney outside of it (13). Effective temperature control by means of a water-heated circulation system requires the use of double-walled, i.e. water-jacketed, vessels and connectors - a double-walled perfusate reservoir, double-walled glass coils and tubes, and provision for heating of the kidney

tray, effluent funnel etc.. Temperature measurement is no longer a problem today as inexpensive devices for this purpose are readily available from consumer electronics stores. Rectal temperature measurement is essential for anesthetized animals (and the operating table must be heated) and the temperatures of the water-baths and circulation thermostats must be monitored. Care should be taken to compensate for heat losses on the way to the perfused organ, insofar as such losses are unavoidable. See the Technical Appendix for details.

9.2. Perfusion flow rate

For pharmacological or physiological studies of the kidney, continuous recording of perfusion flow rate and pressure is strongly recommended. The simplest way to do this is to equip the roller pump with a speed sensor (tachogenerator) and record the number of revolutions of the drive wheel as an analog signal on a potentiometric chart recorder. This type of readout promptly reveals that even slight manipulations of the ureteral catheter can have a direct impact on the flow rate (under constant-pressure operation) or the pressure (in constant-flow mode). This applies to urinary flow rates over 50-100µl/min. At lower urinary flow rates, e.g. when a higher COP (6.5-7.5 g/dl BSA) is used, such unintended changes may otherwise be overlooked. For details of the technique used by us: see chapter 4.2.3. One disadvantage of the method is that arterial leaks can falsify the measurement. If the feedback signal from the perfusion pump's speed sensor is used to control constant-pressure perfusion, a preamplifier is required. For our study of vasoactive substances - which lead to a change in resistance - we modified an infusion technique first described by Joachim Lutz in Würzburg (160), which allows the perfusion rate in constant-pressure mode to be controlled in proportion to the flow rate. This ensures that the final concentration of the substance under investigation remains constant throughout (see Chapter 5, Figs. 5.1.05 and 5.1.06).

Electromagnetic flow measurement is a more expensive option, and requires appropriate technical systems. Less costly techniques based on differences in the travel time of broadband ultrasonic waves are now available which are applicable to pure electrolyte solutions (Transonic T106 flowmeter with cannulating flow probe SN22, Transonic, Ithaca, NY, USA). Both methods have the advantage that they can also be used to measure the venous flow leaving the kidney. (60).

Flow measurement with a rotameter (a float in a conical glass cylinder) is a very simple technique, but the float must be read visually. Depending on the problem, even this technique may be adequate, but has obvious disadvantages compared to continuous measurement and continuous recording.

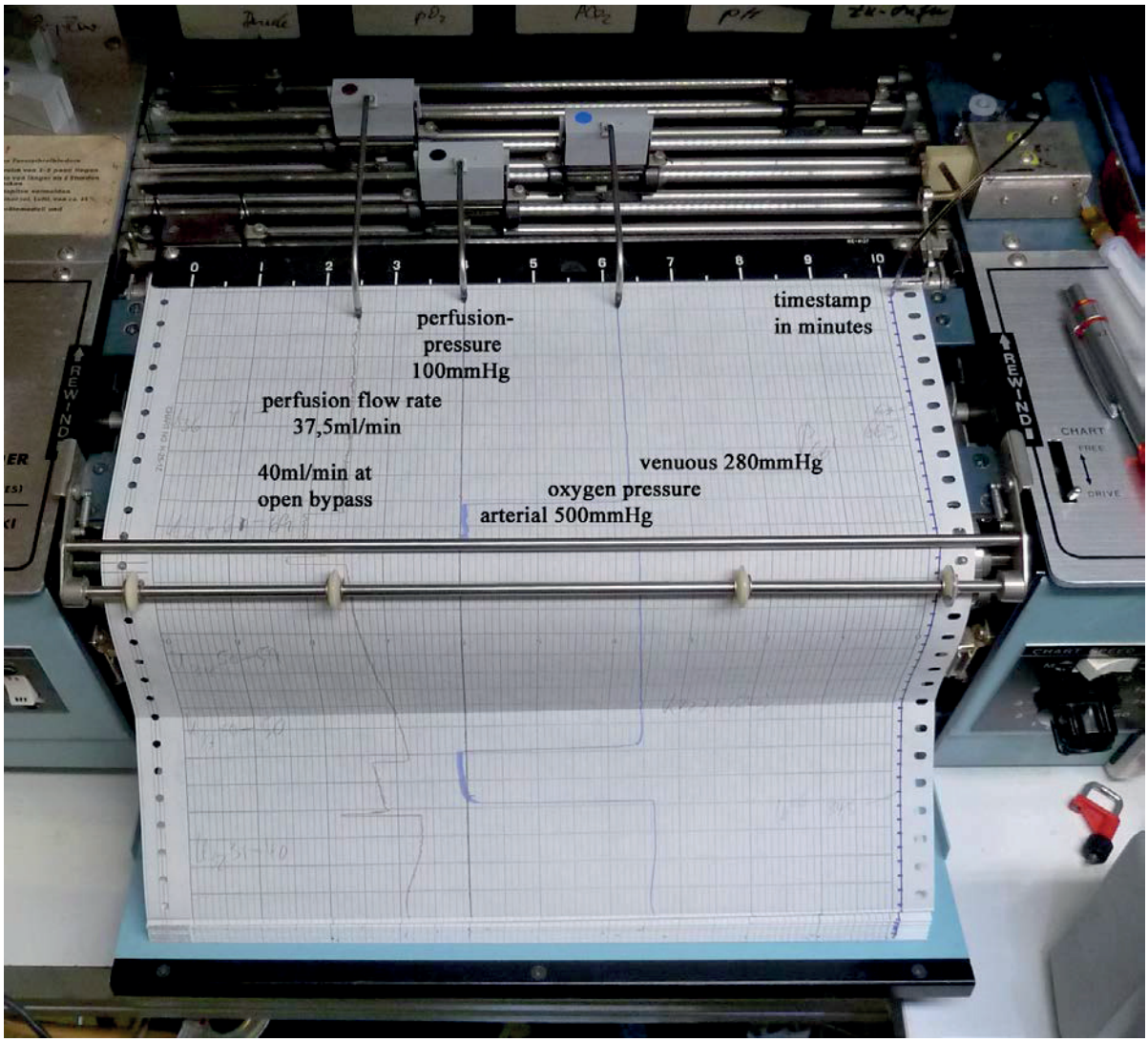

Fig. 9.2.1.: ***Chart recorder protocol from Oct. 7, 2014 (Rikadenki 6-channel chart recorder).*** The experiment used mode-3 perfusion (recirculation with dialysis, Krebs-Henseleit-BSA solution with 5% washed human erythrocytes). On the right is the timestamp (in minutes). The perfusion pressure is 100mmHg (the pressure chosen is indicated on the black bar at the rear (paper output), which is set to 4, zero pressure at 9). The flow rate is 37.5ml/min (30ml/g kidney); in this case, 0 on the black bar is the 50-ml mark, 10 is the zero flow mark. When the arterial bypass is opened the flow rate rises to 40ml/min with no change in the perfusion pressure. In the first switching maneuver (front left), the flow is still low, and the overshoot in the flux peak when the bypass is opened is compensated for manually with the knurled knob (s. Fig. 8.1.2.4.). The oxygen electrode was calibrated with pure oxygen and nitrogen; on the black bar the zero point (N_2 calibration point) for O_2 is 9, the O_2 calibration point is at 2, corresponding to 699mmHg (the barometric pressure was 746mmHg, water vapor pressure at 37°C was 47mmHg). The calculated oxygen consumption was somewhat below 9µmol/min g· kidney.

9.3. Oxygen consumption

When a membrane-coated Clark electrode is used, geometry and calibration of the electrode is somewhat dependent on the hydrostatic pressure acting on the membrane (pO_2-electrode type MT-1-AC from Eschweiler, Kiel, Germany). For this reason, we normally decided not to use one electrode in the venous and a second electrode in the arterial path. It is easier to determine the extent of drift between initial and final calibration easily if only one electrode is in play. We therefore chose to use the same electrode for both venous and arterial measurements. A small roller pump drives an aliquot of the venous effluent past the electrode, which is open to the atmosphere on one side. An electropneumatically operated valve allows arterial perfusate to enter a pre-constricted bypass to the electrode for the determination of the AV difference; a small overflow is allowed in order to avoid sucking external air into the line. Under pressure-constant operation the extra flow through the bypass is actuated and adjusted automatically (s. Fig 9.1.0.). After completion of the calibration at the end of the experiment, the electrode in the chamber should be rinsed free of residues. In recirculation mode, the aliquot used for the pO_2-measurement is recirculated also. Cheung has pointed out that, in the case of cell-free perfusion, drawing samples for discrete measurements with a syringe and/or processing them differently can easily lead to erroneous results. Sampling for this purpose should therefore be done either at a freely draining outlet or using a glass capillary. This problem, which arises because cell-free perfusate contains only physically solved gases (49) while blood samples have a high capacity for blood gases, is negligible with the online-measurement practiced here and can be avoided altogether by using added erythrocytes. At venous pO_2 values above 100mmHg with added red cells, one can calculate the AV-difference directly from the solubility of oxygen and the perfusion flow rate per min per g kidney.

9.4. Urinary flow rate, urinary flow blockage

In Christoph Weiss´ lab, the urinary flow rate was sometimes measured at defined times with a pipette. We prefer to collect the urine in pre-weighed Eppendorf tubes or larger tubes and measure the volume gravimetrically (electronic scale, mg range) at defined intervals. In colloid-free single-pass experiments, 10ml test tubes are required (due to the high rates of filtration and urinary flow). In experiments with BSA in modes 2 and 3 (recirculation, and recirculation with dialysis) 1.5- or 2ml Eppendorf tubes are sufficient. In pure recirculation mode, urine sampling periods can be kept short and the remaining urine can be re-infused, or replaced with an artificial solution that mimics urine, both in its constituents and volume. Reinfusing the remaining urine would be an alternative, but Pegg has noted that urine may contain particles (e.g., tubular cell aggregates or cell debris) that can clog renal capillaries, and he therefore uses a large 0.2-µm filter upstream of the kidney to remove this material (constant sterile filtration). Urine could of course also be passed through minifilters before being returned (196-200). In fact, during cell-free perfusion, the first tubular cells and cell aggregates appear in the urine sediment after about 30 min,

which coincides with the time at which morphologically detectable damage, necrotic TAL segments and P_3 segments first become manifest (7, 42, 63, 263).

If the flow of urine is blocked deliberately (e.g. by twisting of the ureter) and the perfusion flow rate is being continuously recorded, the drop in the flow rate becomes immediately obvious, provided the flow of urine exceeds > 50 µl/min. When the obstruction is removed, the flow rate instantaneously rises again. Obviously, such a blockage is far more difficult to detect with a simple rotameter - in particular at high COP and low urine flow rates. Continuous monitoring is far more sensitive and informative.

9.5. Glomerular filtration rate (GFR) and its measurement

9.5.1. Inulin, polyfructosan, sinistrin

Inulin was affordable when it was still being used for clinical clearance investigation. Meanwhile, sales figures have obviously fallen and the price has correspondingly gone up. In addition, either tritium- or (more commonly) ^{14}C-radiolabeled inulin is used by authors in the field, especially for the recirculation technique with small volumes of perfusate. We have deliberately avoided radioactive markers. In recirculation mode, fluorescence-labelled indicator substances can be used, which are based on polyfructosan resp. sinistrin (61, 156). I myself have no personal experience with such markers. We used inulin and/or polyfructosan for a long time at concentrations of 30-100mg/dl of perfusate, either in single-pass mode or in the recirculation/regeneration mode. Glucose was measured enzymatically with the hexokinase/glucose-6-phosphate dehydrogenase method and polyfructosan was measured with the same assay after acid hydrolysis by incorporating a phosphorhexose isomerase reaction into the procedure (239). Alternatively, we used the anthrone method, which has a glucose error that can be kept low, as Nagel was able to show (176). In the enzymatic inulin analysis, Walter Pfaller´s group used a inulinase for enzymatic cleavage of polyfructosan, a technique first described by Kuehnle (133). This approach avoids the time-consuming acid hydrolysis step at high temperatures, but urine samples must be appropriately diluted.

9.5.2. Creatinine

These days we make use of the rate of creatinine clearance (kinetics of the Jaffé reaction) as a measure of GFR, even though there are no endogenous chromogens in the synthetic perfusate and values for male animals are somewhat (10-20%) higher than those for inulin clearance, due to secretion. We routinely use creatinine at a dose of 2mg/dl (a maximum of 50mg/dl is possible), and add urea where appropriate (6mmol/l). Bowman has argued in favor of creatinine as a marker of GFR because it is easy to measure, the lack of interacting chromogens in the artificial medium “does not matter” and creatinine secretion at high dosage (up to 50mg/dl) can be neglected. Large doses provide a means of depressing the sodium concentration in the final urine by displacement, allowing spectacularly high (and

largely misleading!) fractional sodium reabsorption levels (at high COP, albumin >6g/dl) to be achieved. This high creatinine concentration outstrips the kidney's secretion capacity. We do not use the enzymatic method for creatinine determination (as it yields too many implausible results). The method based on the kinetics of the Jaffé reaction gives more trustworthy values for perfusate and urine, especially because the otherwise interfering chromogens are irrelevant in this setting. However, the method has two drawbacks. First, ketoacids such as oxaloacetate, pyruvate and α-ketoglutarate can falsify the results (281, 309). Secondly, male rats, which we prefer to use because of their more stable hormonal status, secrete creatinine at higher rates than females do (100, 308), giving a clearance quotient creatinine/inulin of <1.2. For the keto acids listed in Table 4.2. (Recipe R2), creatinine measurement with the Jaffé method gives a blanc value of 0.2mg/dl prior to the addition of 2mg/dl creatinine. As long as the level of keto acids actually present in the urine is unknown, any correction would be an arbitrary one, and dilution of the urine could render it irrelevant. Koene's group in Nijmegen has shown that cimetidine inhibits the secretion of creatinine in humans and, as a result, the clearance rate drops to the level measured for inulin (109).

9.5.3. Other markers for determination of GFR

H.M. Brink's group (also in Nijmegen) has used cyanocobalamin (vitamin B12) together with Pluronic F108 as colloid. Interestingly, they measured the level of this pigment in perfusate and urine continuously online via flow cells. Comparative measurements with ^{14}C-inulin were in agreement with the B12 data. Unfortunately, BSA has such a high binding capacity for vitamin B12 that the latter cannot be used as a marker for GFR when albumin is the colloid (45). Thomas Maack used radioactive Polyethylene Glycol (^{3}H-PEG or 14C-PEG) with a molecular weight of 4000 (63, 118).

9.6. Electrolytes Na, K, Ca, Cl, HCO_3

Flame photometric estimation of sodium and potassium, usually with lithium or cesium as standard (for example, Instrumentation Laboratory), remains the gold standard for electrolyte assays. Here, one can select the appropriate calibration for the plasma or urine standard. When automatic analyzers with ion-selective electrodes are used, one must take account of the calibration mode ("protein error"), for these instruments measure the ion activity in the protein-free space, whereas in flame photometry, the total volume is fed into the flame. Modern blood gas analyzers mostly provide for the measurement such as sodium and potassium via ion-selective electrodes, but are not normally calibrated for use with urine. In addition, the measurement of ionized calcium is often possible - and valuable, in that it is quite amazing how far apart theory (initial weight) and reality (ion activity) may be (even when normalized to pH 7.4) in the case of this ion. Chloride, pH and HCO_3 are usually also measurable or can be calculated. In a study published in 1981, Besarab described the very complex interrelationship between total calcium and ionized or ultrafiltratable calcium in vitro (26).

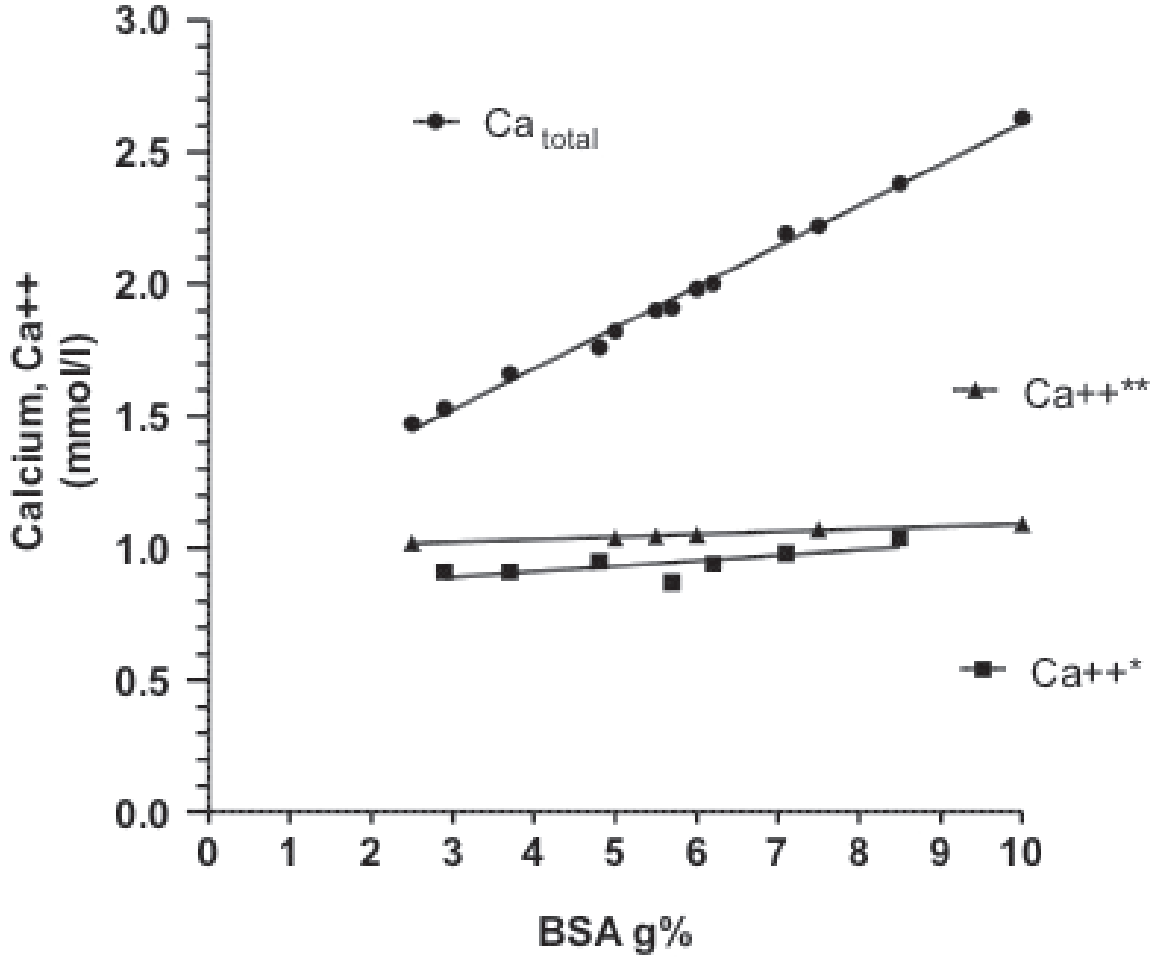

Fig. 9.6.1.: ***Correlation between albumin (BSA) and total calcium/Ca^{++}.*** BSA-medium was dialyzed against a standard-dialysate of the Krebs-Henseleit type at pH 7.4. In recirculation mode with dialysis, the level of ionized calcium in the albumin-containing medium remains constant even when the total calcium concentration in the same medium is increased in parallel with albumin (g/dl). Albumin was measured both chemically and with the Reichert refractometer. Total calcium was measured chemically with an auto-analyzer and Ca^{++} ** with the ICA 113 System, the first device marketed by Radiometer (Copenhagen, Denmark). The latter values were verified with the ABL 505 device* in 2014. On both devices, a conversion to pH 7.4 was possible, resulting in the current analysis in a maximum delta of 0.02mmol/l with a range of 0.85 – 1.04mmol/l, at pH fluctuations of 7.36 to 7.425.

Note: At physiological concentrations of calcium and phosphate in vivo, the protein fetuin acts to dampen fluctuations. Working in vitro means that levels of these ions are always close to their solubility limits. It is therefore essential to keep an eye on their concentrations, especially when the solution is being prepared (check for the Tyndall-effect). Low pH can also guard against exceeding solubility limits (s.a. Chapter 4.1.3.).

9.7. Osmolality and colloid-osmotic pressure

Osmolality

Freezing point depression (Knaur, Gonotec, Berlin, Germany) or vapor pressure osmometry (Wescor, Logan, UT, USA) are both time-consuming (and technically demanding) methods of measurement. Vapor-pressure osmometry requires less material (5-10µl) than the freezing-point method (usually 50 µl). Calibration is onerous, and automatic instruments offer greater precision. For measurements of freezing-point depression on larger numbers of samples, the Osmomat auto (Gonotec, Berlin) provides for automatic processsing (after calibration) of a series of 20 samples with surprisingly high precision (assessed in duplicate samples). The direct cryoscopy approach (Ramsey cryoscope) previously used for the analysis of micropuncture samples required only nl sample volumes (microcups).

Various authors estimate the urine osmolality by calculation (double the sum of U_{Na} and U_K), which is acceptable as a rough approximation (17, 27). Based on my own experience, this can underestimate the "true" (directly measured) osmolality by 5-10% (unpublished). If one wants to determine the osmotic clearance, the free water clearance or free water reabsorption, one should always measure the osmolality directly. Note that osmolality is based on 1 kg solvent (osmole/kg H_2O), osmolarity on 1 liter of solution (osmole/l).

Fig. 9.7.1.: ***Apparatus for serial measurement of freezing-point depression.*** This picture shows the machine (Gonotec, Berlin, Germany) most recently used in our lab, with its (partly concealed) carriage for 20 samples (in the foreground) in which four test tubes are visible. For calibration, tube 1 is filled with double-distilled water, 2 and 3 with calibration solution. All the other slots are available for test samples. The sliding cover in front is retracted stepwise for each measurement, thus minimizing losses due to evaporation.

Colloid-osmotic pressure (COP)

Measurements of COP are very useful when using colloids. One should bear in mind that the relationship between colloid in g/l and the COP is nonlinear, because it represents the sum of two components, the (nonlinear) Donnan equilibrium and the (linear) Van´t Hoff relationship. Fig. 9.7.3 shows the relationship between the concentration of BSA (g/dl) and the COP (mmHg).

Fig. 9.7.2.: ***Colloid osmometer*** (Gonotec, Berlin, Germany). Preferably, the 20,000 Dalton cut-off membrane is used. For calibration, an initial measurement is performed with the waste container on the table, and for the second it is placed on the platform (10 cm higher). The pressure can be expressed in three forms: mmHg, cm H_2O, and kiloPascal. For samples with similar values, serial measurement saves a lot of time, and data protocols can be printed out (software available).

The accuracy of the measurement depends on how closely the test sample resembles the reference solution (usually a Ringer-bicarbonate solution) on the other side of the separating membrane in terms of composition, temperature etc.

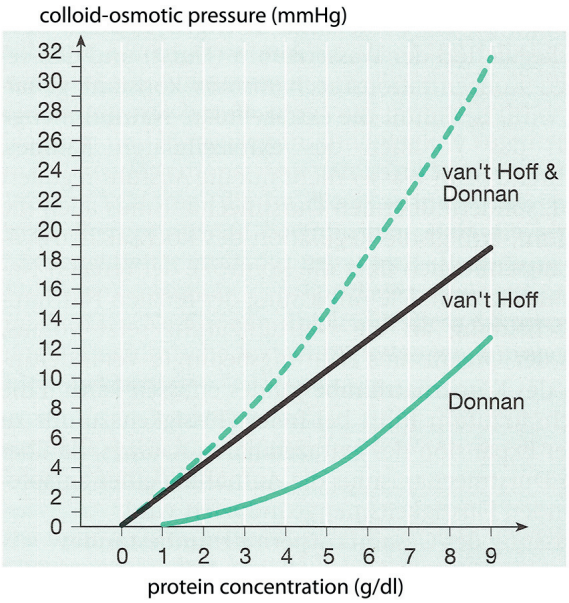

Fig. 9.7.3.: ***Schematic plot of the relationship between COP and protein concentration.*** The COP results from the total number of particles in the solution (which increases linearly with concentration) and the nonlinear Donnan effect exerted by the non-permeable protein (or colloid) fraction, and the resulting imbalance in the diffusion of the permeable particles.

The Figure is taken from our textbook article, Fig. 4.18 (265).

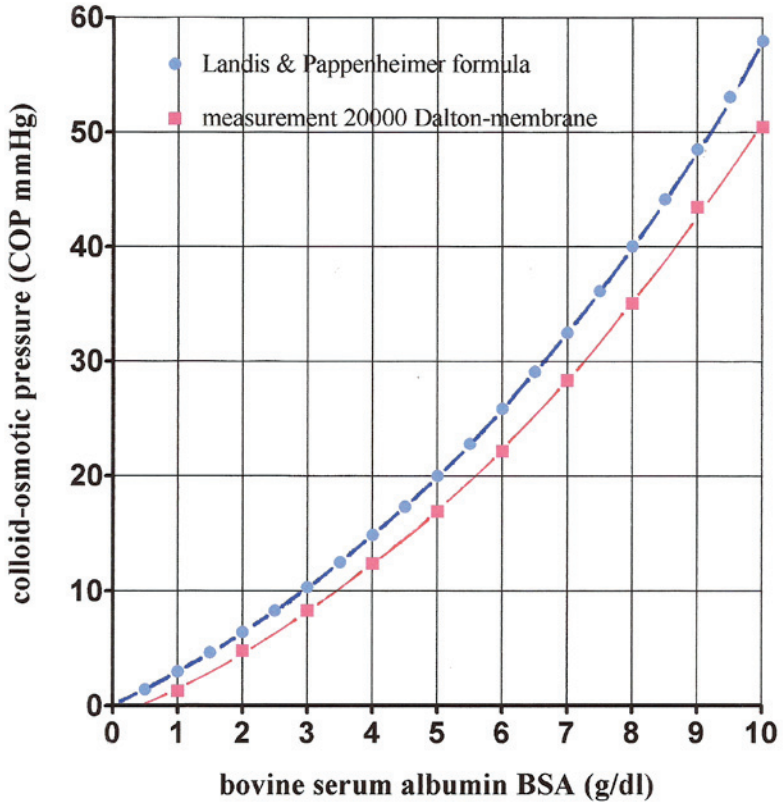

Fig. 9.7.4.: ***Colloid osmotic pressure as a function of the albumin concentration.*** The colloid-osmotic pressure (COP) of bovine serum albumin was measured with a 20,000-Da cut-off membrane at room temperature (Osmomat 50, Gonotec GmbH, Berlin, Germany). The function is not linear, as it reflects the contribution of the (non-linear) Donnan effect and the (linear) Van´t Hoff relationship. According to the Van´t Hoff relationship, the osmotic pressure of a solution is proportional to the number of particles. The test series is from 2014. The measured values are slightly lower, as calculated by the Landis and Pappenheimer formula (140) for albumin ($2.8c + 0.18c^2 + 0.012c^3$, c means the concentration of albumin as g/dl).

9.8. Colloids, substrates incl. amino acids, protein and glucose

9.8.1. Albumin

The most widely used colloid is bovine serum albumin, which must be dialyzed prior to use to remove impurities. In the early years, we simply dissolved the dry powder and dialyzed it at 4°C in cellophane tubing in 10-liter glass containers for 24 hours. Later on, we used disposable (low-flux) dialyzers for 4-8 h and have tried to keep the volume (of the starting 10% solution) constant, then we filtered the solution to sterilize it and stored it frozen in aliquots of 100 ml. Nevertheless, one may still come across batches of albumin that depart from the norm (toxic contaminants, active vasoconstrictors?). Our best results were achieved with a BSA preparation obtained from Armour in USA, which unfortunately is no longer available. A batch purchased from Sigma in 2009 has also proven to be satisfactory. Some authors omit the purification by dialysis and use the impurities bound to albumin as natural substrates in the recirculation mode. This practice was also sometimes followed by Brian D. Ross and his successors in Oxford and Boston. For targeted metabolic studies like those done by J.J. Cohen and coworkers, purification of albumin is of course essential, because only in this way can the initial conditions be controlled. In experiments with fatty acids, Cohen used, in addition to dialysis, activated charcoal to remove bound lipids from albumin. In vivo, albumin is constantly being synthesized in the liver and long-lived, modified albumin molecules are disposed of (203), or go through a recycling process. These replenishing and recycling processes are of course not available in vitro.

There are blood purification methods (referred to as albumin dialysis) that use albumin as a sponge (loading vehicle) in liver disease. In this context, a group in Berlin (MedInnovation GmbH, Berlin-Adlershof, Germany) developed a functional test for albumin. This test assesses the albumin molecule in terms of its physiological function as a transport molecule by measuring its capacity to load and offload ligands. The binding efficiency (BE in %) describes the extent to which the albumin molecule is able to perform its binding function; the efficiency of detoxification (DTE in %) indicates how effectively the molecule can offload toxins, i.e. deliver bound toxins and metabolites to the liver. Initial analyses of our BSA batches give a BE of 65% and a DTE of 61%. These values correspond to the lower end of the distribution for human albumin in the normal population. After dissolving the albumin powder in dialysate, both of the tested batches had been dialyzed extensively in the cold-room before 100ml aliquots of 10% BSA were frozen and stored. The samples were then transported to MedInnovation in dry ice, and analyzed in the local ESR Lab. A systematic study is still pending, which should include analyses of the BSA prior to dialysis, of the perfusate with all the substrate additives, and the effects of treatment with activated charcoal treatment to free up fatty-acid binding sites. If further work validates the technique, this approach could suggest ways of preparing more homogenous batches. Extensive and detailed information on albumin can be found in “All about Albumin” by T.J. Peters (203).

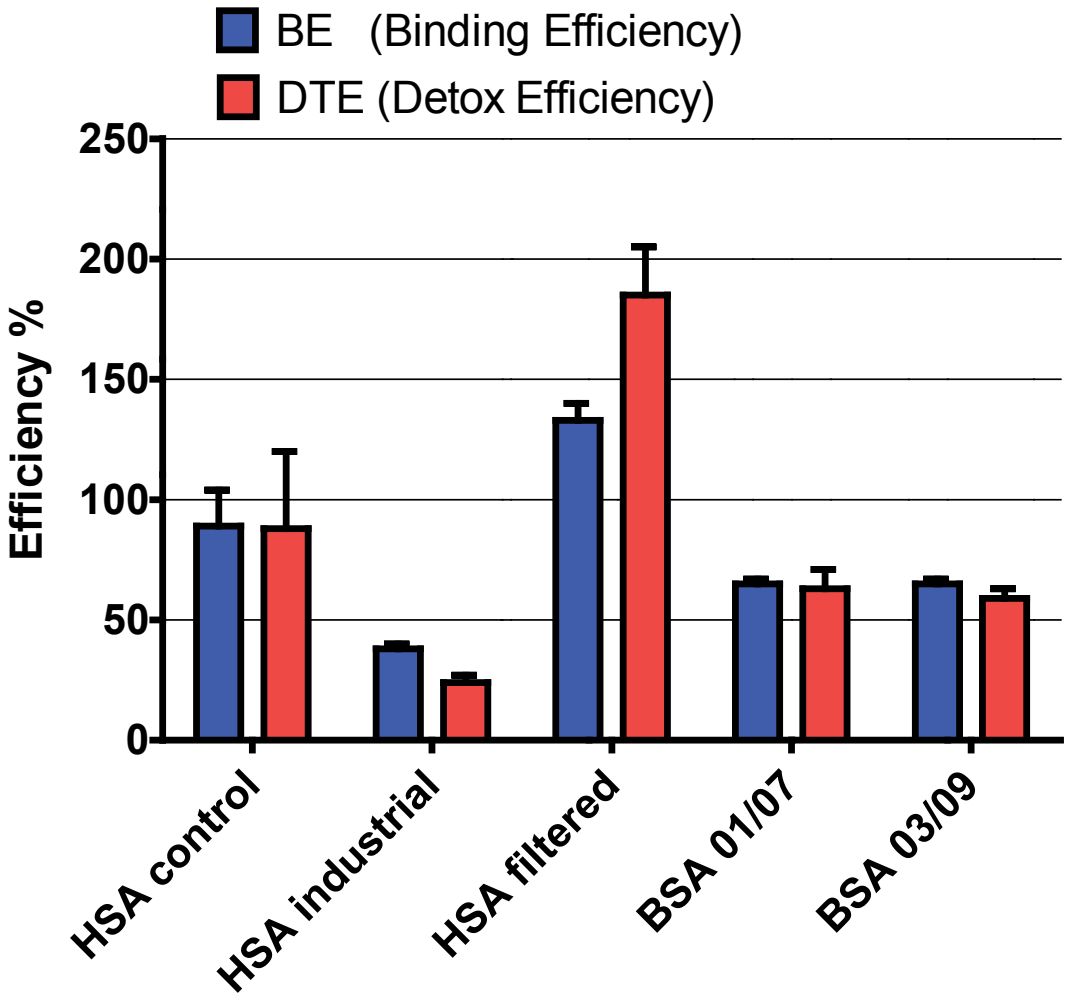

Fig. 9.8.1.: ***Characterization of the functional efficiency of albumin by ESR.*** The binding efficiency (BE in %) quantifies the extent to which the albumin molecule is able to bind and transport substrates; the efficiency of detoxification (DTE in %) indicates how effectively the molecule can offload toxins and metabolites in the liver. Two of our BSA batches were compared with HSA (human serum albumin) from healthy subjects as a control standard, HSA as industrial standard, stabilized by the addition of fatty acids (which is why its BE and DTE are very low), and the latter HSA after passage through a charcoal absorber (Hepalbin^{TM} Absorber) to remove fatty acids. Note the marked rise in BE and DTE in this last case.

9.8.2. Other colloids

9.8.2.1. Dextran

In the first report of the perfusion of the rat kidney published by Christoph Weiss et al., dextran was used as the colloid (307). However, while this work demonstrated that autoregulation of renal blood flow is detectable even in the absence of erythrocytes, dextran is not a particularly good choice of colloid for renal perfusion. At a comparable

COP, it has a significantly higher viscosity than albumin. Moreover, the anthrone-based inulin measurement of GFR must be modified when dextran is present, as the method involves acid hydrolysis at elevated temperature. If this step is carried out at too high a temperature, dextran will be hydrolyzed to dextrose molecules, which also react with the chromogen (176). An alternative approach is to use the enzymatic inulinase method described by Kuehnle (133, 311).

9.8.2.2. Crosslinked gelatin preparations

Our initial experiments in Berlin were performed with urea-crosslinked gelatin (Haemaccel®, Hoechst). The powder was dissolved in distilled water at a final concentration of 46,7g/liter, prefiltered through a glass filter, followed by removal of pyrogens by passage through a Seitz filter of EKS grade with porosities of 3 and 1-1.5 µm in series. The solution was stored in 500ml glass bottles at 4°C after autoclaving at 110°C for 30min. This stock solution was mixed with sterile salt concentrates and metabolites to obtain the defined composition on the day of the experiment, and finally sterilized by passage through 0.2-µm filter (Sartorius flat filter, 142mm diameter). Autoclaving did not increase osmolality. Nevertheless, the low-molecular-weight fraction of Haemaccel presents a problem for the hydrodynamics in the nephron. At the initially high rates of fractional sodium and water reabsorption, the filtered fractions of the colloid increase the viscosity of the tubular fluid. This is indicated by the fact that the flow rate reaches a minimum of about 8ml/min· g kidney after about 20min of perfusion, and P_{tub} is increased to the same level in the proximal and distal tubule*. This points to an increase in resistance around the lamina cribriformis of the papilla due to the increased viscosity, which itself diminishes with time as decreasing reabsorption capacity effectively “dilutes” the urine (Fig. 6.4.2., unpublished findings). Brink and coworkers in Nijmegen made comparable observations when they used Pluronic F108 as colloid (43, 44). The sieving properties were also dependent on the filtration rate. At a GFR of 100µl/ min the sieving coefficient was 0.7, at a GFR of 800-1000µl/min it had dropped to 0.3.

9.8.2.3. Pluronic, HAES

Holger Franke had used Pluronic as the colloid in Christoph Weiss’ lab (81). I myself have had no direct experience with it. The formation of micelles is one attendant difficulty. HAES (hydroxyethyl starch), like other artificial colloids, has the disadvantage of a higher viscosity relative to albumin, which makes it impossible to achieve the high flow rates attainable with BSA. Several authors have used HAES in combination with albumin. We have used HAES for perfusion fixation of kidneys for morphological studies – and the fixed organs were then used for *reperfusion* experiments – our fourth experimental model.

* See also Fülgraff (84b): micropuncture experiments (furosemide diuresis) in vivo.

9.8.3. Metabolic substrates

Glucose

We favor a slightly elevated glucose concentration of 8.4mmol/l (compared to the standard concentration of 5.5 mmol/l). Earlier studies showed that even higher concentration of glucose (for example 20mmol/l) – as the sole substrate added – improved rates of sodium transport (55, 57, 226, 227, 256, 264).

Other metabolic substrates

Systematic studies of the IPRK have shown that a significant improvement in sodium reabsorption, in parallel with the increase in O_2-consumption, is achieved by the addition of amino acids (63, 71, 251), Krebs-cycle intermediates (257) and short-chain fatty acids such as butyrate. The use of long-chain fatty acids (83) also enhanced sodium transport. Whether supplementation with carnitine is beneficial has not yet been investigated systematically. Uptake of butyrate (in contrast to propionate) does not depend on carnitine, and butyrate shows the strongest effects (256). Compounds that serve as substrates for gluconeogenesis in the kidney can theoretically compete for energy resources with energy-intensive sodium transport (222). A substrate such as succinate, which donates electrons via the FAD system to the respiratory chain increases oxygen consumption and reduces rates of sodium transport, since it bypasses the first phosphorylation step in the respiratory chain. At higher succinate concentrations, CO_2 production is so greatly reduced that one has the impression that the Krebs Cycle is being starved (256). Several research groups have taken a closer look at gluconeogenesis in the kidney. In these studies, the recirculation mode was used to enhance the effect (32, 58, 185). Members of F.H. Epstein's group in Boston – in particular Meyer Brezis – have explored the problem of how the level of salt transport in the TAL-segments leads to tissue damages due to lack of oxygen, and elucidated its substrate dependence (40-42).

The following figure shows the effects of butyrate in sodium transport and oxygen consumption in comparison with a perfusion solution that is poor in substrates and contains only 5.5mM glucose. In the early 1970s, with the aim of increasing the input of electrons into the respiratory chain, we tried out mixtures of substrates that use the malate-aspartate shuttle at the mitochondrial membrane to increase sodium transport. This approach was quite successful in the single pass mode with Haemaccel® as colloid (257) as was subsequently confirmed by Brian D. Ross (222). The substrate mixture consisted of glutamate, lactate, oxaloacetate and pyruvate, in addition to the obligatory glucose. Later on (using albumin as the colloid), 8 amino acids were added according to the recipe of Thomas Maack (63), and then the full range of 20 amino acids, as proposed by Franklin H. Epstein (71). The use of 5-liters of dialysate in the mode 3 meant that the supply of substrate was uncritical compared to a mode 2 with pure recirculation, as had been shown

in the case of arginine as NO source (206, 207). On the other hand, the increase in oxygen consumption upon substrate stimulation can exacerbate the hypoxic damage incurred during cell-free perfusion in the critical interbundle area of the outer medulla (41). In this case, the addition of washed erythrocytes alleviates this effect (263).

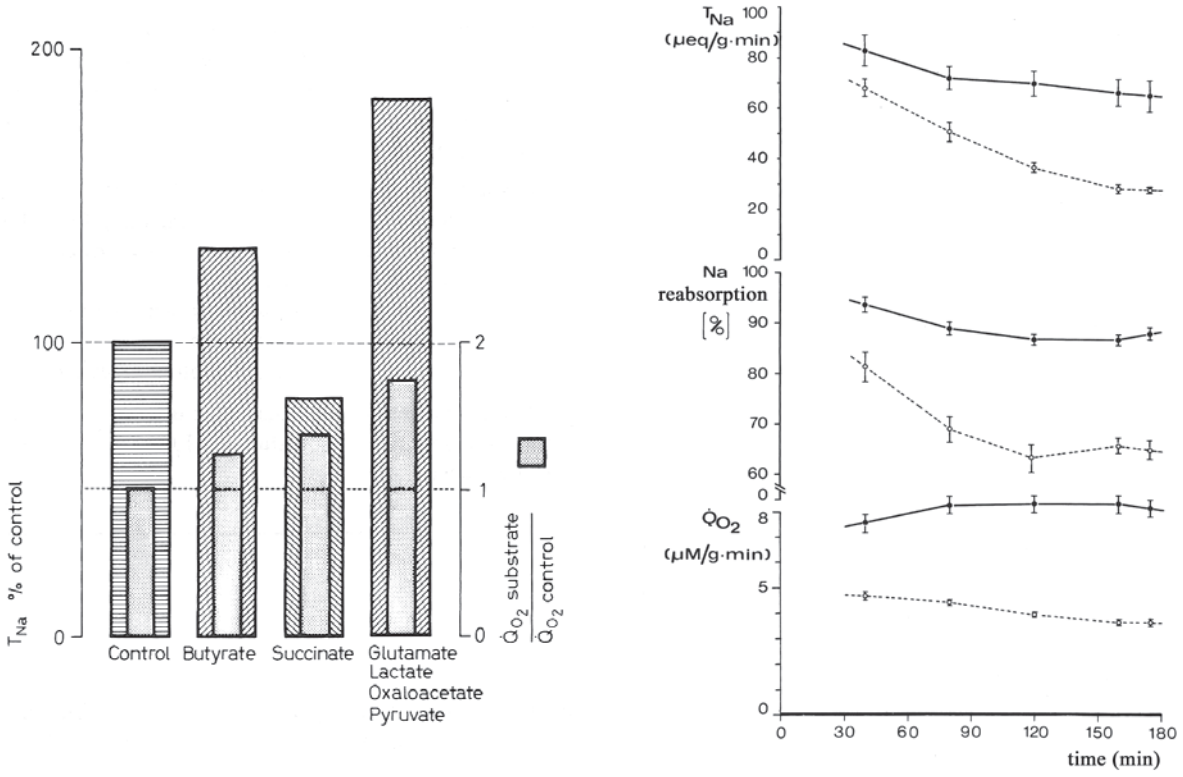

Fig. 9.8.2.: ***Substrate effects on sodium transport and oxygen consumption.*** The left panel shows the effects of additional substrates relative to a control perfusion with 5.5mmol/l glucose as sole substrate. Addition of butyrate increases sodium transport in proportion to oxygen consumption. An even more pronounced effect is seen upon supplementation with a mixture of glutamate, lactate, oxaloacetate and pyruvate, while the addition of succinate increases the oxygen consumption and reduces sodium transport because succinate donates its electrons to the respiratory chain at the level of the FAD system, thus bypassing the first phosphorylating step (NAD system). On the right is the time course of sodium transport (absolute and %) and oxygen consumption in control experiments (5.5mmol/l glucose sole substrate, dotted lines) and with the addition of the substrate mixture of glutamate, lactate, oxaloacetate and pyruvate over 3 h. We performed the experiments in single pass perfusion mode with Haemaccel as the colloid (130, 246, 257).

10. Kidney perfusion: comparison of results

10.1. Single pass perfusion – recirculation with regeneration of perfusate by dialysis

All findings made without any colloid, or with a colloid other than albumin, that are referred to in this chapter are from single-pass experiments. All other data were obtained under mode-3 conditions: recirculation with dialysis and albumin as colloid. With few exceptions, albumin was generally not used in single-pass experiments, largely because of its cost (233, 234, 280). At flow rates of 15-30ml/min per g (rat) kidney, 900-1800ml of perfusate is consumed per hour. A 5-liter batch of medium suffices to perfuse two kidneys for 2 hours. When plasma substitutes such as HAES or gelatin derivatives are used, flow rates are in the range of 10-15ml/min (257). Specific questions may require perfusion of the kidney in the absence of a colloid. In that case, decapsulation of the kidney prior to perfusion is recommended and the perfusion pressure can be reduced to 80-90 mmHg. Without colloid osmotic pressure, the organs swell and perfusion resistance increases if the capsule is intact. On removal of the capsule, flow rates may reach 20-25ml/min·g kidney and a GFR of 1.0 up to 1.6ml/min·g kidney - higher than the in-vivo value – can be attained (at 90mmHg). The following Figures depict our own data, some of which has already been published (250, 251). The diagrams are designed to provide an overview of the functional changes that occur in response to variation of the colloid-osmotic pressure (BSA). Particularly noteworthy is the significant drop in perfusion resistance with increasing COP (albumin concentration), which is apparently induced by the expansion of the vascular bed.

10.1.1. Dependence of perfusion flow rate, urinary flow rate, GFR and filtration fraction on albumin concentration

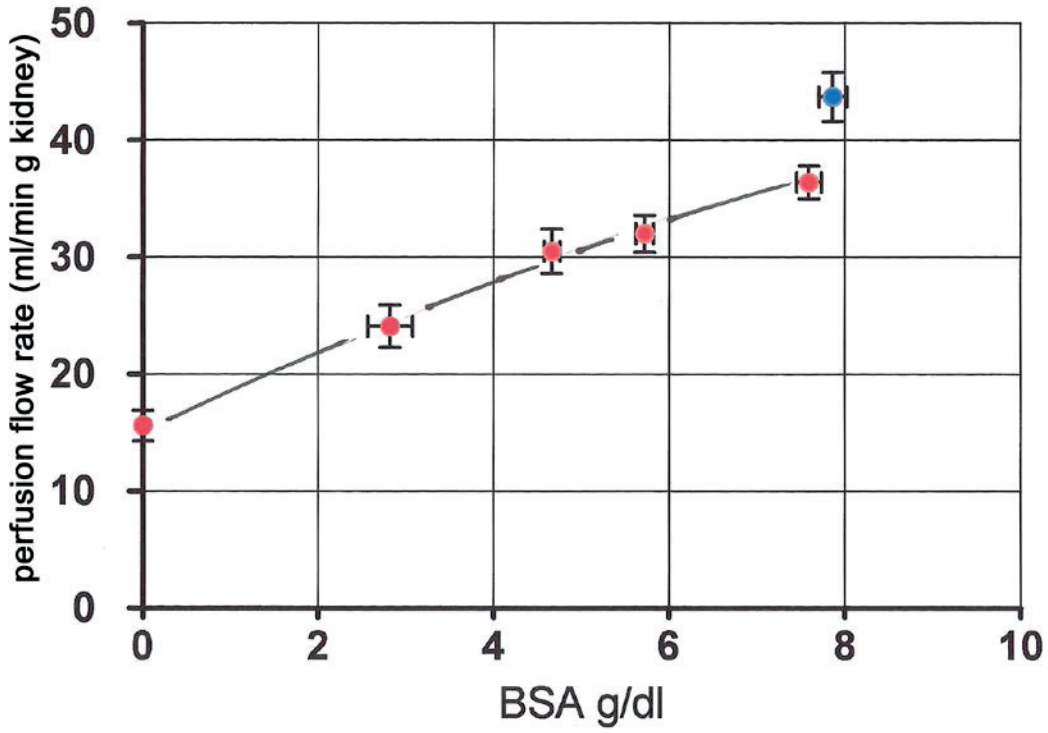

Fig. 10.1.01.: ***Relationship between perfusion flow rate and albumin concentration in the perfusate.*** Perfusion flow rate in the "steady state" phase between 50-70min is plotted against the albumin concentration. Only the colloid-free perfusion was performed in single pass mode (250, 251), here with an intact capsule; the perfusion rate is significantly higher without the capsule – equivalent to that with 2-3g/dl BSA. Data points are mean values ± SEM (perfusion pressure: colloid-free medium 90mmHg, otherwise 100mmHg). In the presence of verapamil (blue) at high BSA concentration, the flow rate is higher. The perfusion pressure required to achieve a comparable GFR of 1ml/min · g kidney (as in experiments using 6g albumin at 100mmHg) was 140mmHg.

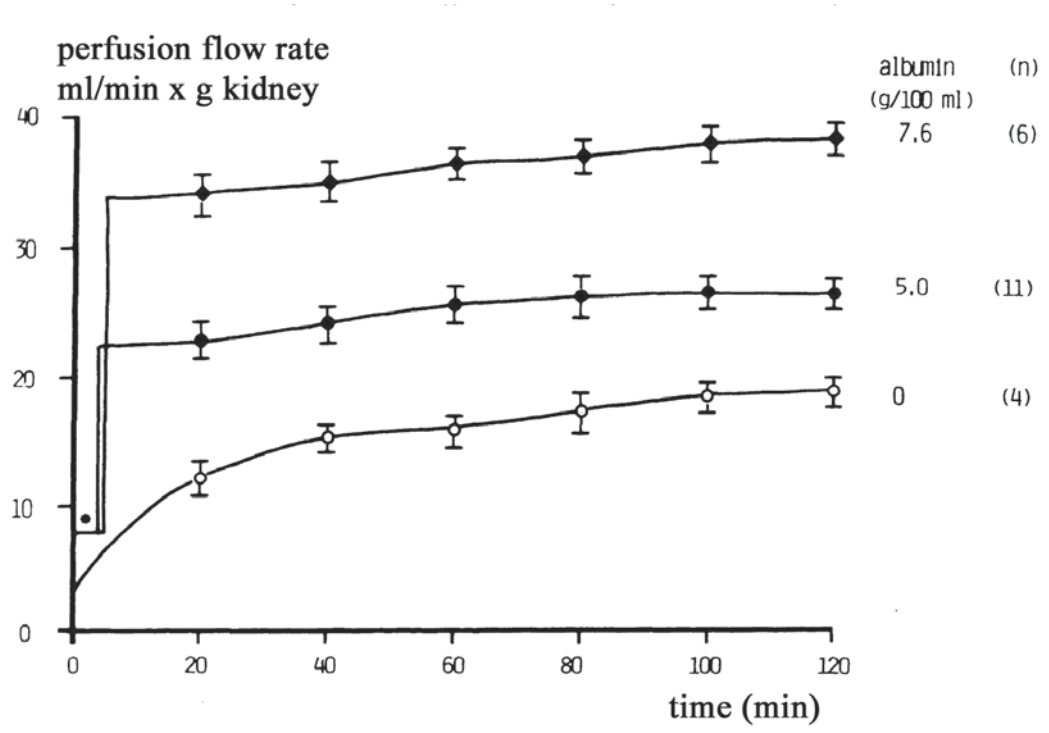

Fig. 10.1.02.: ***Dependence of perfusion flow rate on albumin concentration and duration of perfusion.*** Data points are mean values ± SEM. *Perfusion was initially carried out at a constant flow-rate of 8ml/min until the recirculation circuit was closed, then under constant pressure at 100mmHg. Perfusions without albumin were carried out in the single-pass mode with intact capsule at Pa 90mmHg (mean values ± SEM) (250, 251). In perfusions without albumin, the flow rates are significantly higher if the renal capsule has been removed initially.

Perfusion rates increase in proportion to the concentration of albumin but, despite the attendant increase in oxygen supply, morphological damage in the interbundle area of the outer medulla cannot be fully prevented. Only the addition of erythrocytes as oxygen carriers can provide the required amounts of O_2 (263). Here, one has to keep in mind the fact that, in vivo, although only 8% of the O_2-supply is extracted from the blood overall, areas such as the outer medulla take up to 80%. In cell-free perfusion, the overall extraction level for the whole kidney amounts to about 50% of the physically dissolved O_2. Thus, one can easily imagine that the level of supply becomes critical in the interbundle area of the outer medulla in the absence of erythrocytes.

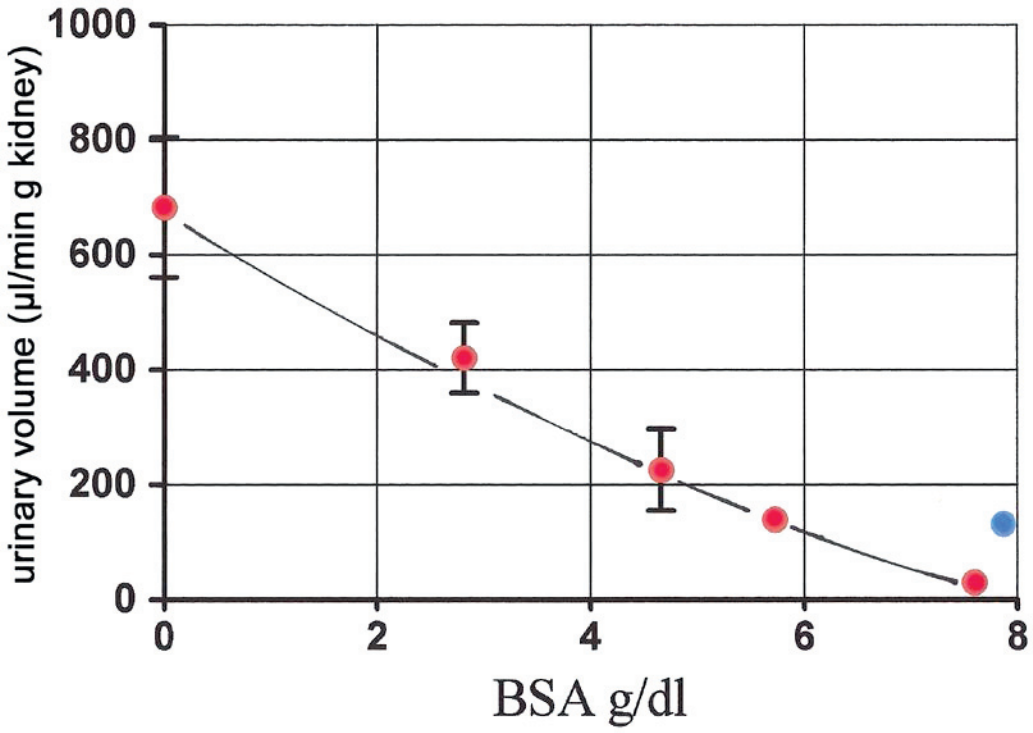

Fig. 10.1.03.: ***Relationship between urinary flow rate and albumin concentration in the perfusate.*** The volume of urine excreted per minute in the steady state phase between 50-70 min is plotted against the BSA concentration. As in Fig. 10.1.01, the blue data point marks the urinary flow rate at elevated perfusion pressure (140 mmHg) in the presence of verapamil. The plot is based on data extracted from the tables in the 1981 publication (250).

The high urinary flow rates attainable in colloid-free perfusion can only be achieved if the kidneys are decapsulated and ureteral catheters are used that build up no back-pressure (see Figs. 4.6.9 - 4.7.1). Parallel filtration rates are higher than in vivo, as one would expect on the basis of Starling´s model (287); see Fig. 10.1.04 below.

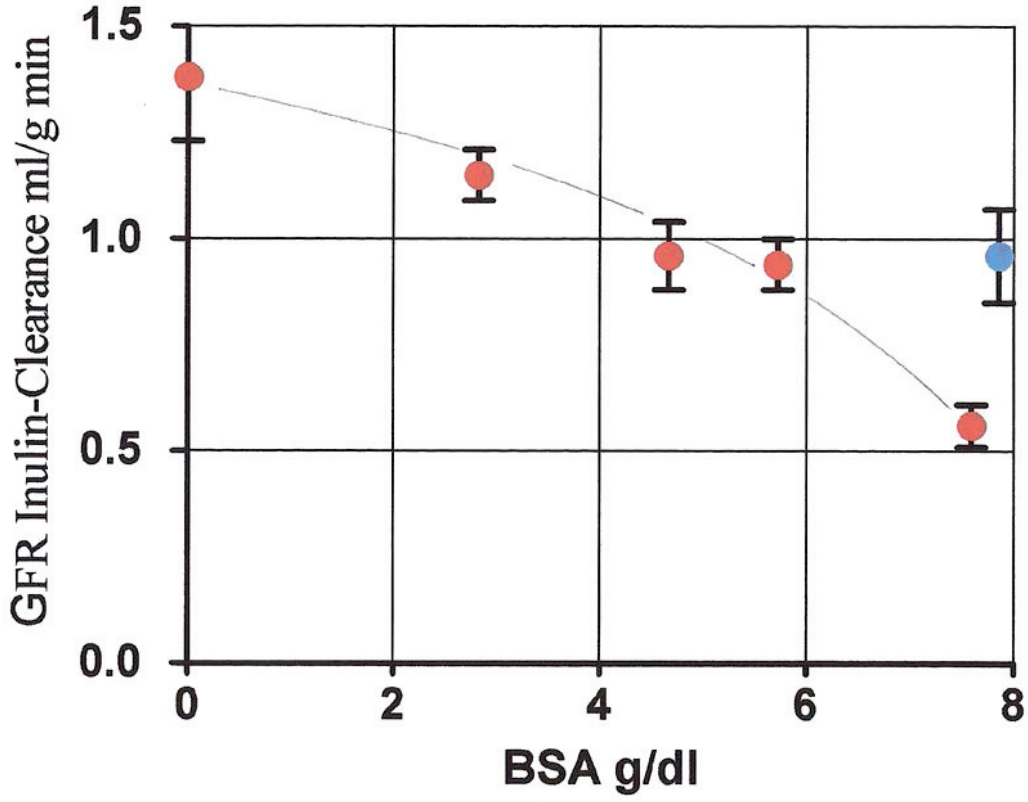

Fig. 10.1.04.: ***Dependence of glomerular filtration rate (clearance of polyfructosan) in the steady state phase (50-70 min) on the albumin concentration.*** Data points are mean values ± SEM. At high COP (BSA 8g/dl), GFR can be enhanced to the level observed in a kidney perfused by 6g/dl BSA by the addition of verapamil and application of a perfusion pressure of 140mmHg. There is a clear relationship between GFR and COP (BSA) as expected from Starlings concept. The problem of "erratic behavior" has been discussed and shown to be an artifact (Chapter 4.6.3, Fig. 4.7.0.). As in Fig. 10.1.01, the blue data point marks the value of GFR when perfusion is carried out at elevated pressure (140 mmHg) in the presence of verapamil. This is a prerequisite for a valid comparison of performance with respect to the absolute and fractional sodium reabsorption between kidneys perfused with 6 g% BSA and 8 g% BSA (see Figs. 10.1.12 – 10.1.14).

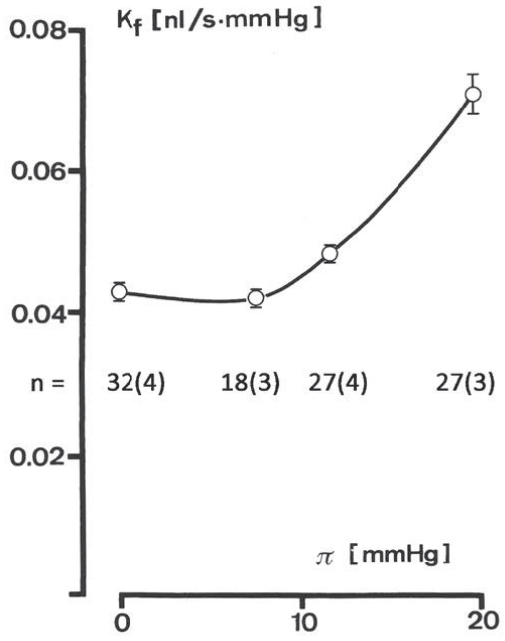

Fig.: 10.1.05.: ***Dependence of the glomerular ultrafiltration coefficient on colloid osmotic pressure (COP).*** The surprising observation that glomerular permeability to water is higher at higher albumin concentrations (250) under in-vivo conditions was made very early on (21). Although this must be considered in light of the fact that filtration conditions in vivo are not as easily characterized as they are in the isolated perfused kidney with its low filtration fraction (see Fig. 10.1.06), a compelling explanation of this phenomenon is still lacking. The data shown here were obtained in micropuncture experiments that measured early proximal tubular free-flow and stop-flow pressures, together with an analysis of single-nephron gfr by sampling under continuous pressure control (250). The figures in parentheses on the plot indicate the numbers of animals used. Micropuncture was performed by Gerd Schwietzer (271), who used the Landis technique (141), and later on by Klaus Hinrich Neumann (181) using the Berlin technique (154).

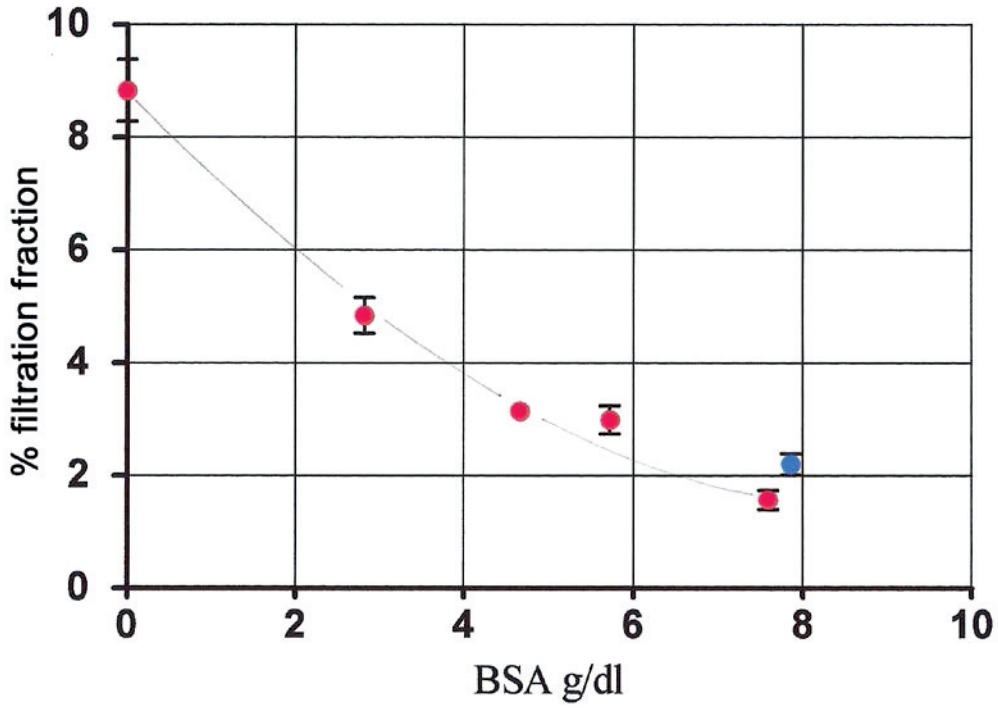

Fig. 10.1.06.: ***Dependence of the filtration fraction in the steady-state phase (50-70 min) on albumin (BSA) concentration*** (250)**.** Data points are mean values ± SEM. The blue data point indicates the value at high perfusion rates in the presence of verapamil (see Fig. 10.1.04).

10.1.2. Kidney weight – a problematic reference parameter

Generally, the weight of the unperfused (but decapsulated) left kidney from the same animal serves as the reference for quantification of the physiological functions of the perfused right kidney (which are expressed per g kidney). Control measurements have shown that the difference in weight between the two kidneys of a pair is generally negligible, which validates the use of this approach. Some authors mention only the average rat weight and therefore relate physiological parameters not to kidney weight, but to perfusion flow rate (i.e., per ml/min).

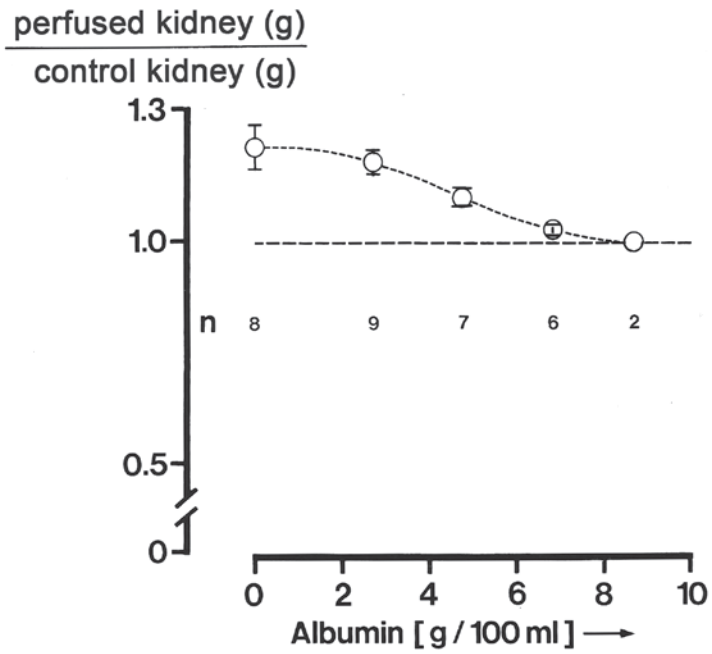

Fig. 10.1.07.: ***Ratio of the weight of the perfused kidney to that of the collateral kidney.*** The concentration of albumin in the perfusate is plotted against the degree of swelling of the perfused kidney or, alternatively, against the intratubular and interstitial increase in pressure and volume. Data points are mean values ± SEM.

The graph is taken from the 1981 paper (250, 251) and is similar to the data described by Little (152). The (colloid-free) perfused kidneys were not decapsulated prior to perfusion, but immediately before weighing, in order to avoid any contribution from the (physiologically irrelevant) lipid residues on the capsule and hilum. If the left collateral kidney has been completely ligated off (i.e. vein and artery together rather than the left renal artery alone) – which is only necessary if, for example, much of the left renal artery is hidden under the vein) – the measured weight of the dissected kidney will be about 0.2 g higher. This is probably attributable to the pressure drop after ligation of the renal artery alone, which allows fluid to leak from tubules and blood to seep from the open veins.

Comparison of wet weight and dry weight in vivo and in vitro

In her 1974 doctoral thesis in Berlin (37), Petra Brandt provided a detailed study of the electrolyte content of renal tissue and the ratio of wet and dry weight, and compared these data for freshly isolated kidneys with those for Haemaccel-perfused kidneys (256). As control samples, she initially used slices of renal cortex obtained from freshly dissected

kidneys; these were then aliquoted and, after weighing, samples were taken for dry weight determination. On average, 100% wet weight was found to correspond of 26.0 ± 0.48 % dry weight. This method proved to be unsuitable for isolated perfused kidneys, because they contain more fluid and therefore lose more liquid when sliced. Thus, the method described by Reinhardt in his *Habilitation* thesis was to flash-freeze kidneys (within 2 seconds), after pinching off hilum, in liquid nitrogen and process tissue samples in the frozen state (216). This approach resulted for the in-vivo controls in values of 20.0 ± 0.31% dry weight (relative to 100% wet weight). For kidneys perfused in single-pass mode with Haemaccel and a standard perfusate with glucose as the sole substrate, the corresponding values were 16.85 ± 0.21% dry weight (based on 100% wet weight). In the context of the simple issue referred to at the top of this paragraph, Reinhardt's procedure appears overelaborate, but its use was crucial for the electrolyte analysis in the work of Petra Brandt. Her thesis also addresses the issue in the context of comparisons between the blood-perfused kidney in vivo and in-vitro perfusion of the organ with cell-free medium (37).

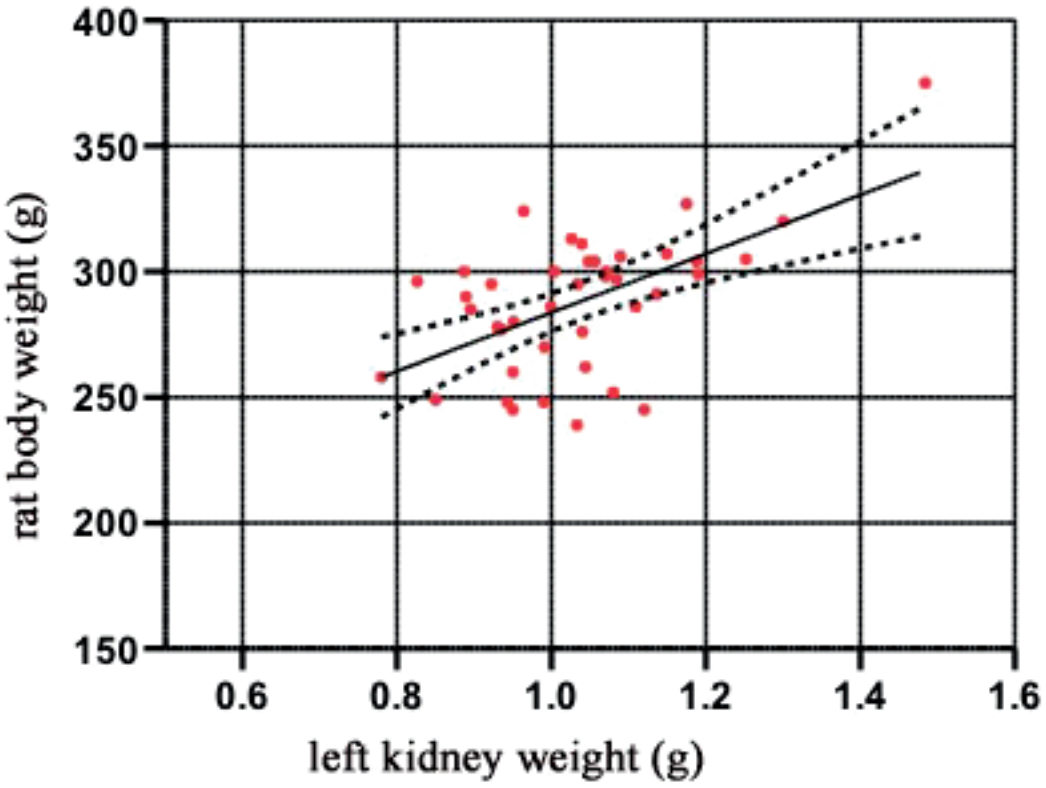

Fig. 10.1.08.: ***Ratio of the weight of the left kidney*** (ligated by the artery) ***to the total weight of the donor rat.*** This parameter was also used as a reference factor to calculate die kidney function/g of the right isolated perfused kidney. Rat strain: Hannover Wistar.

10.1.3. Autoregulation of renal perfusion flow rate

An extensive literature is available on this subject, both for kidneys in vivo and isolated perfused kidneys (92, 93). Here, one must distinguish between cell-free solutions such as blood plasma and artificial colloid-containing solutions, which can be regarded as Newtonian fluids on the one hand, and blood as an inhomogeneous suspension of particles on the other. For Newtonian solutions, the Hagen-Poiseuille equation applies, which already implies that the relationship between pressure and flow is nonlinear (see Fig. 10.1.11). For blood, the situation is even more complicated.

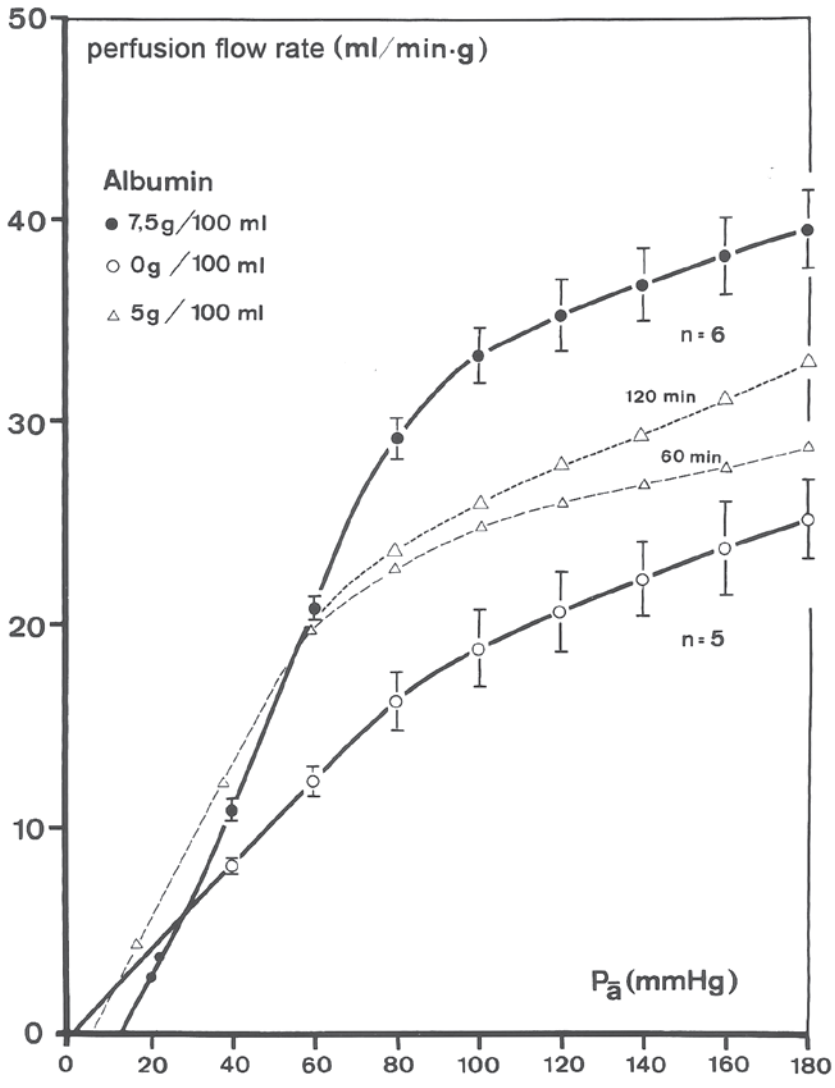

Fig. 10.1.09.: ***Comparison of autoregulation of perfusion flow rate as a function of albumin concentration and COP respectively*** (250). The measurements were conducted over a 2-hour period of cell-free perfusion, during which the pressure was raised in steps of 20 mmHg [minutes time intervals] at albumin concentrations of 0 g and 7.5 g/dl. Autoregulation curves after 60 min and 120 min from a single experiment with 5 g% albumin are also shown. Data points are mean values ± SEM.

The autoregulation curve obtained in the absence of albumin in the perfusate is very flat and is reminiscent of the curve observed when the kidney is replaced by a defined flow resistance (see Fig. 10.1.11). During cell-free perfusion, the tubulo-glomerular feedback (TGF) that would normally complete the autoregulation loop is not detectable (250).

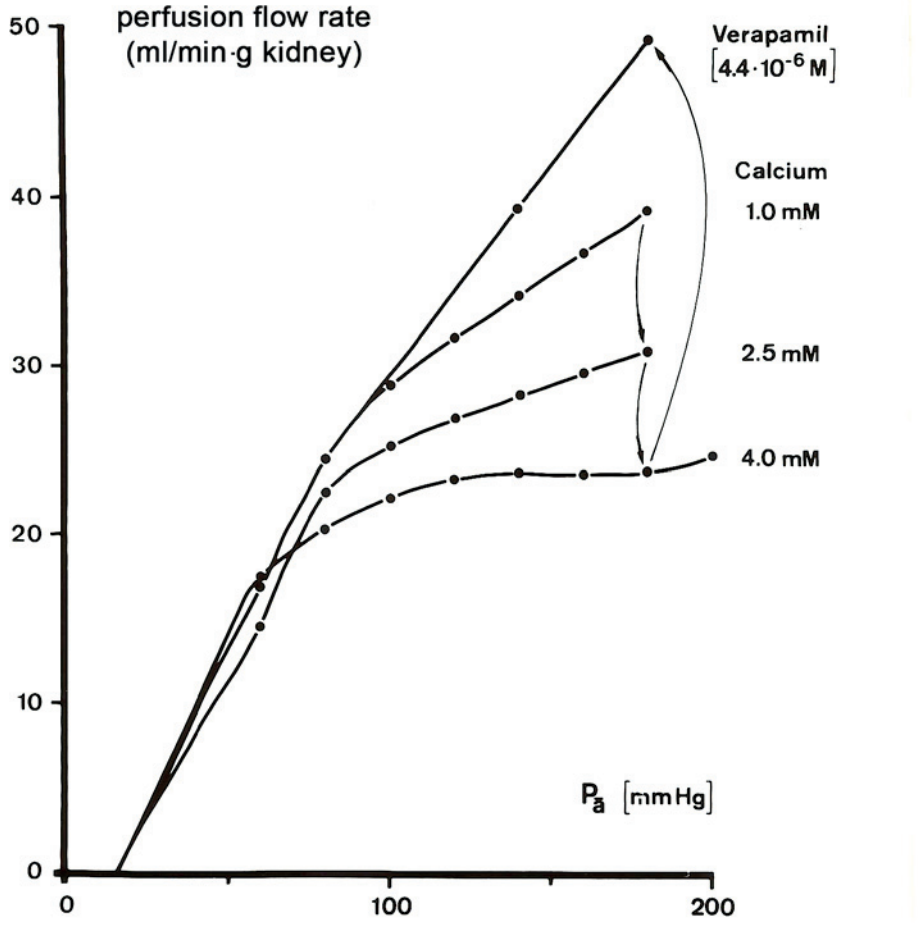

Fig. 10.1.10.: ***Dependence of autoregulation of the perfusion rate on the calcium concentration in the perfusate*** (single experiment). Autoregulation is abrogated by verapamil ($4.4 \cdot 10^{-6}$ M) (175, 250, 253). The nonlinear form of the curve in the presence of verapamil is a reflection of the Hagen-Poiseuille law. The influence of calcium in the perfusate is very clear. In 1976 verapamil was found to inhibit tubulo-glomerular feedback (175), which plays a role in completing the autoregulation loop. The concentration of calcium was calculated from the successive addition (250). At moderate calcium concentration, addition of angiotensin II enhances the autoregulation to the level seen with 4 mmol/l calcium (see Guan et al. (93)). Glucagon abolishes autoregulation of the IPRK completely, as Holger Franke has shown (80).

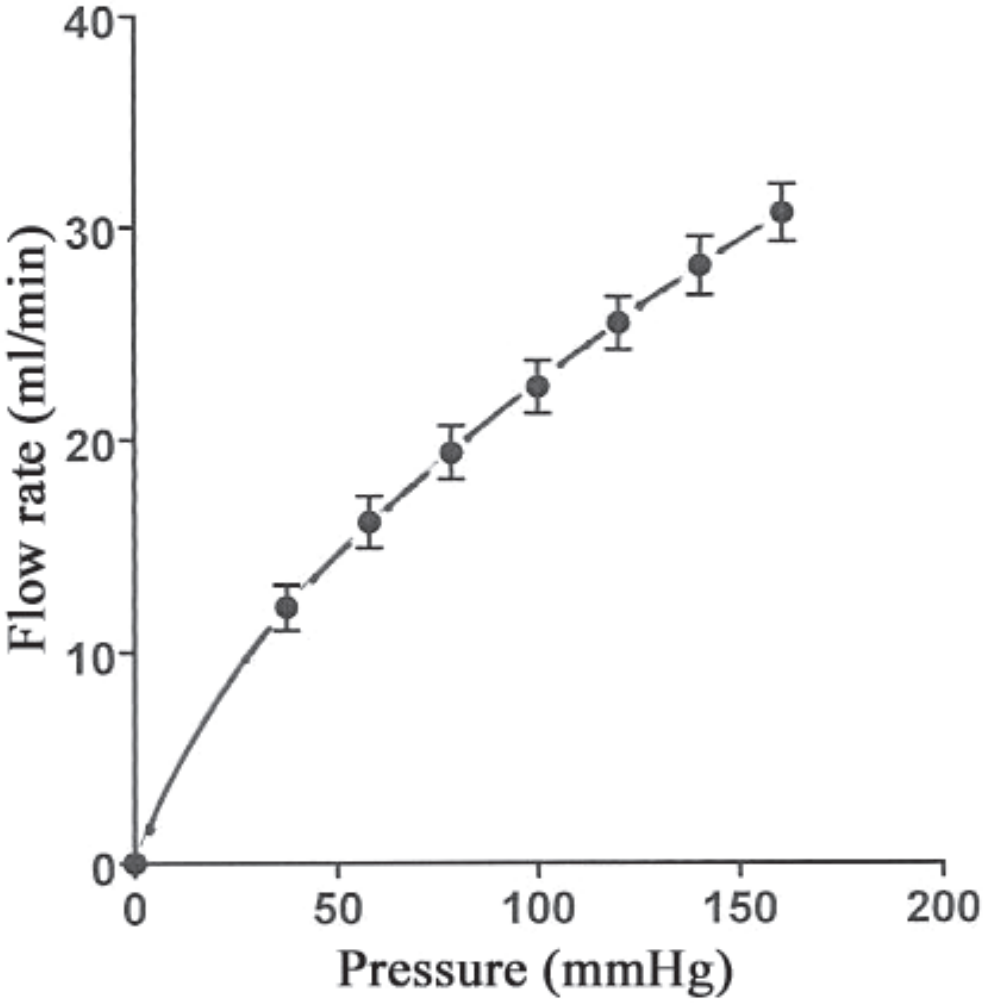

Fig. 10.1.11.: ***Pressure-flow diagram for the apparatus without an in-line kidney.*** The pressure-flow diagram follows the Hagen-Poiseuille law and is therefore non-linear. The curve is determined experimentally at 37°C with a 4% HAES solution and a compressed tube in place of the kidney. The curve observed in the presence of verapamil shown in Fig. 10.1.10 is comparable to the experimentally determined curve for the system without a kidney.

The Hagen-Poiseuille Law:

$$\dot{V} = \frac{dV}{dt} = \frac{\pi \cdot r^4}{8 \cdot \eta} \frac{\Delta p}{l} = -\frac{\pi \cdot r^4}{8 \cdot \eta} \frac{\partial p}{\partial z}$$

$\dot{V}$	= Volumetric rate of flow through a pipe in	m^3/s
r	= Inner radius of the pipe	in m
l	= Length of the pipe	in m
η	= Dynamic viscosity of the flowing fluid	in Pa· s
Δp	= Pressure difference within the pipe	in Pa
z	= Flow direction	
Pa	= Pascal	

Implications for the autoregulation of blood/perfusion flow rate in the isolated kidney model

The pioneering work of Weiss, Passow and Rothstein in 1959 demonstrated (307) that autoregulation requires no red blood cells. Before that, Kinter and Pappenheimer had argued that autoregulation could be attributed to the phenomenon of "plasma skimming" alone (123, 195). Following the demonstration that a cell-free perfusate also exhibits autoregulation of renal perfusion, this notion was no longer be sustainable. Both in the in vivo kidney and the isolated organ, the Bayliss effect (22) is considered to be the basis for the autoregulation phenomena, and this is supplemented by tubulo-glomerular feedback, which is not detectable in the cell-free perfused kidney in our hands (unpublished studies undertaken together with Hans Ulrich Gutsche and Reinhard Brunkhorst in the Hannover Lab). However, Jürgen Schnermann was able to demonstrate a tubulo-glomerular feedback in the blood-perfused dog kidney (240). Nevertheless, one should not exclude plasma skimming as a contributory factor; we see it as a third component, but is not relevant for the cell-free perfused kidney. Findings made by the group led by Bert Flemming and Erdmann Seeliger in Berlin (77, 272) hint at a fourth component. Whether this component plays a role in the isolated kidney cannot be decided at present. Our own experience is that hypoxia attenuates autoregulation in the IPRK model, but that a combination of angiotensin II and an increased calcium concentration improves autoregulation. Indeed, under the latter conditions, it is possible to achieve almost perfect autoregulation without any tubulo-glomerular feedback (see Chapter 12.3., Fig. 12.3.7.). From incidental observations, we conclude that peptide hormones, such as arginine vasopressin (AVP) and – in particular – parathyroid hormone (PTH) may also enhance autoregulation.

10.1.4. Fractional sodium reabsorption and absolute transport rate TNa

The rate of sodium transport is a good criterion with which to assess the function of the isolated kidney. For comparisons of transport capacity, the choice of kidney weight as the reference parameter is just as relevant as in the case of the GFR. A fractional sodium reabsorption of >99%, typically found in vivo, is not attainable in vitro with cell-free perfusate, and at reduced filtration rates only with the addition of erythrocytes combined with other measures, such as supplementation with glutathione and very high levels of creatinine (50mg/dl, s. (162, 163)). Thomas Maack has discussed this in detail in two reviews and recommends the use of high concentrations of albumin in the perfusate as a means to achieve the COP that prevails in the capillary bed of the proximal tubules in vivo, as a consequence of the high glomerular filtration fraction. In the isolated kidney preparation, this can only be achieved - because of the low filtration *fraction* - if one accepts a strongly reduced filtration *rate* (GFR, see Fig. 3.0.1.). The following diagrams demonstrate the strong dependence of sodium transport on the amount of sodium to be filtered (Na-load). The perfusion solutions used here are substrate enriched, as described in 1981 (250, 251).

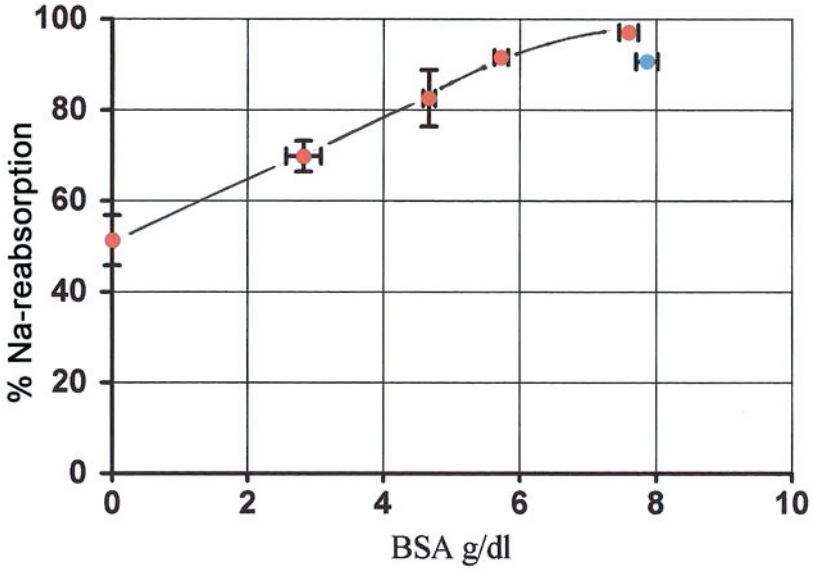

Fig. 10.1.12.: ***Fractional sodium reabsorption in the steady state phase (50-70min) plotted against albumin concentration (BSA).*** In the presence of verapamil, the % Na-reabsorption at a high COP (7.5 g% albumin) remains at the level observed at COP values equivalent to 6g% albumin (at comparable GFR) in its absence. The high fractional sodium reabsorption of >98% can be attained in a cell-free isolated perfused kidney only at reduced GFR with a hyperoncotic perfusate. Data points are mean values ± SEM (see Fig. 10.1.13).

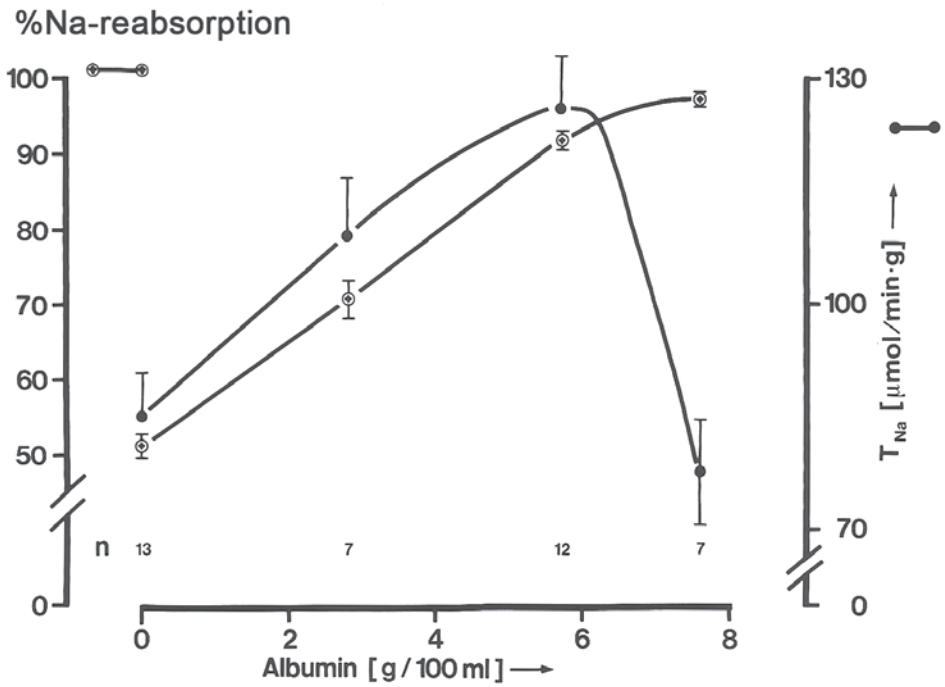

Fig. 10.1.13.: ***Fractional Na-reabsorption and absolute rate of Na-transport TNa in the steady state phase (50-70min) plotted against albumin concentration (BSA).*** With colloid-free media, only 50% of the filtered sodium is reabsorbed. Data points are mean values ± SEM (see Fig. 10.1.14).

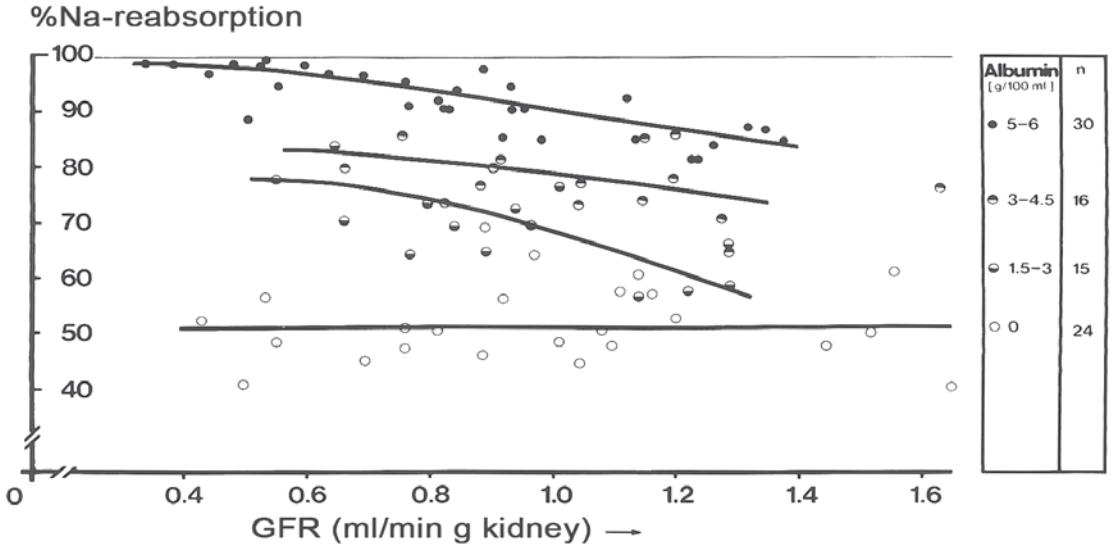

Fig. 10.1.14.: ***Dependence of fractional sodium reabsorption in the steady state phase (50-70min) on COP (BSA) and GFR.*** With colloid-free perfusate, the mean Na reabsorption is equivalent to 50% of the total Na load and is independent of GFR. Note, however, the strong dependence on sodium load at higher COP. Single values (250, 251). The reabsorption rate falls significantly during the 2nd -3rd hours.

10.1.5. Glucose reabsorption

Due to the damage induced by hypoxia in proximal tubuli within the interbundle area of the outer medulla (S_3-segments) in the perfused kidney and the slightly elevated glucose concentration in the perfusate (8.4mmol/l), the fractional (%) glucose reabsorption cannot attain its normal level. Addition of 5% red blood cells prevents damage to the S_3 segments, which explains why % glucose reabsorption under these conditions is higher than that seen in cell-free perfusions.

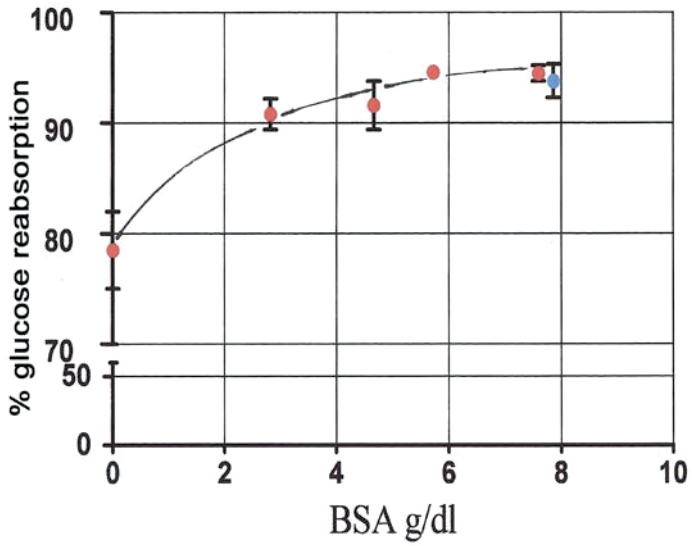

Fig. 10.1.15.: Dependence of ***fractional glucose reabsorption (steady state phase 50-70min) on albumin concentration (BSA).*** With verapamil, the % reabsorption at higher load is only slightly lower than without verapamil. The addition of 5% erythrocytes raises glucose reabsorption to >95% even at low albumin concentration. Mean values ± SEM (250).

10.1.6. Potassium secretion

If one measures the rate of potassium secretion in rats under standard conditions (normal diet) in vivo in the metabolic cage, one finds about 20% of the filtered amount of potassium in the final/excreted urine, corresponding to a value of 0.2 expressed as clearance quotient: $K^{+}_{U/P}$: Creatinine $(Inulin)_{U/P}$. In a paper published in 1975, Silva et al. reported a clearance ratio of 0.41 for the IPRK (in mode 2) and went on to state that they could detect net secretion only in kidneys from animals that had been chronically exposed to high levels of potassium in their food (276). The likely explanation for the low values in their experiments is as follows: The high concentration of albumin in the perfusate – 6.5-6.8g/dl, which corresponds to an increased COP – reduces the GFR and leads to low urine flow rates (small lumen ureteral catheter PE10). In addition, Silva et al. used a substrate-poor perfusate in the recirculation mode with only 5mmol/L glucose. Under our conditions, the results are quite different. We observe a net potassium secretion in the absence of chronic potassium overload, which is dependent both on the urine flow rate and the use of a substrate-enriched perfusate. With albumin concentrations of 5 g% and less, we found higher urinary flow rates, and this may in part be due to a rheogen effect on secretion. Only at very high COP in the perfusate and lower urinary flow rates is potassium secretion reduced such that the clearance ratio falls below 1, i.e., no net secretion. In 1979 Silva's group published data for isolated perfused kidneys from adrenalectomized animals. Upon substitution of aldosterone, these organs exhibited a rapid increase in kaliuresis after that could be inhibited with spironolactone. This effect of aldosterone was only seen if they added more exogenous metabolites other than glucose, such as pyruvate, lactate and α-ketoglutarate (synonym α-oxoglutarate) (282). The net potassium secretion corresponds to the results, published in the initial work of 1975. Potassium secretion reached up to 213% of the filtered potassium amount (257) when the perfusate was substrate-enriched. Thus, we can conclude that the effect of stimulation with aldosterone persists for the entire period of perfusion.

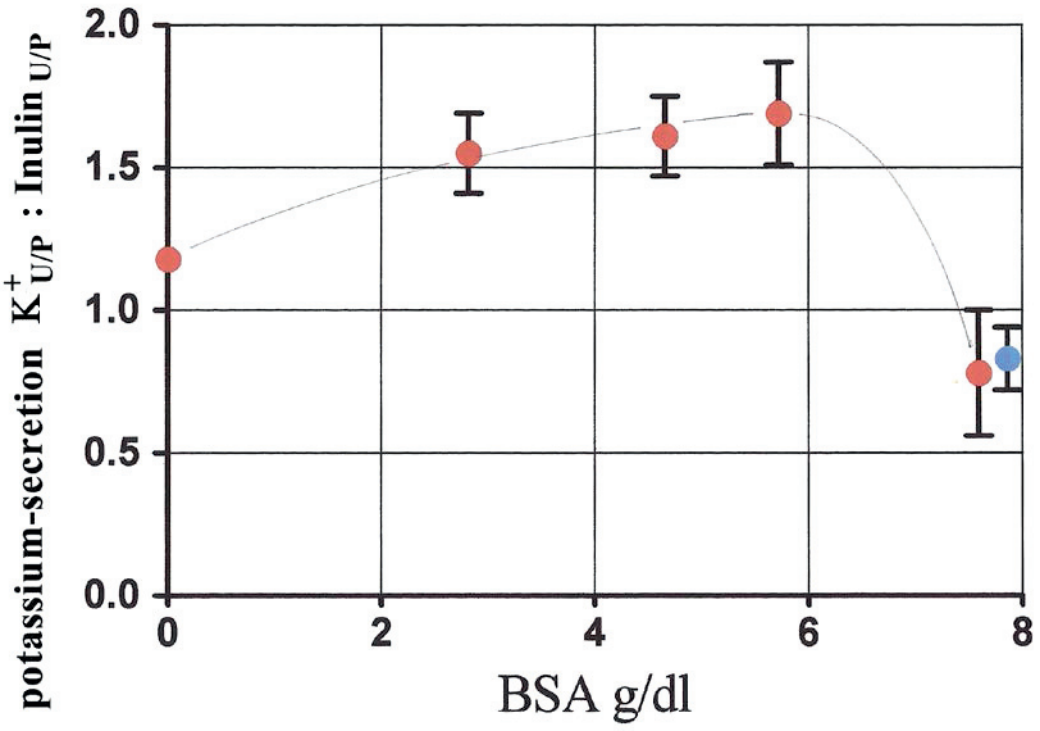

Fig. 10.1.16.: ***Potassium secretion during the steady state phase (50-70min) with substrate-enriched perfusate.*** Potassium secretion [mean values ± SEM (250)] is plotted against albumin (BSA) concentration in the perfusate. Net secretion increases up to an albumin concentration of 6 g%, but ceases abruptly at 7.5 g% albumin, where GFR and urinary flow rate are depressed. The blue data point corresponds to experiments in which the GFR was increased by adding verapamil at a higher perfusion pressure, up to the GFR level attained with 6g % albumin experiments.

The relationship between potassium secretion and the concentration of albumin in the perfusate depicted in Fig. 10.1.16 demonstrates that only at the highest albumin concentration does net secretion cease. At the high urinary flow rates attained in these experiments (using adequate ureteral catheters), the rheogenic-dependent effect on potassium secretion is clearly visible. The findings reported by Silva (276), who observed net potassium secretion only after dietary stimulation, are probably due to two factors –the use of (i) PE10 catheters and (ii) a perfusate containing glucose as sole substrate. In the Figs. 10.1.17 and 10.1.18, we take these factors into account.

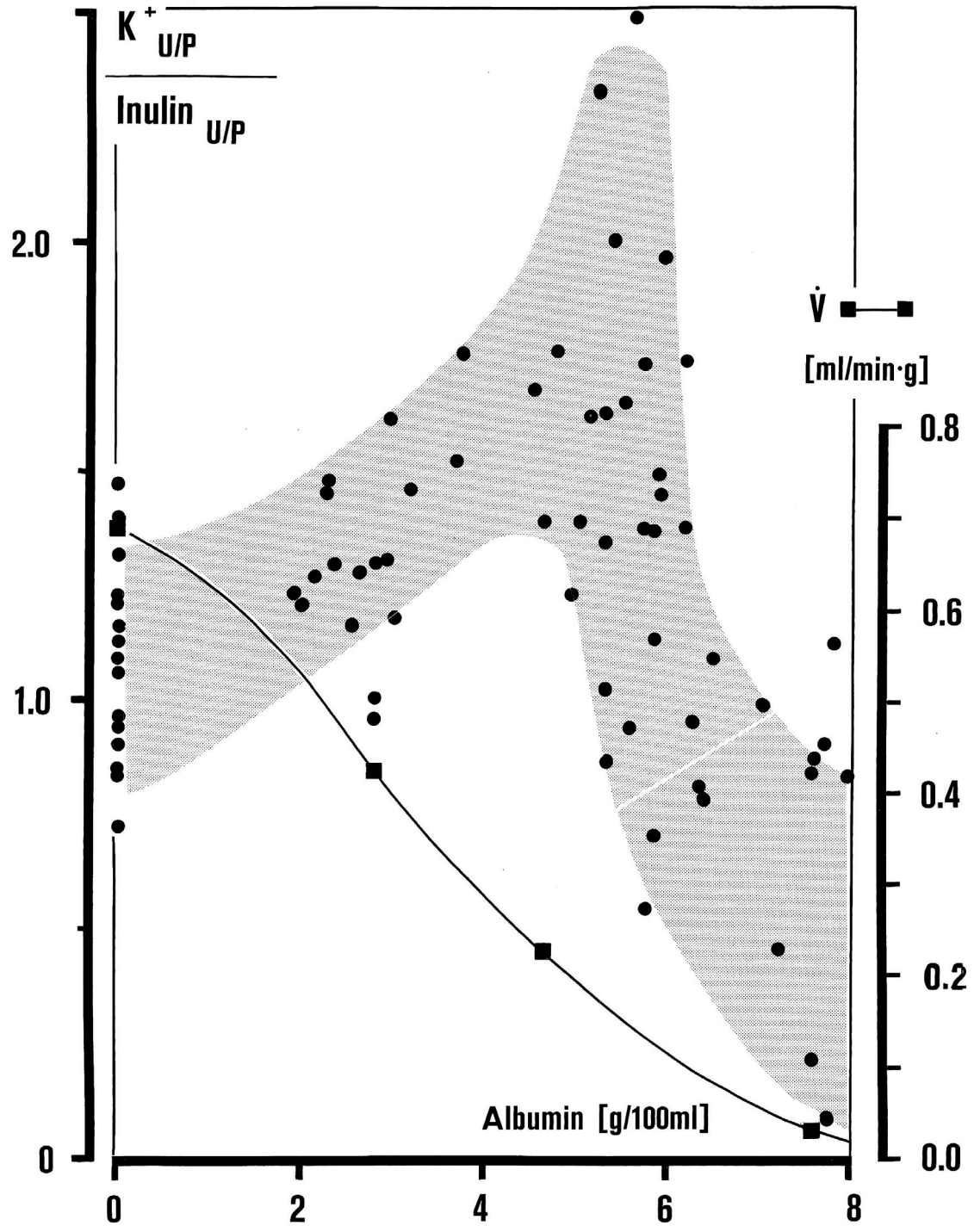

Fig. 10.1.17.: ***Dependence of potassium secretion in the steady state phase (50-70 min) on the concentration of albumin (BSA).*** Individual values are plotted in relation to the urine volume (filled squares), which falls as the concentration of albumin in the perfusate is increased (scale on the right). High secretion rates are a feature of the perfusate enriched with metabolic substrates (s. Fig. 10.1.18.). In vivo, values are around 0.2. Values in this range can be attained in the IPRK only at very high COP values. Most of the measured values fall in the shaded area.

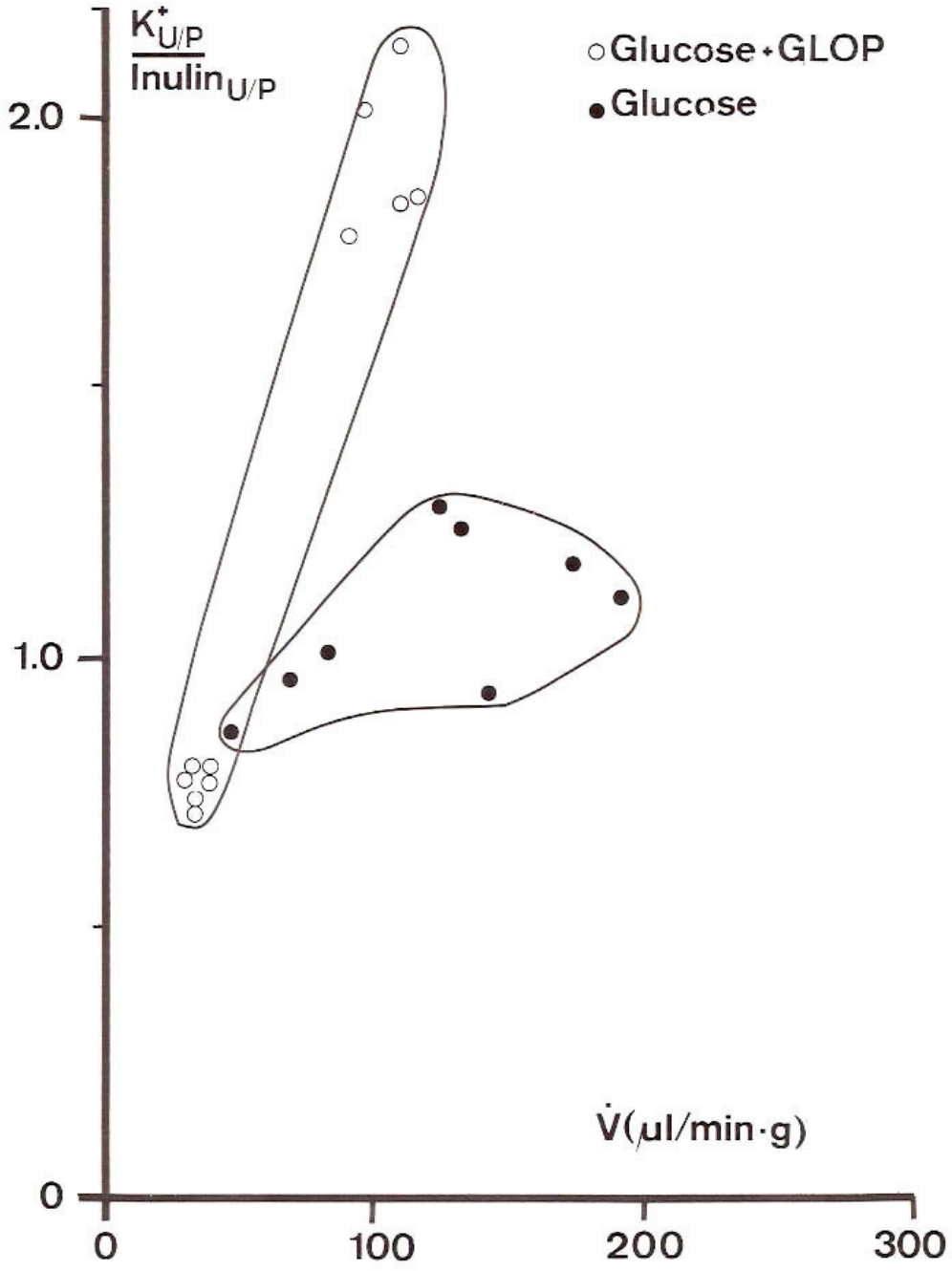

Fig. 10.1.18.: ***Dependence of potassium secretion in the steady state phase (50-70min) on the rate of urine output and the presence of substrate additives***. Individual values are plotted against urinary volume (**$\dot{V}$**). Note the difference between substrate-poor perfusate (glucose alone) and enriched perfusate (glucose plus glutamate, lactate, oxaloacetate, pyruvate and 8 amino acids). The in-vivo clearance ratio based on studies in the metabolic cage on rats fed on the standard diet, i.e., at low urinary volumes ("anti-diuresis") of less than 10 µl/min, is about 0.2.

10.1.7. Efficiency of sodium transport in relation to oxygen consumption

A comparison of rates of sodium transport between the in-vivo kidney and the isolated organ raises the question of why the in vivo kidney is able to transport sodium so much more efficiently. The calculated in-vivo ratios of T_{Na} to $\dot{Q}_{O_2}$ are around 18, i.e., 18 sodium molecules are transported per molecule of oxygen consumed. The isolated kidney reaches a quotient of 15 – at best. So-called back-leak phenomena are thought to underlie this effect, and they may indeed explain the decrease in absolute and fractional sodium reabsorption, which is most clearly seen with colloid-free perfusate. An exceptional situation is described below, in which a value of 18 was reached for a short time.

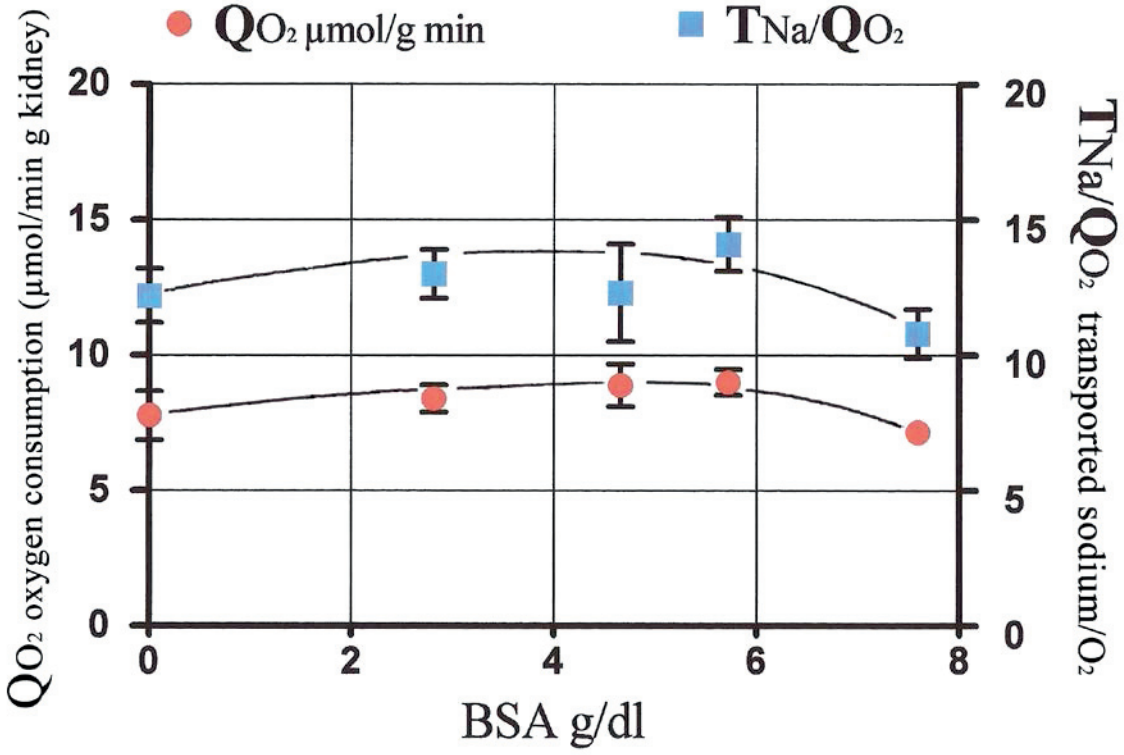

Fig. 10.1.19.: ***Relationship between oxygen consumption and $T_{Na}/\dot{Q}_{O_2}$ in the steady-state phase (50-70min) with substrate-enriched perfusate.*** $\dot{Q}_{O_2}$ and $T_{Na}/\dot{Q}_{O_2}$ are plotted against the concentration of albumin (BSA). Mean values ± SEM.

With the addition of glutathione, cysteine and 5% red blood cells, the in-vivo $T_{Na}/\dot{Q}_{O_2}$ value of 18 can be achieved for a short time (see Table 11.1.6) some 50 min after starting perfusion. At 100 min the ratio had fallen to 16.3. The high efficiency obviously declines with time, but the reason for this is not clear (shedding of the endothelial surface layer and glycocalyx? (204)).

10.2. Recirculation perfusion

With the single-pass perfusions, which we had performed in Berlin using the gelatin preparation Haemaccel® as colloid, we experienced initial problems with regard to the stability of the resistance to perfusion. Switching to sterile perfusion solutions essentially solved this problem, and stability could be maintained for 2-4h (257). In our first perfusion experiments using bovine serum albumin (BSA) and the recirculation mode in Hannover, however, these old problems returned. After 90 minutes, we regularly observed a drop in flow rate and in GFR under pressure-constant perfusion conditions. The use of filters with 8-µm porosity did not fully resolve the problem, but we retained the inline filtration nevertheless. Reflection on the relative stability of the relatively stable single-pass experiments then led to the solution – which would have been obvious to a nephrologist - to regenerate the perfusion continuously with the aid of dialysis. In this way, one could aerate the dialysate with a glass frit and replenish the albumin containing perfusate, and achieve greater stability. A literature search revealed that the dialysis technique had already been used in 1967 by Baumung and Peterlik in Vienna (20) on the isolated rat liver to compensate for the rapid development of acidosis in their preparation (see Section 10.3. below).

Table 10.1. ***Functional parameters of the isolated kidney perfused with 5g albumin/dl and using either a dialyzer circuit (a) and a membrane oxygenator (b)***. Time course. Mean values ± SEM, n = number of the kidneys, Pa 100 mmHg.

Perfusion	a) b)	a) b)	a) b)	a) b)
Time range (min)	**30-50**	**50-70**	**70-90**	**90-110**
Perfusion flow rate (ml/min·g)	22,9±0,9	24,9±1,1	26,2±1,3	27,5±2,1
	26,1±1,9	25,8±1,8	25,3±1,6	*
Urine flow rate $\dot{V}$ (µl/min·g)	128±21	166±25	201±28	255±33
	111±18	121±19	124±22	*
GFR Inulin-Clearance (ml/min·g)	0,96±0,04	0,95±0,03	0,96±0,04	0,98±0,06
	0,85±0,05	0,79±0,06	0,66±0,09	*
T_{Na} (µmol/min·g)	126±6	116±4	113±5	112±8
	112±7	102±7	82±10	*
Na-reabsorption %	91,6±1,6	87±2,1	83,3±2,4	81,3±2,5
	90,8±1,7	89,3±1,4	87,3±1,6	*
Glucose-reabsorption %	94,9±0,3	93,5±0,8	91,9±1,0	90±1,8
	96,9±0,2	95,5±0,5	91,0±1,3	*
K_{UP}/Inulin$_{UP}$	1,50±0,13	1,47±0,09	1,30±0,08	1,22±0,09
	1,15±0,07	1,04±0,07	0,97±0,07	*
$\dot{Q}_{O_2}$ (µmol/min·g)	7,93±0,29	8,2±0,3	8,01±0,32	7,90±0,58
	8,78±0,38	8,5±0,4	7,86±0,03	*
Number of Experiments n =	14	14	14	9
	13	13	13	*

*The experiments in recirculation mode 2 with a membrane oxygenator were terminated after 90 min due to a marked drop in the GFR and a drop in the perfusion flow rate.

Table 10.1. is taken from the work of 1981 (251). For the sake of comparability, all parameters are based on 1g kidney weight. For reference, the unperfused left kidney was decapsulated and weighed after the left renal artery had been tied off prior to perfusion. Given the typically small difference in weight between the right and left kidney in vivo, this is a more reliable reference for the perfused kidney, which almost always gains weight, except when perfused with hyperoncotic perfusate (e.g. BSA>7g%), see also chapter 10.1.2. Hartwig used verapamil in recirculation experiments with a membrane oxygenator, which explains the only slight flow rate and filtrate reduction in comparison (99).

Perfusion experiments on the endocrine function of the kidney

To study the role of the kidney for the homeostasis of peptide hormones, we used the isolated kidney preparation in the recirculation mode, both as a filtering and non-filtering organ (237, 268). This approach enabled us to distinguish metabolic clearance from clearance by filtration, and to quantify both (268). In addition, we were able to show that metabolic clearance of homologous rat insulin was more efficient than that of heterologous porcine insulin (237). Furthermore, we unexpectedly discovered that peptide hormones such as insulin and parathyroid hormone (PTH) are not broken down by the non-filtering kidney* (165, 171, 237, 268). However, this is compatible with the fact that an IPRK with a normal GFR is a better model for these studies than one with hyperoncotic perfusate and reduced filtration rates as used by Rabkin (205). Moreover it is necessary to comply with the conditions specified by Johnson and Maack for the non-filtering kidney: a hyperoncotic 10g% BSA, a lower perfusion pressure (70mmHg) (118) and ligation of the ureter (in contrast to Maude, who sought to stop urinary flow only at reduced perfusion pressure (168)). By injecting a Lissamine bolus, we have directly confirmed that no filtration occurs under these conditions, as Maack had previously reported (162).

However, other aspects of the kidney's function in hormonal homeostasis, such as the conversion of cholecalciferol (Vit D) and the metabolism of steroid hormones, could be investigated and elucidated (107, 108, 220). In addition to our studies on insulin, C-peptide and PTH, we have examined other hormonal processes, such as the conversion of thyroxine [T_4] to triiodothyronine [T_3] and quantified the export of T_3 from the kidney to other tissues. We were able to demonstrate (99, 314) that an optimized and substrate enriched perfusate with added erythrocytes as oxygen carriers supports a much higher conversion rate than that reported by Ferguson (75). Earlier, we had investigated the clearance of both hormones in the single-pass mode without colloid and those results were published in 1980 (4). Under such conditions (i.e., in the absence of binding proteins) we found a high, non-saturable resorption capacity even at non-physiologically high concentrations (100 times the normal values). Michael Hartwig used equilibrium-dialysis to recover the free hormone fraction from an albumin-containing perfusate (99).

* This assertion refers to the fact that there is no change when measured by RIA, but a certain degree of fragmentation is detectable by column chromatographic methods (171).

To overcome the increase in resistance that regularly occurred after the first 60-90 min of recirculation without replenishment, in the investigations carried out by Hartwig we made use of verapamil from the beginning, and were thus able to keep the flow rate stable (99). Earlier work had shown that autoregulation and tubulo-glomerular feedback can be suppressed also in vivo (175) (see Fig. 10.2.1.). Based on experiments on the isolated rabbit kidney, Pegg has pointed out that the return of the urine into the perfusate may facilitate blockage of capillaries by debris from the tubule cells. This is detectable by microscopy after about 30-40min perfusion with cell-free medium in the urine sediment (218), but can be avoided by the addition of 5% erythrocytes, as revealed by the fact that no necrosis occurs (218, 263).

Using small volumes of substrate-poor perfusate (30 ml/g kidney) Ferguson and Jennings measured the amount of T_3 formed in kidney tissue, as well as the level of T_3 secreted into the medium (75). Fig. 10.2.1 shows their data for the T_3 exported to the perfusate. At these relatively low conversion rates, no saturation appears, even at levels up to 10 times the physiological concentration of T_4. In contrast, the conversion rate measured by Gisela Wruck in her doctoral thesis is some 10 times higher than that reported in Ferguson´s publication (in the physiological range of T_4), but at a T_4 concentration of 75µg/dl conversion it is not linearly enhanced, but only 3 times higher (314). The crucial methodological differences here were the following. (i) The perfusate was substrate enriched and included glutathione precursor substrates and glutathione; (ii) erythrocytes were added to prevent oxygen deficiency damage, and (iii) the ratio of perfusate volume to kidney mass was 150ml/g kidney - and thus 5 times higher than in Ferguson´s work. These measures ensure that the kidney is supplied with higher levels of metabolically active substrates. The correspondingly lower T_3 levels were measured with a newly developed and highly sensitive RIA (314).

In the work of Michael Hartwig the concentration of T_4 used was further increased to 145µg/dl. The use of verapamil allowed perfusion resistance to be held stable into the second hour, and the deliberate restriction of the pO_2 to about 400mmHg increased the rate of export of T_3 furthermore. However, at the highest concentration of T_4, the T_3 export rate fell in the second hour from 79.7±6.5 down to 51.5±4,0 ng/h·g kidney, indicating that a saturation threshold had been reached. It follows that a process of model optimization can facilitate the approach to in-vivo conditions. Nevertheless, Ferguson had already shown that there was no difference in the conversion rate between a filtering and a non-filtering kidney. Wruck confirmed this finding, at even higher levels of export. In the physiological concentration range of 10ug/dl T_4, the filtering kidney exported 5.8±1.2ng/h·g kidney T_3 and the value for the non-filtering kidney was 6.7±0.8ng/h·g kidney. At a T_4 concentration of 75µg/dl, the rate of export was 16.6±2.6 in the filtering and 15.5±1.8ng/h·g kidney in the non-filtering kidney. However, Ferguson and Jennings brought filtration to a halt by lowering the perfusion pressure to 50-60mmHg (BSA unchanged at 7.5 g/dl) and interpreted the cessation of urine flow and the constancy of the T_4 concentration as evidence for the non-filtering function. In contrast, the non-filtering kidney in Wruck´s work was prepared by the method described by Maack, which involves ligation of the ureter,

elevation of BSA to 10g/dl, reduction of the perfusion pressure to 70mmHg, and the demonstration in a pilot experiment that an injected Lissamine-green bolus does not appear in collapsed lumina of tubuli.

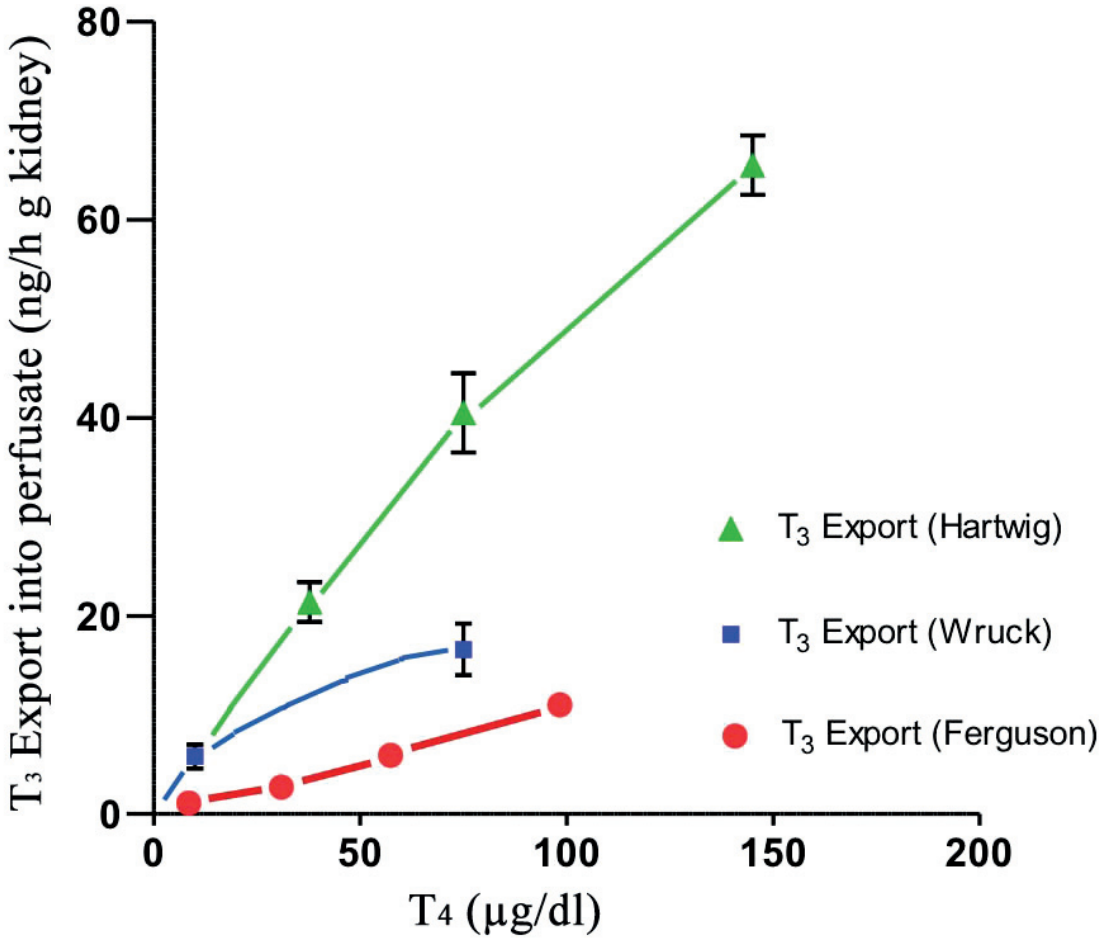

Fig. 10.2.1.: ***Comparison of the rates of conversion of thyroxine (T_4) to triiodothyronine (T_3) in the isolated perfused kidney.*** The diagram shows the amount of T_3 exported into the medium. Methodological differences account for the major discrepancies between the results depicted (s. text). The data from Ferguson (75) were calculated from the plot in the original paper. Gisela Wruck's results (314) are plotted as mean values ± SEM (n = 5, and 4 respectively) and Michael Hartwig's data (99) as mean values ± SD (n = 4). The latter data are taken from Hartwig's doctoral thesis (written in German). They can be accessed from the Medical University of Hannover (MHH) and the National Library in Berlin.

10.3. Recirculation with regeneration of the perfusate by dialysis

The functional stability of the isolated perfused kidney is enhanced when a hyperoncotic albumin solution is used, but this gain comes at the expense of a reduced GFR. Conversely, the use of 5g/dl BSA results in a normal GFR of 1ml/min·g kidney but, unless erythrocytes are included, the renal function clearly declines already in the second hour. Based on my experience with single-pass perfusion (and Haemaccel® as colloid), which provided stable perfusion flow rates over 2-3 hours, I introduced the use of bovine serum albumin combined with replenishment by dialysis in Hannover. At first we used an initial perfusate volume of 200 ml (150 ml in recirculation) and 2000 ml dialysate. Later on, we increased the dialysate volume to 5000 ml and that of the perfusate to 250/200 ml. This meant that substrates needed to be weighed out only for the dialysate; the albumin stock solution could then be diluted and the perfusate equilibrated by dialysis in preparation for the experiment. For details of the preparation of large volumes of dialysate see Chapter 4.1.3.

As mentioned in the previous section (10.2), a literature review showed that Baumung and Peterlik in Vienna had already used dialysis technique on the isolated rat liver in 1967 to compensate for the emergence of acidosis in their preparation (perhaps due to hypoxic lactic acidosis or bicarbonate consumption through urea synthesis). Dialyzers in those days were made from cellophane tubes (2.8cm in diameter and 160cm in length) in the manner of the Kolff-Watschinger coil-type dialyzer. The original publication gives a detailed description (20). We first obtained a reliable dialyzer in 1976. It had been developed by Josef Hoeltzenbein in Münster (112) and Travenol® in Belgium - see Fig. 4.4.11 and 4.4.12 - then produced this so-called capillary plate dialyzer (Type M1000) commercially. One outstanding feature of the device was the small filling volume of the blood compartment and the optimized diffusion distances.

Table 10.1. (Chapter 10.2) presents the comparison of recirculation with oxygenator and recirculation with regeneration of the perfusate by passage through this dialyzer. It clearly shows the superior performance obtained with the latter technique compared to recirculation with an oxygenator. This opened up the possibility of performing micropuncture experiments over 2-3 hours. Early-proximal micropuncture samples could be analyzed for albumin, thus allowing the sieving coefficient to be calculated under various experimental conditions (244, 245, 248, 250, 252, 266, 290-292) after microdisc gradient-gel electrophoresis. In parallel with the introduction of the dialysis method for regeneration of the albumin-containing perfusate we used the standard substrates glucose, lactate, pyruvate, oxaloacetate and glutamate, and also the mixture of 8 amino acids described by De Mello and Maack in 1976 (63). Later, we became aware that the inclusion of arginine in the dialysate helped to avoid rapid depletion of this precursor of NO, and we suspected that this might have contributed to the improved long-term stability of this preparation. The issue was then systematically investigated in cooperation with Jörg Radermacher in our

experimental set-up in Hannover, and our hypothesis was confirmed (206, 207). Owing to its swift consumption, arginine deficiency sets in rapidly in the non-replenishing recirculation system, but its effects may be mitigated when perfusion is performed with hyperoncotic media. Under these latter conditions, the vascular bed shows the lowest perfusion resistance. This is even more obvious at concentrations of albumin of 5 g/dl and below (with pure recirculation). Administration of L-NNA (N omega-nitro-L-arginine), an inhibitor of nitric oxide synthase, had the same effect as arginine depletion. These findings clearly showed why long-term stability was improved by including arginine in the dialysate. On this empirical basis, a series of studies with micropuncture techniques was undertaken (181, 182, 184, 245). The first tubular pressure measurements had been performed in Berlin on the single-pass preparation with Haemaccel®. We noted that proximal and distal tubule pressures were almost identical in the early phase, during which the flow rate sank to a minimum before rising again (see Fig. 6.4.2). We interpreted this drop in perfusion pressure as indicating that the filtered gelatin increased the viscosity in the lumen of the tubule at this stage, when fractional sodium and fluid resorption rates are still high. These rates fall off later on, and the pressure in the distal tubule also decreases.

The first measurements of tubular pressure in the albumin-perfused kidney were performed by Gerd Schwietzer, who used the Landis technique (141), which was a standard method in the laboratory of Karl-Heinz Gertz at that time. In subsequent studies, we were able to use the system developed by the Berlin group (154) in the version built by Hampel in Frankfurt. Klaus Hinrich Neumann performed the studies with this micropuncture technique, having acquired his expertise in the Gertz laboratory in Hanover and in Floyd Rector´s group in San Francisco. The dialyzers we have used most recently are low-flux dialyzers from FMC, initially the Polysulfone type F4, then the FX5 (Helixone®, Polysulfone improved) with a 1-m² surface and a filling volume of 54ml (blood side). So-called high-flux dialyzers are unsuitable due to their high permeability for albumin under these experimental conditions.

10.4. The anatomically fixed kidney as a tool for analyzing the glomerular filter

The micropuncture experiments used for the characterization of glomerular permeability for macromolecules are extremely laborious. This factor motivated a search for a simpler method, which resulted in the fixation technique and the published material summarized in Chapter 12.4.

10.4.1. Perfusion fixation of the isolated kidney for reperfusion

We preperfused the kidneys initially by the standard method at 100 mmHg with a substrate-enriched Krebs-Henseleit solution containing 5% BSA over 15 min in mode-3 recirculation with dialysis and in the presence of verapamil ($4.4 \cdot 10^{-6}$ mol/l). The perfusion

pressure was then raised to 150 mm Hg just before the fixation, and the kidney was perfused with the warmed fixation solution at the same pressure over 5-9min.

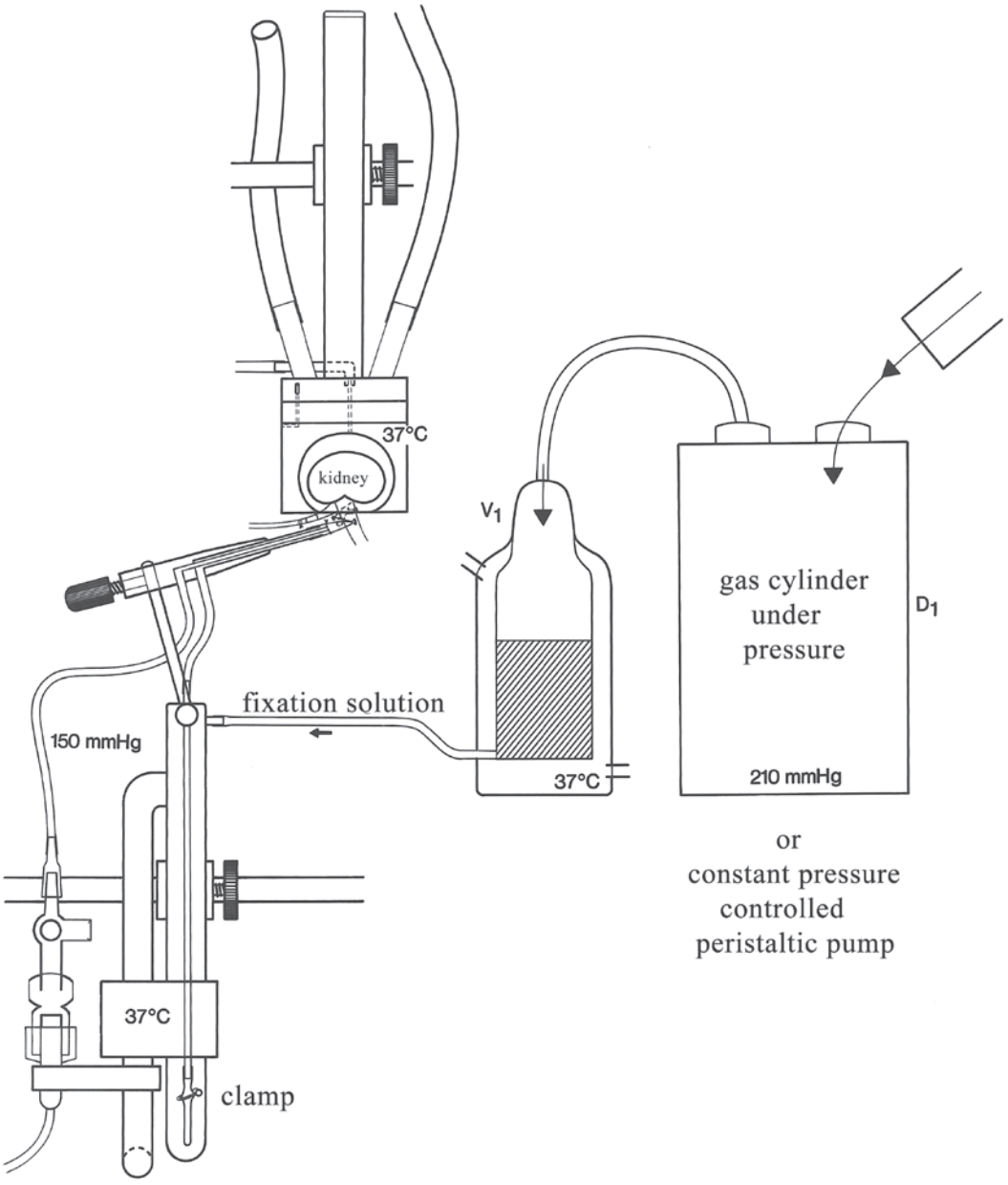

Fig. 10.4.1.: ***Set up for anatomical fixation.*** The arterial bypass serves as an inflow for the fixation solution, which is warmed up to 37°C and as driving force we used compressed air. Compressed air fills a reservoir as driving force, near the set or a pressure-controlled peristaltic pump replace what is lost. To start fixation seamlessly we clamp the inflow of standard perfusate and open the influx of fixation solution. We record the perfusion pressure during fixation.

10.4.2. Fixation solution for reperfusion experiments

The starting material was a 6g% HAES solution in 0.9% NaCl (FMC), which was concentrated by ultrafiltration to half the volume to yield a 12g% solution. In addition, we used an 8% solution of monomeric glutaraldehyde, diluted with phosphate buffer (7.1 pH) and mixed 1:1 with the HES solution to give a final concentration of 1.25% glutaraldehyde. The rational for the use of HAES is the following: If one uses colloid-free fixing solution, a dramatic increase of perfusion resistance occurs immediately after the transition to the perfusion fixation. This can be avoided by using a non-proteinaceous colloid-solution, which in turn permits better and more homogeneous fixation of kidney tissue, based on morphological criteria as assessed by light and transmission electron microscopy (s. Chapter 12.2.).

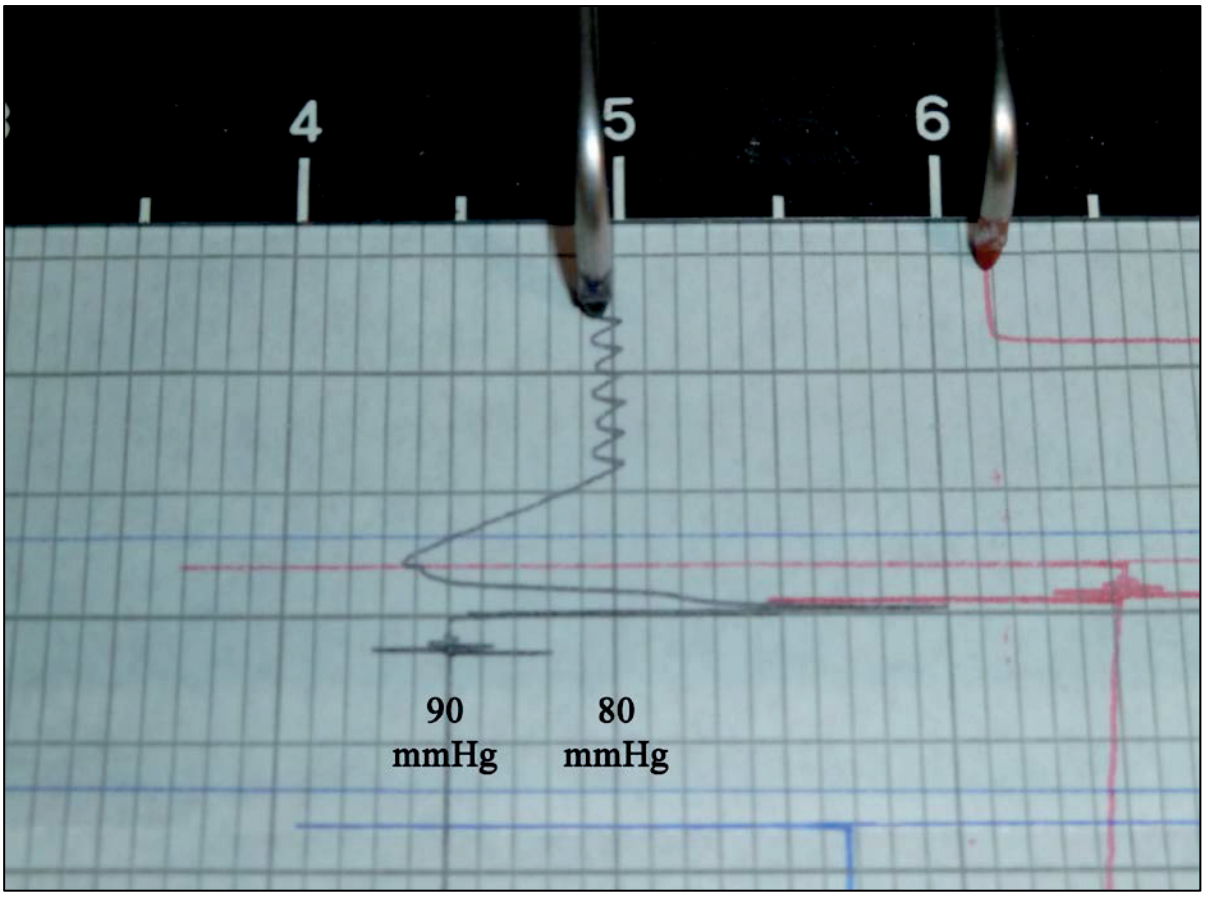

Fig. 10.4.2.: ***Pressure recording in the fixation phase.*** The recorder protocol shows the transient oscillation of the perfusion pressure (black line) following the abrupt rise on the transition to fixation. The initial pressure is 90mmHg; at the onset of the transition, there is a brief drop in pressure, which then rises to just over 90 mmHg before settling down to the preset fixation pressure (here 80 mmHg). The train of pulses coincides with the restart of the aerating peristaltic pump to keep the pressure in the gas reservoir near the set perfusion pressure of 80 mmHg. In this case, the fixation was carried out specifically for morphological studies. For fixation of kidneys for use in reperfusion experiments an effective pressure of 150 mmHg is used.

11. Tabellarium

Abbreviations used in the following Tables and in Chapter 13.

Parameter	Dimensions	Meaning
ffp (P_{ff}) °	mmHg	free flow pressure early proximal
sfp (P_{sf}) °	mmHg	stop flow pressure early proximal
efp (P_{uf}) °	mmHg	effective filtration pressure
gcp	mmHg	glomerular capillary pressure
K_f *	nl/s·mmHg	glomerular ultrafiltration coefficient
k	nl/s·mmHg·cm²	effective hydraulic permeability
K	µl/min·mmHg	coefficient of hydraulic conductance of the whole kidney
TF/P_{Inulin}		ratio of inulin to tubular fluid/perfusate
gfr, SNGFR	nl/min	single nephron filtration rate
$\dot{Q}$**	nl/min	perfusion rate of single nephron
GFR	ml/g·min	glomerular filtration rate (Inulin) of the whole kidney
RPF	ml/g·min	renal perfusion flow of the whole kidney
FF	%	filtration fraction GFR/RPF
T_{Na}	µmol/g·min	absolute sodium reabsorption rate
$\dot{Q}_{O_2}$	µmol/g·min	oxygen consumption rate
$\dot{V}$	µl/g·min	urinary volume per minute
COP/π	mmHg	colloid-osmotic (oncotic) pressure of perfusate
$K_{U/P}/Inulin_{U/P}$		clearance ratio of potassium

* Calculated from **K_f** of the whole kidney/$3 \cdot 10^4$ nephrons in a rat kidney (approximate number)

** Calculated from total perfusion rate/$3 \cdot 10^4$ nephrons of a rat kidney

Table 11.1.1.: ***Effects of increasing concentrations of albumin (COP) in the medium on functional parameters of the IPRK (measured 50-70min after the start of perfusion).*** Albumin (bovine serum albumin BSA) was the sole colloid. The COP was calculated with the Landis and Pappenheimer (L & P) formula: $2{,}8c + 0{,}18c^2 + 0{,}012c^3$ where c is the albumin concentration in g/dl. The measured COP values were read off from a calibration curve obtained experimentally with a 20000-Da membrane. The data for colloid-free perfused kidneys are from single-pass (mode 1) perfusions, the others from mode 3 (recirculation with regeneration of the perfusate by dialysis). The effective perfusion pressure Pa in colloid-free perfusate was at 90mmHg and otherwise at 100mmHg. In order to achieve a GFR at high COP comparable/equivalent to that observed at "normal" COP, it was necessary to increase the effective perfusion pressure from 100 to 140 mmHg and add verapamil ($4.4 \cdot 10^{-6}$ mol/l); this is listed in the last column. Single nephron flow rate and single nephron gfr was calculated based on $3 \cdot 10^4$ nephrons / kidney. The material in this Table was first published in 1981 (250, 251). n = number of the animals, mean ± SEM.

						Verapamil
Albumin (g/100ml)	**0**	**2,82±0,26**	**4,66±0,09**	**5,72±0,1**	**7,59±0,14**	**7,86±0,16**
π COP L&P-formula (mmHg)	0	9,6±0,89	18,2±0,35	24,2±0,42	36,9±0,68	39,0±0,79
πCOP measured (mmHg)	0	7,5	15,3	20,8	32,3	34
Perfusion rate (ml/min·g)	15,6±1,3	24,1±1,8	30,5±1,9	32,0±1,6	36,4±1,4	43,7±2,1
Urine flow rate $\dot{V}$ (µl/min·g)	683±122	421±61	226±71	140±17	30,6±8,8	132±22,1
GFR Inulin-Clearance (ml/min·g)	1,38±0,15	1,15±0,06	0,96±0,08	0,94±0,06	0,56±0,05	0,96±0,11
T_{Na} (µmol/min·g)	96,8±15,5	109,1±7,8	108±7	126±7	77,7±7,1	119±16
Na-Reabsorption %	51,3±5,5	69,8±3,4	82,6±6,2	91,6±1,3	97,1±1,0	90,7±1,2
$T_{Glucose}$ (µmol/min·g)	9,17±1	8,71±0,62	7,48±0,63	7,73±0,65	4,32±0,29	8,72±1,44
Glucose-Reabsorption %	78,5±3,5	90,8±1,4	91,6±2,2	94,6±0,6	94,5±0,7	93,8±1,5
K_{UP}/Inulin$_{UP}$	1,18±0,03	1,55±0,14	1,61±0,14	1,69±0,18	0,78±0,22	0,83±0,11
$\dot{Q}_{O_2}$ (µmol/min·g)	7,77±0,9	8,4±0,51	8,89±0,79	9,0±0,48	7,15±0,14	n.m.
T_{Na}/ $\dot{Q}_{O_2}$	12,2±1,03	13,0±0,86	12,3±1,8	14,1±1,0	10,8±0,9	n.c.
Filtration-fraction %	8,83±0,55	4,84±0,32	3,14±0,15	2,99±0,25	1,57±0,17	2,20±0,19
Single nephron flow rate (nl/min)	532±45	821±60	1140±71	1034±51	1117±43	1310±63
Single nephron gfr (nl/min)	47,0±5,2	39±2,0	35,7±2,8	30,2±2,0	17,0±1,5	28,9±3,2
Number n =	4	7	3	12	7	5

The colloid-free perfused kidneys in this group were not systematically decapsulated before the start of perfusion (although spontaneous decapsulation often occurred during the course of perfusion). Hence the perfusion rates are significantly lower than for perfusions that were initiated only after removal of the renal capsule.

Table 11.1.2.: ***Albumin free perfused rat kidney.*** Effects of perfusion with and without ureteral back pressure on overall renal function and nephron hydrodynamics. Data are means ± SEM. n = number of tubules (in parentheses, the number of animals). Pa = 100mmHg. The single nephron-gfr and K_f are calculated on the assumption that the rat kidney comprises $3 \cdot 10^4$ nephrons. Functional parameters were measured at 50-70 min (whole kidney) and at 30-115 min (single nephrons). For colloid free perfusate the stop flow pressure (sfp) = the glomerular capillary pressure (gcp). The ureter of the control kidney was cannulated with a short glass cannula extended with a PE50 tubing, the ureteral backpressure was applied via a PP10 catheter (10cm length) inserted in the ureter, s.a. Fig. 4.7.0. The data displayed in this Table was first published in 1981 (250) (251).

	control	with ureteral back pressure
Parameter IPRK Number n =	n = 32 (4)	n = 21 (4)
Perfusion flow rate (ml/min·g)	15,6±1,3	15,0±1,1
Urine flow rate $\dot{V}$ (µl/min·g)	683±122	279±30
GFR Inulin-Clearance (ml/min·g)	1,34±0,05	0,54±0,01
T_{Na} (µmol/min·g)	96,8±15,5	37,7±3,9
Na-Reabsorption %	51,3±5,5	49,6±3,9
$T_{Glucose}$ (µmol/min·g)	9,17±1	3,32±0,3
Glucose-Reabsorption %	78,5±3,5	84,2±1,2
$K_{UP}/Inulin_{UP}$	1,18±0,03	1,21±0,15
$\dot{Q}O_2$ (µmol/min·g)	7,77±0,9	7,23±0,32
***$T_{Na}/\dot{Q}O_2$**	12,2±1,0	5,23±0,54
Filtration-fraction %	8,83±0,55	3,33±0,25
Single nephron data		
Free flow pressure ffp (mmHg)	55,4±1,6	47,7±1,8
Stop flow pressure sfp (mmHg)	73,8±1,3	68,9±1,4
Effective filtration pressure efp	18,4±0,6	21,2±1,1
Single nephron flow rate (nl/min)	520	500
Single nephron gfr (nl/min)	46,1±1,5	19,4±0,3
Ultrafiltration-coefficient K_f (nl/s mmHg)	0,0426±0,0015	0,0161±0,0011

The pressure drop along the thin PP 10 catheter was set to about 22mmHg at a urine flow rate of 279µl / min (s.a. Fig.: 4.4.3.).

*Note the slight difference in oxygen consumption relative to the amount of sodium transported, **T_{Na}**. The **$T_{Na}/\dot{Q}O_2$** ratio falls from 12.5 to 5.2. This could be due to backleak phenomena in the proximal tubule.

Table 11.1.3.: ***Comparison of functional parameters of the isolated rat kidney perfused a) without colloid in single pass mode and b) with 7g/dl albumin in mode 3 (recirculation with regeneration by dialysis) at various phases of the experiment.***
Values are means ± SEM. n = number of kidneys. Pa = 100mmHg.
Note that the capsule was not systematically removed prior to colloid-free perfusion. The material in this Table was first published in 1981 (250, 251).

Perfusion a) / Perfusion b)	a) / b)	a) / b)	a) / b)	a) / b)
Period (min)	**30-50**	**50-70**	**70-90**	**90-110**
Perfusion flow rate (ml/min·g)	14,5±1,0	16,8±1,4	19,4±1,7	21,0±1,7
	33,1±2,1	35,4±1,4	35,0±1,8	34,6±1,8
Urine flow rate $\dot{V}$ (µl/min·g)	556±80	703±59	718±61	778±97
	15±2,7	26,8±5,7	33,3±7,6	28,2±6,8
GFR Inulin-Clearance (ml/min·g)	1,18±0,13	1,40±0,07	1,37±0,07	1,40±0,1
	0,58±0,09	0,63±0,04	0,58±0,06	0,49±0,08
T_{Na} (µmol/min·g)	87,3±9,6	97,4±5,4	89,2±5,2	86,6±3,1
	84,1±12,8	89,6±7,6	82,7±8,3	69,7±10,6
Na-Reabsorption %	54,7±3,2	50,9±2,3	47,8±2,3	45,6±3,1
	99,1±0,2	98,4±0,4	97,1±0,7	94,4±1,1
Glucose-Reabsorption %	86,6±2,2	83,4±2,3	82,4±3,8	79,1±5,0
	95,9±0,4	95,8±0,3	95,4±0,3	94,4±1,1
K_{UP}/Inulin$_{UP}$	1,15±0,05	1,09±0,06	1,08±0,07	1,05±0,09
	0,43±0,07	0,67±0,13	0,67±0,13	0,77±0,12
$\dot{Q}O_2$ (µmol/min·g)	7,26±0,45	7,29±0,36	7,43±0,45	7,58±0,60
	7,12±0,20	7,33±0,2	7,44±0,21	7,42±0,17
$T_{Na}/\dot{Q}O_2$	12,02	13,36	12,01	11,42
	11,81	12,22	11,12	9,39
Number of Experiments n =	10	10	8	7
	6	6	6	6

The fact that oxygen consumption does not differ significantly between the colloid-free and BSA-perfused kidneys during the first 90 minutes is reflected in the amount of sodium transported, **T_{Na}.** Only during the latest phase of the experiment does the ratio **$T_{Na}/\dot{Q}O_2$** in colloid-free perfused kidneys fall off significantly. Note also that no ureteral backpressure was applied (see Table 11.1.2).

Table 11.1.4.: ***Hydrodynamics of superficially accessible nephrons*** (early proximal tubules) and functional parameters of the whole kidney with increasing concentration of albumin (BSA) from 0 to 4.9 g / dl. Pa = 100 mmHg, n = number of tubules, in parentheses the number of animals. The material in this Table was first published in 1981 (250).

Period 50-70 min

Albumin BSA (g/100ml)	**0**	**2,82±0,26**	**4,66±0,09**
π COP L & P (mmHg)	0	9,60±0,89	18,17±0,35
Perfusion flow rate (ml/min·g)	15,6±1,3	24,1±1,8	30,5±1,9
Urine flow rate $\dot{V}$ (µl/min·g)	683±122	421±61	226±71
GFR Inulin-Clearance (ml/min·g)	1,38±0,15	1,15±0,06	0,95±0,08
TNa (µmol/min·g)	96,8±15,5	109±7,8	108±7,3
Na-Reabsorption %	51,3±5,5	69,8±3,4	82,6±6,2
Glucose-Reabsorption %	78,5±3,5	90,8±1,4	91,6±2,2
K_{UP}/Inulin$_{UP}$	1,18±0,03	1,55±0,14	1,61±0,14
$\dot{Q}_{O_2}$ (µmol/min·g)	7,77±0,90	8,40±0,51*	8,46±1,19
T_{Na}/ $\dot{Q}_{O_2}$	12,2±0,90	13,0±0,86*	13,6±2,0
Filtration-fraction %	8,83±0,55	4,84±0,32	3,14±0,15
Filtration coefficient whole kidney (µl/min·mmHg)	76,6±2,8	82,3±2,0	127,4±8,5
Number n =	4	7 (5*)	3

Period 30-107 min

Albumin BSA (g/100ml)	**0**	**2,76±0,08**	**4,9±0,08**
π COP L&P (mmHg)	0	9,35±0,23	19,5±0,4
πCOP measured (mmHg)	0	7,4	16,5
Free flow pressure ffp (mmHg)	55,4±1,6	35,4±0,4	29,8±1,1
Stop flow pressure sfp (mmHg)	73,8±1,3	49,5±0,5	39,2±1,5
glomerular capillary pressure gcp (mmHg)	73,8±1,4	59,0±0,6	58,7±1,5
Filtration pressure Δp (gcp - ffp)	18,4±0,6	23,6±0,49	28,8±0,7
Effective filtration pressure efp	18,4±0,7	14,0±0,3	9,4±0,6
Ultrafiltration coefficient K_f (nl/s mmHg)	0,0426±0,0015	0,0458±0,0011	0,0708±0,0047
Single nephron flow rate $\dot{Q}$ (nl/min)	535±44	810±59	1136±70
Single nephron gfr (nl/min)	46,1±1,5	37,8±0,7	36,7±1,3
Number n =	32 (4)	46 (7)	27 (3)

$\dot{Q}$, gfr und K_f were calculated on the basis of $3 \cdot 10^4$ nephrons / kidney

π COP L & P (mmHg) was calculated using the Landis and Pappenheimer formula (see Section 9.7.1, Fig. 9.7.4)

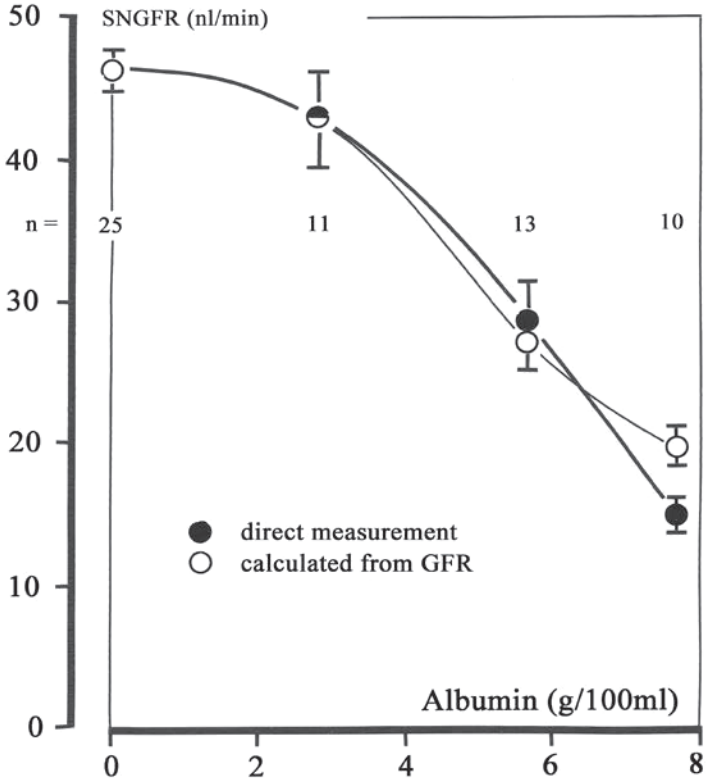

Fig. 11.1.1.: ***Comparison of SNGFR with the GFR of the whole kidney*** (250). The SNGFR was measured directly by micropuncture. The calculation is based on an average number of 30000 nephrons per rat kidney. The single-nephron filtration rate (SNGFR) was measured at subcortical nephrons under constant pressure control (181). Measured and calculated values are in good agreement as long as the colloid osmotic pressure of the perfusate is within the physiological range. At hyperoncotic perfusate, the SNGFR determined by micropuncture of nephrons is significantly lower than the SNGFR calculated from the total GFR. Here, the higher SNGFR of juxtamedullary glomeruli may have an impact. The GFR was measured as the rate of polyfructosan clearance, using the double-enzymatic method (macro- and microversions) according to Schmidt, (181, 182, 184, 239, 250, 251).

Table 11.1.5.: ***Data plotted in Fig. 11.1.*** The colloid-osmotic pressure calculated from the albumin concentration using the Landis & Pappenheimer formula (250).

Albumin concentration (g/100ml)	COP (mmHg)	SNGFR (nl/min)	SNGFR (nl/min)	Number of nephrons (kidneys)	Kidney-weight (g)
		Measured	Calculated (GFR/30000)		
0		n.m.	46,1±1,5	32 (4)	1,02±0,08
2,79±0,07	9,5	43,2±3,4	42,3±2,4	11 (4)	0,93±0,07
5,64±0,12	23,7	29,0±2,6	27,4±2,0	14 (5)	0,92±0,05
7,67±0,04	37,5	15,3±1,3	20,1±1,1	10 (3)	0,96±0,05

Table 11.1.5.: ***Hydrodynamics of superficially accessible nephrons (early proximal tubule)***. These data are for kidneys with ureteral backpressure (due to the use of narrow-bore ureteral catheters; see Table 11.1.1.) perfused with the indicated concentrations of albumin (BSA). Pa = 100 mmHg. n = number of tubules (in parentheses, the number of animals). The data are taken from the Habilitation thesis of 1981 (250), s.a. Fig. 4.7.0.

Period 50-70 min

Albumin BSA (g/100ml)	**0**	**2,54±0,16**	**4,85±0,17**
π COP L&P (mmHg)	0	8,47±0,53	19,18±0,67
Perfusion rate (ml/min·g)	15,0±1,1	19,8±1,4	24,8±0,6
Urine flow rate $\dot{V}$ (µl/min·g)	279±30	350±40	208±33
GFR Inulin-Clearance (ml/min·g)	0,50±0,03	0,88±0,04	0,90±0,05
T_{Na} (µmol/min·g)	37,7±3,9	84,7±5,1	106,4±7,0
Na-Reabsorption %	49,6±3,9	67,6±2,7	82,6±3,7
Glucose-Reabsorption %	84,2±1,2	92,5±0,6	90,3±2,0
K_{UP}/Inulin$_{UP}$	1,21±0,15	1,18±0,08	1,49±0,21
$\dot{Q}_{O_2}$ (µmol/min·g)	7,23±0,23	8,02±0,66	8,50±0,58
T_{Na}/ $\dot{Q}_{O_2}$	5,32±0,54	10,3±0,6	12.6±1,1
Filtration-fraction %	3,49±0,55	4,46±0,53	3,64±0,19
Filtration coefficient whole kidney (µl/min·mmHg)	28,9±1,8	70,7±3,2	91,5±1,9
Number n =	(4)	(3)	(4)

Period 37-115 min

Albumin BSA (g/100ml)	0	2,67±0,03	4,9±0,08
π COP L&P (mmHg)	0	8,99±0,14	19,5±0,2
πCOP (20000 Dalton membrane) (mmHg)	0	7,1	16,5
Free flow pressure ffp (mmHg)	47,7±1,8	52,0±0,5	36,4±0,9
Stop flow pressure sfp (mmHg)	68,9±1,4	66,1±0,5	46,7±0,9
Glomerular capillary pressure gcp (mmHg)	68,9±1,5	75,2±0,5	66,3±0,9
Filtration pressure Δp (gcp - ffp)	21,2±1,1	23,2±0,6	29,9±0,8
Effektive filtration pressure efp	21,2±1,1	14,1±0,6	10,3±0,24
Ultrafiltration coefficient K_f (nl/s mmHg)	0,0161±0,0011	0,0393±0,0018	0,0508±0,001
Single nephron flow rate Q (nl/min)	540±68	731±50	856±33,2
Single nephron gfr (nl/min)	19,4±0,3	32,2±0,7	31,9±0,6
Number n =	22 (4)	21 (3)	21 (4)

$\dot{Q}$, gfr und K_f were calculated on the basis of $3 \cdot 10^4$ nephrons / kidney

π COP L&P (mmHg) was calculated using the Landis and Pappenheimer formula (see Section 9.7.1, Figure 9.7.4)

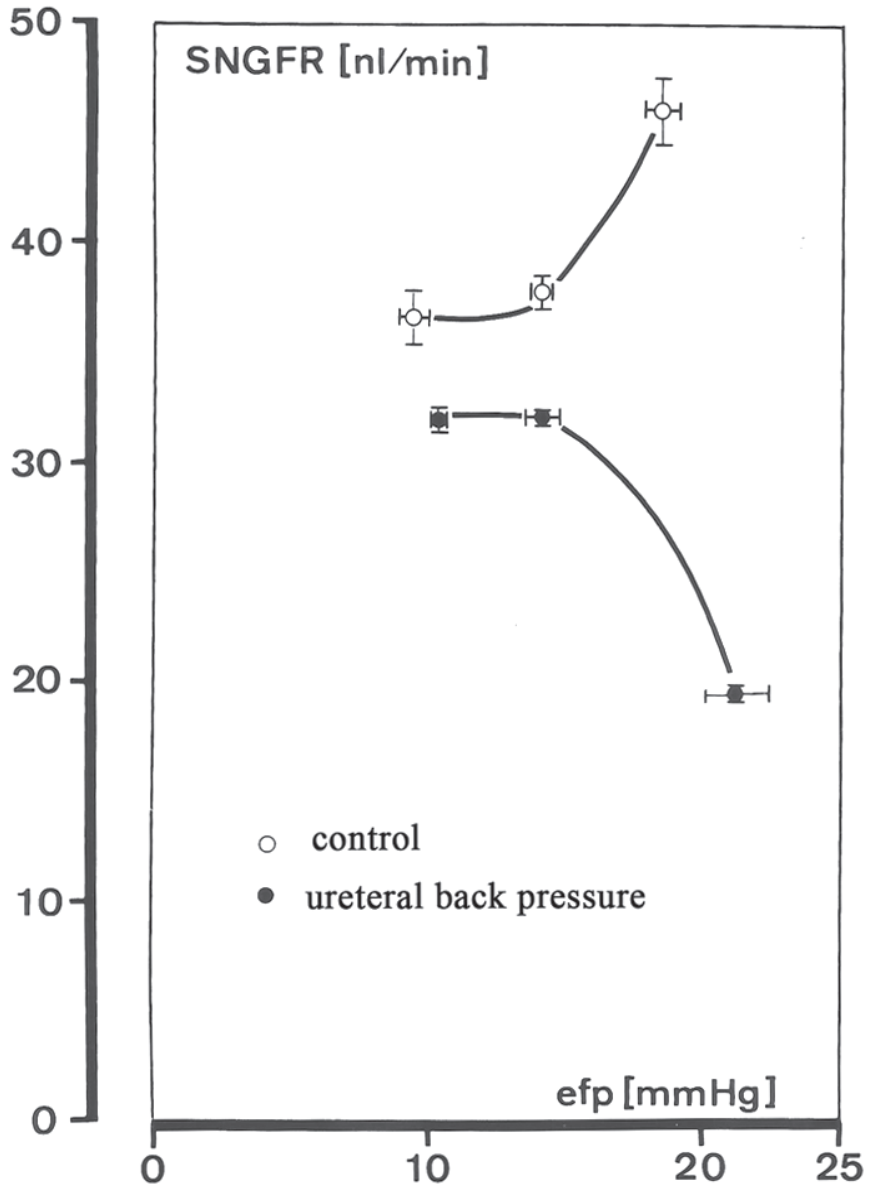

Fig. 11.1.2.: ***Effect of inadequate ureteral catheterization on the single nephron gfr.*** The strongest impact on the single nephron gfr is observed under colloid-free perfusion and ureteral backpressure due to the use of a ureteral catheter that is too narrow. This phenomenon, which was described as "erratic behavior of GFR" by two research groups (34, 152), was subsequently shown to be a consequence of inadequate ureteral catheterization (250, 251). Tables 11.1.3 and 11.1.5 present the basic data. The findings imply that under perfusion with a colloid-free medium, perturbation of post-renal outflow leads to a drastic reduction in hydraulic conductivity at an otherwise adequate effective filtration pressure. See Fig. 10.1.05, which shows that at a COP of between 10 and 20mmHg the ultrafiltration coefficient increases significantly; i.e. the hydraulic conductivity of the glomerular capillaries increases significantly (250).

Table 11.1.6.: ***Effects of enriched perfusate on functional parameters of the isolated perfused rat kidney after 50 and 100 minutes.*** After the addition of the indicated additives (glutathione, cysteine and washed human erythrocytes (5% hematocrit)) for perfusate. Perfusion in mode 3 with regeneration of the perfusate by dialysis, 5g / dl BSA, basic formula R1 (Table 4.2.) and R2 (Table 4.3). The perfusion pressure was 100mmHg in groups 1-3, 90mmHg in the 4th group in order to obtain comparable glomerular filtrates.
* Significance compared to the control (unpaired t-test Student), from (263).

Parameter	Group 1 Control n = 8		Group 2 Glutathione + Cysteine n = 3		Group 3 Erythrocytes n = 5		Group 4 As Gr 2 + Erythrocytes n= 5	
	50min	100min	50min	100min	50min	100min	50min	100min
Perfusion flow rate (ml/min·g)	25±2	28±2	25±2	26±2	21±2	22±3	21±1	23±1
Urine flow rate $\dot{V}$ (µl/min·g)	142±20	225±33	153±13	198±46	**77±29***	**115±27***	**80±12***	**134±19***
Inulin-Clearance (ml/min·g)	0,96±0,04	0,98±0,07	0,91±0,09	0,81±0,02	0,76±0,09	0,77±0,08	1,04±0,05	0,94±0,07
T_{Na} (µmol/min·g)	123±7	112±8	116±11	96±5	99±10	95±9	143±7	119±8
Na-Reabsorption %	90±2	81±2	90±1	83±3	94±2	89±3	95±1	**88±2***
Glucose-Reabsorption %	95±1	90±2	96±1	92±1	96±1	**95±1***	96±1	**96±1***
$K_{UP}/Inulin_{UP}$	1,59±0,07	1,22±0,09	1,62±0,012	1,35±0,01	1,12±0,007	1,04±0,008	1,17±0,023	1,49±0,008
$\dot{Q}_{O_2}$ (µmol/min·g)	8,2±0,4	7,9±0,6	6,7±0,5	6,3±0,3	7,6±0,5	7,3±0,4	7,8±0,2	7,3±0,5
$T_{Na}/\dot{Q}_{O_2}$	**17,3**	**14,2**	**17,3**	**15,2**	**13,0**	**13,0**	**18,3**	**16,3**

In control kidneys, unlike IPRKs under pure recirculation, GFR remains stable (see Table 10.1.). Addition of glutathione and cysteine had no effect on GFR but was associated with a striking reduction in oxygen consumption. Addition of erythrocytes increased sodium and water reabsorption, resulting in constant fractional glucose reabsorption, perhaps because red blood cells prevent morphological damage to proximal S_3-segments and TAL-segments (263). Another surprising finding in Group 4 is the quotient **$T_{Na}/\dot{Q}_{O_2}$** of 18 in the first hour after the start of perfusion, which is comparable to the value under in-vivo conditions. The Table is from the 1985 publication (263).

12. Annex

12.1. Biochemical studies on the energy metabolism of the IPRK

In the early single-pass experiments with Haemaccel® (urea-crosslinked polygelatin) as colloid, we perfused control kidneys, and kidneys that had been subjected to short-term "pre-perfusion" with basic medium, with perfusates containing various substrate additives. We then analyzed various metabolites after flash-freezing with the Wollenberger technique (313), modified to exclude the renal hilum and the papilla.

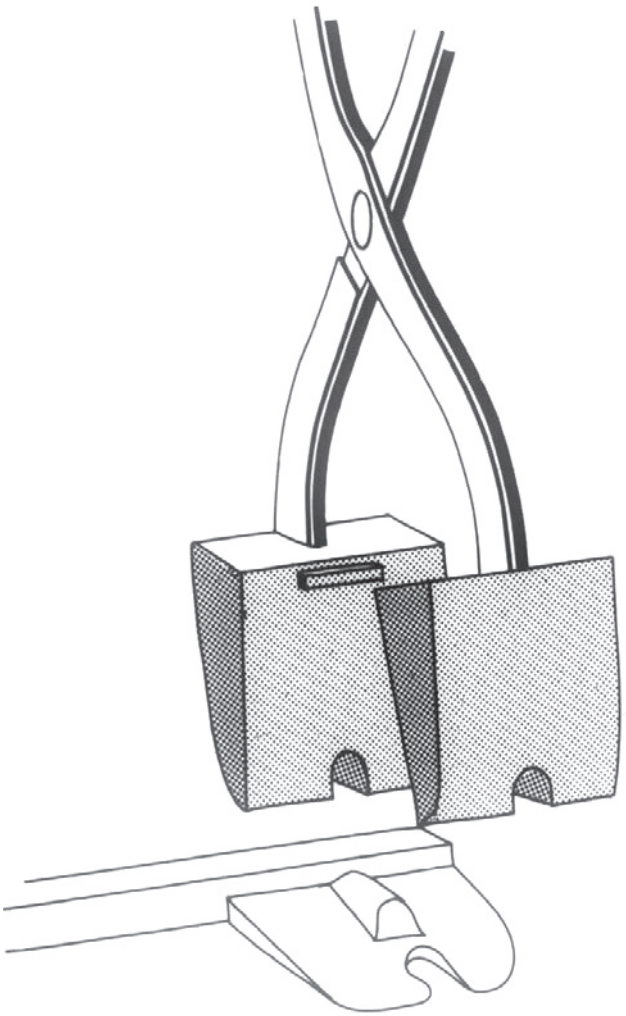

Fig. 12.1.: ***Freeze stop tongs (jaws of copper) with spacers*** (253) (after Wollenberger, modified). The kidney is supported on a plexiglass mount with a molded spacer; the cut-outs at the base of the tongs are designed to exclude the papilla and the renal hilum. We modified the freeze tongs described by Wollenberger (313) so that the metal spacer enabled us to obtain tissue slices of defined thickness from the perpendicularly oriented kidney, while excluding the papilla and hilum. Before clamping, the fat capsule is removed, the cranially located adrenal gland is dissected away, and the kidney is oriented on the Plexiglas mount. In this way, flash-freezing could be performed in situ under normal circulation conditions, or on the isolated perfused kidney oriented on its kidney support.
Thereby, we could exclude papilla and hilum.

When comparing the in-vivo data with the data for the IPRK one must consider that, after a short period of perfusion, the wet weight of the isolated kidney is greater (by 16.8 to 24.4%) than that of the in-vivo control. Thus, for example, the decrease in the ATP concentration is only 33% of the in vivo value. If we take into account the ATP content of blood as our in-vivo situation, the relative decrease compared to the blood-free perfusate (free of ATP) is still modest, and is comparable to the values measured in kidneys under micropuncture conditions in vivo (Roland Kirsten, personal communication, FU Berlin).

Table 12.1.: ***Metabolite concentrations in flash-frozen kidney tissue*** (256) The data are expressed in units of 10^{-9} mol / g wet weight. The results for succinate were later extended by Ingrid Krause in her dissertation (s. Tab. 12.2.).

	in vivo		in vitro		
Substrate	Control	Blood	Control	Oxaloacetate	Succinate
				1mmol/l	10mmol/l
G6P	58,3 ± 2,3		34,0 ± 11,2	32,1 ±3,1	17,8 ± 4,05
F6P	16,1 ± 0,2		13,5 ± 4,0	9,5 ± 1,7	
2-P-Glycerate	7,2 ± 2,1		8,1 ± 5,7	25,0 ± 7,2	
3-P-Glycerate	78,7 ± 4,8		58,6 ± 3,4	112,0 ± 20,2	
PEP	29,0 ± 2,2		27,8 ± 10,4	120,0 ± 37,3	
Pyruvate	88,5 ± 5,3	74,8	43,5 ± 10,1	208,0 ± 3,6	35,9 ± 11,3
Lactate	828,0 ± 82,8	1728,0	523,5 ± 66,8	580,0 ± 45,7	410,4 ± 47,1
L/P	9,4	23,1	12,0	2,8	11,4
ATP	1734,0 ± 34,1		972,8 ± 50,7	734,0 ± 64,6	475,2 ± 85,4
Citrate	209,0 ± 13,7		42,0 ± 6,6	94,2 ±10,7	45,0 ± 11,2
Malate	123,8 ± 16,9			78,1 ± 10,9	
MW ± SEM	n = 6	n = 6	n = 6	n = 4	n = 6

Table 12.2.: ***Effect of increasing concentrations of succinate in the perfusate on the metabolite content of flash-frozen tissue*** (130). The data are expressed in units of 10^{-9} mol / g wet weight. n = 6.

	Control	Succinate	Succinate	Succinate
Substrate		1mmol/l	4mmol/l	10mmol/l
ATP	806 ± 67	1025 ± 23*	754 ± 83**	507 ± 38***
ADP	590 ± 29	467 ± 17	455 ± 35	553 ± 38
AMP	414 ± 42	299 ± 28	313 ± 26	1145 ± 226****
ATP/ADP	1,37	2,19	1,66	0,92
∑ Adenine nucleotides	1810	1790	1522	2205
2-PG	71 ± 6	405 ± 30	78 ± 4	50 ± 5
PEP	162 ± 13	177 ± 18	189 ± 15	84 ± 15
Pyruvate	27 ± 3	50 ± 6	55 ± 2	37 ± 5
Lactate	907 ± 111	838 ± 205	632 ± 107	870 ± 95
L/P	33,6	16,8	11,5	23,5
Malate	122 ± 8	148 ± 119	357 ± 25	415 ± 44
MW ± SEM	n = 6	n = 5	n = 5	n = 6

*p<0,025 **p<0,02 ***p<0,005 ****p<0,0025

The metabolite content in flash-frozen tissue is expressed relative to the wet weight of the organ. As discussed above, values relative to dry weight differ less from those of the in-vivo controls, as we know from the electrolyte analysis carried out by Petra Brandt on in-

vivo kidneys and isolated perfused kidneys (37). The mean dry weight of in-vivo kidneys was 20.0 ± 0.31% of their wet weight. The corresponding figure for isolated perfused kidneys was 16.85 ± 0.21%, which gives a conversion factor of 1.187. Applying this conversion factor yields a value for the ATP concentration in the in-vitro controls of $1155 \cdot 10^{-9}$mol/g wet weight instead of $973 \cdot 10^{-9}$mol/g wet weight. This, however, ignores the fact that the vascular beds in the isolated and cell-free perfused kidney are devoid of cells. In vivo, the erythrocytes, leukocytes and thrombocytes all contain ATP.

Functional and morphological evidence of an oxygen deficit in the cell-free perfused rat kidney.

Weiss and his group in Hamburg and Kiel (142, 306) and Ochwadt`s team in Göttingen (67) have presented strong evidence for a relative lack of oxygen in the cell-free perfused kidney. Based on micropuncture studies, in 1976 De Mello and Maack defined a functional defect in the isolated kidney (63), which they localized to the TAL-segments. In 1978, Venkatachalam attributed morphological damage in specific areas in the medullary rays of the cortex and outer medulla to a shortage of O_2 (300). Three years later, Alcorn described similar changes in the isolated, cell-free perfused rat kidney (7). We studied this topic in parallel with Franklin Epstein´s group in Boston (38-42) and were able to develop our own ideas based on comparisons with in-vivo studies on the exposed kidney (117, 243, 250, 259-261, 263). In cooperation with Wilhelm Kriz in Heidelberg, we were able to place morphologically defined tissue damage in a functional context (263) and these findings stimulated further investigations. A conversation with Christian Bauer during a stroll along the Vltava River in Prague in 1982 raised the question of whether glomeruli are actually exposed to arterial blood, as was the general view in those days. With the support of Horst Baumgärtl and Dietrich W. Lübbers at the MPI in Dortmund, we were able to establish a technique for measuring pO_2 in superficial glomeruli and tubules in our laboratory in Hannover. In addition to the platinum microelectrodes encased in glass provided by Horst Baumgärtl, we also adapted the gold multiwire electrode technique of Herrmann Metzger in Hannover. This then led to several studies (117, 259-261) which demonstrated the existence of preglomerular oxygen shuntdiffusion. Two students, Uwe Jost and Harald Bertram, contributed significantly to this work. Harald Bertram completed his dissertation thesis on the topic (entitled “The significance of preglomerular shuntdiffusion of blood gases in the renal cortex for the intrarenal localization of erythropoietin synthesis: A comparison of experimental results on the rat kidney with a mathematical model of shuntdiffusion”) in 1991 at the Hannover Medical School (Medizinische Hochschule). Both students were among the authors of the resulting publications (260, 261). The following micrographs, which were taken in Wilhelm Kriz’s laboratory in Heidelberg, were obtained from kidneys perfused in mode 3 (recirculation with aeration and regeneration by dialysis) in Hannover and then anatomically fixed, and are taken from the 1985 paper (263).

12.2. Morphological studies of the isolated kidney, perfused either cell-free or with erythrocyte-containing medium (250, 263)

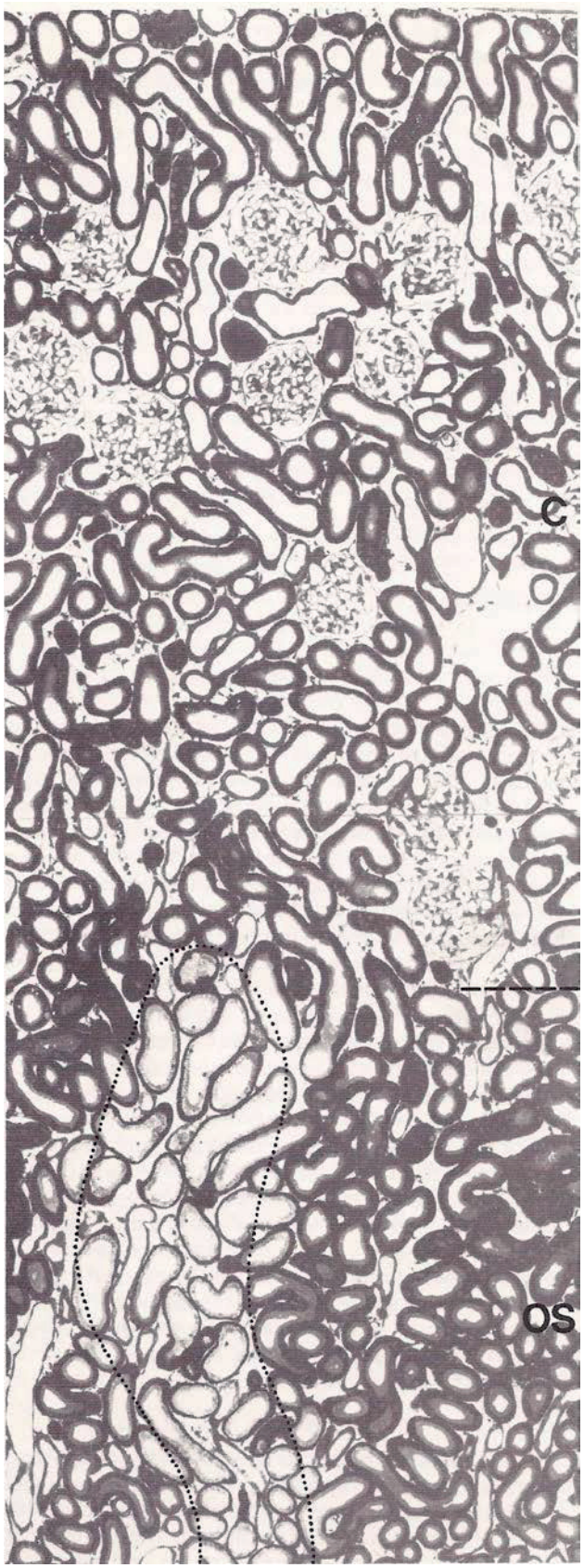

Wilhelm Kriz (263) performed the morphological analysis and prepared the Figures. One micrograph was contributed by Karlwilhelm Kuehn (Figure 12.2.08). The data shown come from four experimental groups:

Group 1: Control group, kidneys perfused (cell-free) with the basic medium supplemented with glucose, oxaloacetate, pyruvate, lactate, glutamate and the 8 amino acids from the protocol of DeMello and Maack and 10mU AVP (Pitressin®) (see R2 Table 4.3.).

Group 2: Protocol as for group 1, with the addition of reduced glutathione (0.2mmol/l) and cysteine (0.5mmol/l) to perfusate and dialysate.

Group 3: protocol as group 1, plus 5% washed human erythrocytes without in-line filter.

Group 4: protocol as group 2, plus 5% washed human erythrocytes. Perfusion pressure was reduced (90mmHg) to obtain a comparable GFR (see Table 11.1.6).

Fig. 12.2.01.: ***Longitudinal section through the cortex (C) and the outer stripe (OS) of the outer medulla.***
Group 2, cell-free perfusion with addition of glutathione. Within the cortex, glomeruli, tubules and vessels are structurally intact. In the outer stripe, necrotic P_3 segments are arranged in columns (dotted line), beginning in the basal portion of the medullary rays and extending to the border between outer and inner stripes. For further details, see Fig. 12.2.02. Epon section, 1µm thick, stained with methylene blue and azure II; Light micrograph (LM), magnification 100x.
Only at higher magnification does the true extent of the damage to the P_3 segments become clear (see Fig. 12.2.03.).

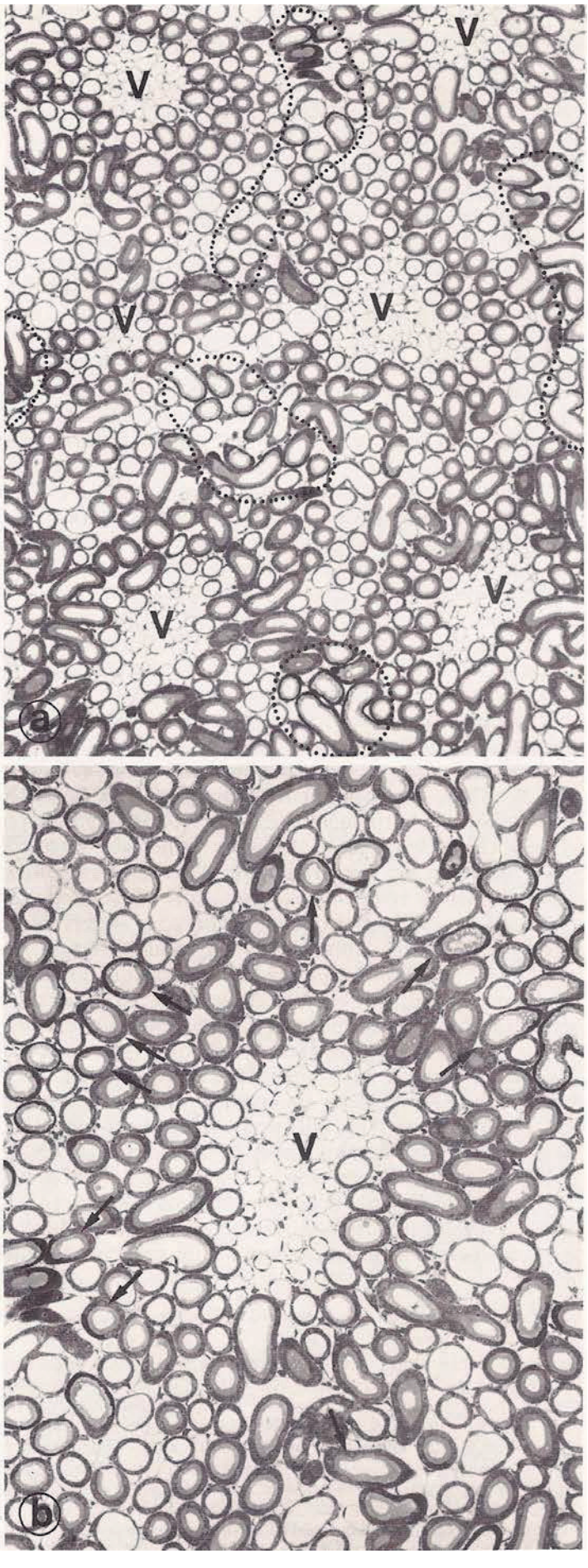

Fig. 12.2.02.: ***Cross sections through the outer stripe of the outer medulla.***
Group 1, cell-free standard perfusion over 2h.
a. Distribution of areas containing degenerated P_3 segments (dotted lines), which are consistently located farthest from vascular bundles (V). Damaged epithelia are characterized by their dark, condensed appearance. Epon section, 1µm thick. Magnification 100x (LM).
b. Damaged P_3 profiles around the vascular bundle (V) often exhibit a split between a degenerated and an intact half. The latter (arrows) generally face the vascular bundle. Epon section, 1µm thick; magnification 160x (LM).

Radial diffusion of oxygen from the vascular bundles helps to supply the tubules. As a consequence of the low oxygen-carrying capacity of the cell-free perfusate, the vascular bundles in the more remote areas are underserved. The characteristic feature of necrosis in the P_3-segments is coagulation necrosis. As water loss from the cells causes shrinkage of the cytoplasm and nucleus, the microvilli condense and become narrower, before being shed into the lumen. Different stages of the processes can be observed in one and the same tubule, where cells on one side may be intact while the opposite side shows defects.
(See the following Figs.).

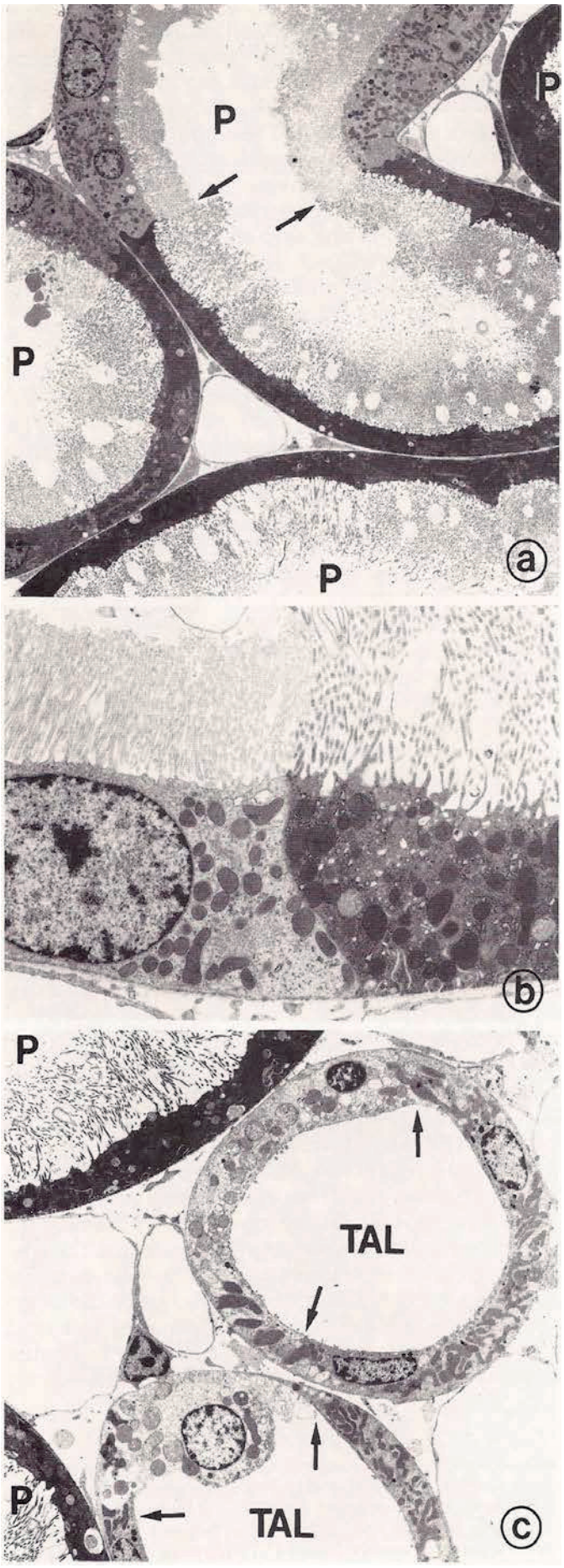

Fig. 12.2.03.: ***Electron micrographs of structural damage.***
Group 1 (**a** and **b**) and Group 2 (**c**). Cell-free standard perfusion for 2 h (**a**, **b**), with addition of glutathione (**c**).

a) The micrograph shows a group of four damaged P_3 segments (P). Damaged cells are shrunken and exhibit coagulation necrosis. Borders between damaged and intact cells are sharp (arrows).
Magnification: 1200x (EM).

b) Detailed view of the interface between an intact and a damaged (early phase) P_3 cell. All components of the cell, including the microvilli, are electron dense and appear dark, and shedding of the microvilli has begun.
Magnification: 5000x (EM).

c) Center of the damaged area in the outer stripe. Among necrotic P_3 segments (P) one can find thick ascending limb profiles (TAL) of loops of Henle, which contain degenerated cells sharply separated from intact cells (arrows).
Magnification: 2000x (EM).

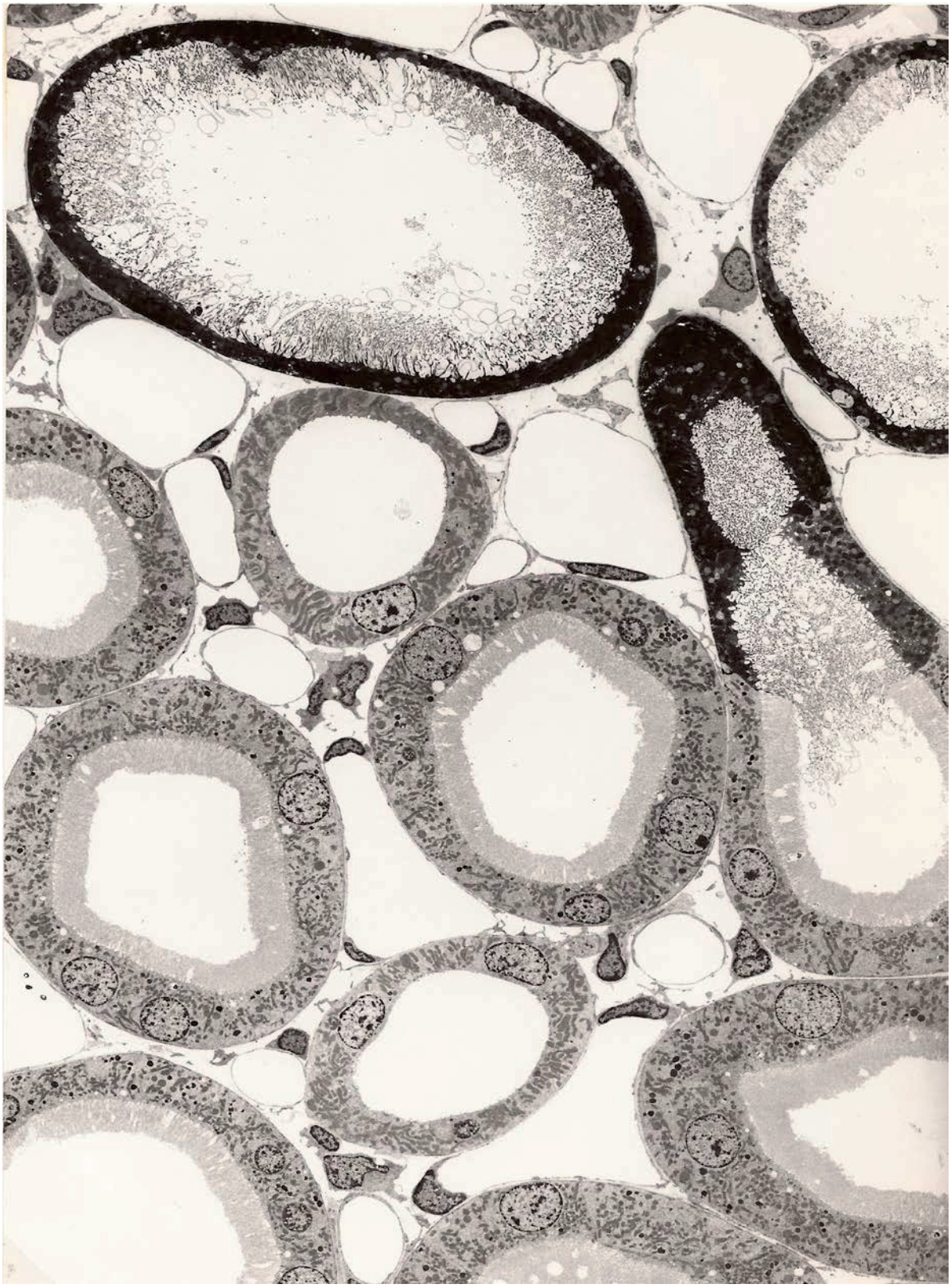

Fig. 12.2.04.: ***Cross section of the outer stripe of the outer medulla.***
Note the coagulation necrosis of proximal P_3 segments. On the right is a tubule with very darkly stained cells directly adjacent to somewhat less condensed cells. Many of the microvilli that make up the cells' brush borders have already been shed into the lumen.
Magnification: 3575x (EM).

The following Fig. 12.2.05. – 12.2.08 show intact structures.

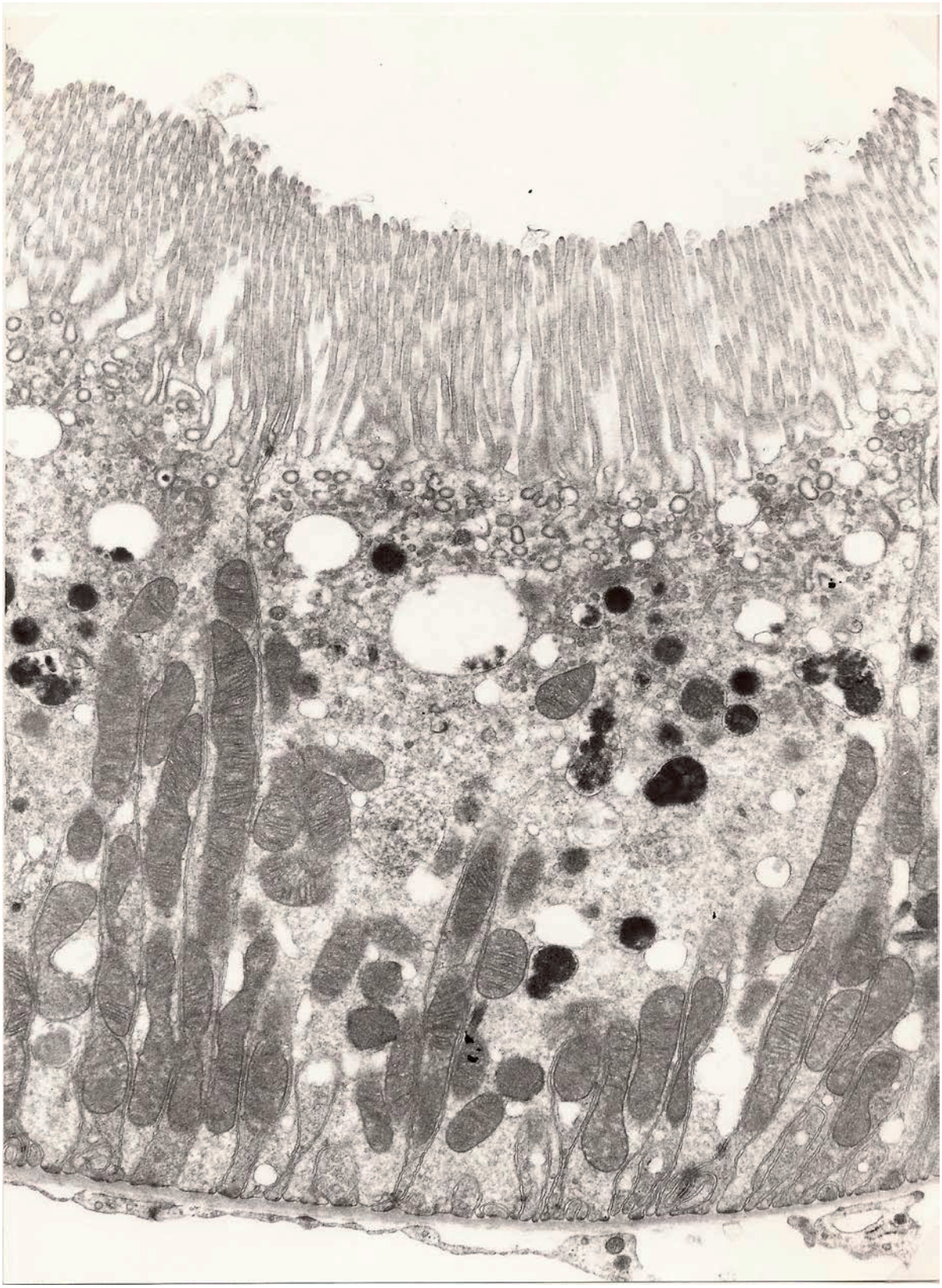

Fig. 12.2.05.: longitudinal section of a proximal tubule (S_1, S_2 segments).
The ultrastructure is intact after 120min of perfusion with 5g% albumin in standard perfusate (corresponding to group 1). Perfusion fixation, magnification: 28125x (EM).

Fig. 12.2.06.: ***Longitudinal section of a distal tubule.***
Ultrastructure is intact. Magnification: 28125x (EM).

Fig. 12.2.07.: ***Distal tubule, macula densa cells.***
Note the typical perinuclear vacuoles, which disappear when transport is inhibited with loop diuretics. Magnification: 11875x (EM).

Fig. 12.2.08. ***Detailed image of a glomerular capillary.***
Perfusion fixation after 2 hours of perfusion. Ultrastructure is intact. The characteristic ring structure seen at the lower margin of the image is an assembly line for the production of basement membrane. The micrograph was taken by Karlwilhelm Kuehn. Magnification: 24000x (EM).

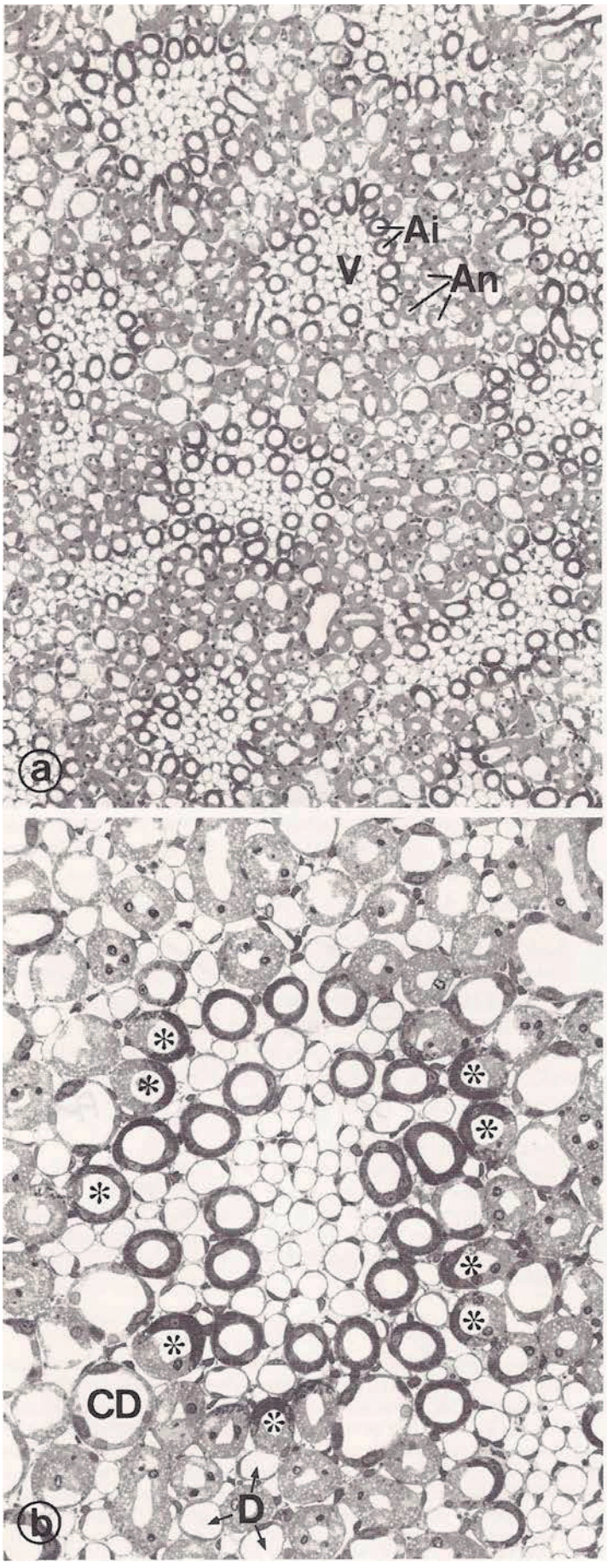

Fig. 12.2.09.: ***Cross-sections through the innermost one-third of the inner stripe.***
Group 2, perfused for 2 hours with cell-free standard medium supplemented with glutathione.

a) The regular pattern of damage around the vascular bundles (V) is obvious. Thick ascending limbs situated immediately around the bundles are structurally intact (Ai), while those farthest from the bundles are necrotic (An). All other tubular segments are intact.
Magnification: 100x (LM).

b) Vascular bundle with surrounding thick ascending limb profiles (asterisks), which are intact on the side facing the bundles and damaged on the opposite side. Collecting ducts (CD) and descending thin limbs of loops of Henle are structurally intact.
Magnification: 300x (LM).

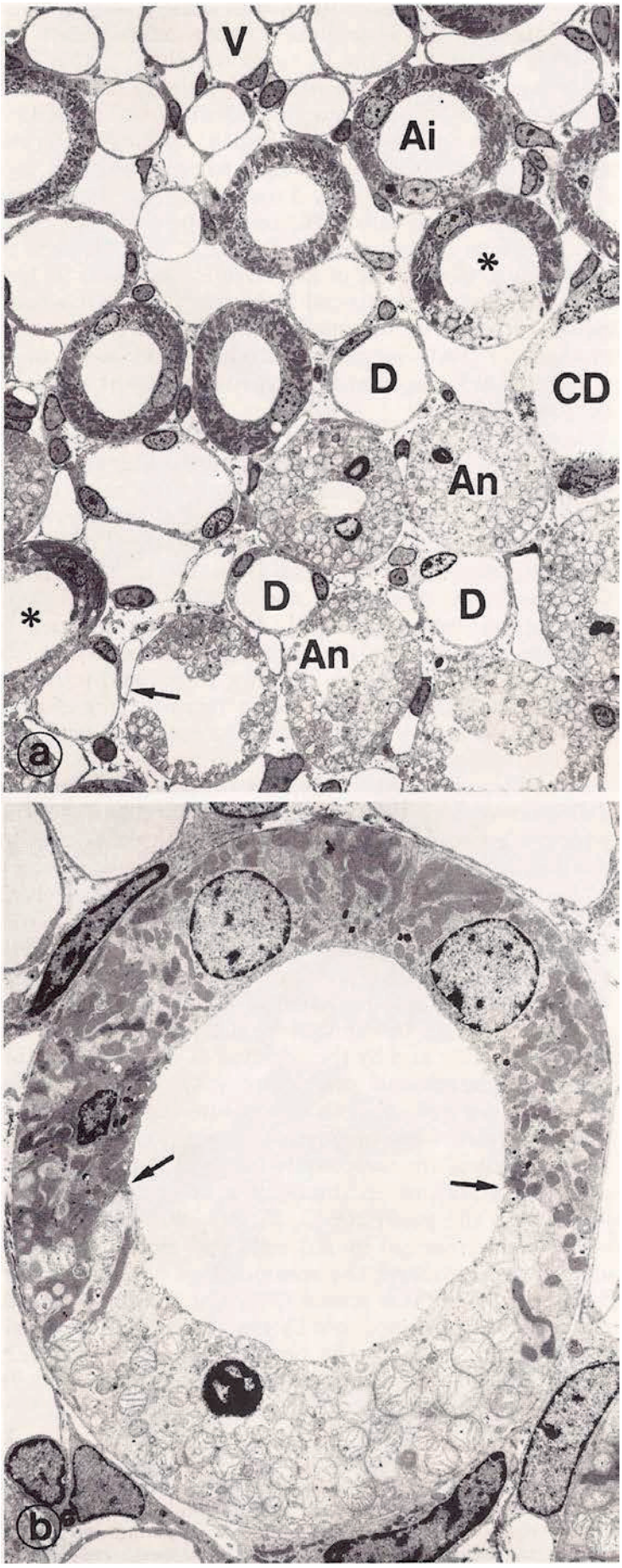

Fig. 12.2.10.: ***Electron micrographs of cell damage in the inner stripe of the outer medulla.***
Group 2, perfused for 2 hours with cell-free standard medium supplemented with glutathione.

a) Thick ascending limbs in the vicinity of vascular bundles (V) are intact (Ai), while those farthest from V are necrotic (An). In between these same thick ascending limbs (asterisk) is one that exhibits a damaged and an intact half. The type of necrosis seen here is a hydropic degeneration with extensive cytoplasmic and mitochondrial swelling; the nuclei are pyknotic. In the most severely damaged tubules, the circumferential outline of the tubule is maintained only by the basement membrane (arrow). Collecting ducts (CD) and descending thin limbs (D) are intact.
Magnification: 750x (EM).

b) Thick ascending limb profile with an intact and a necrotic half (border indicated by arrows). Note the swollen mitochondria and the pyknotic nucleus.
Magnification: 2300x (EM).

Fig. 12.2.11.: ***Electron micrographs depicting details of defective TAL-segments.*** Swollen mitochondria fill almost the whole cell; only small wisps of cytoplasm remain. Note the nuclei in various stages of pyknosis. Collecting ducts on the left and right are intact. Magnification: 6875x (EM).

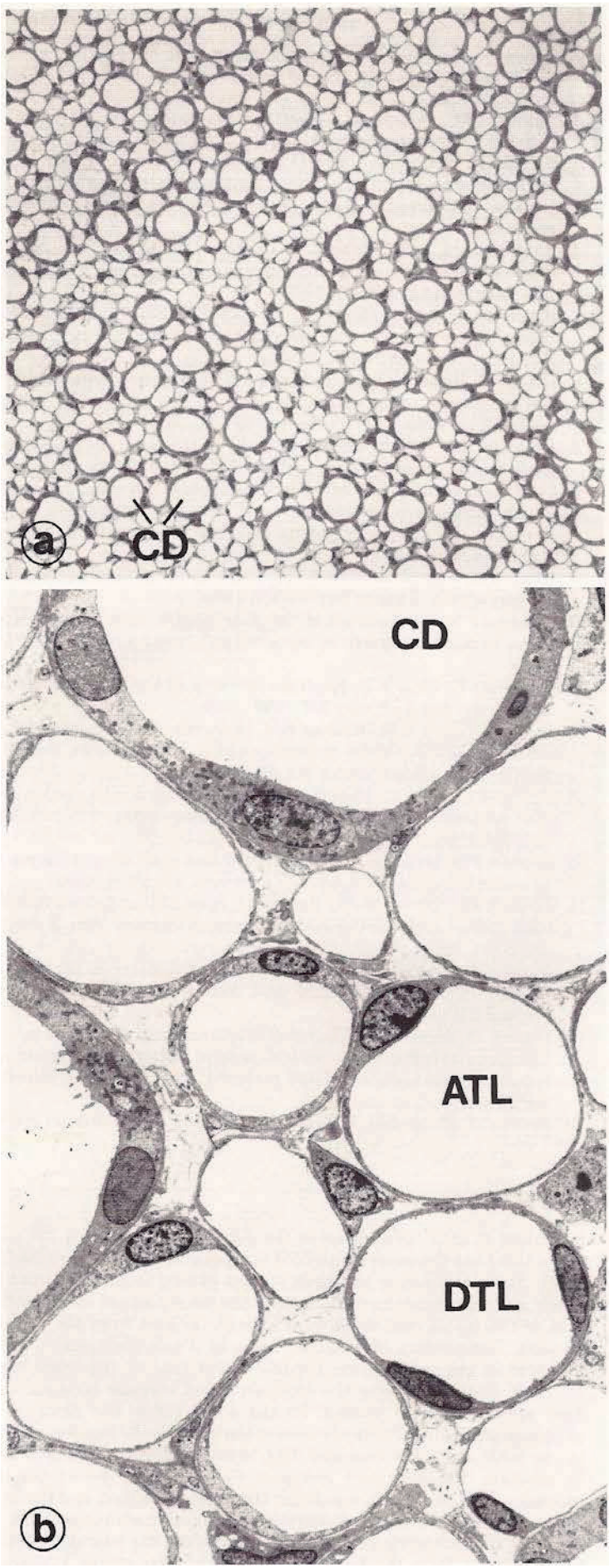

Fig. 12.2.12.: ***Cross-section of the inner medulla.***
Group 1, perfused with cell-free standard medium for 2 hours.

a. ***Survey light micrograph.*** Collecting ducts (CD) are structurally intact.
Magnification: 170x (LM).

b. ***Detailed view.*** All tubules and collecting ducts are structurally intact. ATL, ascending thin limb; DTL, descending thin limb.
Magnification: 1600x (EM).

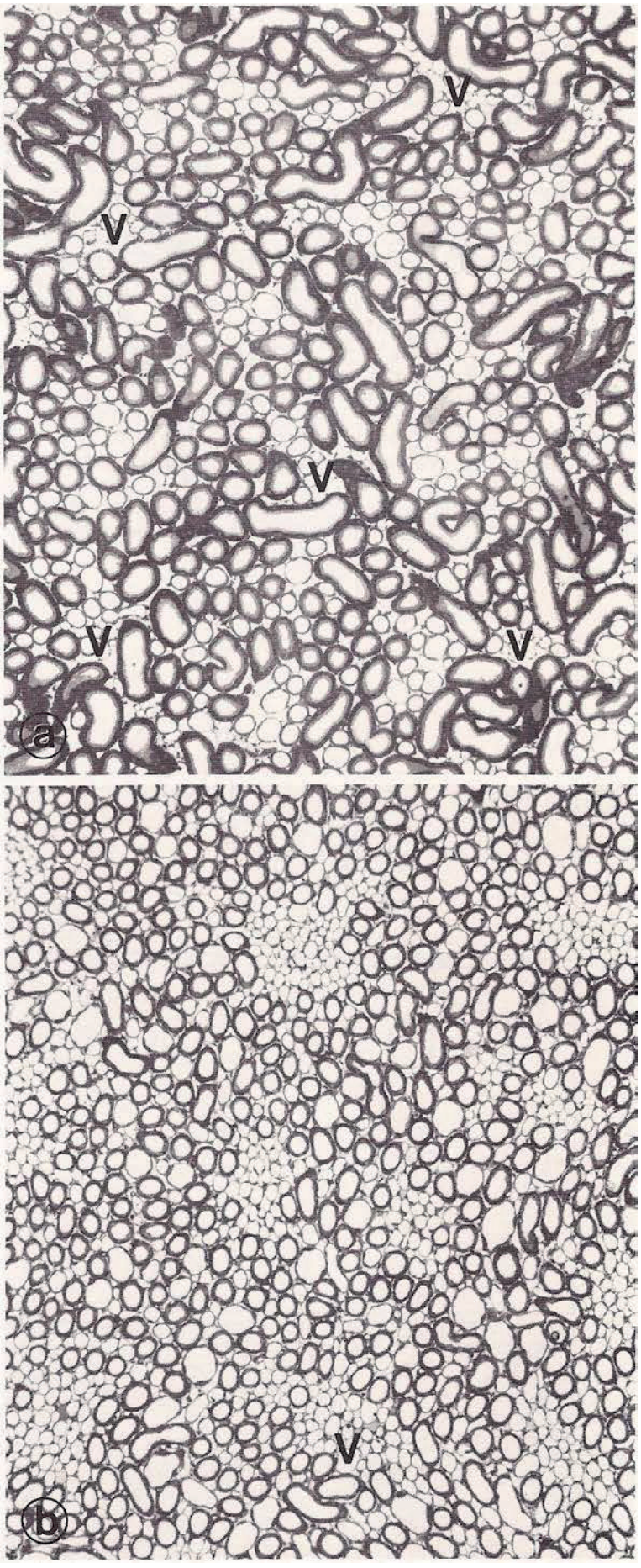

Fig. 12.2.13.: ***Cross-section through the outer stripe (a) and inner stripe (b) of the outer medulla.***
Group 4, perfused for 2 hours with the addition of 5% erythrocytes.

a. ***Outer stripe.*** Unlike the case in cell-free perfused kidneys, no necrosis is visible.
Magnification: 75x (LM).

b. ***Inner stripe.*** All tubules appear structurally intact. V, vascular bundle.
Magnification: 60x (LM).

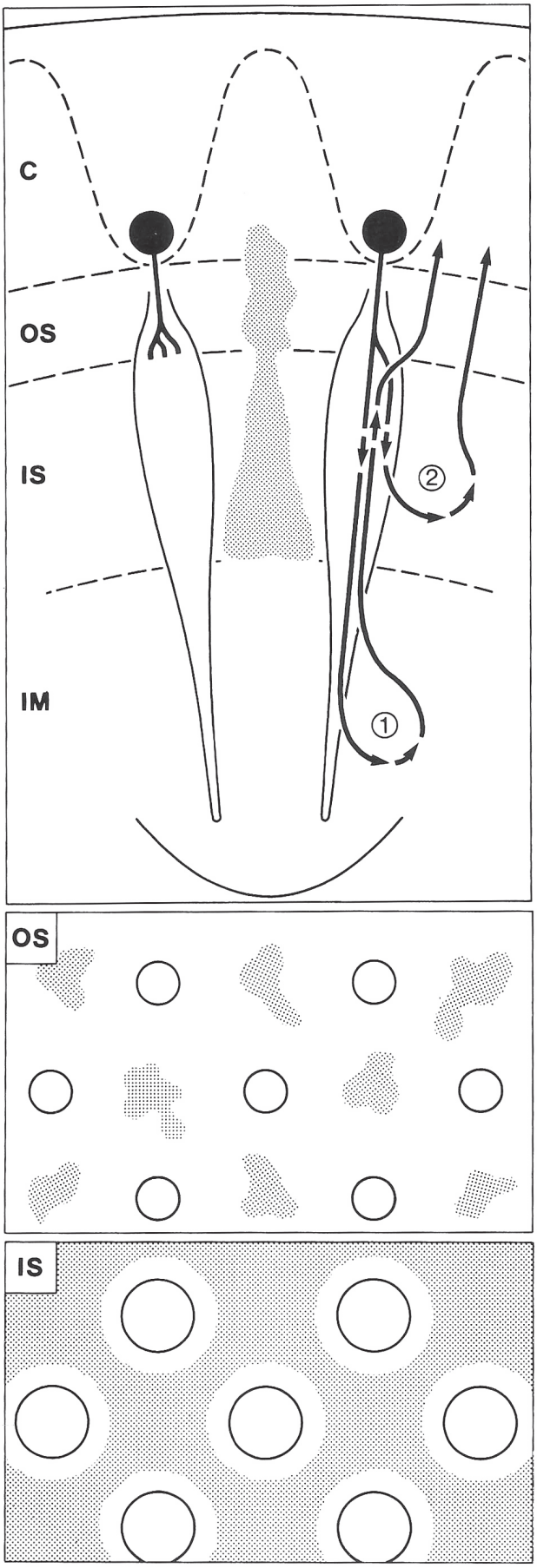

Fig. 12.2.14.: ***Schematic diagram to demonstrate distribution of damaged areas (shaded) within the kidney.*** Two vascular bundles are depicted at the top, beginning at their glomeruli in the cortex (C), traversing the outer stripe (OS) and the inner stripe (IS) and penetrating the inner medulla (IM). Areas containing damaged tubules (indicated by shading) extend from the border between outer and inner medulla up into the basal portions of the medullary rays of the cortex, and are always located farthest from the vascular bundles. The distribution of damaged areas in a cross-sectional plane of the outer stripe (middle) differs from that in the inner stripe (bottom); circles represent the cross-sectional vascular bundles and damaged areas are again shaded. In the outer stripe, the damaged P_3 segments are confined to the centers of the interbundle regions, whereas in the inner stripe the damaged TAL-segments form a confluent area. In addition, the top panel indicates the course of descending and ascending vasa recta responsible for the supply of blood (resp. perfusate) to the inner medulla and inner stripe.

Pathway 1 represents the inner medullary circulation, with the ascending vasa recta rising within the vascular bundles, and spreads out from the bundles within the outer stripe.

Pathway 2 represents the inner medullary circulation, in which the oxygen depleted ascending vasa recta mostly ascend individually between the vascular bundles to the corticomedullary border. The traversing ascending vasa recta [see references (131, 132)] mainly supply blood to the tubules in the outer stripe.

12.3. Hypothesis to account for oxygen deficiency in the cell-free perfused kidney

The assumption that perfusion without oxygen carriers, i.e., with cell-free perfusate, does not provide an organ such as the kidney with sufficient oxygen goes back to the idea that there are regions in the kidney, such as the outer medulla, which even under normal conditions in vivo consume up to 80% of the available oxygen (39, 56). One striking feature of this region is that the TAL-segments have a very high density of mitochondria, and levels of glycolytic enzymes are ten times higher than in the cells of the proximal tubules (18). This high capacity of glycolysis can only be explained if there are phases of oxygen deficiency which lead to gene activation by (as is now known) HIF1α (hypoxia-inducible factor-1α) (273-275), which is also responsible for the activation of the erythropoietin gene. The morphological damage described in section 12.2 can be explained by the fact that, in the cell-free perfused rat kidney, the tubuloglomerular feedback (TGF) loop is not operative (unpublished data from Ulrich Gutsche and Reinhard Brunkhorst in my laboratory in Hanover in June 1979). In contrast, Schnermann demonstrated that the TGF is present in the blood perfused dog kidney (240). In vivo, the TGF acts to reduce the SNGFR when oxygen levels in the TAL segment become critical and the cells must draw on anaerobic glycolysis for energy. Reabsorption of NaCl becomes insufficient and consequently the NaCl concentration at the macula densa increases. One indication of this switch from aerobic to anaerobic energy production are oscillations in tubular pressures, first described by Paul Leyssac in 1983 (143) and followed up by Holstein-Rathlou (113, 114). Using a microconductivity probe (95) Hans-Ulrich Gutsche detected oscillations of equal frequency in the NaCl concentration in the tubular fluid of the distal convoluted tubule, which were, however, phase-shifted with respect to the oscillations in tubular pressures. The oscillations were observed only under light halothane anesthesia (94, 119, 120), when barbiturate was used they were not detectable (94). We found furthermore that the oscillations in tubule pressure and distal sodium concentrations are also reflected in measurements of oxygen pressure in superficially located tubules and glomeruli, as shown in Fig. 12.3.1.

Perfusion of the renal medulla, proceeding via the vascular bundles of descending and ascending vasa recta, is postglomerular, which is a prerequisite for the development of osmotic gradients through the shunt diffusion of solutes such as urea. Shunt diffusion of blood gases also occurs, with a continuous drop in the pO_2 between the cortico-medullary border and the papilla, and a concomitant increase in pCO_2 (trapping). The vascular bundles are linked by alternately meshed, individual capillary networks, which are supplied with more or less depleted pO_2. In a remarkable piece of work, Bastin has uncovered a clear distinction between the proximal tubule and the TAL-segment with respect to the relationship between levels of ATP on the one hand, and the levels of glucose seconds after ischemia / hypoxia on the other. The proximal tubule loses its stock of ATP very quickly, while the glucose level remains stable for much longer (18).

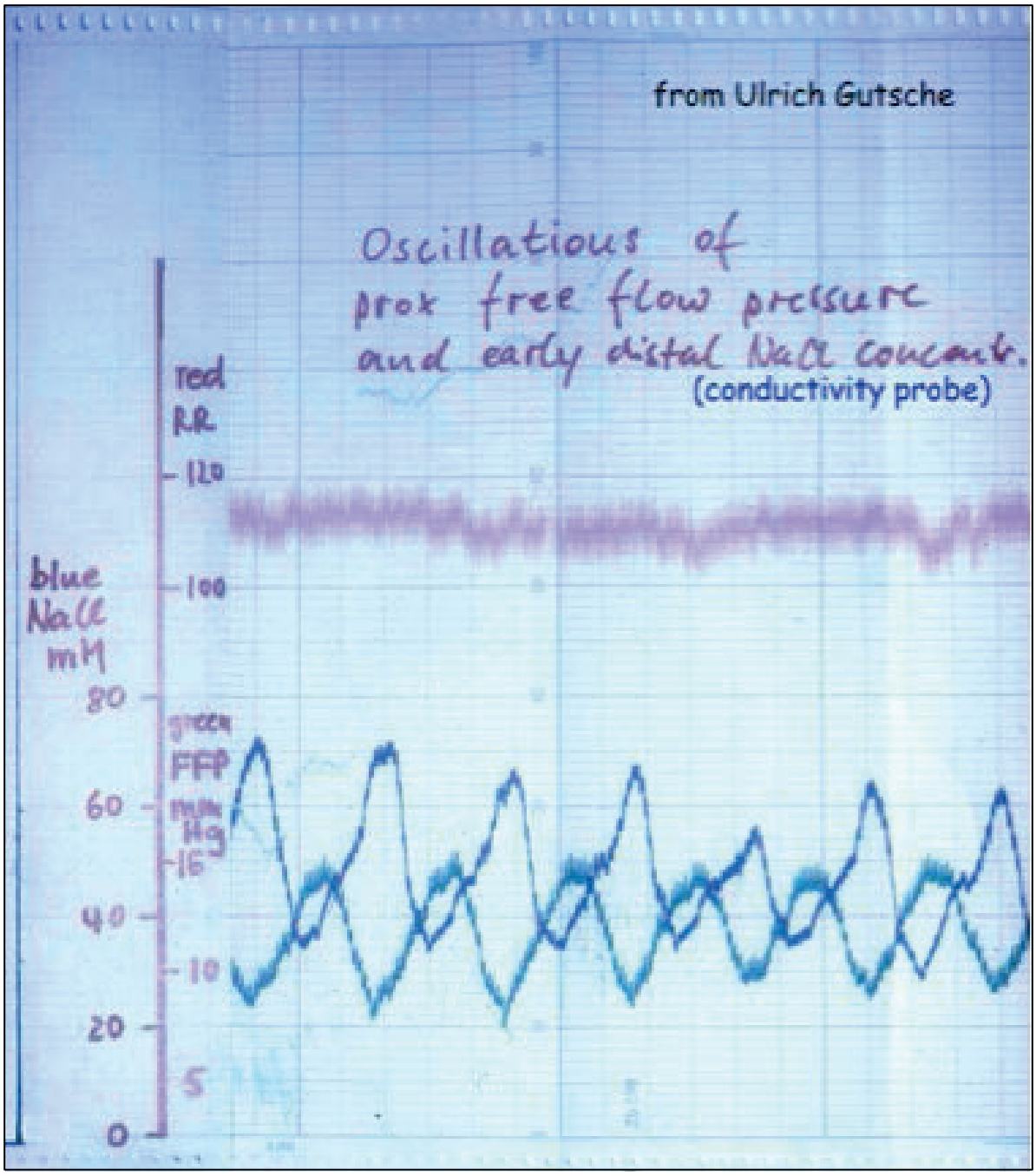

Fig. 12.3.1.: ***Original recording of the oscillations in the free-flow pressure in the proximal tubule and the NaCl concentration in the fluid of the early distal tubule*** (measured as electrical conductivity) (95). The red trace at the top corresponds to the blood pressure registered in the carotid artery, the green line to the pressure in the proximal tubule (8-16mmHg), the blue trace to the conductivity as NaCl equivalent (30-75mmol/l). Hans Ulrich Gutsche provided the image personally. The finding emerged from a collaboration with Paul Leyssac´s laboratory in Copenhagen (94).

The TAL segment consumes its stock of glucose via anaerobic glycolysis within 2 minutes, which allows it to maintain its ATP level for almost 60 seconds. I have extracted the graph shown in Fig. 12.3.2. from the Tables in this work (18).

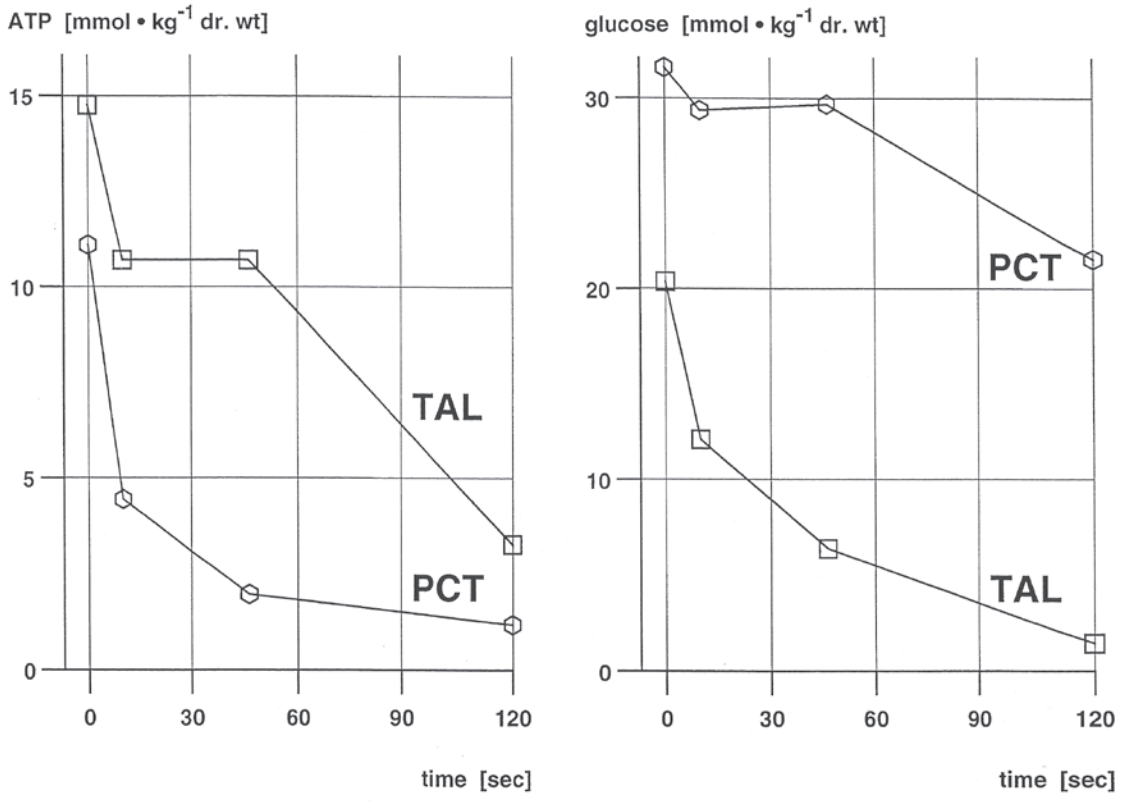

Fig. 12.3.2.: ***Comparison of ATP (A) and glucose (B) levels following the onset of hypoxia in the proximal tubule and TAL segment.*** The proximal tubule (PCT) quickly loses its energy reserves in the form of ATP, without a correspondingly dramatic change in its glucose stock. However, under hypoxia the TAL segment consumes its glucose by glycollysis within 2 minutes, so that its pool of ATP can be maintained for nearly 60 seconds. This reflects the high potential of TAL-segments for glycolysis, in contrast to the proximal tubule (the plot is based on Bastin´s data (18)).

This temporal profile is compatible with the generation of the oscillation frequency in those nephrons whose amount of filtrate exceeds the reabsorption capacity of the associated TAL-segment. Thus, the TGF protects the proximal tubule from damage that would otherwise be induced by oxygen deficiency. Shunt diffusion of blood gases is not only present in the renal medulla but also in the renal cortex, as had long been suspected but was first definitively confirmed by measurements on superficial glomeruli of Munich-Wistar-Froemter rats (260). This is compatible with the finding that a significant portion of the renal cortex is not as well supplied with oxygen as the high venous pO_2 values suggested by the rather bright red color of renal venous blood. This was the starting point for our subsequent in-vivo studies on the pO_2 at the kidney surface using multiwire gold microelectrodes, which revealed oscillations of the oxygen pressure in a subset of nephrons. As with Leyssac´s observations, this was detectable only under light halothane anesthesia. The following Figures show recordings of glomerular and tubular pO_2 pressures at the renal surface in Munich-Wistar-Froemter rats.

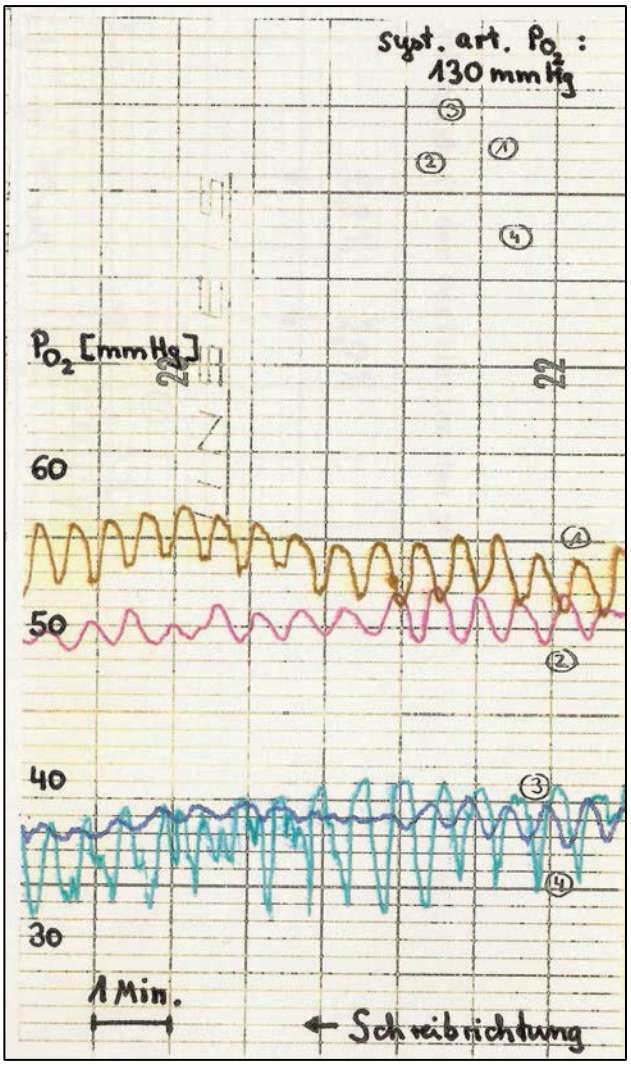

Fig. 12.3.3.: ***Original recording of pO_2 at the kidney surface in a Munich-Wistar-Froemter rat in-vivo and in-situ.*** The systemic arterial pO_2 of 130 mmHg was measured with an O_2 macroelectrode (bottom) inline of a femoro-femoral arterio-venous shunt under continuous blood flow (driven by the rat´s heart) and under ventilation with 25% O_2 .

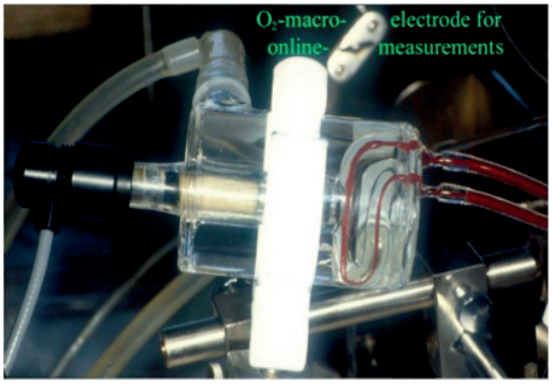

Wires 1 & 2 of the multiwire (8) gold microelectrode were positioned directly above the glomerulus (ochre and red traces), wires 3 and 4 (blue/green) above the proximal tubules. The mean frequency of oscillation was 2 cycles per min or 33mHz. The pO_2 pressures above glomeruli and tubules are clearly distinguishable in height. This Figure, like the following, is taken from the thesis by Oliver Johns (117, 259). The traces run from right to left (Schreibrichtung).

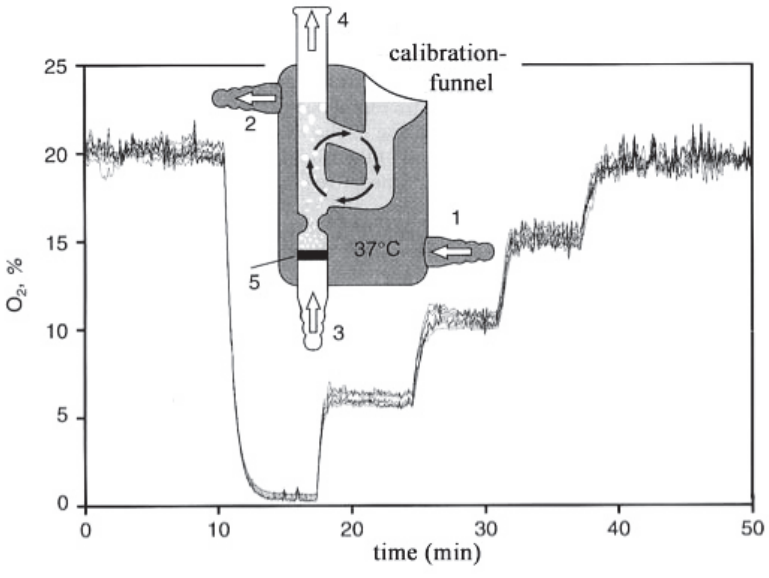

Fig. 12.3.4. ***Sketch of the temperature-controlled calibration chamber (1, 2).***
The calibration gas is passed through the frit (5) in vent 3/4 and causes the calibration fluid to rotate as in an Ussing chamber, without allowing gas bubbles to enter the calibration funnel. The figure shows the calibration of all 8 gold wires from an original calibration.
For more details, see original publication (117, 259).

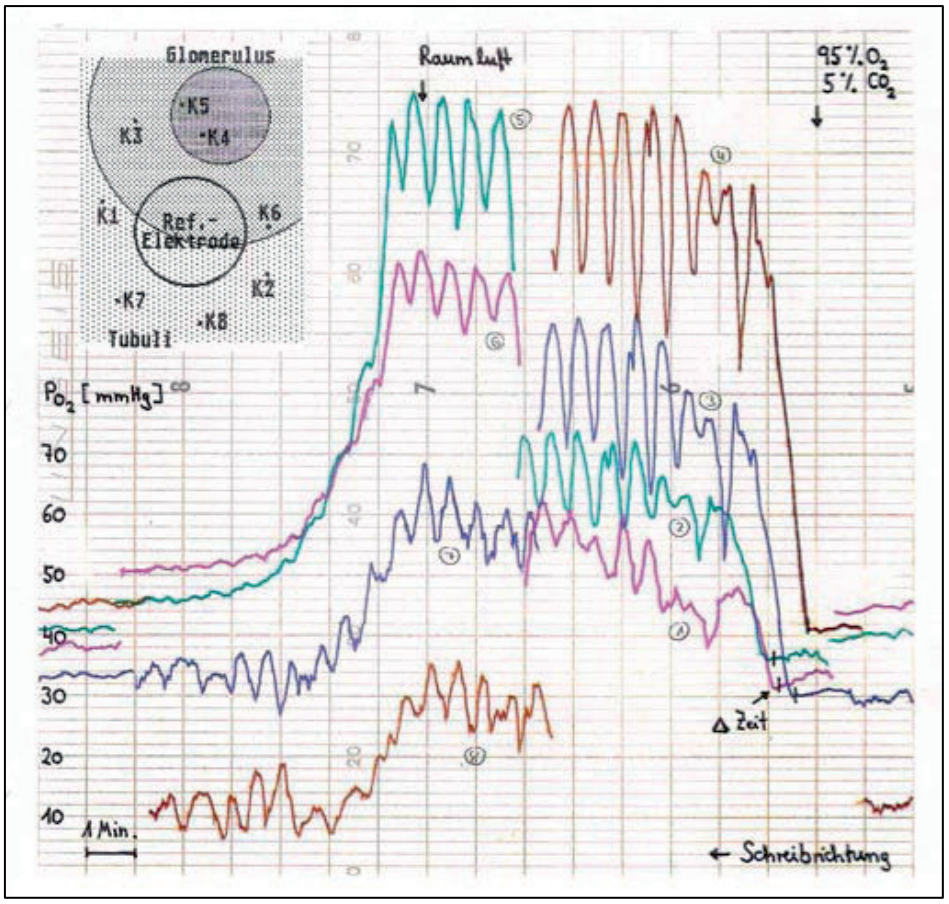

Fig. 12.3.5.: ***Original recordings of all 8 wires of gold electrode during the transition from air to 95% O_2 and back.*** The geometric disposition of the detection wires of the electrode in relation to the glomerulus is depicted at the top left. K4 and K5 are directly above the glomerulus. The starting point of the recording is on the right-hand side. At first only weak oscillations are seen, but strong pressure oscillations set in immediately after switching to 95% O_2 and reach a maximum of 130mmHg. The corresponding systemic arterial pO_2 reached 600mmHg under ventilation (261). K3 and K6 are implaced in a tubuloglomerular intermediate region, K1, K2 and K7, K8 are supratubular records. Since the compensation recorder had only 4 channels, we switched this recording from the first 4 on to the next 4 wires in the middle. For further details see original publication (117, 259).

The oscillations are observed in only a small portion of the nephrons under "normal conditions". Most nephrons operate at a constant level. A physiological perturbation like that shown in Fig. 12.3.5 or its converse - hypoxia - induces more nephrons to oscillate. Cortical, subcortical and midcortical nephrons, whose TAL-segments are further away from the vascular bundles of the renal medulla are more susceptible to oscillations than juxta-medullary nephrons. The TAL-segments of the latter benefit from the radial diffusion of oxygen because they directly surround the vascular bundles. This allows these groups of nephrons to adjust their SNGFR over a much wider range. Holstein-Rathlou has presented evidence that nephrons that are associated with an interlobular artery can oscillate synchronously as a group (113).

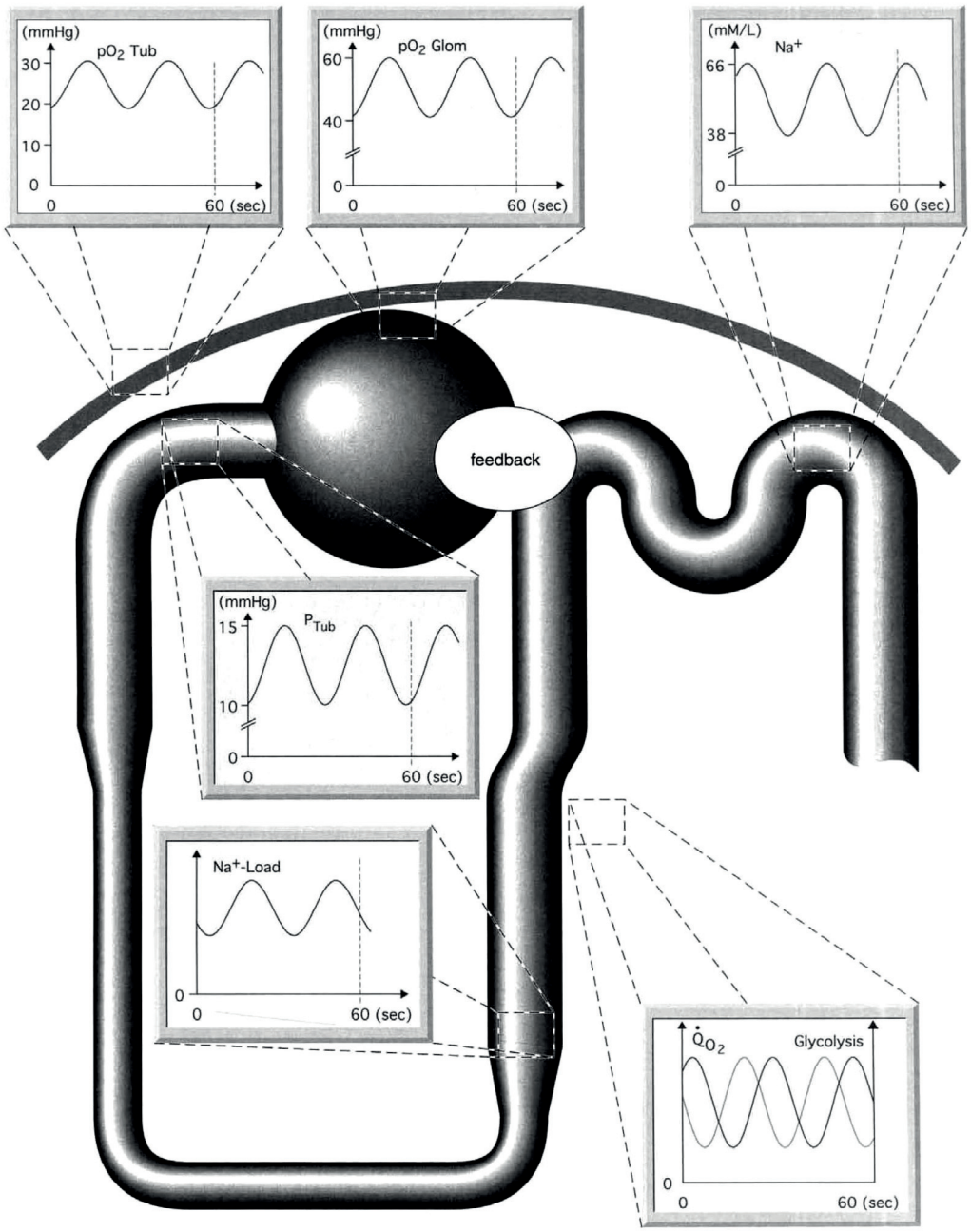

Fig. 12.3.6.: ***Synopsis of an oscillating nephron.*** Oscillations of equal frequency can be detected in (proximal) tubular pressure, and (phase shifted) in the sodium concentration (conductivity) in distal tubules and the oxygen pressure at both supraglomerular and supratubular positions on the renal surface. Consequently, the amount of sodium will oscillate with the same frequency (at the entrance to TAL segment) as the tubular flow rate, and the cells of the TAL segment convert the flow signal into a change in the concentration of sodium if their metabolism switches from aerobic to anaerobic ATP production. The oscillating sodium concentration at the macula densa can use the TGF to adapt the tubular transport to the oxygen supply, making it the driver and the source of this regulatory oscillation phenomenon (259). The pacemaker nephron then takes over the synchronization of the whole group of nephrons around a pair of interlobular vessels (113).

Summary of the components of the hypothesis

In vivo, only 8% of the oxygen that passes through the mammalian kidney is consumed by the organ. Nevertheless, some areas of the kidney are constantly on the brink of oxygen deficiency. This may be one reason why evolution has relocated the site of erythropoietin synthesis from the liver in the fetus to the kidney in the adult organism. Here, reductions in both the oxygen carrying-capacity of the blood (for example, due to blood loss) and the ambient oxygen pressure such as at high altitude (above sea level) can be readily detected. Another reason may be that efficiency of renal function is essentially proportional to the overall level of metabolism and thus more or less directly reflects the magnitude of the latter (see for example, performance adjustment of the kidneys in pregnancy).

1. In vitro studies of the normothermic perfused rat kidney reveal an uptake of 40-50% of the oxygen available in a cell-free perfusate that has been equilibrated with 95% oxygen. Under these conditions, there are physiological signs of functional insufficiency of S_3 segments of the proximal tubule and of TAL segments, which manifest morphologically in the form of necrosis due to oxygen deficiency. Under cell-free perfusion, radial diffusion of oxygen from the vascular bundles of the medulla cannot meet the demands of the affected structures. In vivo, the particular architecture of the vessels of the renal medulla indeed allows the kidney to set up concentration gradients down to the papilla, thus maintaining their concentrating ability by shunt diffusion of solutes in the vascular bundles. However, this inevitably involves the shunt diffusion of blood gases, which leads to a greatly reduced pO_2 and elevated CO_2 (“trapping") in the renal medulla. In vivo, the kidney can cope with the consequences, but not when perfused with cell-free medium lacking oxygen carriers.

2. In vivo studies on MWF rats that have a large number of glomeruli in superficial locations show that half the oxygen disappears on the way from the renal artery to the superficial glomerulus due to highly efficient shunt diffusion within the renal cortex, specifically via the vasa interlobulares. This implies that, in spite of high circulation rates, there are also areas of oxygen deficiency in the renal cortex.

3. In vivo studies under light halothane anesthesia have detected oscillations in the hydrostatic pressure of the proximal tubule which are reflected in - phase shifted – oscillations in the sodium concentration in the early distal tubule and in the oxygen pressure in superficial glomeruli and tubules. These findings indicate that nephron efficiency oscillates as a function of its transport capacity. The critical factor here is the transport capacity of the TAL-segments, which depends on oxygen availability. When the TAL-segment is forced to shift from aerobic to anaerobic energy generation, this serves not so much as an emergency reserve but as a metabolic switch that triggers an oscillatory adjustment to the functional transport capacity of the

nephron. The tubulo-glomerular feedback thus has a vital function in inhibiting necrosis not only in TAL-segments. In addition, it protects the proximal tubule (which has a weak capacity for glycolysis) against oxygen deficiency by reducing and adjusting the single-nephron filtration rate. Persson and coworkers have shown that the oncotic pressure substantially affects the feedback response, i.e. that a high colloid osmotic pressure (COP) – which is associated with a high filtration fraction - ensures a high feedback response rate in the efferent arteriole, and conversely a lower COP leads to a significant weakening of the feedback response (201, 202). In the cell-free perfused kidney, the filtration fraction is always below 10%, which may explain why the lack of feedback does not further depress the filtration rate – in response to the limiting O_2 supply - and thus enables damage due to O_2 deficiency. An observation made by Zoltan Endre (70) and coworkers is interesting in this context: they found that an isolated kidney perfused with 2% added erythrocytes, and thus under slight hypoxia, shows damage to proximal tubules but not to TAL-segments. This may mean that the added erythrocytes specifically protect TAL-segments, but that simply shifts the problem to the proximal tubules, which suffer from overloading due to defective tubuloglomerular feedback. Thus, when confronted with a high sodium load proximal tubules - with their weak glycolytic capacity - cannot handle oxygen deficiency.

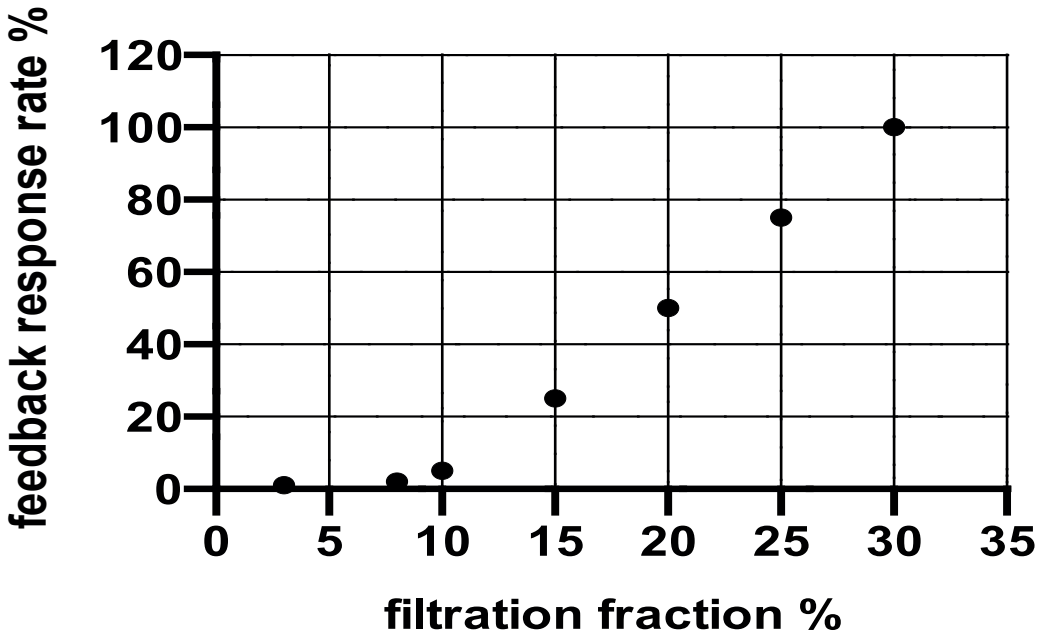

Fig. 12.3.7.: ***Hypothetical relationship between filtration fraction and feedback response in the IPRK .*** The filtration fraction of the IPRK ranges between 1.5 and 8% while the mean for the rat kidney in vivo is 30%.

Summary:

The balancing act between concentrating ability, adequate oxygen supply and erythropoietin secretion, which the kidney performs so well in vivo, is beyond the capacity of the isolated cell-free perfused kidney. The latter´s concentrating ability is severely limited by the high perfusion of the medulla; hence, the necessary concentration gradient along the corticomedullary axis cannot be established or maintained.

The oscillations in oxygen pressure detectable in glomeruli and tubules at the surface of the kidney in vivo, together with the associated pressure fluctuations in proximal tubules and conductivity fluctuations in distal tubules, point to an oscillating functional state of the nephron in relation to its transport capacity. The crucial factor is the transport capacity of the thick ascending limb of the loop of Henle (TAL-segment) under oxygen-deficiency conditions: It is not surprising that the cells in this TAL segment contain large numbers of mitochondria and display a high capacity for glycolytic activity. As a result, this segment can react to oxygen deficiency by flipping a metabolic toggle switch which triggers an oscillatory adjustment of the affected nephron to the level of available oxygen (by means of its shift kinetics).

In the isolated cell-free perfused kidney (IPRK), oxygen capacity is insufficient - despite the high partial pressures employed – to meet the demands of the interbundle area of the outer medulla which, even under in vivo conditions, takes up no less than 80% of the oxygen supplied. Since the TGF in the cell-free perfused kidney is too insensitive and does not work, the GFR cannot be adapted to the reduced transport capacity of TAL segments and proximal tubuli. This results in morphological damage to the vulnerable structures of the interbundle area, such as the S_3 segments of the proximal tubule and the TAL segments. In contrast, structures nearer the vascular bundle profit from radial diffusion of oxygen and therefore remain morphologically intact.

In vivo, the fact that nephrons operate at the brink of oxygen deficiency enables them to sensitively monitor the supply of, and demand for oxygen, and to control the synthesis of erythropoietin. Although the IPRK can synthesize erythropoietin, it is unable to accomplish the required balance between concentrating ability, oxygen sufficiency and adaptation of the rate of erythropoietin synthesis.

The key to the lack of long-term stability of the isolated kidney and the resulting loss of function of isolated kidneys lies in the fact that the integrity of the endothelium is lost during artificial perfusion. The complexity of circulating whole blood and its permanent reconditioning is a crucial prerequisite for the integrity of the endothelial barrier and its glycocalyx. The glycocalyx builds up an endothelial surface layer whose components are drawn from the bloodstream, and this layer defines the integrity and local permeability of the endothelium under in vivo conditions (97, 204). Another significant factor may be the

unfavorably narrow margin between oxygen deficiency and oxygen intoxication in the isolated kidney. In order to remain within the optimal range, one must mimic the conditions that prevail in vivo, which provide for a high oxygen capacity at low (i.e. normal) oxygen pressure (i.e. lower perfusion flow rates). For the isolated liver, this principle was established a long time ago with the result that, for example, the oxygen consumption was higher than at reduced hemoglobin levels and high pO_2 partial pressures (1, 2, 169). In addition, lysosomes remain intact for much longer (up to 8 hours) than in the case of the conventional perfusion (low Hb, high O_2 partial pressure) technique.

Another approach would be to improve the stability of albumin function. In vivo, albumin has a limited half-life and is constantly replenished. In vivo, aged and defective albumin is removed by mechanisms which are not available in vitro. Siliconization of the interior surfaces of the perfusion apparatus would be worthwhile, as would measures to minimize contact of the perfusate with air and avoid foaming as far as possible. With the latter aim in view, we used a sensor in the draining funnel which controlled a tube valve, thus allowing perfusate to flow back as a column of liquid with no air bubbles in between. This can reduce an unnecessary denaturation. In the laboratory in Muenster we had abandoned this principle for the sake of simplicity, which was perhaps a mistake. Whether these scruples are realistic may be another field of research.

12.4. Overview of the contributions of our group to the four different techniques of renal perfusion

1 Single pass perfusion (with/without colloid, i.e. polygelatine as Haemaccel®)
2 Recirculation with bovine serum albumin (BSA), with/without red cells
3 Recirculation with dialysis and BSA, with/without red cells
4 Reperfusion of the perfusion-fixed kidney

1a Single pass perfusion with Haemaccel® as colloid

Sodium transport and metabolism (Free University Berlin)

1970 Na-Reabsorption in the IPRK. Dependency on substrates and Na-load (264)
1971 Na-Reabsorption and O_2-consumption in the IPRK under ethacrynic acid (255)
1972 Effects of added substrates (pyruvate, oxaloacetate, butyrate and succinate) on transport and metabolism in the IPRK (256).
1975 Definition of the basic requirements for the function of the isolated cell-free perfused rat kidney (257)
1975 Influence of ouabain and ethacrynic acid on sodium transport and the sodium-potassium ATPase in the IPRK (254).
1976 Effects of the Ca antagonist verapamil on inhibition of renal sodium transport by ouabain (253).
1976 In vivo study: Acute and reversible inhibition of tubuloglomerular feedback-mediated afferent vasoconstriction by the calcium-antagonist verapamil (175, 253).
1984 The effect of succinate on Na-reabsorption and the metabolism of the isolated perfused rat kidney, IPRK (130) 256).

1b Single pass perfusion without colloid (Medical University Hannover)

The effect of albumin on the function of the IPRK compared to "colloid-free perfusion"

1981 Effect of albumin on the function of perfused rat kidney (251).

The renal clearance of thyroid hormones by the IPRK

1978/1980 The renal clearance of thyroid hormones in the IPRK (4).

The effects of AVP and dDAVP on free-water reabsorption in the IPRK

2011 Analysis of aquaporin-2 regulation in the IPRK (262). (Laboratory of Experimental Nephrology in Münster)

2015 Laborhandbuch: Nierenperfusion (320)

2 Recirculation with bovine serum albumin, BSA (with/without red cells)

Conversion of thyroxine to tri-iodothyronine in the IPRK (with red cells)

1986 On conversion of thyroxine to trijodthyronine in the IPRK (314).
1988 The conversion of thyroxine to trijodthyronine with an analysis of free T_4 by equilibrium dialysis (99).

Renal metabolism of peptide hormones and uremic middle molecules

1979 Renal handling of polypeptide hormones (insulin, C-peptide, h-PTH) as studied in the IPRK (268).
1980 Renal handling of homologous and heterologous insulin in the IPRK (236, 237).
1980 Renal handling of uremic middle molecules (158, 233, 234, 290).

Renal metabolism of leukotrienes

1991 Metabolism of cysteinyl leucotrienes by the IPRK (with/without BSA) (73).

3 Recirculation with BSA, regeneration and aeration of perfusate by dialysis

Glomerular permeability for albumin in the IPRK, functional characterization. *Mikropuncture studies are indicated in bold italics*

1977 ***Direct assessment of the glomerular sieving coefficient for albumin in the rat kidney*** (290).
1978 ***Micropuncture experiments on albuminuria in the IPRK*** (252).
1979 ***A comparison of micropuncture studies in the IPRK with the in vivo experimental conditions*** *(292)*.
1980 Glomerular permeability for water and albumin in the IPRK (247).
1984 ***Glomerular albumin leakage and morphology after neutralization of polyanions I*** (12, 284).
1984 Glomerular albumin leakage and morphology after neutralization of polyanions II. Discrepancy between protamin induced albuminuria and fine structure of the glomerular filtration barrier (284).
1986 ***The „repaired defect" hypothesis of the glomerular capillary wall. Analysis in the IPRK*** (244).
1992 ***The physiological and pathophysiological basis of glomerular permeability for plasma proteins*** (266).
1994 Mechanisms of glomerular proteinuria and hematuria (248).

Various aspects of renal function which were studied in the IPRK
Micropuncture studies are indicated in bold italics

1981 Effect of albumin on the function of perfused rat kidney (251).
The micro-puncture data raised in parallel have been published only in the habilitation work (250).
1984 Single nephron function after unilateral nephrectomy in rats treated with Cyc A (267).
1984 Studies on the pathophysiology of glomerular water permeability (181).

1985 Morphological and functional evidence for oxygen deficiency in the IPRK (263).
1986 Effective hydraulic permeability of the glomerular capillary wall in rats after unilateral nephrectomy (184).
1986 Influence of Cyc A on adaptive hypertrophy after unilateral nephrectomy in the rat (116) (267).
1989 Renal mesangium is a target for calcitonin gene-related peptide (136).
1990 Role of erythropoietin in adaptation to hypoxia (241).
1991 Oxygen dependent erythropoietin production by the IPRK (242).
1991 Effect of arginine depletion on glomerular and tubular kidney function. Studies in the IPRK (206).
1992 Importance of NO/EDRF for glomerular and tubular function. Studies in the IPRK (207).
2004 Age-dependent thickening of glomerular basement membrane has no major effect on glomerular hydraulic conductivity (182).
2016 Studies on the "repaired defect" hypothesis of the glomerular capillary wall (218).

4 The reperfusion model of a perfusion-fixed rat kidney

Studies on the importance of the electric charges of the glomerular filtration barrier

1990 The significance of the negative charges in the glomerular basement membrane for proteinuria (78).
1994 On glomerular permeability for charged and uncharged macromolecules (317).

1999 Roles of size, charge and conformation of dissolved molecules and of fixed charges on the filtration barrier in glomerular permselectivity (50).
1999 Role of albumin and glomerular capillary wall charge distribution on glomerular permselectivity. Studies on the perfused-fixed rat kidney model (53).
2001 The "fixed" charge of glomerular capillary wall as a determinant of permselectivity (51).
2003 Dynamic alterations of glomerular charge density in fixed rat kidneys suggest involvement of endothelial cell coat. Studies in the IPRK (52).

Klaus Hinrich Neumann

13. Special aspects of micropuncture experiments on the IPRK

13.1. Studies on the isolated perfused rat kidneys

Micropuncture techniques permit one to investigate tubular and glomerular functions of surface nephrons in the IPRK under conditions similar to those that prevail in vivo. However, they require certain modifications of the experimental set up normally used in studies on the IPRK and some special aspects must be considered. The placement of the experimental kidney in the temperature controlled kidney tray is similar to that employed for the in-vivo preparation. One major advantage for micropuncture experiments lies in the absence of the renal movements associated with respiration, which inevitably complicate the puncturing of superficial cortical nephrons in situ. On the other hand, as a consequence of perfusion with cell-free medium, peritubular capillaries are less clearly defined, which hampers precise placement of puncturing glass capillaries under stereomicroscopic control.

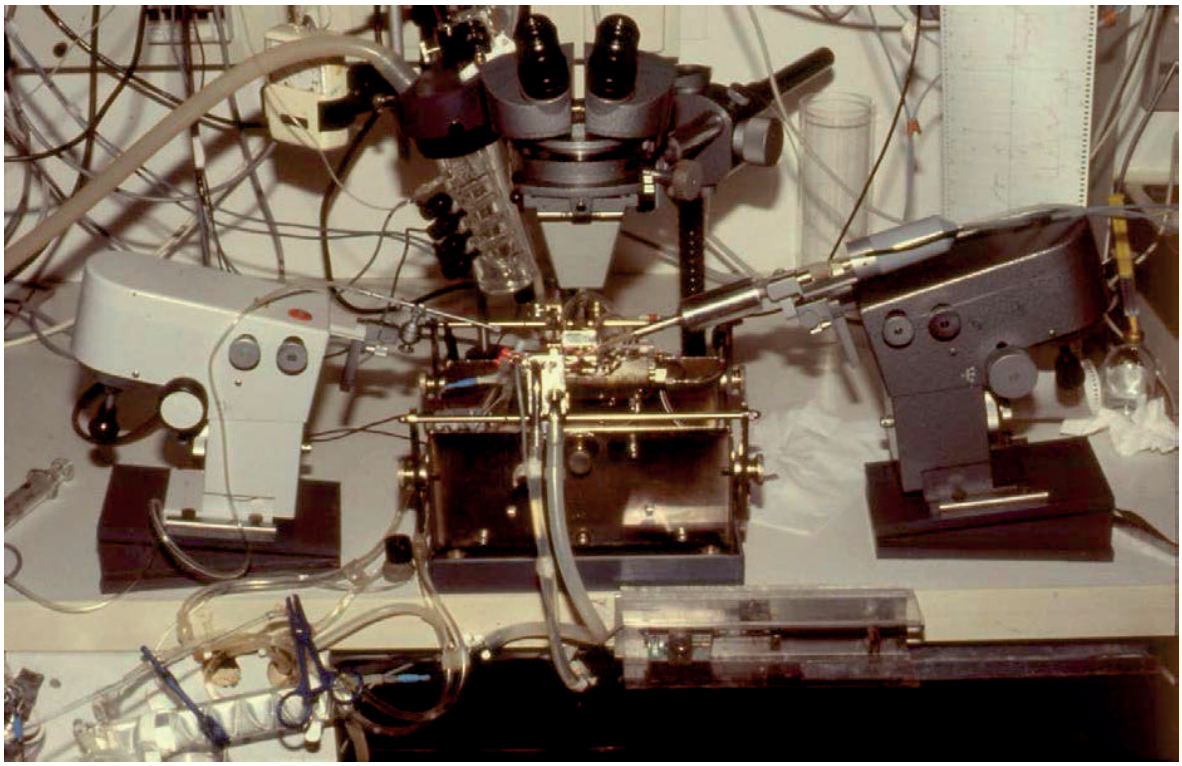

Fig. 13.1.1.: ***Set-up for micropuncture experiments in the IPRK.*** Micromanipulators are positioned on both sides of the kidney tray, which are used to estimate single nephron gfr, to measure tubular pressures and for indirect determination of glomerular capillary pressure by means of the stop-flow technique described by Gertz (86). The holder for the glass pipette for collection of tubular fluid is mounted on the left micromanipulator. The micromanipulator on the right is used to direct the pipette mounted on the microperfusion pump with the micropressure transducer. The stereomicroscope in the center is a Leitz model, equipped with episcopic illumination, a 4x objective and 10x eyepieces.

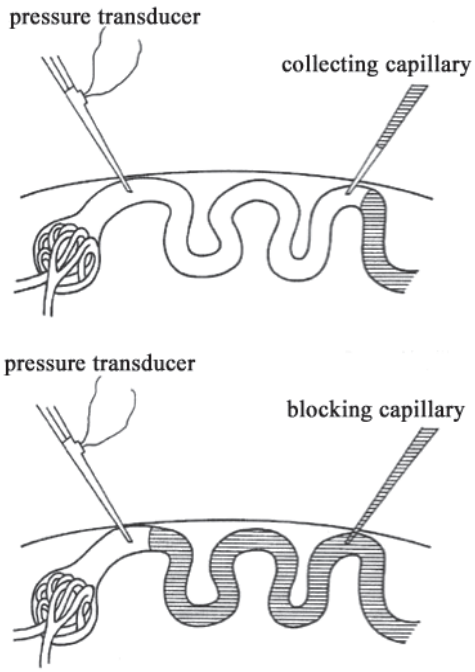

To achieve the highest possible contrast for visualization of cortical tubules, the surface of the isolated kidney is illuminated tangentially by cold light sources. When viewed with vertically directed incident light the level of contrast at the surface of the cell-free perfused kidney is extremely low.

Fig. 13.1.2.: ***Schematic view of the positioning of micropuncture pipettes.*** The upper panel shows the disposition used for collection of tubular fluid (top), the lower panel depicts the arrangement used for measurement of tubular free flow ($P_{FF)}$ and stop flow (P_{SF}) pressure (bottom). The latter enable one to measure the single nephron GFR (SNGFR) and calculate the effective filtration pressure (181).

Proximal convoluted tubules of surface nephrons are punctured with sharpened glass pipettes (tip size 8-10 µm) filled with isotonic sodium chloride solution containing 0.1% Lissamine green (Serva, Heidelberg, Germany) for better visualization. For measurements of pressure and tubular perfusion the pipettes are mounted on the lucite pipette holder of the microperfusion pump (W. Hampel, Frankfurt, Germany) which is filled with silicon oil (AH35 Wacker Chemie, Munich) and connected via a side-arm to a micropressure transducer (type Epi-080-25, Entran Devices, Little Falls, NJ, USA). The transducer signal is recorded by a chart recorder (Linseis Messgeräte, Selb, Germany). The microperfusion pump including the pressure transducer [this system was developed in Berlin (154)] is mounted on a micromanipulator (Leitz, Wetzlar, Germany). The pipette tip is placed in a proximal tubule (under stereomicroscopic control). Then the free flow pressure (P_{FF}) is recorded and the tubule is perfused for a short period of time with the colored solution. If an early proximal tubule has been punctured, as indicated by the number of colored loops visible downstream (at least 4, range 4-7, mean 5.3), the pressure pipette is left in place. Since the number of proximal surface loops in Wistar rats has been reported to be 5.2 on average, it can be assumed that the pressure pipette is located in the earliest accessible part of the proximal tubule. The last proximal surface loop is then punctured with a second pipette filled with colored paraffin oil and, after the introduction of a small droplet of oil into the lumen of the tubule, fluid is collected for specific period (5-8 min). The collection rate is adjusted so that the continuously recorded tubular pressure is held at the initial P_{FF} level and the oil droplet is kept distal to the collection pipette. When collection is complete, the pipette is withdrawn and the tubule distal to the pressure pipette is blocked with paraffin oil using another pipette. The stop flow pressure (P_{SF}) is then recorded and the position of the tubule is noted for later identification (181). Since the tubulo-glomerular

feedback mechanism is not operative in this isolated perfused kidney preparation, any possible influence of proximal collection of tubular fluid on hydraulic pressure in the glomerular capillary can be disregarded. At the end of the experiment, the kidney is perfused at the original perfusion pressure with a 1.25% glutaraldehyde solution in phosphate buffer containing 6g% hydroxyethyl starch as the colloid. The tubules previously studied are then gently injected in the retrograde direction with Microfil (Canton Biomedical Products, Boulder Co, USA) so that the marked glomeruli can subsequently be identified in histological sections, based on the presence of small particles of Microfil in Bowman´s capsule.

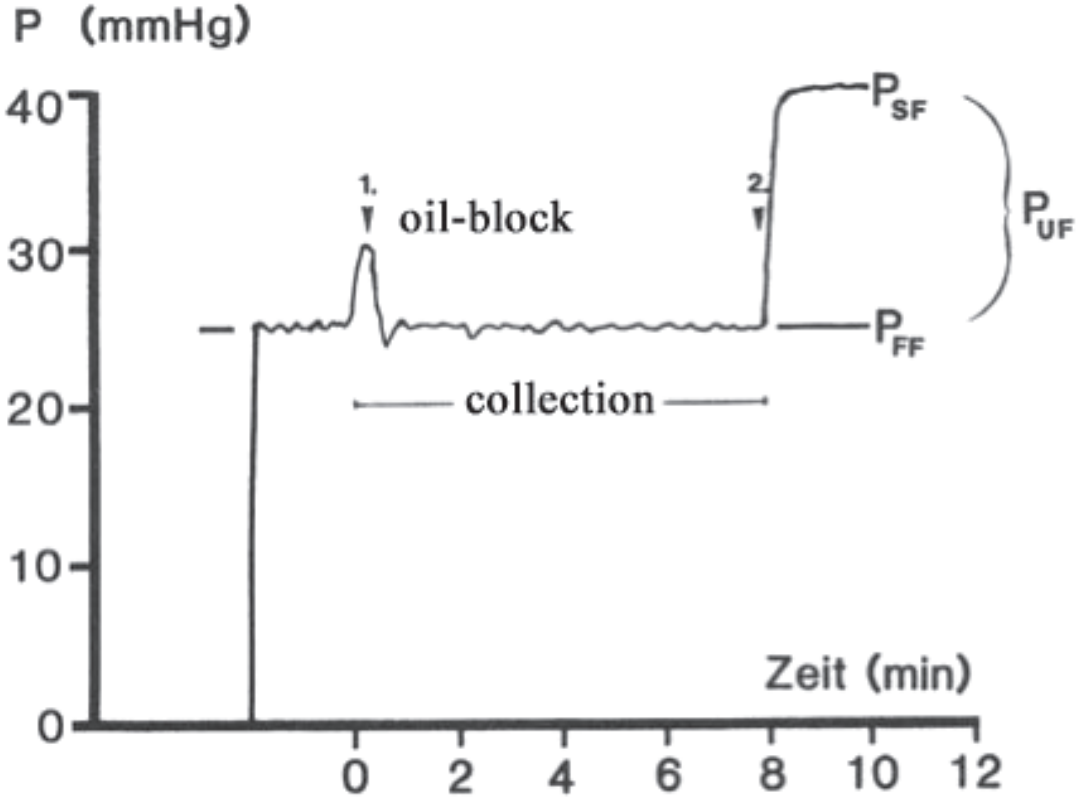

Fig. 13.1.3.: ***Schematic diagram of continuous tubular pressure registration during pressure controlled collection of tubular fluid***. The pressure pipette is located in the earliest accessible loop of the proximal tubule and the free flow pressure (P_{FF}) is registered. The last proximal surface loop is then punctured with a second pipette filled with colored paraffin oil, and a timed collection (5-8 min) of tubular fluid is begun after insertion of a small droplet of oil into the tubular lumen (arrow 1). The collection rate is adjusted so that the continuously recorded pressure is held at the original P_{FF} and the oil droplet is kept distal to the collection pipette. After collection is completed, the pipette is withdrawn and the tubule distal to the pressure pipette is blocked by injecting paraffin oil from another pipette. Then the stop flow pressure (P_{SF}) is recorded (see arrow 2), (181).

Calculations: The volume of tubular fluid (V) obtained in timed collections is estimated from the length of the fluid column in a calibrated constant bore capillary glass tube measured with an eye-piece micrometer. The inulin concentration in microsamples of tubular fluid (TF) and perfusion fluid (P) is measured with a downscaled adaptation of the macro-analytical technique.

$$\mathbf{SNGFR = \dot{V}\,(TF/P)_{Inulin}} \qquad \mathbf{P_{UF} = P_{SF} - P_{FF}}$$

Under the conditions prevailing in the isolated perfused rat kidney the glomerular ultrafiltration pressure (P_{UF}) can be calculated as the difference between the stop flow pressure and the free flow pressure (P_{FF}):

Derivation:

(1) $P_{UF} = (P_{GC} - P_{FF}) - (\pi_{GC} - \pi_{TF})$, $\pi_{TF} = 0$

(2) $P_{SF} = P_{GC} - \pi_{GC}$ $P_{GC} = P_{SF} + \pi_{GC}$

Hence $P_{UF} = P_{SF} + \pi_{GC} - P_{FF} - \pi_{GC}$

$P_{UF} = P_{SF} - P_{FF}$

P_{UF} : glomerular ultrafiltration pressure P_{FF} : tubular free flow pressure

P_{GC} : hydrostatic pressure in glomerular capillary P_{SF} : tubular stop flow pressure

π_{GC} : colloid osmotic pressure in glomerular capillary, and of tubular fluid: π_{TF}

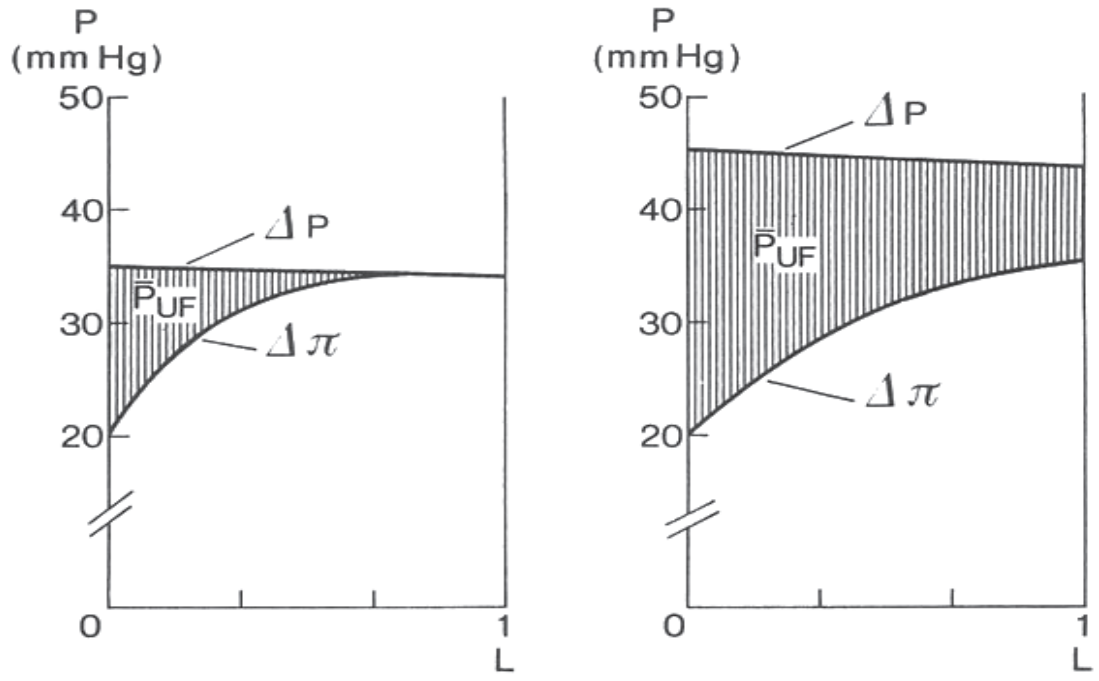

Fig. 13.1.4.: ***Schematic depiction of glomerular pressure profiles in vivo:*** The panel on the left shows how "filtration pressure equilibrium" (P_{UF} = 0) along the glomerular capillary is achieved under hydropenic conditions. The panel on the right depicts the "filtration pressure disequilibrium" observed under euvolemic conditions with positive P_{UF} at the end of the glomerular capillary length. The shaded area represents the effective filtration pressure. ΔP represents the hydrostatic pressure difference, which falls slightly along the length of the capillary, Δπ stands for the colloid-osmotic pressure difference, which increases along the capillary during the filtration process (181).

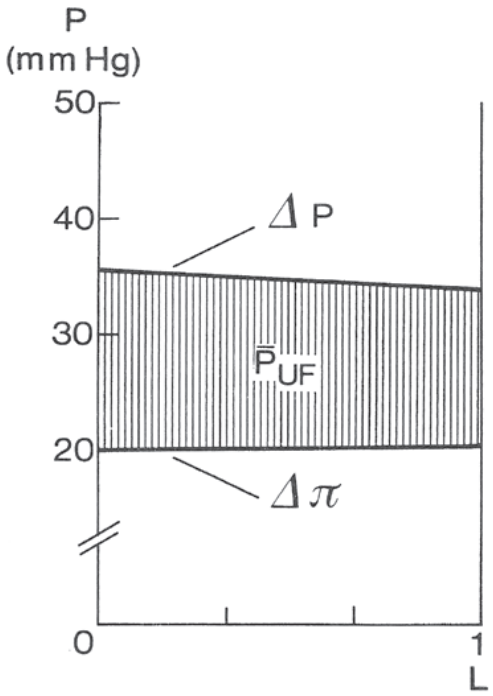

Fig. 13.1.5.: ***Schematic depiction of glomerular pressure profiles in the IPRK:*** Due to the high perfusion rates at "normal" GFR, the filtration fraction is low (2 - 8%). The colloid-osmotic pressure consequently rises only minimally, thus providing almost constant filtration conditions along the glomerular capillary. Therefore, the effective glomerular filtration pressure can be easily and unequivocally calculated in this model (181). If the colloid-osmotic pressure is high (e.g. when a perfusion solution with 7g/ 100ml albumin is used), the filtration fraction can be as low as 2%, whereas it can rise up to 8% with a colloid-free perfusion solution due to the very high filtration rates (up to 1.6ml/g·min).

Estimation of the glomerular hydraulic conductivity

Due to its unique features the IPRK is well suited as an experimental model in which to quantify the determinants of glomerular ultrafiltration and calculate the glomerular ultrafiltration coefficient K_f. Since K_f is the product of the hydraulic conductivity of the glomerular capillary wall (k) and the glomerular capillary surface area (S), in order to calculate k from K_f ($k = K_f/S$), it is necessary to measure the glomerular surface area. The actual anatomical site of the glomerular hydraulic resistance has not been clearly defined. Therefore, the effective hydraulic conductivity k is usually calculated from the total area of the inner surface of the glomerular capillaries for the purpose of comparability.

This method was applied in the context of the following issues:

- Dependence of the effective hydraulic permeability on age (122, 181)
- Adaptation hypertrophy after unilateral nephrectomy (122, 184) and
- Suppression of adaptation hypertrophy under the influence of cyclosporine A (116, 267)

13.2. Glomerular morphometry

Glomerular capillary surface area is measured using the technique described by Aeikens (5, 6). After perfusion fixation of the kidney, wedges of tissue - each containing the nephron that had been investigated and marked by particles of synthetic colored silicone rubber (Microfil) - are dehydrated and embedded in Araldite (Serva, Heidelberg, Germany). Beginning at the kidney surface, 400 – 600 serial sections (0.9 µm thickness) of which about 150 include the marked glomerulus, are cut on an ultramicrotome (MT-22-B Serval DuPont

Instruments, Miami, FL, USA). The thickness of sections is monitored interferometrically. The sections are stained with methylene blue and covered with a coverslip.

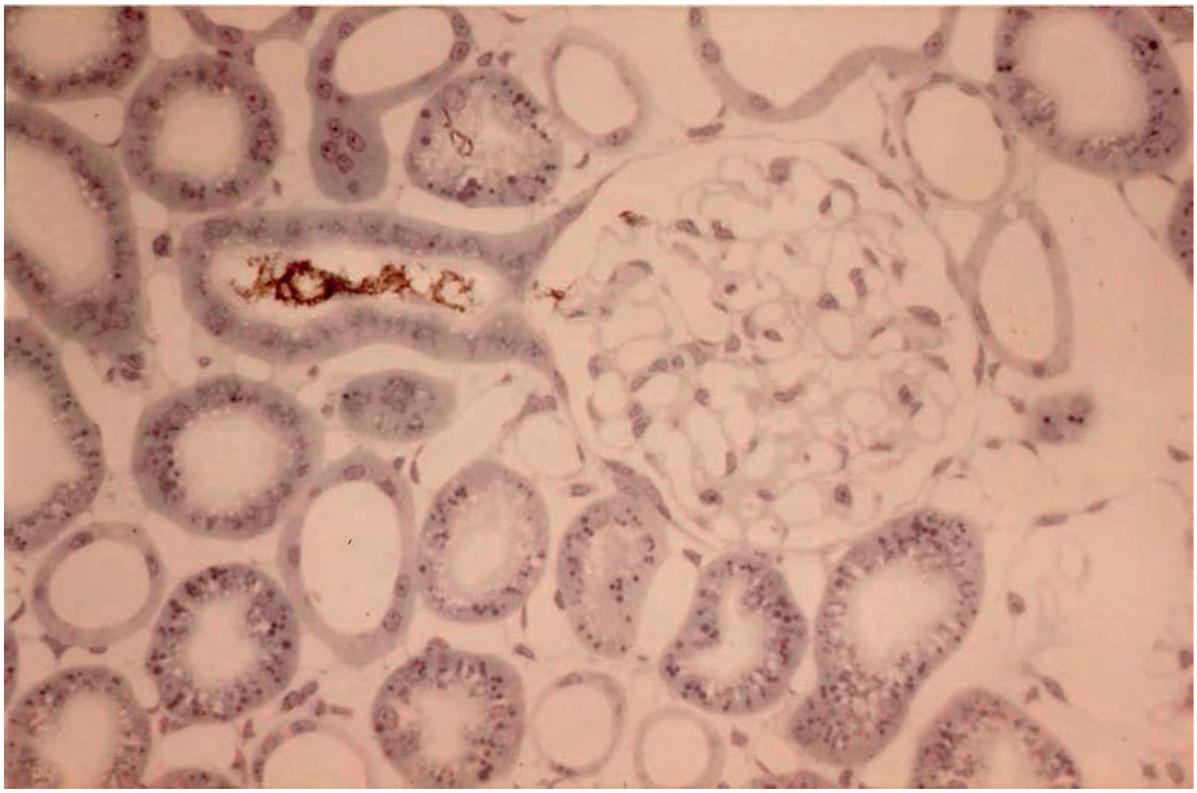

Fig. 13.2.1.: ***Light micrograph of a glomerulus from an isolated perfused kidney of a 2-month-old rat.*** Particles of Microfil are present in Bowman´s capsule and in the proximal tubule [methylene blue, from (181)].

Morphometry of glomerular structures is interactively performed on serial light microscopic sections using an ASM Leitz image analysis system (Leitz, Wetzlar, Germany). The system consists of a digitizer linked to a computer (LSI11, Digital Equipment, Maynard, Ma, USA; see Fig. 13.2.1). The movement of an electronic pencil with a diode at the tip over an induction table is projected onto the light microscopic image of the structure under investigation via a system of prisms. The inner surfaces of the glomerular capillaries are outlined with an electronic pencil and their circumferences are calculated by the computer program. The computed sum of the capillary circumferences is then multiplied by the thickness of the sections to obtain the total capillary surface area. Aeikens (6) has shown that when measuring a microscopic structure of the size of a glomerulus a magnification factor of 1:680 results in an error of less than 1% (S.D.). For the histomorphometric measurements, the changes in size due to fixation and embedding of the material must be taken into account. According to Aeikens (5, 6), perfusion fixation results in a 6% enlargement of area and embedding causes a reduction in area of 9% relative to measurements on frozen sections. These changes are taken into account in the calculations.

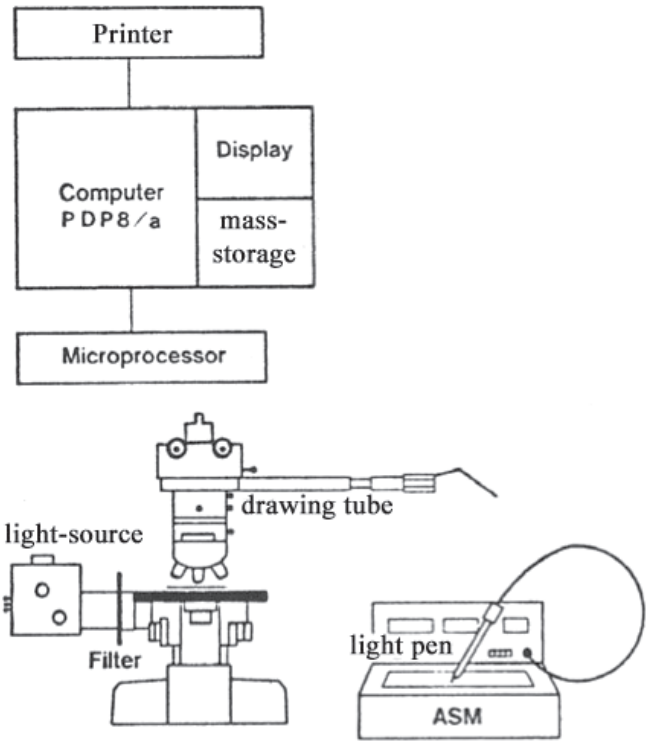

Fig. 13.2.2.: ***Schematic representation of the morphometric analysis system for the determination of the capillary surface from serial sections.*** The movement of the light pen on the induction table is projected via a system of prisms onto the microscopic image and processed by the PDP8 computer. The microprocessor was attached to the ASM image analyzer and the drawing tube of the microscope (181).

Frank Schweda

14. The isolated perfused mouse kidney

After isolated perfused kidneys of different species - especially rats - had been used in medical research for over half a century, adaptation of the model to mouse kidneys became desirable early in the new millennium. With the establishment and dissemination of the transgene and knockout technology in mouse, detailed investigation of specific gene products became possible. For instance, the function of transport proteins or ion channels for which no specific pharmacological tools are available could now be investigated in vivo by genetic manipulation of the respective gene. Apart from the other problems encountered in the analysis of genetically manipulated mice, the significance of any direct effect on kidney function in such experiments is often limited by the systemic phenotype, which can potentially influence kidney function as well. For example, mice with global genetic deletion of the endothelial NO-synthase (eNOS) or of the receptor for the cardiac natriuretic peptides ANP and BNP (guanylyl cyclase-A, GC-A) each exhibit arterial hypertension because eNOS and GC-A both play important roles in the cardiovascular system (48, 65, 87, 155). Since this systemic phenotype has a major impact on kidney function, a detailed analysis of the direct effects of eNOS or GC-A on kidney function is not possible in vivo. This sort of scenario presents an ideal opportunity for the isolated perfused kidney model, which, as has been discussed in detail in the preceding chapters, allows the investigation of kidney function ex situ under controlled conditions, and therefore without the confounding influences of the systemic phenotype of the mice. Of course, systemic effects of the genetic manipulation and the resulting systemic phenotype might result indirectly in functional (e.g., changes in receptor expression levels, vessel contractility, etc.) or structural (e.g., fibrosis) changes in the kidney, which could influence kidney function even in the isolated perfused organ. Obviously, such eventualities should be carefully considered when interpreting the results of such experiments.

14.1. Perfusion techniques

All the perfusion techniques that have been employed in published experiments using isolated perfused mouse kidneys so far are based on the methods used for kidneys from other mammals. The technique was described in detail in a recent Video Article (62). The perfusion medium consists of a modified Krebs-Henseleit buffer, which is continuously aerated with a mixture of 95% O_2 and 5% CO_2 (209, 270, 289). Some studies have used perfusion medium that contained neither albumin nor erythrocytes (288, 289, 303), while both bovine serum albumin (BSA) and erythrocytes were included in the perfusate in other cases (48, 209, 270). The effects of BSA and erythrocytes on the function and integrity of isolated perfused mouse kidneys has been addressed in only one published study so far (209). It was shown that reduction of the BSA concentration in the perfusate resulted in a marked increase in urine excretion (at 4% BSA: ca. 40 µl / min per g kidney weight,

equivalent to more than 10 times the rate of diuresis in vivo) and in the fractional excretion of sodium (FE_{Na} at 4% BSA: 11.6%), as was already known from the IPRK (251). Moreover, the glomerular filtration rate was markedly attenuated compared with the in vivo situation. In that study, a BSA concentration of 6.7% resulted in the reduction of urine excretion to such small volumes that the collection of sufficient urine over reasonable time periods was impossible. Hence, a concentration of 5.5% of BSA was chosen as a compromise between preservation of kidney function and the production of sufficient volumes of urine for analysis. With this concentration of BSA almost physiological values for urine volume (22 µl /min per g kidney weight), GFR (400 µl/min per g kidney weight) and FE_{Na} (1.5%) were observed. While the addition of rat erythrocytes (hematocrit 1%) to the 5.5% BSA perfusate did not significantly alter GFR or diuresis, the fractional excretion of sodium was further reduced to 0.3% and therefore to physiological values. This study very clearly underlines the high-energy demand of tubular transport and the resulting need to use a perfusate containing erythrocytes at least in studies focusing on tubular transport. This conclusion is further corroborated by the fact that the use of a perfusate without erythrocytes results in markedly pronounced damage to tubular cells in the inner stripe of the outer medulla (209, 263). However, since some structural tubular damage was also detected when a hematocrit of 1% was used, the addition of higher concentrations of erythrocytes to the perfusate would seem advisable. Importantly, none of the tested perfusates resulted in reasonably physiological renal vascular resistance (209), which can most probably be attributed to the lack of vasoconstrictor hormones in the perfusate.

The diameters of human and rat erythrocytes are quite similar (ca. 7.5 µm) so that the use of human erythrocytes for the perfusion of rat kidneys should not induce marked mechanical alterations of the renal vasculature. Since mouse erythrocytes are significantly smaller (mean diameter 5.6 µm), human or rat erythrocytes might well be too large for the glomerular capillaries in mouse kidneys. Their use for the perfusion of mouse kidneys could perhaps be expected to cause perturbations in renal perfusion, glomerular filtration and therefore renal function. However, Rahgozar and colleagues demonstrated in pilot experiments that the use of erythrocytes from rats, mice or sheep (mean diameter 4µm) had no detectable impact on renal perfusion (209). These results are in good agreement with unpublished studies from our group, which addressed the effect of the size and source of erythrocytes (mouse vs. human) on renal vascular resistance and renal endothelial function.

In light of the above-mentioned studies, which demonstrated that: (i) the presence of erythrocytes in the perfusion medium is essential for nearly physiological renal function; (ii) a hematocrit of 1 % is not sufficient to preserve the integrity of the kidney for a perfusion time of 1 hour, and (iii) the use of larger erythrocytes from a different species does not appear to have major effects on renal hemodynamics or renal function, we chose to use a perfusion medium containing human erythrocytes at a hematocrit of 7 – 10%. Due to the relatively large numbers of erythrocytes necessary for kidney perfusion, the use of mouse blood as a source is neither feasible nor ethically justifiable.

As with the perfusion of kidneys from other species, mouse kidneys can be perfused at either a constant flow rate (289) or a constant perfusion pressure (270). In contrast to the perfusion of kidneys from larger species, which require high rates of perfusion with a complex and expensive perfusate and therefore necessitate its recirculation, perfusion of mouse kidneys can be performed in single-pass mode due to the low flow rates (see Chapter 2).

Use of the isolated perfused mouse kidney for the investigation of renal renin release and renal vascular resistance

In the Institute for Physiology and the Collaborative Renal Research Center 699 on Structural, Physiological and Molecular Determinants of Kidney Function at the University of Regensburg, Germany, several groups are working on the regulation of renin secretion and the control of renal perfusion. Since, as indicated above, genetically manipulated mice allow new and detailed insights into these topics, the technique used for the perfusion of isolated rat kidneys, which was described in detail in the preceding chapters, was adapted to mouse kidneys. They have since been used successfully in the investigation of renin release and renal perfusion (8, 65, 91, 101, 111, 137, 138, 167, 192, 238, 269, 270, 304). Although determination of the glomerular filtration rate and of the tubular function can be successfully performed using this technique, our approach to these tasks (cannulation of the ureter using a glass capillary micropipette, usage of FITC-labeled sinistrin for the determination of the GFR) is not yet fully mature, so that a detailed description of the method would not be appropriate at this stage. Instead, the interested reader is referred to the publication by Rahgozar (209) in which a different method of urine collection is described. Alternatively, the author of this chapter can contacted directly.

14.2. Perfusion medium

A modified Krebs-Henseleit buffer (see Table 4.1) serves as the basic perfusion medium, which is supplemented with substrates according to formula R2, table 4.2. A commercially available solution (Aminoplasmal AS10, Braun AG, Melsungen, see table 4.3.) is used as the source of amino acids. Butyrate is not used in our perfusate. A 5-liter batch of perfusate is freshly prepared on the day of the experiment and sterile filtered (see figure 4.5.1, 4.5.2). Bovine serum albumin is then dissolved in this sterile medium (6 g BSA per 100mL) using a magnetic stirring bar and the resulting albumin solution is subsequently sterile filtered. In order to remove bound substances such as hormones from the albumin solution, dialysis can be performed, but we do not use this step for routine experiments.

To ensure an adequate supply of oxygen to the kidney, the albumin solution is supplemented with human erythrocytes at a hematocrit of 7-10%. As source of erythrocytes, packed red blood cells, which are just past their expiry date, are purchased from the local blood bank. Red blood cells are repeatedly washed with sterile modified Krebs-Henseleit

buffer without albumin (see above) at least three times or until the supernatant after centrifugation is clear (see chapter 4.1.6.3). For an experiment of 2 hours duration and perfusion in single-pass mode, approximately 250 ml of perfusate is needed.

14.3. Perfusion apparatus

Perfusion of mouse kidneys is carried out at a constant pressure of 90 or 100 mmHg in the single-pass mode. In order to avoid alterations in the composition of the perfusate (modified Krebs-Henseleit-buffer + BSA + human erythrocytes) during the perfusion period (owing to the release of potassium from erythrocytes as a result of hemolysis, for instance) and to ensure adequate oxygenation of the perfusate, continuous dialysis of the perfusate is performed (see Chapter 4.4.5., the dialyzer as the "kidney´s lung"). As dialysate, the modified Krebs-Henseleit buffer without albumin and erythrocytes is used. The dialysate is continuously aerated with a mixture of 95% O_2 and 5% CO_2.

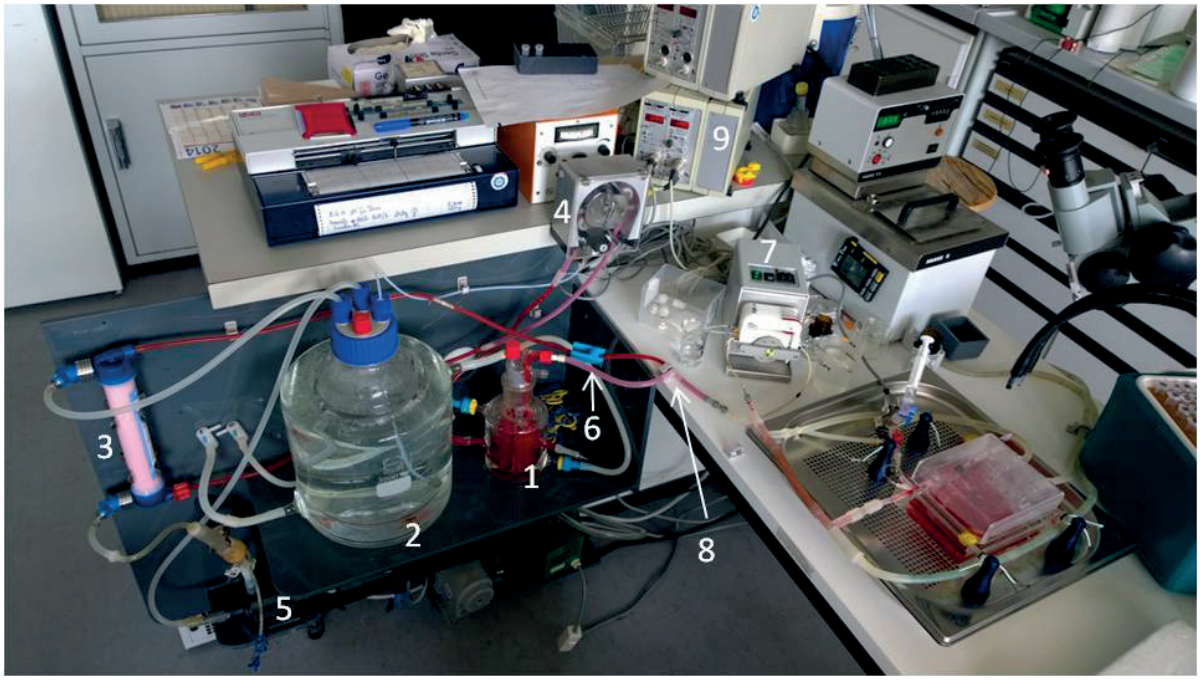

Fig. 14.3.1.: ***Apparatus for the perfusion of mouse kidneys at constant perfusion pressure in the single-pass mode:*** Complete setup (Fig. 14.3.0) and detailed view of the dialysate and perfusate circuits (Fig. 14.3.1).

The perfusion pump (7), electronic control unit (9) and perfusion chamber (5 in Fig. 14.3.3) shown in Figs. 14.3.1 – 14.3.3 were purchased from Hugo Sachs Electronic – Harvard Apparatus GmbH, Germany.

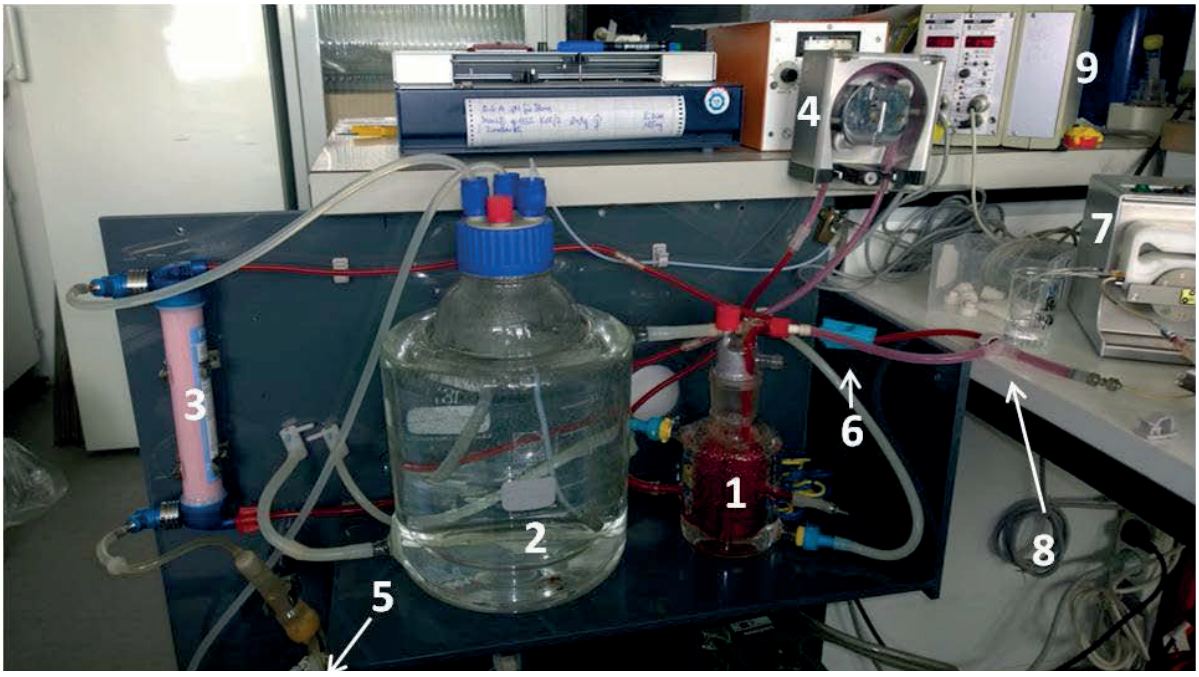

Fig. 14.3.2.: ***Detailed view of the dialysate and perfusate circuits.***

The numbers in the Figures refer to the following components:

1. Temperature-controlled perfusate reservoir
2. Temperature-controlled dialysate reservoir
3. Dialyzer for solute and gas exchange between perfusate and dialysate
4. Roller pump for the circulation of the perfusate
5. Centrifugal pump of the dialysate circuit
6. Variable clamp for the adjustment of the hydrostatic pressure in the perfusate circuit
7. Roller pump for perfusion of the kidney, which can be pressure dependently regulated by the attached electronic control unit (9).
8. T-junction for the withdrawal of perfusate for kidney perfusion
9. Electronic control unit for pressure-dependent regulation of perfusion pump (7). The temperature-controlled perfusion chamber and the pressure transducer are shown on the right in Fig. 14.3.1 (and in greater detail in Fig. 14.3.3).

The perfusate and dialysate reservoirs are enclosed in water-jacketed containers ([1] and [2] in Figs. 14.3.1 and 14.3.2) and the perfusate is heated immediately before entering the kidney and the (temperature-controlled) perfusion chamber (see below), ensuring that, when it leaves the perfusion cannula, the perfusate temperature is 37°C. Perfusate (250 ml) and dialysate (3.5 l) circuits are connected via a dialyzer ([3] in Figs. 14.3.1 & 14.3.2) and are driven by a roller pump (perfusate, [4] in Figs. 14.3.1 & 14.3.2) and a centrifugal pump (dialysate, [5] in Figs. 14.3.1 & 14.3.2) respectively. After filling the respective fluid circuits with perfusate and dialysate, and before beginning the experiment, the pressure within the perfusate circuit must be adjusted, either by changing the flow rate of the roller pump ([4] in Figs. 14.3.1 & 14.3.2) or by altering the setting of the variable pressure clamp ([6] in Figs. 14.3.1 & 14.3.2), so that fluid transfer between perfusate and dialysate is avoided.

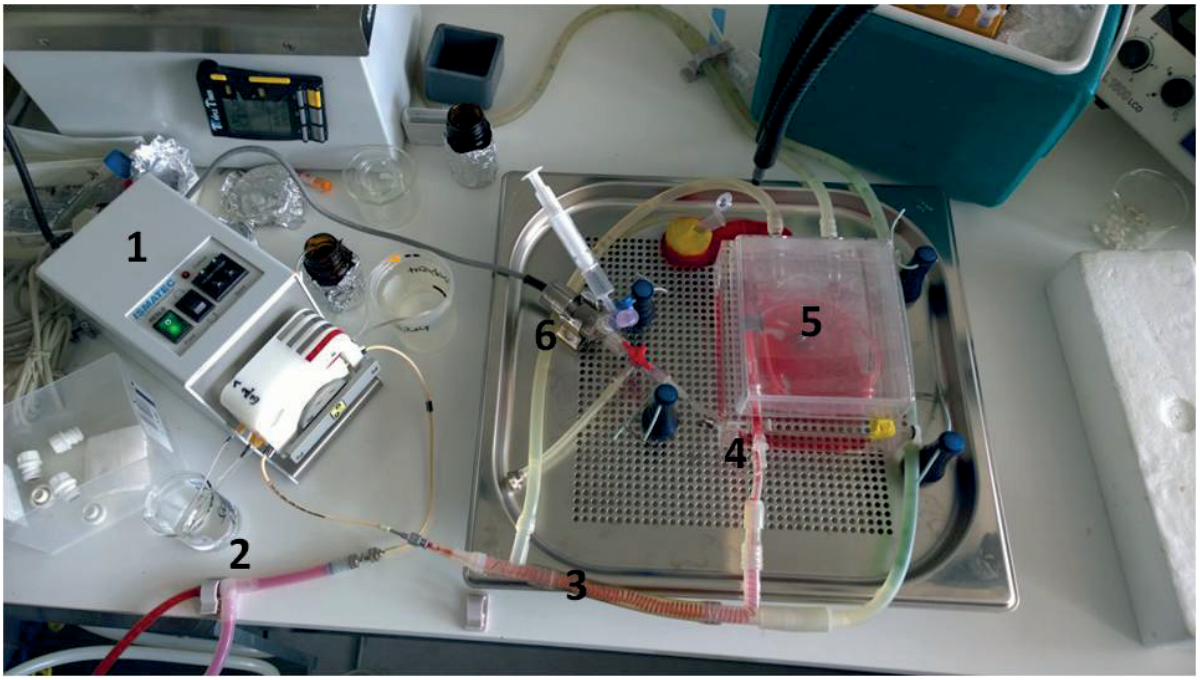

Fig. 14.3.3.: ***Set-up used for the perfusion of mouse kidneys at constant pressure in single-pass mode.*** 1. Roller pump for perfusion of the kidney, pressure dependently regulated by the attached electronic control unit. 2. T-junction for the withdrawal of perfusate for the kidney perfusion. 3. Temperature-controlled helical tube. 4. T-junction for the determination of perfusion pressure. 5. Temperature-controlled perfusion chamber with kidney (shown in greater detail and without lid in Fig. 14.4.1). 6. Pressure transducer for the determination of perfusion pressure.

The perfusion of the kidney is driven by a roller pump (4-channel, 8 rollers; [7] in Figs. 14.3.1 & 14.3.2; [1] in Fig. 14.3.3), which withdraws the necessary amount of perfusate from the perfusate circuit via a T-junction ([8] in Figs. 14.3.1 & 14.3.2; [2] in Fig. 14.3.3). On its way to the kidney, the perfusate, which has been prewarmed in its storage container, passes through a thermostated helical tube ([3] in Fig. 14.3.3) and reaches the thermostated perfusion chamber ([5] in Fig. 14.3.3) via a further T-junction ([4] in Fig. 14.3.3). This one provides for determination of the hydrostatic pressure in the perfusate circuit by a pressure transducer ([6] in Fig. 14.3.3). The pressure serves as the feedback signal for the electronic control unit ([9] in Figs. 14.3.1 & 14.3.2) of the perfusate pump to maintain a constant perfusion pressure. Note here that, due to the rather narrow inner diameter of the perfusion cannula, a pressure is built up in the perfusate tube, so that the pressure determined by the pressure transducer in the perfusate circuit is higher than the actual pressure in the renal artery. In accordance with the Hagen-Poiseuille law, this systematic error increases disproportionately with decreasing inner diameter of the perfusion cannula. Accordingly, a cannula with the highest possible diameter should be used. Moreover, the pressure build-up in the perfusate tube has to be determined for each cannula and must be taken into account when the perfusion pressure is adjusted via the electronic control unit of the roller pump.

14.4. Surgical preparation and cannulation of the renal artery

Basically, the preparation of the mouse kidney follows the procedure described for rats in Chapter 8.2. For the operation, the anesthetized mouse is placed in the thermostated perfusion chamber. Anesthesia is performed using a combination of ketamine and xylazine. After abdominal midline incision, the aorta is dissected and is clamped distal to the right renal artery, so that perfusion of the right kidney is not disturbed during the subsequent insertion of the perfusion cannula into the abdominal aorta distal to the clamp. The mesenteric artery is ligated, and a metal perfusion cannula (outer diameter 0.6 – 0.9 mm) is inserted into the abdominal aorta. After removing the aortic clamp, perfusion is started immediately at a low flow rate (100 µl/min) to prevent clotting in the cannula. Subsequently, the cannula is advanced to the origin of the right renal artery and fixed in this position. The aorta is ligated proximal to the right renal artery and the perfusion rate is increased until a perfusion pressure of 90 – 100 mmHg is achieved. Alternatively, perfusion mode can be switched to “constant pressure” at this time point. Use of the cannulation technique mentioned above avoids any significant ischemia of the right kidney. Finally, the right kidney is excised, placed in the humid and thermostated chamber, and perfusion at constant pressure (100 mmHg) is established. In order to facilitate the subsequent cannulation of the V. cava superior, a part of the liver, which partially encircles the V. cava, should be excised together with the kidney en bloc. Finally, the V. cava is cannulated proximally (polypropylene catheter, approximately 1.5 mm outer diameter, the largest possible diameter should be used) and distally ligated. The venous effluent is drained outside the moistened perfusion chamber and collected for determination of renin activity and venous blood flow.

The perfusate flow rate can be determined from the speed (rpm) of the perfusate pump and the renal vascular resistance can be calculated if the pump has been calibrated. Note that the perfusate flow rate will be markedly overestimated if any leakage should occur in the arterial limb (e.g., if a side branch of the aorta has not been properly ligated). An alternative way to determine the renal perfusion rate is to measure venous blood flow. This can be done either by using electronic flowmeters, which can be easily integrated into the venous outflow tubing, or by the sampling of the venous effluate over a certain time interval and determination of its volume. The disadvantage of the latter method is that the renal blood flow will be underestimated in the event of a venous leakage. However, with this method one can be certain that all of the sampled blood has in fact passed through the kidney, which is eminently important if the experiment focuses on the secretion of a certain hormone or substance. Since our experiments on the regulation of renin secretion require the sampling of the venous blood in any case, we routinely use the latter method for the determination of renal blood flow (see Fig. 14.4.1). In addition to the renin activity in the venous effluate of isolated perfused mouse kidneys, we have determined the concentration and renal secretion of the cyclic nucleotides cAMP and cGMP, and of adenosine and ATP.

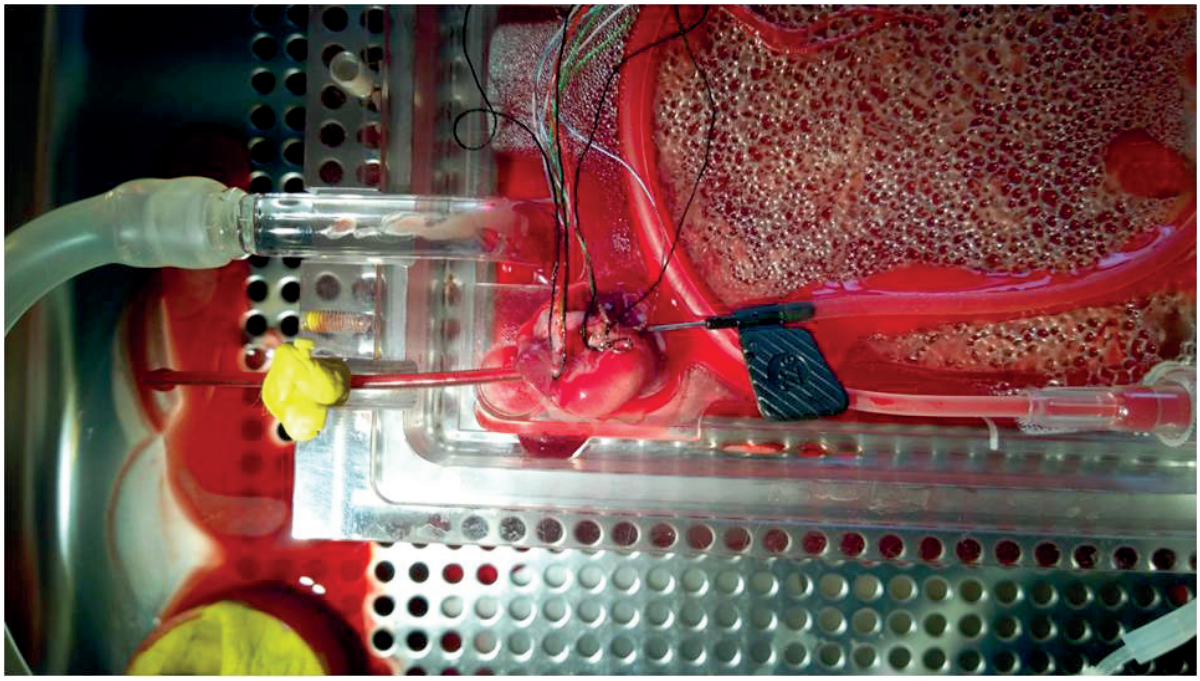

Fig. 14.4.1.: ***Perfusion chamber with open lid.*** Kidney with perfusion cannula (right, black plastic wing of cannula visible) and venous catheter (left) for the drainage of the perfusate out of the perfusion chamber. The venous catheter is attached to the perfusion chamber by plasticine.

Ad 14.2 Appendix

Sheep erythrocytes as O_2 carriers during perfusion of the isolated mouse kidney. Contributed by **Jan Czogalla**, Institute of Anatomy, University of Zurich, Switzerland.

Raw material: Defibrinated sheep whole blood obtained from EOlabs (Burnhouse, Bonnybridge, UK) is used. The donor sheep are kept in quarantine (under veterinary supervision) and supplied with food, and water *ad libitum* (ISO 17025:2005). The blood is withdrawn in cycles, thus guaranteeing a constant animal hematocrit above 35%. The blood is withdrawn into gamma-irradiated blood collecting bags under sterile conditions from the jugular vein, and subsequently agitated at 4°C until full defibrination is achieved. It is then stored at 4°C under sterile conditions (ISO Grade 5/GMP Grade B) and dispatched within 48 hours. Quality control: (ISO9001:2008): Columbia-Agar is inoculated with the blood and plates are monitored for the growth of microorganisms for 14 days. The cost of 3 liters of blood prepared in this fashion is 99 GBP (136€).

Shipment: Blood is packed in units of 3x1 liter in Styrofoam boxes. Two cooling bags (0°C) are included, separated from the blood by a Styrofoam panel. The order is sent by International Priority via FedEx and reaches Zurich within 20h, at which point the temperature is approximately 8°C. The cost of shipment is 78€.

Storage and stability: Erythrocytes are stored at 4°C. The shelf life stated by the supplier side is 1 month. Functional tests with the isolated perfused kidney with 1-month-old erythrocytes were successful (flow, pressure, gfr and urinary output were the same as with 3-day-old blood).

Protocol: On the day of the perfusion, three times the final erythrocyte volume needed is withdrawn under sterile conditions. The blood is then centrifuged in 12-ml Falcon tubes for 8 min at 3000g. Blood plasma and the upper 0.5cm of the erythrocyte layer are removed and replaced by the dialysis buffer used for kidney perfusion. This step is then repeated three times. After the last step, the clear supernatant is removed and the erythrocytes are filtered (Machery-Nagel MN 615 paper filter, 4-12µm pore size) and added to the final perfusion buffer (final hematocrit approximately 10%). For two mouse kidneys, 700ml of perfusion buffer is used.

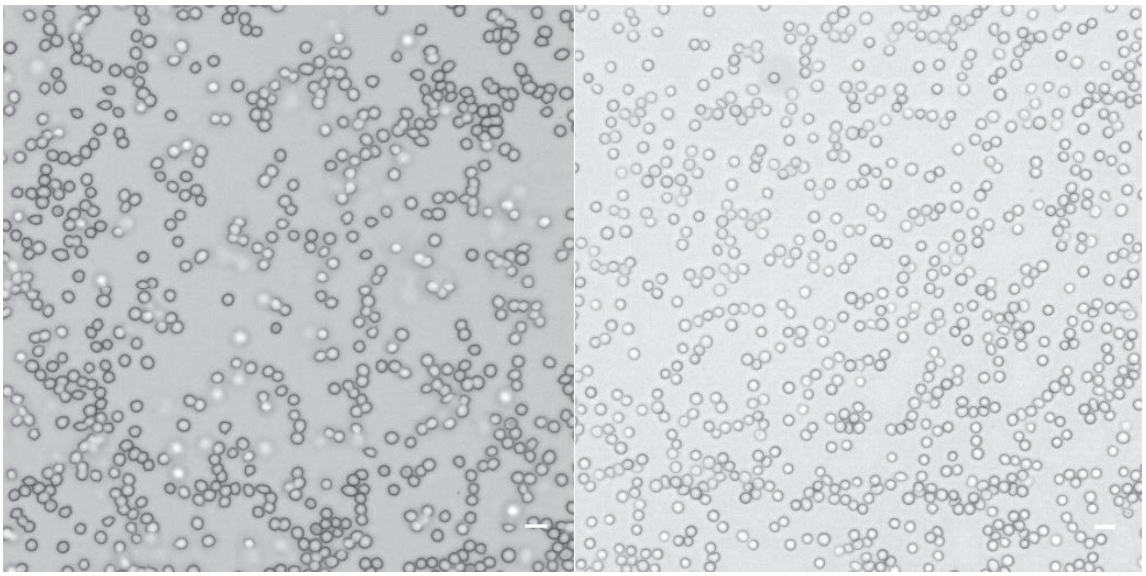

Fig. 14.2.1.: ***Sheep Erythrocytes from EOlabs in smear, diluted.***
Left: Erythrocytes after 2 hours of continuous dialysis.
Right: Erythrocytes after 2 hours of continuous dialysis and passage through the isolated kidney, taken from the renal vein. Scale bar: 10µm.

H.J. Schurek´s P.s.:

There is an interesting new way – not yet used in the IPRK - to enhance oxygen capacity by using the extracellular macro-hemoglobin of the marine annelid worm Arenicola marina. This path has been developed by the French biologist Dr. Franck Zal and his company´s name is Hemarina. One may expect that this macro-hemoglobin will not be filtered at the glomerular capillaries and its large size may not contribute to the colloid-osmotic pressure (296b).

15. Technical appendix

Fig. 15.0.1.: ***Ensemble for humidification and heating of gases.*** Gases are pre-warmed in the water-jacketed glass coil at the top, humidified by passage through the ground-glass frit into distilled water in the Erlenmeyer flask which is placed in a water bath (see Fig. 5.1.01). Gas is reheated by passage through the glass coils in the lower panel, thus avoiding transfer of condensate into the perfusate. The 4-fold coil was originally designed for studies (in the single-pass mode) of the effects of different substrates on sodium transport. Up to 4 Woulff bottles, each filled with 2 liters of a different perfusate, could be connected in series (256, 257).

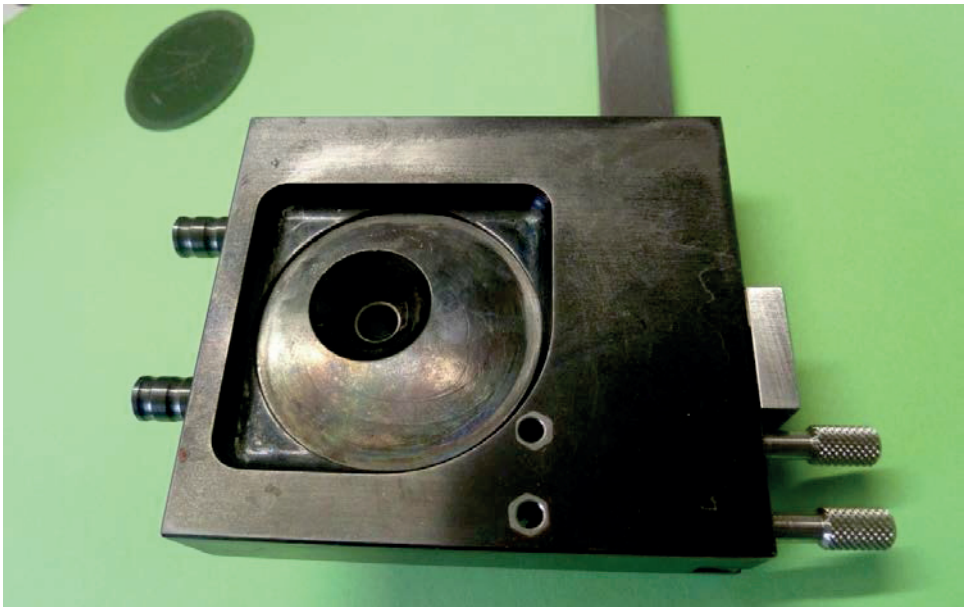

Fig. 15.0.2.: ***Mount for the collecting funnel, with venous cannula holder and valve block. Upper panel:*** The current collecting funnel, made of stainless steel, is positioned below the kidney tray and is equipped with a threaded hose adapter (for perfusate outflow). On the left are connections for water circulation (temperature control). The two apertures at the front serve to accommodate the arterial bypass and the tube used to tap the venous cannula via a T-junction. ***Lower panel:*** The bar inserted below the screws controls two clamping pins, which are driven by compressed air via a solenoid valve, and alternately direct or block the arterial or venous inflow to the O_2 electrode. The compressed air cylinder connects to the bracket on the right. The collecting funnel originally used in Hannover was made of nickel-plated brass. The later versions employed in Hannover and Münster were constructed of stainless steel in the research workshop, and provided for adequate temperature control. The dark color resulted from an attempt to create a diamond-like surface by exposing the unit to a physical plasma (with acetylene) in vacuum. The plate on the right is used to mount the block.

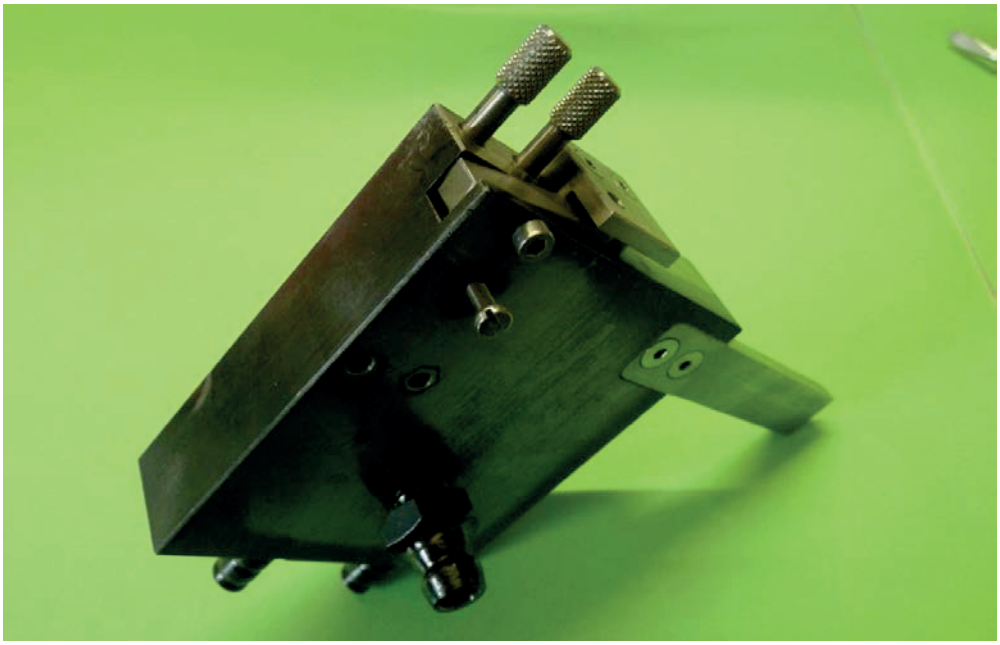

Fig. 15.0.3.: ***The venous cannula.*** The cannula is fitted with a stepped T-junction that connects the bypass to the O_2 measuring cell. On the right is a Luer connector for spot-check measurements and venous sampling.

The reluctance of experimenters to cannulate the renal vein is understandable. However the method we used gives us enough time to monitor the success of the maneuver under continuous flow control on the recorder after the start of perfusion. When the funnel has been positioned and perfusion at constant pressure is underway, the venous cannula in the mounting block can be brought close to the vena cava inferior from the cranial side (right) and the vein is then slipped over the cannula with the aid of two watchmaker's forceps, and the upper cava ligature is fixed. The lower cava ligature can then be fixed so that the perfusate drains quantitatively via the cannula. This procedure is quite simple, because the cannula is rotatable about the axis of the lower T-arm and can be firmly arrested with the fixing screw, while monitoring flow on the recorder.

Choice of plastic tubing.

Pegg et al. published an analysis of different plastic tubes concerning gas permeability and adsorption of fatty acids which should make the selection easier. At that time Tygon was not available.

Pegg et al.: Cryobiology 9, 569-571 (1972)

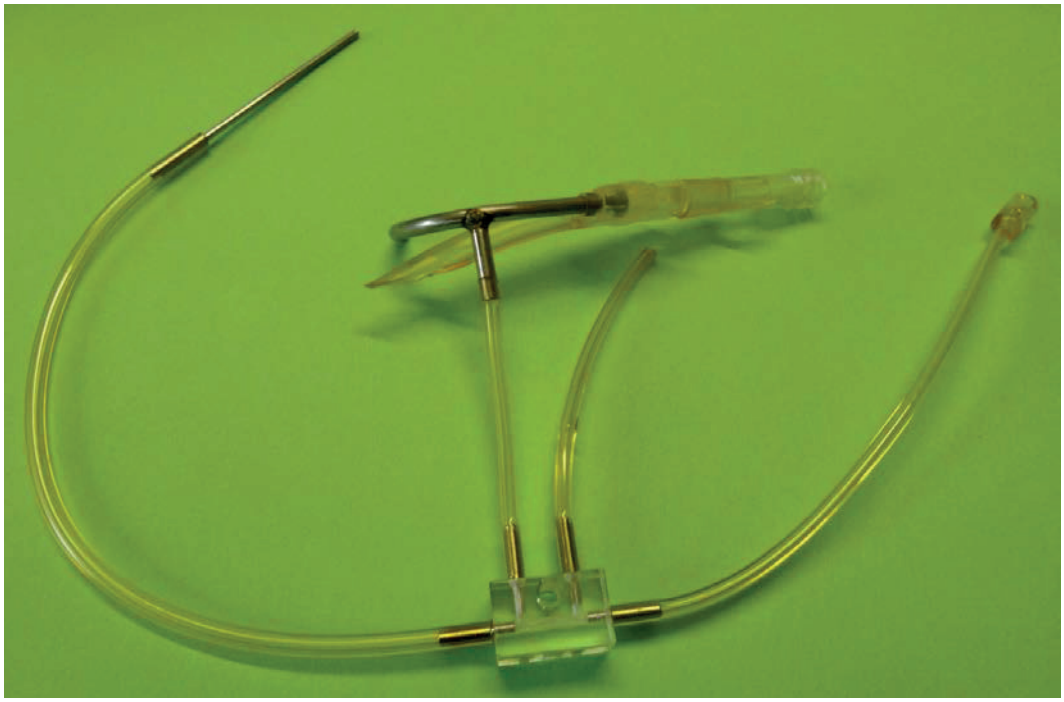

Fig. 15.0.4.: ***Linkage of the venous cannula and arterial bypass, and outlet to the oxygen-measuring cell.*** The Tygon® tube connects the venous cannula to a 4-way manifold, to which the tube for the arterial bypass, with the outlet to the O_2 measuring cell (on the right) and the open overflow, which is recycled into the funnel.

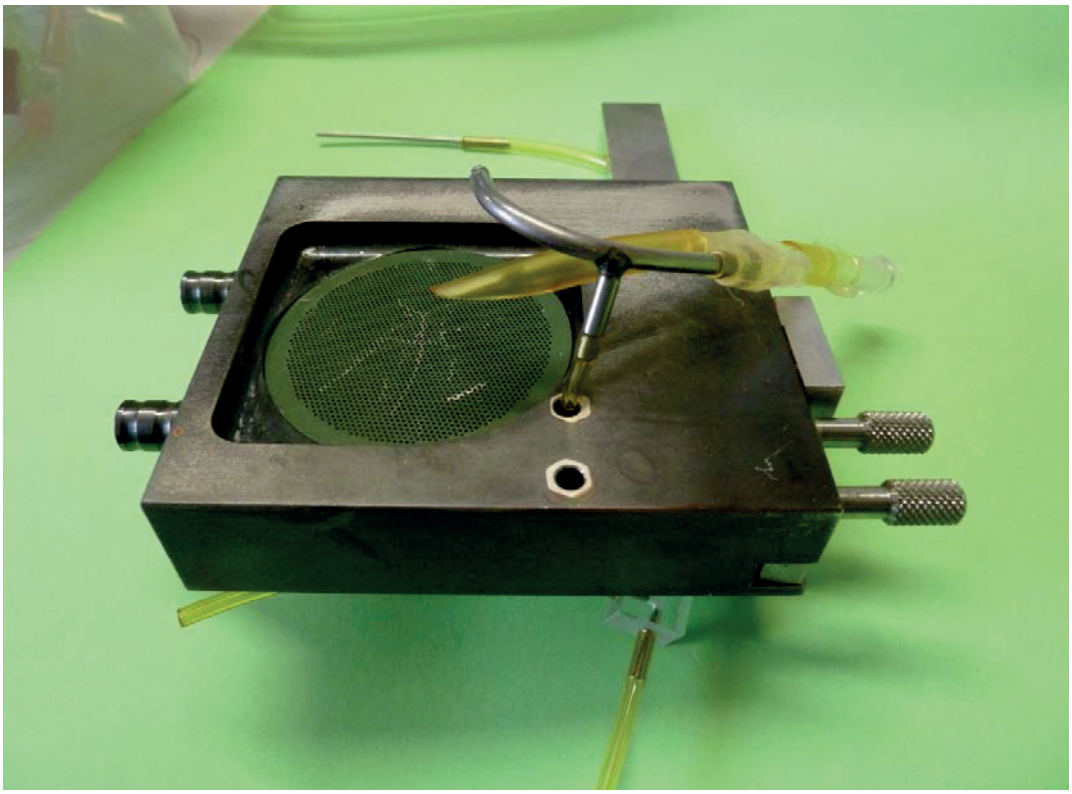

Fig. 15.0.5.: ***Disposition of the tubing on the mounting block*** (seen from above)**.** The tubing system is prepared for installation.

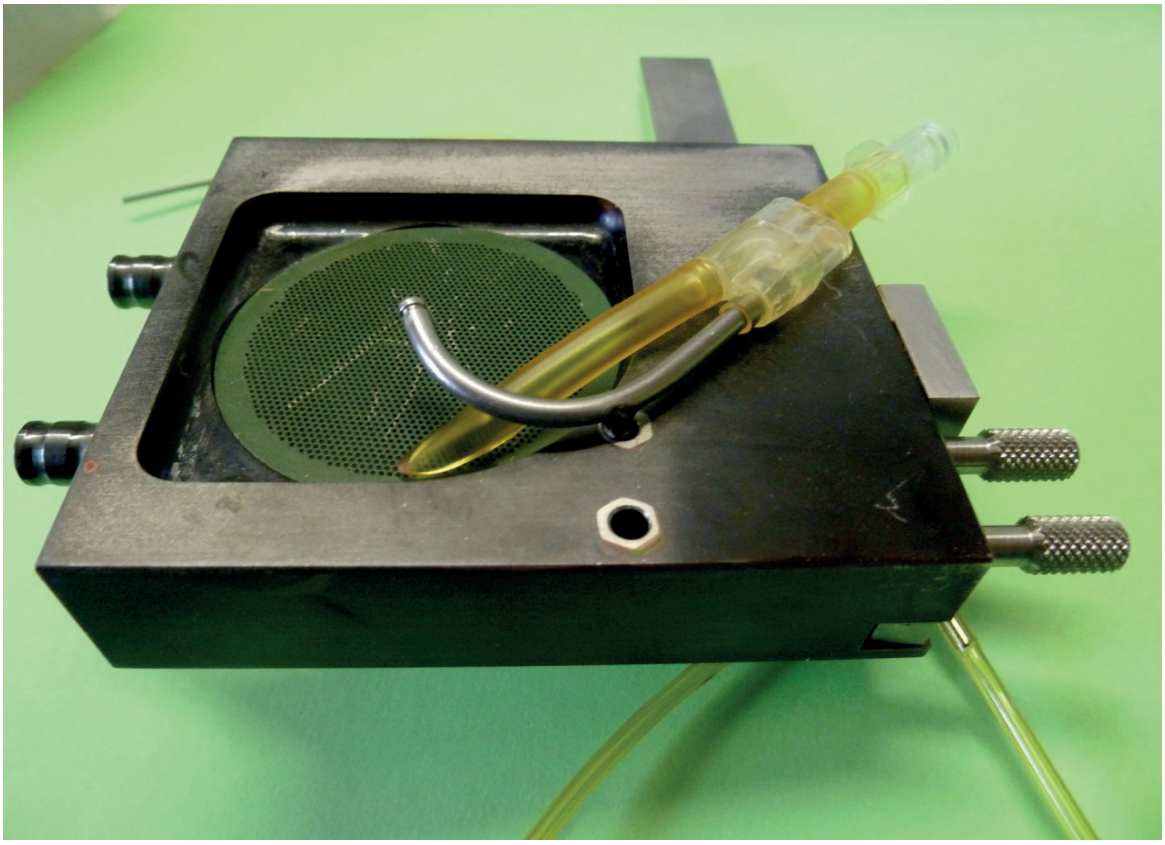

Fig. 15.0.6.: ***Final assembly*** (seen from above). The venous cannula is positioned and temporarily fixed. It is rotatable about the axis of the T-outlet and is pivoted into the inferior vena cava from the cranial side with opening directed toward the renal vein. The tube for the arterial bypass must still be threaded from below through the front hole.

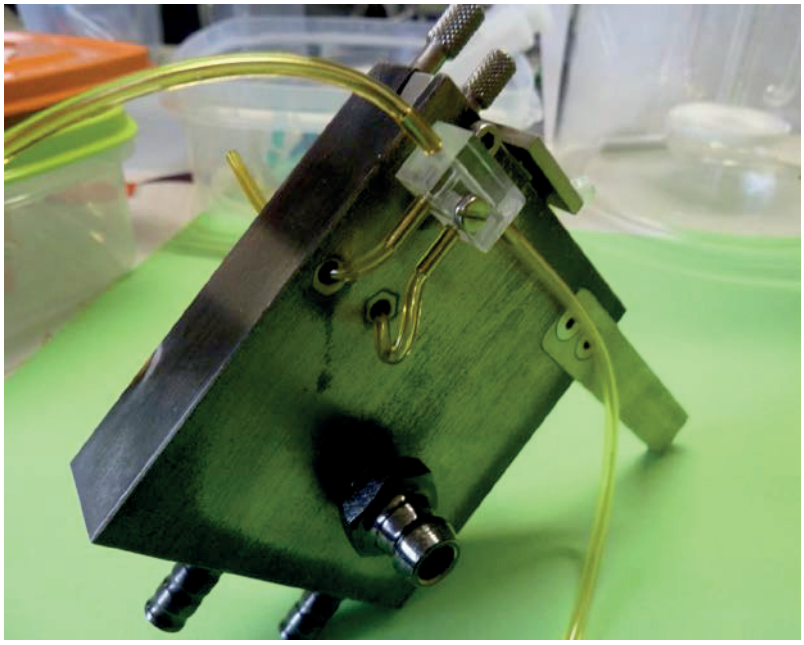

Fig. 15.0.7.: ***Final assembly*** (seen from below). The 4-way manifold is screwed to the bottom of the block, and the tube for arterial bypass is pushed through and is clamped off by the valve bar by spring pressure. The plate (bottom right) is used to position the funnel under the operating table. The effluent tube is attached to the large-bore nozzle, and leads to the reservoir or (in single-pass mode) a waste receptacle. For sensor-controlled recycling of the effluent via a valve for foam reduction (which allows effluent to be recycled without intervening air segments) a smaller nozzle is sufficient (and more effective).

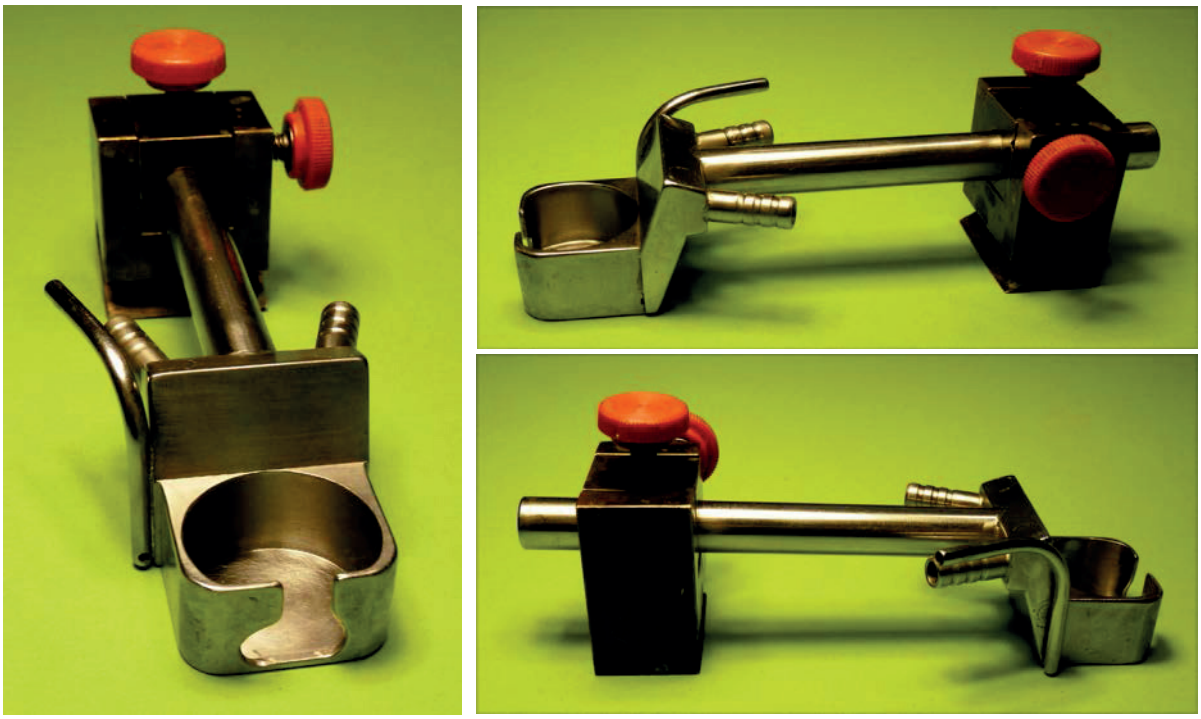

Fig. 15.0.8.: ***Views of kidney tray last used, with its mounting block.*** The two-part mounting block is made of brass, the tray is stainless steel. The heated water is circulated via a U-shaped channel within the inclined back-plate of the tray, which connects the inlet and outlet ports. The suction tube* is laser-welded to one side of the tray, opens forward and, when in use, this end should be underlain with a wide silicone half-tube in order to prevent aspiration of fat globules. Dimensions of tray: width 28 mm, height of the front wall 15mm, total height 29mm, depth 20,5mm, connectors 6 / 4mm, suction tube 3mm. Mounting rod 10 mm diameter, 90 mm long. Dimensions of mounting block: width 30mm, height 35mm, depth 20mm, the inner part is 16mm wide and has a horizontal groove on the right to accommodate the fixing screw.

*After the start of perfusion, when the aorta and vena cava have been severed, this tube is used to suck the blood into a suitable container (e.g., an Erlenmeyer flask with a ground glass neck). In Berlin we used a water-jet pump for this; nowadays, the inlet nozzle of a small compressor is connected to the Erlenmeyer flask.

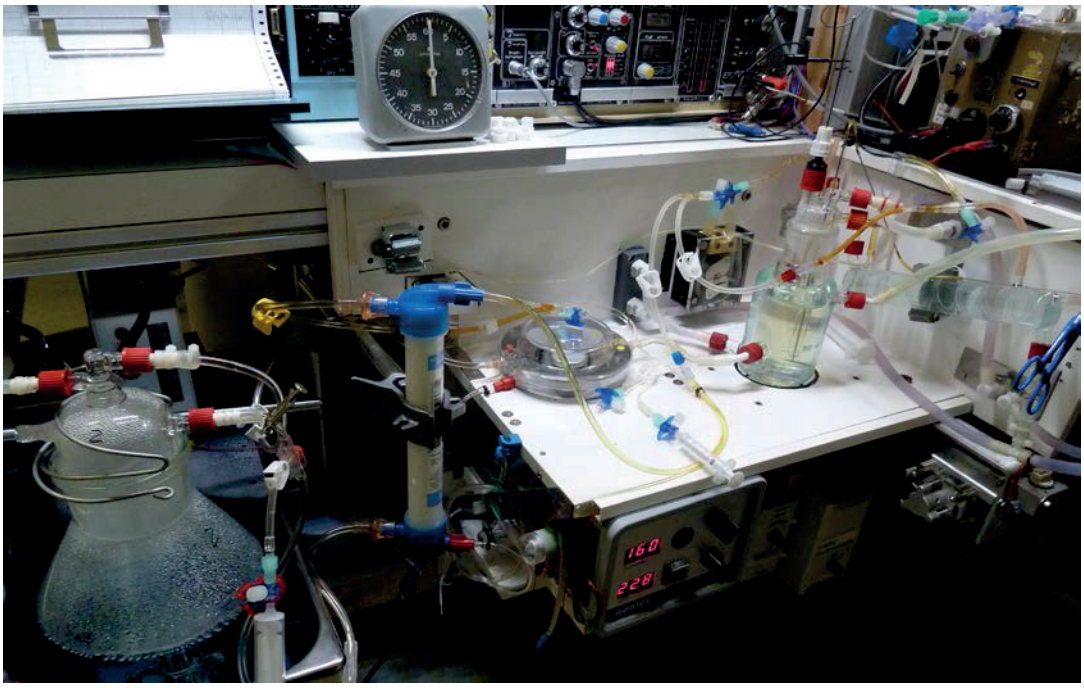

Fig. 15.0.9.: ***Conditioning in preparation for mode-3 perfusion before addition of erythrocytes.*** On the left is the bottle containing 5 liters of dialysate, in the middle is the capillary dialyzer (FX5), which is driven by the two-way pump behind it. The inlet for dialysate is on the top left, that for perfusate on the top right, behind the feedback-controlled perfusion pump and the reservoir for perfusate.

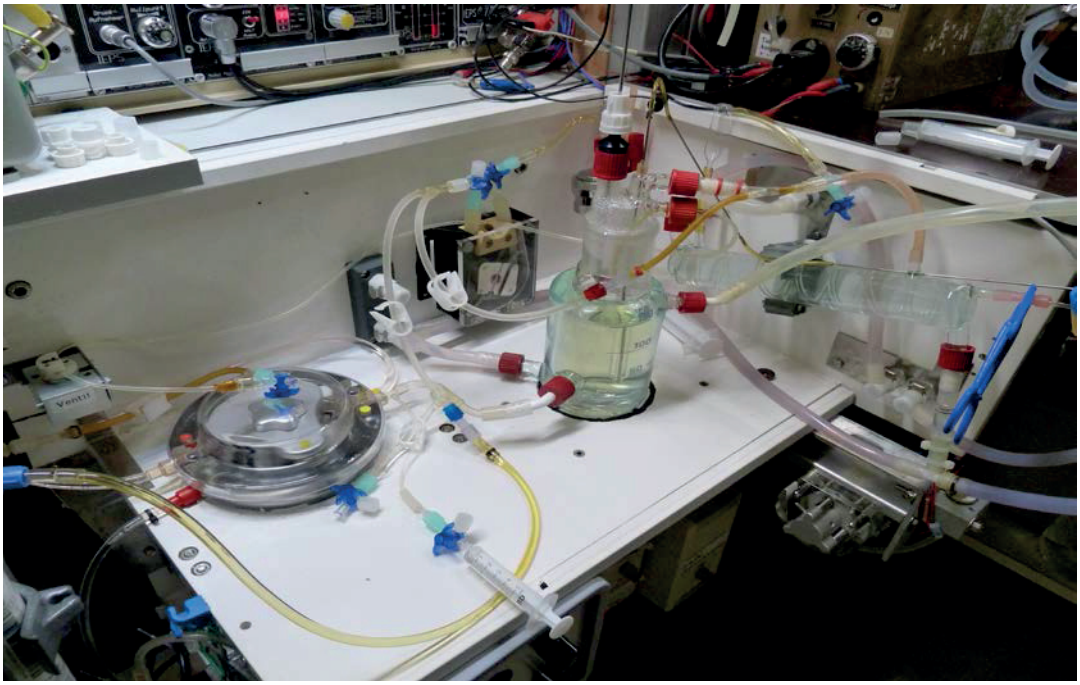

Fig. 15.1.0.: ***Detailed view of the complete assembly.*** On the left is the tube valve (normally closed), which is opened to add dialysate to the perfusate when the level of liquid in the perfusate reservoir drops below that of the scanning probe; the control volume is equivalent to about 1% of the filling volume (i.e., 2ml). Suitable electronic water switches (e.g. Kemo M158) are available from specialized retailers. The blue clamp on the right cuts off the connection to the kidney, while the bypass (to the left of the clamp) is open.

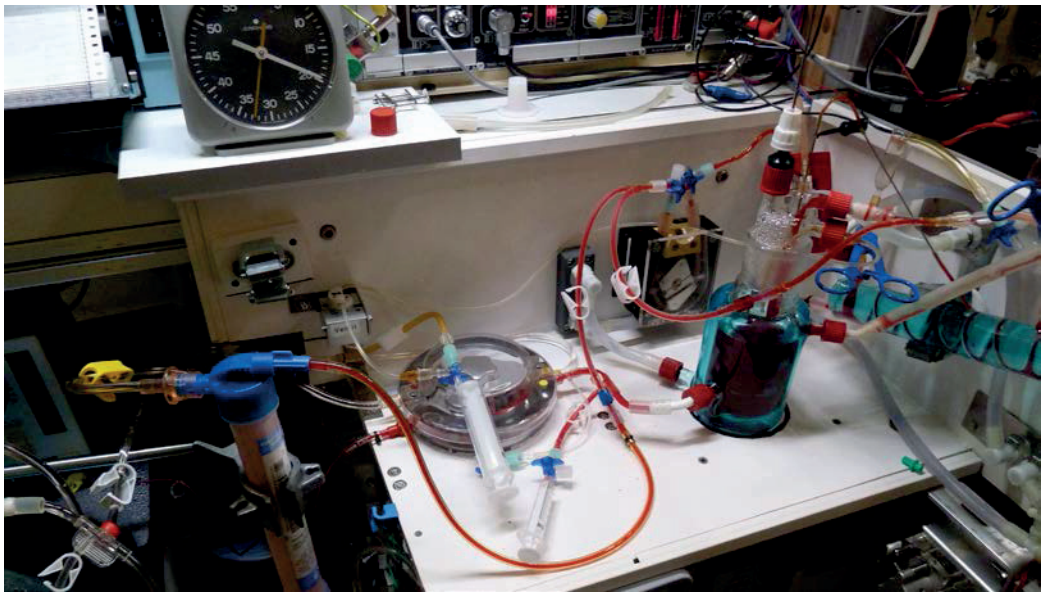

Fig. 15.1.1.: ***After erythrocyte addition and initiation of perfusion (19th minute).*** A hematocrit of 5% is sufficient to prevent morphologically visible damage indicative of oxygen deficiency (253). In the perfusate reservoir, a magnetic stirring bar (coupled to a stirrer placed below the reservoir) prevents settling of the erythrocytes.

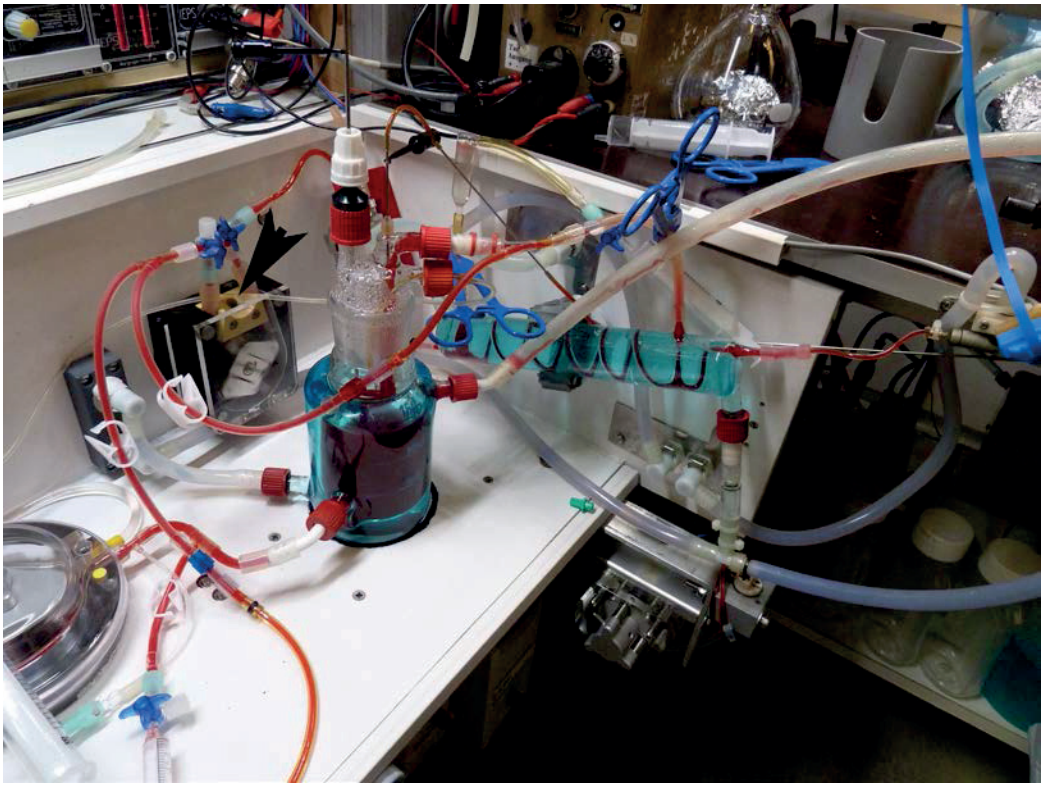

Fig. 15.1.2.: ***Close-up view of part of the assembly.*** The thin tubing between the two ports of the perfusion pump (black arrow) leads directly to the reservoir. This tube is used to supply dialysate to offset losses of perfusate as urine and during ultrafiltration in the dialyzer. Volume losses due to withdrawal of perfusate samples are compensated for by lowering the sensing probe. During perfusion, the bypass from the glass coil to the reservoir is closed (blue clamp).

Fig. 15.1.3.: ***Detailed view of perfusate reservoir with level control.*** The sensing probe on the left is adjustable in height, and serves as one of the electrodes for the refill control to compensate for losses during ultrafiltration of the dialyzer and withdrawal of urine samples. The thin stainless steel tube on the right serves both as a second electrode and as the return path for aliquots used for oxygen pressure measurements. See Fig. 5.3.2.

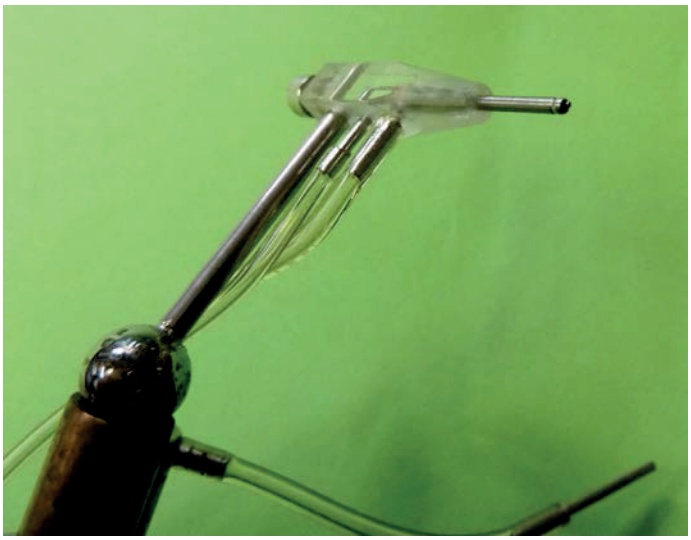

Fig. 15.1.4.: ***Mobile double-barreled aortic cannula attached to a magnetic ball joint.*** The ball moves freely in the pan. The perfusion cannula itself is screwed firmly to the rod axis (IBS Magnet, Berlin; ibsmagnet.de).

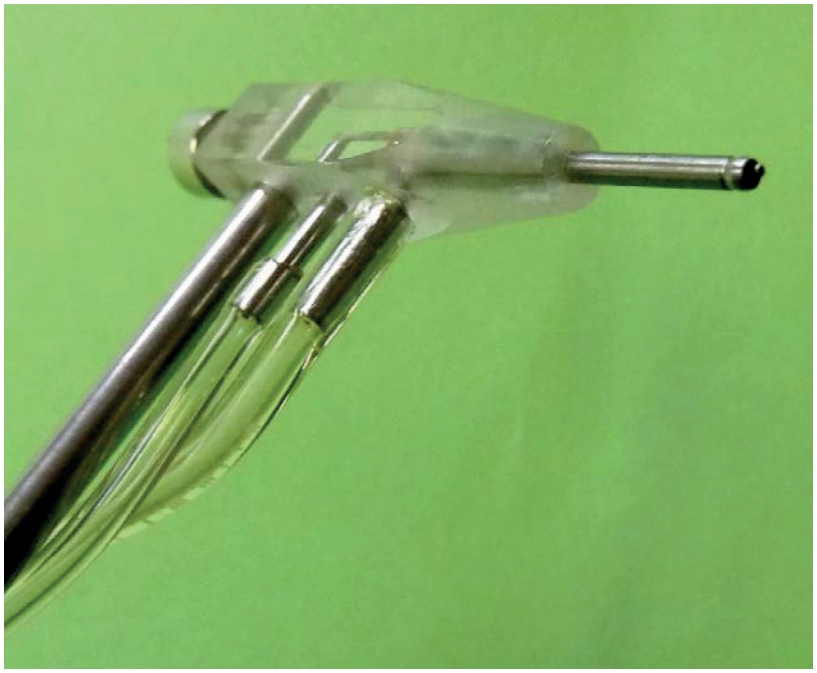

The detailed view of the cannula (below left) shows the extended inner cannula used for pressure transmission to the pressure transducer. The outer cannula has a frontal notch to secure the fixing thread.
The exact dimensions of the cannula are given in Fig. 4.6.4.

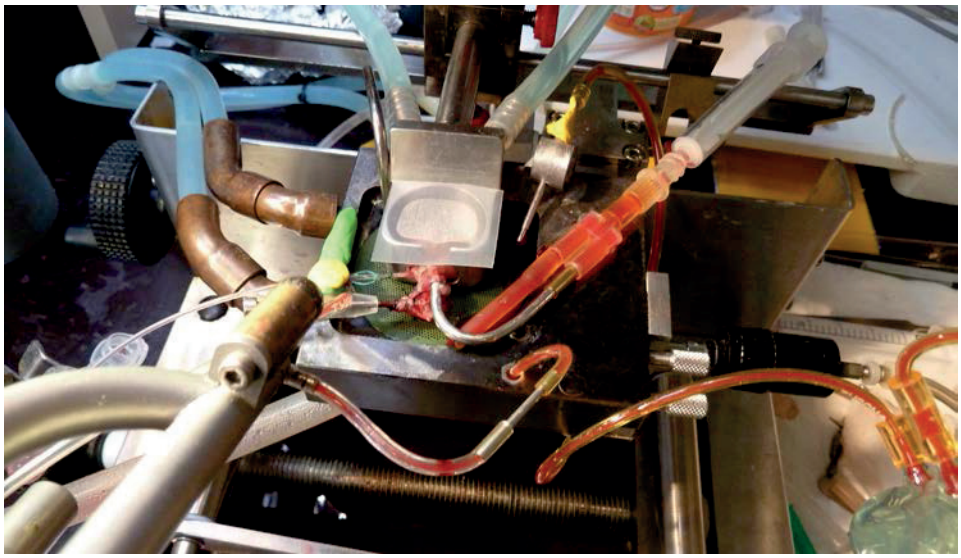

Fig. 15.1.5.: ***Perfused kidney with cannulas in aorta and vena cava and ureteral catheter.*** The venous effluent is drained via the sieve-plate under the kidney tray. The tray itself is covered with Parafilm, and the ureteral catheter is fixed with plasticine. The ureteral catheter on the left leads to the collecting vial. In front, the bypass for arterial pO_2 measurement, on the right the Tygon tube leads to the measuring cell. The black cylinder on the right is the compressor inlet that pneumatically activates the switch bar for venous or arterial pO_2 measurement.

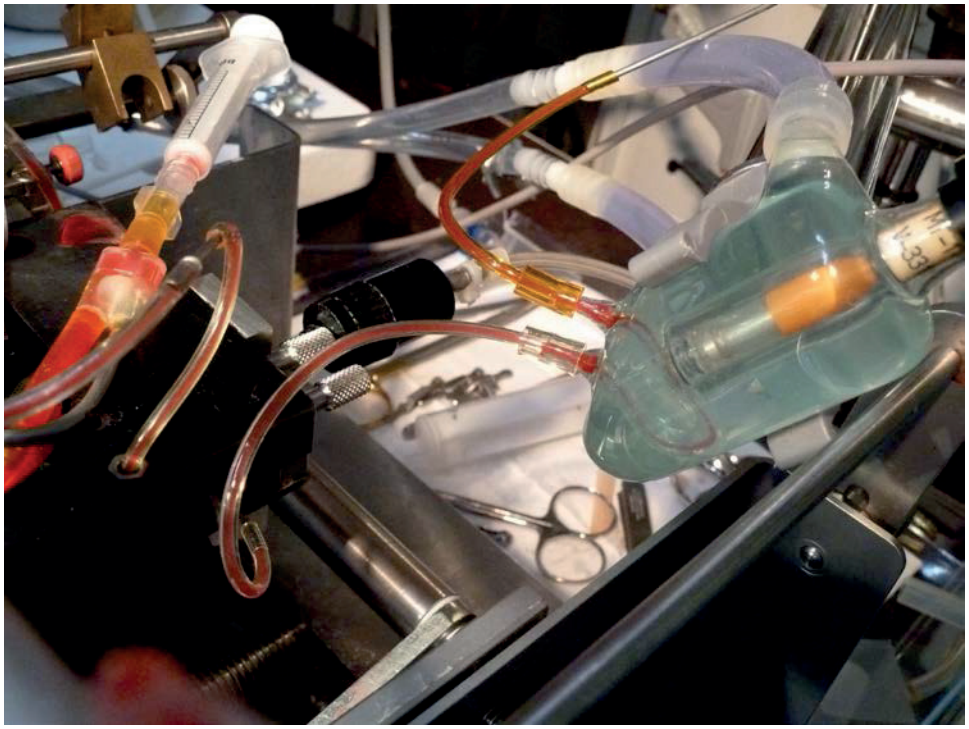

Fig. 15.1.6.: ***Detailed view of the pO_2 probe (Type MT-1-AC, Eschweiler, Kiel) in its cuvette.*** A multiple cuvette for measurement of pO_2, pCO_2 and pH can also be used, but calibration requires considerable effort. Such measurements show that fluctuations in pH and pCO_2 are significantly greater in cell-free perfusate.

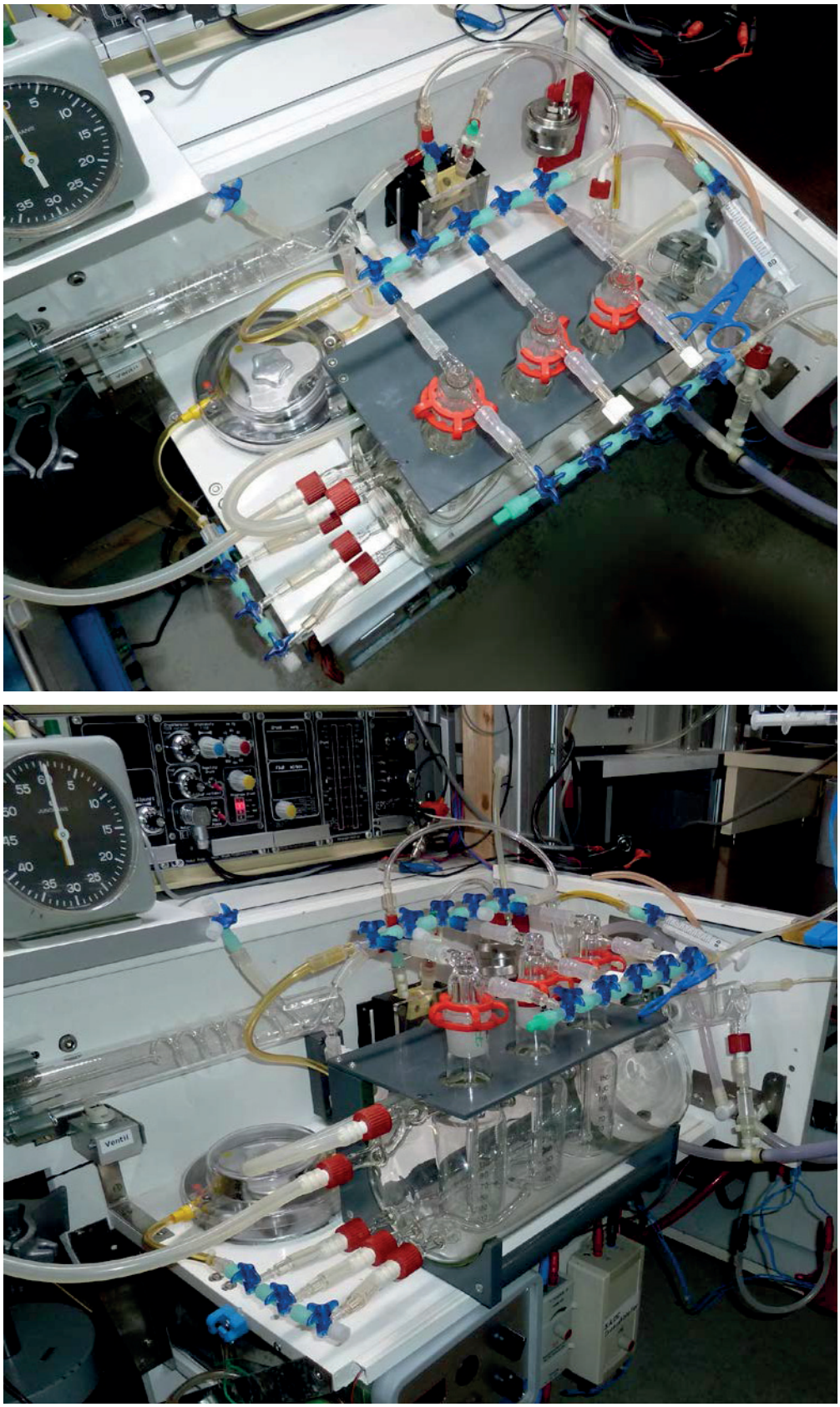

Fig. 15.1.7.a/b.: ***Set-up used for reperfusion of anatomically fixed kidneys.*** A water-jacketed glass container supplies three separate reservoirs, allowing for recirculation and variation of perfusate composition. For rinsing purposes, we use warm NaCl solution delivered via the glass coil on the left.

16. Appendix on the history of renal perfusion 1849–1908

Chronology of the development of perfusion equipment *modified by BD Ross from the work of* ***K. Skutul*** *from the Pharmacology Laboratory of the St. Vladimir University of Kiev* (277)*:* ***Über Durchströmungsapparate. Pflügers Arch 123: 249-273, 1908***

1849 ***Carl Eduard Loebell: De conditionibus quibus secretiones in glandulis. Doctoral dissertation (in Latin), Marburg University*** (153)*. Loebell describes his initial attempts to perfuse the isolated porcine kidney with defibrinated blood and measure urine output, so-called pass-through tests. Particularly noteworthy is his observation that when the bright red arterial blood emerged from the renal vein, it was darker in color and contained more solids, while a completely clear liquid came out of the ureter, which contained considerable amounts of protein (see Ernst Bidder´s commentary on Loebell´s work for remarks on the quality of the Latin).*

1862 ***Ernst Bidder: Doctoral dissertation (in German), Imperial University of Dorpat (modern-day Tartu in Estonia)*** (29)*. Bidder is quite critical of the work of Loebell, but cites the above observation as an important result. Interestingly, Bidder himself noted that at very low urinary flow rates more protein was excreted than at higher flow rates.*

1869 ***Alex Schmidt: In Carl Ludwig´s laboratory in Leipzig.*** *Beginning in 1867, Schmidt improved methodology by heating the defibrinated blood to 36-40°C and by achieving continuous flow through the kidney (Annual Report of the Physiological Institute in Leipzig 1869, p.99).*

1877 ***G. Bunge and O. Schmiedeberg*** (47). *These authors reported the synthesis of hippuric acid, based on 'pass-through' experiments on the isolated canine kidney.*

1885 ***Frey and Gruber*** *constructed an apparatus equipped with an oxygenator (artificial lung) and a pulsatile pump for the circulation of blood.*

1890 ***C. Jacobj introduces his so-called "Haematisator" in Strasbourg****. Designed by Jacobj, this machine used a water-driven two-valve pump and provided for oxygenation of the blood, thus more closely approximating natural circulation.*

1892 ***W. von Sobieranski and C. Jacobj*** *make use of a biological lung as oxygenator, thus avoiding direct contact of the blood with ambient air. Skutul refers to this set-up as a "double Haematisator". Pulsatile perfusion as above.*

1895 ***O. Langendorff in Rostock develops the first successful perfusion apparatus for the heart,*** *the principle of which has hardly changed since. He studied the function of the beating heart and was able to record the contractions. As a pressure source he used a 17.5-liter glass bottle filled with water, and kept the pressure constant by steadily replenishing the water (the gasometer principle).*

1903 ***T. G. Brodie in London described a recirculation apparatus*** *with variable pump and adjustable constant perfusion pressure, and a small recirculation volume. With increasing experience, he later installed filters in the venous and arterial legs of the system, which were retained in the arterial branch (or were "re-discovered") up to modern times. The perfusion of surviving organs. J Physiol 29: 266-275, 1903*

1904 ***Sakusow in St. Petersburg*** *described in his dissertation thesis (in Russian) an improved temperature control with a water-filled glass coil heated in a water bath.*

1904 ***A. Siewert in Kiev*** *(work published in German) perfused isolated hearts with a modified Langendorff apparatus with a temperature-controlled glass coil placed immediately before the heart, enabling him to preheat the perfusate so that the organ reached normothermia. Pflügers Archiv 102: 364-372, 1904.*

1908 ***K. Skutul in Kiev carried out a survey of existing equipment*** *(with the exception of Brodie´s work). After careful study of the defects and deficiencies of his predecessors' designs, he went on to develop his own apparatus.* (277) *(Publication in German).*

Selection of historic graphs, photos

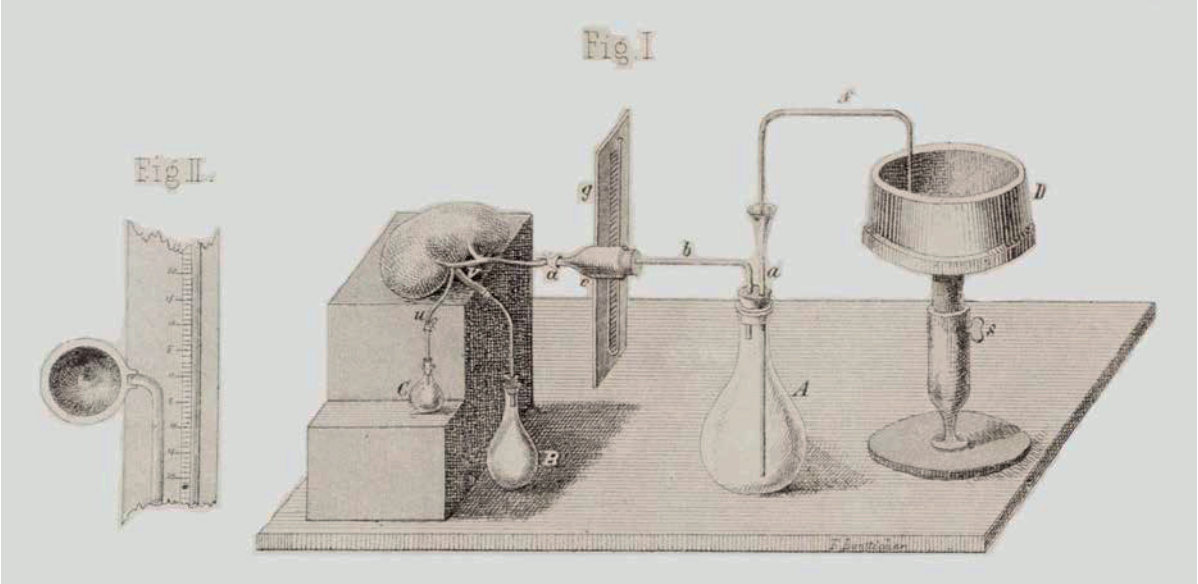

Fig. 16.0.1.: The apparatus used by Ernst Bidder. The illustration is taken from the dissertation (in German) he submitted in 1862 to the Imperial University of Dorpat, now Tartu in Estonia (29).

Jacobj C: XXIII Work from the Laboratory of Experimental Pharmacology at Strasbourg. 78. Apparat zur Durchblutung isolirter Organe. **Archiv f. experimentelle Pathologie u. Pharmakologie Volume XXVI: pp 388-400, 1890.** The journal is now published by Springer Science Publishing as Naunyn-Schmiedeberg's Archives of Pharmacology, and is accessible in digital form (115). Copyright permission of Springer.

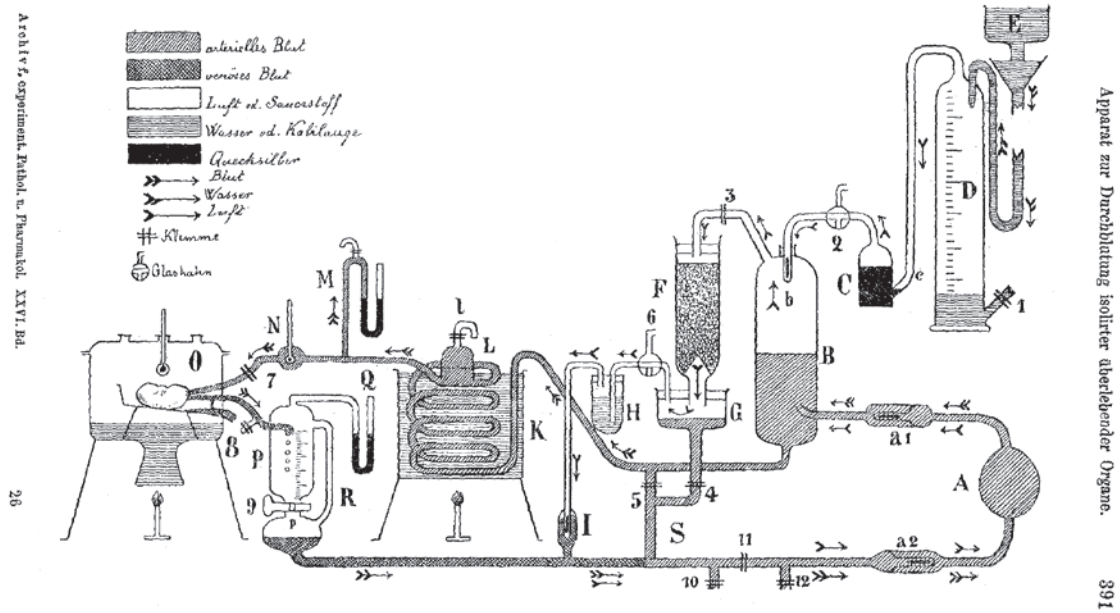

Fig. 16.0.2: ***Diagram of the historical apparatus used for perfusion of the canine kidney by Jacobj at the Pharmacology Institute of the University of Strasbourg.*** It consists of three subsystems for (1) arterial blood, (2) venous blood, and (3) air or oxygen circulation for “arterialization” of blood. On the right is the "artificial heart" (A) a bellows pump with two valves, driven in pulsatile fashion by a rocker powered by a water motor. The total volume of defibrinated blood in reservoir B and the main circuit was 300 ml, and it was compressed and aerated by the oxygen gasometer D. The shunting circuit could be closed at S, and acted as a buffer on the output of the pump. Oxygen, derived from CO_2 by passage through potassium hydroxide solution, was added at I. Temperature control was achieved with the aid of a glass spiral immersed in a water bath (K) which was heated by Bunsen burners, and temperature was monitored at N. Jacobj used the calibrated chamber P to measure the venous flow rate, and mercury-filled U-tubes for pressure measurement. The input oxygen pressure was measured in the cylinder D. The oxygen in the gasometer D was displaced in portions by the inflow of water into E and expelled via a mercury return-valve into the reservoir for arterial blood where it mixed with CO_2. Pure oxygen was mixed with the blood at I, and thus arterialized (F had a defoaming function). The protocols in the study show that the flow rates per minute were quite low at 10-33ml for a dog kidney of 28 g of wet weight. On the other hand, swine kidneys that were obtained directly from the slaughterhouse and had been devoid of perfusion for only 45 min showed significantly higher values, but they exhibited high levels of oxygen consumption, indicating a perfusion deficiency (see Nizet in the 20th century (186)). Two years later, Jacobj, together with von Sobieranski, used a biological lung in the second circuit to overcome the drawbacks of the system described in the 1890 publication.

Jacobj C and v. Sobieranski W: II Scientific work from the Laboratory of Experimental Pharmacology at Strasbourg. 89. Ueber das Functionsvermögen der künstlich durchbluteten Niere. **Archiv für experimentelle Pathologie und Pharmakologie 29: 25-40, 1891. (today: Naunyn-Schmiedeberg´s Archives of Pharmacology)**

In this work the authors complain about the difficulties caused by fluctuations in urban water pressure, and consider how one might overcome this problem.

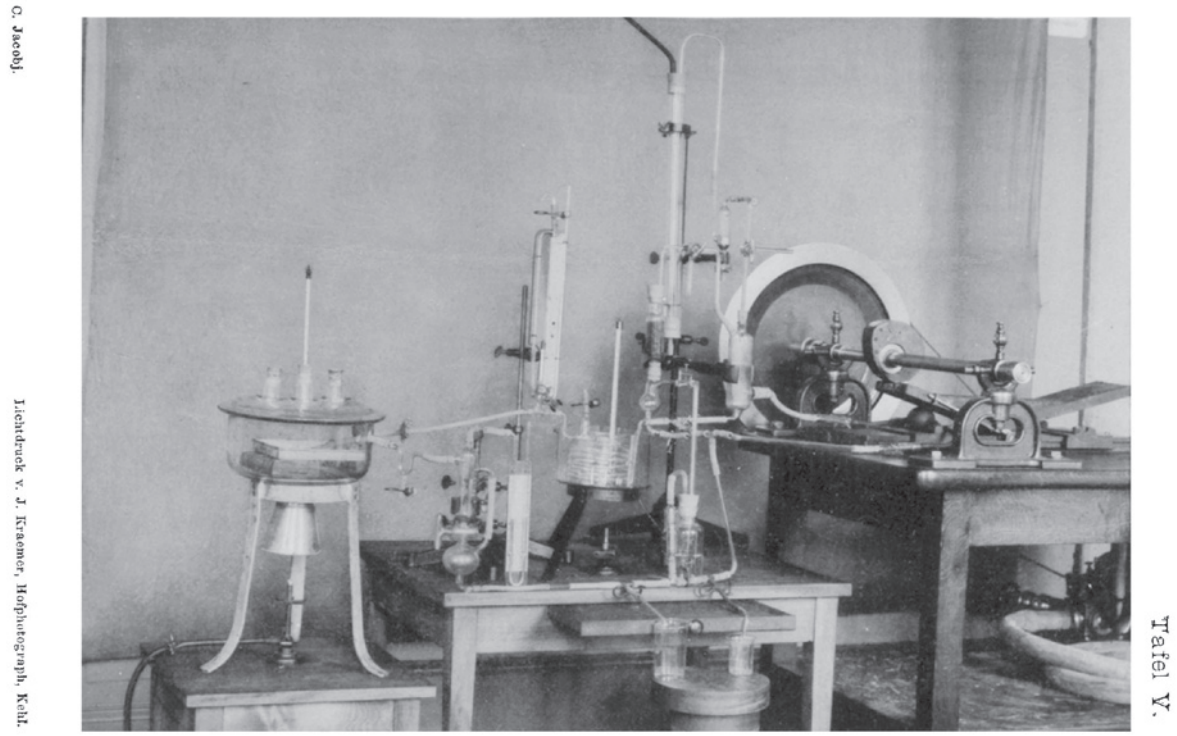

Fig. 16.0.3.: ***C. Jacobj´s 1890 apparatus.*** This picture, taken by a court photographer from the neighboring town of Kehl, shows the elaborate mechanical rocker (on the right) with which the rubber ball (substituting for a ventricle) is compressed via the camshaft. The system was powered by a water-driven motor like those used in many washing machines (which were then cheaper than electrical machines) up to the 1950s. One can also see the two Bunsen burners under the organ chamber (on the left) and the water bath for the glass coil (in the middle). The U-shaped mercury manometers at venous output and arterial inflow can also be seen.

17. References

1. ***Abraham R, Dawson W, and Gangolli SD**. The isolated perfused rat liver in toxicological studies. Naunyn Schmiedebergs Arch Exp Pathol Pharmakol 259: 203, 1968.*
2. ***Abraham R, Dawson W, Grasso P, and Golberg L**. Lysosomal changes associated with hyperoxia in the isolated perfused rat liver. Exp Mol Pathol 8: 370-387, 1968.*
3. ***Adlkofer F, Ramsden DB, Wusteman MC, Pegg DE, and Hoffenberg R**. Metabolism of thyroid hormones by the isolated perfused rabbit kidney. Horm Metab Res 9: 400-403, 1977.*
4. ***Adlkofer F, Schurek HJ, and Soerje H**. The renal clearance of thyroid hormones in the isolated perfused rat kidney. Horm Metab Res 12: 400-404, 1980.*
5. ***Aeikens B**. Untersuchungen über den Kapillaraufbau des Glomerulum und morphometrische Messungen am Glomerulum. Habilitation. Medizinische Hochschule Hannover, 1982.*
6. ***Aeikens B, Eenboom A, and Bohle A**. Untersuchungen zur Struktur des Glomerulum. Virchows Arch A Pathol Anat Histol 381: 283-293, 1979.*
7. ***Alcorn D, Emslie KR, Ross BD, Ryan GB, and Tange JD**. Selective distal nephron damage during isolated kidney perfusion. Kidney Int 19: 638-647, 1981.*
8. ***Aldehni F, Tang T, Madsen K, Plattner M, Schreiber A, Friis UG, Hammond HK, Han PL, and Schweda F**. Stimulation of renin secretion by catecholamines is dependent on adenylyl cyclases 5 and 6. Hypertension 57: 460-468, 2011.*
9. ***Arendshorst WJ, and Gottschalk CW**. Glomerular ultrafiltration dynamics: euvolemic and plasma volume-expanded rats. Am J Physiol 239: F171-F186, 1980.*
10. ***Arendshorst WJ, and Gottschalk CW**. Glomerular ultrafiltration dynamics: historical perspective. Am J Physiol 248: F163-F174, 1985.*
11. ***Assel E**. Polykationeninduzierte Erhöhung der Durchlässigkeit für Albumin ohne morphologische Veränderungen der Fußfortsätze. Untersuchungen mit Protamin an der isoliert perfundierten Rattenniere. Dissertation. Medizinische Hochschule Hannover, 1982.*
12. ***Assel E, Neumann KH, Schurek HJ, Sonnenburg C, and Stolte H**. Glomerular albumin leakage and morphology after neutralization of polyanions. I. Albumin clearance and sieving coefficient in the isolated perfused rat kidney. Ren Physiol 7: 357-364, 1984.*
13. ***Bahlmann J, Giebisch G, Ochwadt B, and Schoeppe W**. Micropuncture study of isolated perfused rat kidney. Am J Physiol 212: 77-82, 1967.*
14. ***Bainbridge FA, and Evans CL**. The heart, lung, kidney preparation. J Physiol 48: 278-286, 1914.*
15. ***Baines AD, Adamson G, Wojciechowski P, Pliura D, Ho P, and Kluger R**. Effect of modifying O_2 diffusivity and delivery on glomerular and tubular function in hypoxic perfused kidney. Am J Physiol 274: F744-F752, 1998.*
16. ***Baines AD, Christoff B, Wicks D, Wiffen D, and Pliura D**. Cross-linked hemoglobin increases fractional reabsorption and GFR in hypoxic isolated perfused rat kidneys. Am J Physiol 269: F628-F636, 1995.*
17. ***Baines AD, and Ross BD**. Nonoxidative glucose metabolism a prerequisite for formation of dilute urine. Am J Physiol 242: F491-F498, 1982.*
18. ***Bastin J, Cambon N, Thompson M, Lowry OH, and Burch HB**. Change in energy reserves in different segments of the nephron during brief ischemia. Kidney Int 31: 1239-1247, 1987.*

19. ***Bauman AW, Clarkson TW, and Miles EM***. *Functional evaluation of isolated perfused rat kidney. J Appl Physiol 18: 1239-1246, 1963.*
20. ***Baumung H, and Peterlik M***. *[On the use of an "artificial kidney" in the perfusion of the isolated rat liver]. Med Pharmacol Exp Int J Exp Med 16: 275-281, 1967.*
21. ***Baylis C, Ichikawa I, Willis WT, Wilson CB, and Brenner BM***. *Dynamics of glomerular ultrafiltration. IX. Effects of plasma protein concentration. Am J Physiol 232: F58-F71, 1977.*
22. ***Bayliss WM***. *On the local reactions of the arterial wall to changes of internal pressure. J Physiol 28: 220-231, 1902.*
23. ***Bekersky I***. *Use of the isolated perfused kidney as a tool in drug disposition studies. Drug Metab Rev 14: 931-960, 1983.*
24. ***Belzer FO, Ashby BS, Huang JS, and Dunphy JE***. *Etiology of rising perfusion pressure in isolated organ perfusion. Ann Surg 168: 382-391, 1968.*
25. ***Bertermann H, Franke H, Huland H, and Weiss C***. *CO_2-production by the isolated perfused rat kidney from ^{14}C-labelled substrates. Res Exp Med (Berl) 161: 1-14, 1973.*
26. ***Besarab A, DeGuzman A, and Swanson JW***. *Effect of albumin and free calcium concentrations on calcium binding in vitro. J Clin Pathol 34: 1361-1367, 1981.*
27. ***Besarab A, Silva P, Landsberg L, and Epstein FH***. *Effect of catecholamines on tubular function in the isolated perfused rat kidney. Am J Physiol 233: F39-F45, 1977.*
28. ***Besarab A, Silva P, Ross B, and Epstein FH***. *Bicarbonate and sodium reabsorption by the isolated perfused kidney. Am J Physiol 228: 1525-1530, 1975.*
29. ***Bidder E***. *Beiträge zur Lehre von der Function der Nieren. Dissertation. Dorpat, today Tartu, Estland: Universität Tartu, 1862.*
30. ***Boesken WH, Mamier A, Neumann H, and Engelhardt R***. *[Proteinuria by fever?] Gibt es die "febrile Proteinurie". Klin Wochenschr 61: 917-922, 1983.*
31. ***Bohrer MP, Deen WM, Robertson CR, and Brenner BM***. *Mechanism of angiotensin II-induced proteinuria in the rat. Am J Physiol 233: F13-F21, 1977.*
32. ***Bowman RH***. *Gluconeogenesis in the isolated perfused rat kidney. J Biol Chem 245: 1604-1612, 1970.*
33. ***Bowman RH***. *The perfused rat kidney. Methods Enzymol 39: 3-11, 1975.*
34. ***Bowman RH, and Maack T***. *Effect of albumin concentration and ADH on H_2O and electrolyte transport in perfused rat kidney. Am J Physiol 226: 426-430, 1974.*
35. ***Bowman RH, and Maack T***. *Glucose transport by the isolated perfused rat kidney. Am J Physiol 222: 1499-1504, 1972.*
36. ***Boyce NW, and Holdsworth SR***. *Glomerular permselectivity in the isolated perfused rat kidney. Am J Physiol 249: F780-F784, 1985.*
37. ***Brandt P***. *Der Elektrolytgehalt im Nierengewebe von intakten und adrenalektomierten Ratten. Untersuchungen an in vivo Nieren und an isoliert perfundierten Nieren. Dissertation. Freie Universität Berlin, 1974, p. 1-85.*
38. ***Brezis M, and Rosen S***. *Hypoxia of the renal medulla - its implications for disease. N Engl J Med 332: 647-655, 1995.*
39. ***Brezis M, Rosen S, Silva P, and Epstein FH***. *Renal ischemia: a new perspective. Kidney Int 26: 375-383, 1984.*
40. ***Brezis M, Rosen S, Silva P, and Epstein FH***. *Transport activity modifies thick ascending limb damage in the isolated perfused kidney. Kidney Int 25: 65-72, 1984.*

41. ***Brezis M, Rosen S, Spokes K, Silva P, and Epstein FH***. *Substrates induce hypoxic injury to medullary thick limbs of isolated rat kidneys. Am J Physiol 251: F710-F717, 1986.*
42. ***Brezis M, Rosen S, Spokes K, Silva P, and Epstein FH***. *Transport-dependent anoxic cell injury in the isolated perfused rat kidney. Am J Pathol 116: 327-341, 1984.*
43. ***Brink HM, Moons WM, and Slegers JF***. *Glomerular filtration in the isolated perfused kidney. I. Sieving of macromolecules. Pflügers Arch 397: 42-47, 1983.*
44. ***Brink HM, Moons WM, and Slegers JF***. *Glomerular filtration in the isolated perfused kidney. II. Glomerular hemodynamics. Pflügers Arch 397: 48-53, 1983.*
45. ***Brink HM, and Slegers JF***. *Instantaneous measurement of glomerular filtration rate in the isolated perfused rat kidney. Pflügers Arch 383: 71-73, 1979.*
46. ***Brull L, and Louis-Bar D***. *Toxicity of artificially circulated heparinized blood on the kidney. Arch Int Physiol Biochim 65: 470-476, 1957.*
47. ***Bunge G, and Schmiedeberg O***. *Über die Bildung der Hippursäure. Archiv für Experimentelle Pathologie & Pharmakologie 6: 233-255, 1876.*
48. ***Castrop H, Schweda F, Mizel D, Huang Y, Briggs J, Kurtz A, and Schnermann J***. *Permissive role of nitric oxide in macula densa control of renin secretion. Am J Physiol Renal Physiol 286: F848-F857, 2004.*
49. ***Cheung K, Hickman PE, Potter JM, Walker NI, Jericho M, Haslam R, and Roberts MS***. *An optimized model for rat liver perfusion studies. J Surg Res 66: 81-89, 1996.*
50. ***Ciarimboli G***. *Role of size, charge and conformation of dissolved molecules and of fixed charges of the filtration barrier in glomerular permselectivity. Dissertation. FB Biologie. Universität Hannover 1999, p. 1-83.*
51. ***Ciarimboli G, Boekenkamp A, Schurek HJ, Fels LM, Kilian I, Maess B, and Stolte H***. *The "fixed" charge of glomerular capillary wall as determinant of permselectivity. Ren Fail 23: 365-376, 2001.*
52. ***Ciarimboli G, Hjalmarsson C, Boekenkamp A, Schurek HJ, and Haraldsson B***. *Dynamic alterations of glomerular charge density in fixed rat kidneys suggest involvement of endothelial cell coat. Am J Physiol Renal Physiol 285: F722-F730, 2003.*
53. ***Ciarimboli G, Schurek HJ, Zeh M, Flohr H, Boekenkamp A, Fels LM, Kilian I, and Stolte H***. *Role of albumin and glomerular capillary wall charge distribution on glomerular permselectivity: studies on the perfused-fixed rat kidney model. Pflügers Arch 438: 883-891, 1999.*
54. ***Cohen JJ***. *Is the function of the renal papilla coupled exclusively to an anaerobic pattern of metabolism? Am J Physiol 236: F423-F433, 1979.*
55. ***Cohen JJ, Gregg CM, Merkens LS, Brand PH, Garza-Quintero R, Pashley DH, and Black AJ***. *Comparison of the oxidation rates of glucose and lactate in relation to support of Na^+ reabsorption. Curr Probl Clin Biochem 8: 418-423, 1977.*
56. ***Cohen JJ, and Kamm DE***. *Renal Metabolism: Relation to Renal Function. In: The Kidney, edited by Brenner BM, and Rector FC, Jr. Philadelphia: WB Saunders, 1981, p. 147, 155-157.*
57. ***Cohen JJ, Kook YJ, and Little JR***. *Substrate-limited function and metabolism of the isolated perfused rat kidney: effects of lactate and glucose. J Physiol 266: 103-121, 1977.*
58. ***Cohen JJ, and Little JR***. *Lactate metabolism in the isolated perfused rat kidney: relations to renal function and gluconeogenesis. J Physiol 255: 399-414, 1976.*
59. ***Cortell S, Davidman M, Gennari FJ, and Schwartz WB***. *Catheter size as a determinant of outflow resistance and intrarenal pressure. Am J Physiol 223: 910-915, 1972.*

60. ***Cowin GJ, Leditschke IA, Crozier S, Brereton IM, and Endre ZH***. *Regional proton nuclear magnetic resonance spectroscopy differentiates cortex and medulla in the isolated perfused rat kidney. MAGMA 5: 151-158, 1997.*
61. ***Cowley AW, Jr., Ryan RP, Kurth T, Skelton MM, Schock-Kusch D, and Gretz N***. *Progression of glomerular filtration rate reduction determined in conscious Dahl salt-sensitive hypertensive rats. Hypertension 62: 85-90, 2013.*
62. ***Czogalla J, Schweda F, and Loffing J***. *The mouse isolated perfused kidney technique. J Vis Exp 2016.*
63. ***De Mello G, and Maack T***. *Nephron function of the isolated perfused rat kidney. Am J Physiol 231: 1699-1707, 1976.*
64. ***de Seigneux S, Nielsen J, Olesen ETB, Dimke H, Kwon TH, Frokiaer J, and Nielsen S***. *Long-term aldosterone treatment induces decreased apical but increased basolateral expression of AQP2 in CCD of rat kidney. Am J Physiol Renal Physiol 293: F87-F99, 2007.*
65. ***Demerath T, Staffel J, Schreiber A, Valletta D, and Schweda F***. *Natriuretic peptides buffer renin-dependent hypertension. Am J Physiol Renal Physiol 306: F1489-F1498, 2014.*
66. ***Döring HJ, and Dehnert H***. *Das isoliert perfundierte Warmblüter-Herz nach Langendorff. Biomesstechnik-Verlag March GmbH, Germany, 1985.*
67. ***Dume T, Koch KM, Krause HH, and Ochwadt B***. *[Critical venous oxygen tension on the erythrocyte-free perfused isolated rat kidney]. Pflügers Arch Gesamte Physiol Menschen Tiere 290: 89-100, 1966.*
68. ***Edwards A, Silldorff EP, and Pallone TL***. *The renal medullary microcirculation. Front Biosci 5: E36-52, 2000.*
69. ***Eisenbach GM, Liew JB, Boylan JW, Manz N, and Muir P***. *Effect of angiotensin on the filtration of protein in the rat kidney: a micropuncture study. Kidney Int 8: 80-87, 1975.*
70. ***Endre ZH, Ratcliffe PJ, Tange JD, Ferguson DJ, Radda GK, and Ledingham JG***. *Erythrocytes alter the pattern of renal hypoxic injury: predominance of proximal tubular injury with moderate hypoxia. Clin Sci (Lond) 76: 19-29, 1989.*
71. ***Epstein FH, Brosnan JT, Tange JD, and Ross BD***. *Improved function with amino acids in the isolated perfused kidney. Am J Physiol 243: F284-F292, 1982.*
72. ***Evans RG, Gardiner BS, Smith DW, and O'Connor PM***. *Intrarenal oxygenation: unique challenges and the biophysical basis of homeostasis. Am J Physiol Renal Physiol 295: F1259-F1270, 2008.*
73. ***Fauler J, Wiemeyer A, Yoshizawa M, Schurek HJ, and Froelich JC***. *Metabolism of cysteinyl leukotrienes by the isolated perfused rat kidney. Prostaglandins 42: 239-249, 1991.*
74. ***Felts JM, and Whayne TF, Jr.*** *A small oxygenator for use with an organ perfusion system. IEEE Trans Biomed Eng 20: 382-384, 1973.*
75. ***Ferguson DC, and Jennings AS***. *Regulation of conversion of thyroxine to triiodothyronine in perfused rat kidney. Am J Physiol 245: E220-E229, 1983.*
76. ***Fisher MM, and Kerly M***. *Amino acid metabolism in the perfused rat liver. J Physiol 174: 273-294, 1964.*
77. ***Flemming B, Arenz N, Seeliger E, Wronski T, Steer K, and Persson PB***. *Time-dependent autoregulation of renal blood flow in conscious rats. J Am Soc Nephrol 12: 2253-2262, 2001.*

78. ***Flohr H**. Die Bedeutung der negativen Ladungen in der glomerulären Basalmembran für die Proteinurie. Untersuchungen an dem neu etablierten Modell der reperfundierten, isolierten und anatomisch fixierten Rattenniere. Dissertation. Medizinische Hochschule Hannover, 1990, p. 1-77.*

79. ***Folkman J, Winsey S, Cole P, and Hodes R**. Isolated perfusion of thymus. Exp Cell Res 53: 205-214, 1968.*

80. ***Franke H, Gronow G, and Petersen K**. Glucagon induced functional changes of isolated perfused rat kidney. Curr Probl Clin Biochem 8: 424-434, 1977.*

81. ***Franke H, Huland H, Weiss C, and Unsicker K**. Improved net sodium transport of the isolated rat kidney. Z Gesamte Exp Med 156: 268-282, 1971.*

82. ***Franke H, Malyusz M, and Runge D**. Improved sodium and PAH transport in the isolated fluorocarbon-perfused rat kidney. Nephron 22: 423-431, 1978.*

83. ***Franke H, Malyusz M, and Weiss C**. Substrate oxidation and inhibition of sodium transport in the isolated perfused rat kidney. Curr Probl Clin Biochem 4: 169-174, 1975.*

84. ***Franke H, Sobotta EE, Witzki G, and Unsicker K**. [Function and morphology of isolated rat kidney following cellfree perfusion with various plasmaexpanders (author's transl)]. Anaesthesist 24: 231-238, 1975.*

84b. ***Fülgraff G, Greven J, Meiforth A und Osswald H.** Hydrostatische Drucke in proximalen und distalen Kopnvoluten und in peritubulären Capillaren von Rattennieren nach Furosemid und Acetazolamid. Naunyn-Schmiedebergs Arch. Pharmak. 264: 76-85, 1969.*

85. ***Garsen M, Rops AL, Rabelink TJ, Berden JH, and van der Vlag J**. The role of heparanase and the endothelial glycocalyx in the development of proteinuria. Nephrol Dial Transplant 29: 49-55, 2014.*

86. ***Gertz KH, Mangos JA, Braun G, and Pagel HD**. Pressure in the glomerular capillaries of the rat kidney and its relation to arterial blood pressure. Pflügers Arch Gesamte Physiol Menschen Tiere 288: 369-374, 1966.*

87. ***Godecke A, Decking UK, Ding Z, Hirchenhain J, Bidmon HJ, Godecke S, and Schrader J**. Coronary hemodynamics in endothelial NO synthase knockout mice. Circ Res 82: 186-194, 1998.*

88. ***Green R, Windhager EE, and Giebisch G**. Protein oncotic pressure effects on proximal tubular fluid movement in the rat. Am J Physiol 226: 265-276, 1974.*

89. ***Grosse-Siestrup C, Unger V, Fehrenberg C, Baeyer H, Fischer A, Schaper F, and Groneberg DA**. A model of isolated autologously hemoperfused porcine slaughterhouse kidneys. Nephron 92: 414-421, 2002.*

90. ***Grosse-Siestrup C, Unger V, Meissler M, Nagel S, Wussow A, Peiser C, Fischer A, Schmitt R, and Groneberg DA**. Hemoperfused isolated porcine slaughterhouse kidneys as a valid model for pharmacological studies. J Pharm Sci 92: 1147-1154, 2003.*

91. ***Gruenberger C, Obermayer B, Klar J, Kurtz A, and Schweda F**. The calcium paradoxon of renin release: calcium suppresses renin exocytosis by inhibition of calcium-dependent adenylate cyclases AC5 and AC6. Circ Res 99: 1197-1206, 2006.*

92. ***Guan Z, Gobe G, Willgoss D, and Endre ZH**. Renal endothelial dysfunction and impaired autoregulation after ischemia-reperfusion injury result from excess nitric oxide. Am J Physiol Renal Physiol 291: F619-F628, 2006.*

93. ***Guan Z, Willgoss DA, Matthias A, Manley SW, Crozier S, Gobe G, and Endre ZH**. Facilitation of renal autoregulation by angiotensin II is mediated through modulation of nitric oxide. Acta Physiol Scand 179: 189-201, 2003.*

94. ***Gutsche HU, Holstein-Rathlou NH, and Leyssac PP***. *Oscillating tubulo-glomerular feedback, proximal hydrostatic pressure fluctuations in relation to early distal salt concentration. Unpublished results, 1988.*
95. ***Gutsche HU, Mueller-Suur R, Hegel U, and Hierholzer K***. *Electrical conductivity of tubular fluid of the rat nephron. Micropuncture study of the diluting segment in situ. Pflügers Arch 383: 113-121, 1980.*
96. ***Hamilton RL, Berry MN, Williams MC, and Severinghaus EM***. *A simple and inexpensive membrane "lung" for small organ perfusion. J Lipid Res 15: 182-186, 1974.*
97. ***Haraldsson B, Nystrom J, and Deen WM***. *Properties of the glomerular barrier and mechanisms of proteinuria. Physiol Rev 88: 451-487, 2008.*
98. ***Haraldsson BS, Johnsson EK, and Rippe B***. *Glomerular permselectivity is dependent on adequate serum concentrations of orosomucoid. Kidney Int 41: 310-316, 1992.*
99. ***Hartwig M***. *Zur Konversion von Thyroxin zu Trijodthyronin an der isoliert perfundierten Rattenniere mit Bestimmung des freien Thyroxins durch Equilibriumsdialyse. Dissertation. Medizinische Hochschule Hannover, 1988, p. 1-52.*
100. ***Harvey AM, and Malvin RL***. *Comparison of creatinine and inulin clearances in male and female rats. Am J Physiol 209: 849-852, 1965.*
101. ***Hautmann M, Friis UG, Desch M, Todorov V, Castrop H, Segerer F, Otto C, Schutz G, and Schweda F***. *Pituitary adenylate cyclase-activating polypeptide stimulates renin secretion via activation of PAC1 receptors. J Am Soc Nephrol 18: 1150-1156, 2007.*
102. ***Hemingway A***. *A comparison of methods used for oxygenating blood in perfusion experiments. J Physiol 72: 344-348, 1931.*
103. ***Hemingway A***. *Some observations on the perfusion of the isolated kidney by a pump. J Physiol 71: 201-213, 1931.*
104. ***Hemmingsen L, and Skaarup P***. *Urinary excretion of ten plasma proteins in patients with febrile diseases. Acta Med Scand 201: 359-364, 1977.*
105. ***Hems R, Ross BD, Berry MN, and Krebs HA***. *Gluconeogenesis in the perfused rat liver. Biochem J 101: 284-292, 1966.*
106. ***Heringlake M, Wagner K, Schumacher J, and Pagel H***. *Urinary excretion of urodilatin is increased during pressure natriuresis in the isolated perfused rat kidney. Am J Physiol 277: F347-F351, 1999.*
107. ***Hierholzer K, Lichtenstein I, Siebe H, Tsiakiras D, and Witt I***. *Renal metabolism of corticosteroid hormones. Klin Wochenschr 60: 1127-1135, 1982.*
108. ***Hierholzer K, Schoneshofer M, Siebe H, Tsiakiras D, and Weskamp P***. *Corticosteroid metabolism in isolated rat kidney in vitro. I. Formation of lipid soluble metabolites from corticosterone (B) in renal tissue from male rats.*
Pflügers Arch 400: 363-371, 1984.
109. ***Hilbrands LB, Artz MA, Wetzels JF, and Koene RA***. *Cimetidine improves the reliability of creatinine as a marker of glomerular filtration. Kidney Int 40: 1171-1176, 1991.*
110. ***Hochel J, Lehmann D, Fehrenberg C, Unger V, Groneberg DA, and Grosse-Siestrup C***. *Effects of different perfusates on functional parameters of isolated perfused dog kidneys. Nephrol Dial Transplant 18: 1748-1754, 2003.*
111. ***Hoecherl K, Gerl M, and Schweda F***. *Proteinase-activated receptors 1 and 2 exert opposite effects on renal renin release. Hypertension 58: 611-618, 2011.*
112. ***Hoeltzenbein J***. *Die künstliche Niere. Ferdinand Enke Verlag, Stuttgart, 1969.*
113. ***Holstein-Rathlou NH***. *Synchronization of proximal intratubular pressure oscillations: evidence for interaction between nephrons. Pflügers Arch 408: 438-443, 1987.*

114. ***Holstein-Rathlou NH, and Leyssac PP***. *TGF-mediated oscillations in the proximal intratubular pressure: differences between spontaneously hypertensive rats and Wistar-Kyoto rats. Acta Physiol Scand 126: 333-339, 1986.*
115. ***Jacobj C***. *Apparat zur Durchblutung isolirter überlebender Organe. Archiv für Experimentelle Pathologie & Pharmakologie 26: 388-400, 1890. now: Naunyn-Schmiedeberg´s Archives of Pharmacology.*
116. ***Jesinghaus WP***. *Zum Einfluß von Cyclosporin A auf die Anpassungshypertrophie nach unilateraler Nephrektomie. Dissertation. Medizinische Hochschule Hannover, 1987.*
117. ***Johns O***. *Oszillierende Sauerstoffpartialdrücke in der Nierenrinde. Ausdruck einer durch den tubuloglomerulären Feedback Mechanismus geregelten Nephron-funktion? Dissertation. Medizinische Hochschule Hannover, 1994.*
118. ***Johnson V, and Maack T***. *Renal extraction, filtration, absorption, and catabolism of growth hormone. Am J Physiol 233: F185-F196, 1977.*
119. ***Kaczmarczyk G, Goepel M, and Reinhardt HW***. *[Arterial blood-gas in Wistar rats during barbiturate and halothane long term anesthesia in normothermia]. Pflügers Arch 332: Suppl, 1972.*
120. ***Kaczmarczyk G, and Reinhardt HW***. *Arterial blood gas tensions and acid-base status of Wistar rats during thiopental and halothane anesthesia. Lab Anim Sci 25: 184-190, 1975.*
121. ***Karakashian A, Timmer RT, Klein JD, Gunn RB, Sands JM, and Bagnasco SM***. *Cloning and characterization of two new isoforms of the rat kidney urea transporter: UT-A3 and UT-A4. J Am Soc Nephrol 10: 230-237, 1999.*
122. ***Kellner C***. *Morphometrische Untersuchungen corticaler Glomerula an Rattennieren zur Bestimmung der glomerulären effektiven hydraulischen Permeabilität. Dissertation. Medizinische Hochschule Hannover, 1986.*
123. ***Kinter WB, and Pappenheimer JR***. *Role of red blood corpuscles in regulation of renal blood flow and glomerular filtration rate. Am J Physiol 185: 399-406, 1956.*
124. ***Kleinzeller A, Malek J, Longmuir I, Kovac L, Cerkasov J, Chaloupka J, Kotyk A, and Burger M***. *Manometrische Methoden und ihre Anwendung in der Biologie und Biochemie. VEB Gustav Fischer Verlag Jena (deutsch) & Tschechoslowakischer Verlag für Medizinische Literatur Prag (Original tschechisch), 1965.*
125. ***Klokkers J***. *Atriales natriuretisches Peptid und Stickstoffmonoxid antagonisieren die durch Vasopressin erhöhte Wasserpermeabilität in innermedullären Sammelrohr-zellen. Dissertation. FB Biologie. WWU Münster , 2010, p. 1-141.*
126. ***Kohan DE, Rossi NF, Inscho EW, and Pollock DM***. *Regulation of blood pressure and salt homeostasis by endothelin. Physiol Rev 91: 1-77, 2011.*
127. ***Kokko JP, and Rector FC, Jr.*** *Countercurrent multiplication system without active transport in inner medulla. Kidney Int 2: 214-223, 1972.*
128. ***Koury ST, Bondurant MC, and Koury MJ***. *Localization of erythropoietin synthesizing cells in murine kidneys by in situ hybridization. Blood 71: 524-527, 1988.*
129. ***Koury ST, Bondurant MC, Koury MJ, and Semenza GL***. *Localization of cells producing erythropoietin in murine liver by in situ hybridization. Blood 77: 2497-2503, 1991.*
130. ***Krause I***. *Der Einfluss von Succinat auf die Natriumresorption und den Metabolismus der isoliert perfundierten Rattenniere. Dissertation. Freie Universität Berlin, 1984, p. 1-45.*
131. ***Kriz W***. *Structural organization of renal medullary circulation. Nephron 31: 290-295, 1982.*

132. ***Kriz W***. *Structural organization of the renal medulla: comparative and functional aspects. Am J Physiol 241: R3-16, 1981.*
133. ***Kuehnle HF, von Dahl K, and Schmidt FH***. *Fully enzymatic inulin determination in small volume samples without deproteinization. Nephron 62: 104-107, 1992.*
134. ***Kurtz A, Eckardt KE, Tannahill L, and Bauer C***. *Regulation of erythropoietin production. Contrib Nephrol 66: 1-16, 1988.*
135. ***Kurtz A, Götz KH, Hamann M, and Sandner P***. *Mode of nitric oxide action on the renal vasculature. Acta Physiol Scand 168: 41-45, 2000.*
136. ***Kurtz A, Schurek HJ, Jelkmann W, Muff R, Lipp HP, Heckmann U, Eckardt KU, Scholz H, Fischer JA, and Bauer C***. *Renal mesangium is a target for calcitonin gene-related peptide. Kidney Int 36: 222-227, 1989.*
137. ***Kurtz A, and Schweda F***. *Osmolarity-induced renin secretion from kidneys: evidence for readily releasable renin pools. Am J Physiol Renal Physiol 290: F797-F805, 2006.*
138. ***Kurtz L, Schweda F, de Wit C, Kriz W, Witzgall R, Warth R, Sauter A, Kurtz A, and Wagner C***. *Lack of connexin 40 causes displacement of renin-producing cells from afferent arterioles to the extraglomerular mesangium. J Am Soc Nephrol 18: 1103-1111, 2007.*
139. ***Lacombe C, Da Silva JL, Bruneval P, Fournier JG, Wendling F, Casadevall N, Camilleri JP, Bariety J, Varet B, and Tambourin P***. *Peritubular cells are the site of erythropoietin synthesis in the murine hypoxic kidney. J Clin Invest 81: 620-623, 1988.*
140. ***Landis E, and Pappenheimer JR***. *Circulation: Exchange of substances through capillary walls. In: Handbook of Physiology, edited by WF H, and P D. Washington D.C.: American Physiological Society, 1963, p. 961-1034.*
141. ***Landis EM***. *The capillary pressure in frog mesentery as determined by microinjection methods. Am J Physiol 75: 548-570, 1926.*
142. ***Leichtweiss HP, Lübbers DW, Weiss C, Baumgärtl H, and Reschke W***. *The oxygen supply of the rat kidney: measurements of intrarenal pO_2. Pflügers Arch 309: 328-349, 1969.*
143. ***Leyssac PP, and Baumbach L***. *An oscillating intratubular pressure response to alterations in Henle loop flow in the rat kidney. Acta Physiol Scand 117: 415-419, 1983.*
144. ***Lieberthal W***. *Stroma-free hemoglobin: a potential blood substitute. J Lab Clin Med 126: 231-232, 1995.*
145. ***Lieberthal W, Stephens GW, Wolf EF, Rennke HG, Vasilevsky ML, Valeri CR, and Levinsky NG***. *Effect of erythrocytes on the function and morphology of the isolated perfused rat kidney. Ren Physiol 10: 14-24, 1987.*
146. ***Lieberthal W, Vasilevsky ML, Valeri CR, and Levinsky NG***. *Interactions between ADH and prostaglandins in isolated erythrocyte-perfused rat kidney. Am J Physiol 252: F331-F337, 1987.*
147. ***Lieberthal W, Wolf EF, Merrill EW, Levinsky NG, and Valeri CR***. *Hemodynamic effects of different preparations of stroma free hemolysates in the isolated perfused rat kidney. Life Sci 41: 2525-2533, 1987.*
148. ***Lilienfein H***. *Die Wirkung des Sauerstoffträgers MP4 auf die Nekrosebildung im Hautlappenmodell an SKH-1/hr haarlosen Mäusen. Dissertation. Ruhr-Universität Bochum, 2011, p. 1-98.*
149. ***Lindemann B***. *Hans Ussing, experiments and models. J Membr Biol 184: 203-210, 2001.*
150. ***Lippman RW***. *Mechanism of proteinuria; effect of parenteral bovine albumin injections on hemoglobin excretion in rats. Am J Physiol 154: 532-536, 1948.*

151. ***Lippman RW**. Mechanism of proteinuria; identity of urinary proteins in the rat following parenteral protein injection. Proc Soc Exp Biol Med 71: 546-549, 1949.*
152. ***Little JR, and Cohen JJ**. Effect of albumin concentration on function of isolated perfused rat kidney. Am J Physiol 226: 512-517, 1974.*
153. ***Loebell CE**. De conditionibus quibus secretiones in glandulis perficiuntur. Dissertation. Universität Marburg, 1849.*
154. ***Lohfert H, Lichtenstein I, Butz M, and Hierholzer K**. Continuous measurement of renal intratubular pressures with a combined pressure transducer microperfusion system. Pflügers Arch 327: 191-202, 1971.*
155. ***Lopez MJ, Wong SK, Kishimoto I, Dubois S, Mach V, Friesen J, Garbers DL, and Beuve A**. Salt-resistant hypertension in mice lacking the guanylyl cyclase-A receptor for atrial natriuretic peptide. Nature 378: 65-68, 1995.*
156. ***Lorenz JN, and Gruenstein E**. A simple, nonradioactive method for evaluating single-nephron filtration rate using FITC-inulin. Am J Physiol 276: F172-F177, 1999.*
157. ***Loutzenhiser R, Horton C, and Epstein M**. Flow-induced errors in estimating perfusion pressure of the isolated rat kidney. Kidney Int 22: 693-696, 1982.*
158. ***Lustenberger N, Schindhelm K, Nordmeyer C, Schurek HJ, and Stolte H**. Renal handling of middle molecules in uremic patients and in the isolated rat kidney. Artif Organs 4 Suppl: 110-114, 1981.*
159. ***Lutz J**. Druckkonstante Perfusion von Teilkreisläufen mittels einer druckgesteuerten Rollenpumpe mit analoger Durchströmungsregistrierung. Pflügers Arch 333: 1289, 1972.*
160. ***Lutz J**. Eine linearproportionale regelbare Dauerinfusionspumpe zur stetig abstufbaren Applikation von Pharmaka. Naunyn Schmiedebergs Arch Pharmacol 275: 24-30, 1972.*
161. ***Lutz J, and Henrich H**. [Vascular contractions in situ during constant pressure and flow perfusion of the intestinal vascular system and their dependence upon the initial pressure]. Pflügers Arch 319: 68-81, 1970.*
162. ***Maack T**. Physiological evaluation of the isolated perfused rat kidney. Am J Physiol 238: F71-F78, 1980.*
163. ***Maack T**. Renal clearance and isolated kidney perfusion techniques. Kidney Int 30: 142-151, 1986.*
164. ***Maack T**. Renal handling of low molecular weight proteins. Am J Med 58: 57-64, 1975.*
165. ***Maack T, and Kau ST**. Renal handling of parathyroid hormone. Contrib Nephrol 20: 103-113, 1980.*
166. ***Marcus AJ, Broekman MJ, Drosopoulos JH, Islam N, Alyonycheva TN, Safier LB, Hajjar KA, Posnett DN, Schoenborn MA, Schooley KA, Gayle RB, and Maliszewski CR**. The endothelial cell ecto-ADPase responsible for inhibition of platelet function is CD39. J Clin Invest 99: 1351-1360, 1997.*
167. ***Mathar I, Vennekens R, Meissner M, Kees F, Van der Mieren G, Camacho Londono JE, Uhl S, Voets T, Hummel B, van den Bergh A, Herijgers P, Nilius B, Flockerzi V, Schweda F, and Freichel M**. Increased catecholamine secretion contributes to hypertension in TRPM4-deficient mice. J Clin Invest 120: 3267-3279, 2010.*
168. ***Maude DL, Handelsman DG, Babu M, and Gordon EE**. Handling of insulin by the isolated perfused rat kidney. Am J Physiol 240: F288-F294, 1981.*
169. **Mayes PA, and Felts JM**. *Liver function studied by liver perfusion. Proc. European Soc. Study of Drug Toxicity 7: 16-29, 1966 (Amsterdam).*

170. ***Mehta D, Ravindran K, and Kuebler WM**. Novel regulators of endothelial barrier function. Am J Physiol Lung Cell Mol Physiol 307: L924-935, 2014.*
171. ***Meier W**. Untersuchungen zum Parathormon-Abbau an der isoliert perfundierten Rattenniere. Dissertation. Medizinische Hochschule Hannover, 1981, p. 1-67.*
172. ***Michels L, and Harvey R**. Effects of perfusate viscosity on the perfused rat kidney. Microvasc Res 12: 169-175, 1976.*
173. ***Miki M, Tamai H, Mino M, Yamamoto Y, and Niki E**. Free-radical chain oxidation of rat red blood cells by molecular oxygen and its inhibition by alpha-tocopherol. Arch Biochem Biophys 258: 373-380, 1987.*
174. ***Miller LL, Bly CG, Watson ML, and Bale WF**. The dominant role of the liver in plasma protein synthesis; a direct study of the isolated perfused rat liver with the aid of lysine-epsilon-^{14}C. J Exp Med 94: 431-453, 1951.*
175. ***Mueller-Suur R, Gutsche HU, and Schurek HJ**. Acute and reversible inhibition of tubuloglomerular feedback mediated afferent vasoconstriction by the calcium-antagonist verapamil. Curr Probl Clin Biochem 6: 291-298, 1976.*
176. ***Nagel W, Wolff G, Gigon JP, and Enderlin F**. [On determination of inulin clearance in the presence of dextran]. Klin Wochenschr 45: 137-140, 1967.*
177. ***Nakane H, Nakane Y, Reach G, Corvol P, and Menard J**. Aldosterone metabolism in isolated perfused rat kidney. Am J Physiol 234: E472-E479, 1978.*
178. ***Nawata CM, Evans KK, Dantzler WH, and Pannabecker TL**. Transepithelial water and urea permeabilities of isolated perfused Munich-Wistar rat inner medullary thin limbs of Henle's loop. Am J Physiol Renal Physiol 306: F123-F129, 2014.*
179. ***Neher E, and Sakmann B**. The patch clamp technique. Sci Am 266: 44-51, 1992.*
180. ***Neher E, and Sakmann B**. Single-channel currents recorded from membrane of denervated frog muscle fibres. Nature 260: 799-802, 1976.*
181. ***Neumann KH**. Untersuchungen zur Pathophysiologie der glomerulären Wasserpermeabilität. Habilitation. Medizinische Hochschule Hannover, 1984.*
182. ***Neumann KH, Kellner C, Kühn KW, Stolte H, and Schurek HJ**. Age-dependent thickening of glomerular basement membrane has no major effect on glomerular hydraulic conductivity. Nephrol Dial Transplant 19: 805-811, 2004.*
183. ***Neumann KH, and Rector FC, Jr.** Mechanism of NaCl and water reabsorption in the proximal convoluted tubule of rat kidney. J Clin Invest 58: 1110-1118, 1976.*
184. ***Neumann KH, Schurek HJ, Kellner C, Kühn KW, and Aeikens B**. Effective hydraulic permeability of the glomerular capillary wall in rats after uninephrectomy. Ren Physiol 9: 270-278, 1986.*
185. ***Nishiitsutsuji-Uwo JM, Ross BD, and Krebs HA**. Metabolic activities of the isolated perfused rat kidney. Biochem J 103: 852-862, 1967.*
186. ***Nizet A**. The isolated perfused kidney: possibilities, limitations and results. Kidney Int 7: 1-11, 1975.*
187. ***Nizet A, and Cuypers Y**. [Extraction of two fractions with vasoconstrictor actions on the kidneys by partition of erythrocytes]. Arch Int Physiol Biochim 65: 642-647, 1957.*
188. ***Nizet A, Cuypers Y, Deetjen P, and Kramer K**. Functional capacity of the isolated perfused dog kidney. Pflügers Arch 296: 179-195, 1967.*
189. ***Nizet A, Cuypers Y, Massillon L, and Lambert S**. [Demonstration of factors reducing renal blood flow liberated by erythrocytes]. Arch Int Physiol Biochim 65: 568-588, 1957.*
190. ***Nordsletten DA, Blackett S, Bentley MD, Ritman EL, and Smith NP**. Structural morphology of renal vasculature. Am J Physiol Heart Circ Physiol 291: H296-H309, 2006.*

191. ***O´Connor P, Anderson W, Kett M, and Evans R***. *Renal preglomerular arterial-venous O_2 shunting is a structural defence mechanism of the renal cortex. Clin Exp Pharmacol Physiol 33: 637-641, 2006.*
192. ***Oppermann M, Gess B, Schweda F, and Castrop H***. *Atrap deficiency increases arterial blood pressure and plasma volume. J Am Soc Nephrol 21: 468-477, 2010.*
193. ***Pagel H***. *Zum glomerulären Mechanismus der renalen Proteinausscheidung. Dissertation. FB Biologie. Universität Hannover, 1986, p. 1-106.*
194. ***Pagel H, and Stolte H***. *On the glomerular mechanism of the renal protein excretion. Studies in the isolated perfused rat kidney. Ren Physiol Biochem 15: 249-256, 1992.*
195. ***Pappenheimer JR, and Kinter WB***. *Hematocrit ratio of blood within mammalian kidney and its significance for renal hemodynamics. Am J Physiol 185: 377-390, 1956.*
196. ***Pegg DE, and Farrant J***. *Vascular resistance and edema in the isolated rabbit kidney perfused with a cell-free solution. Cryobiology 6: 200-210, 1969.*
197. ***Pegg DE, and Green CJ***. *Renal preservation by hypothermic perfusion. I. The importance of pressure-control. Cryobiology 10: 56-66, 1973.*
198. ***Pegg DE, and Green CJ***. *Renal preservation by hypothermic perfusion. III. The lack of influence of pulsatile flow. Cryobiology 13: 161-167, 1976.*
199. ***Pegg DE, and Green CJ***. *Renal preservation by hypothermic perfusion. IV. The use of gelatin polypeptides as the sole colloid. Cryobiology 15: 27-34, 1978.*
200. ***Pegg DE, Green CJ, and Foreman J***. *Renal preservation by hypothermic perfusion. II. The influence of oxygenator design and oxygen tension. Cryobiology 11: 238-247, 1974.*
201. ***Persson AEG, Mueller-Suur R, and Selen G***. *Capillary oncotic pressure as a modifier for tubuloglomerular feedback. Am J Physiol 236: F97-102, 1979.*
202. ***Persson AEG, Schnermann J, and Wright FS***. *Modification of feedback influence on glomerular filtration rate by acute isotonic extracellular volume expansion. Pflügers Arch 381: 99-105, 1979.*
203. ***Peters T J***. *All about Albumin. Academic Press Elseviers, 1995.*
204. ***Pries AR, Secomb TW, and Gaehtgens P***. *The endothelial surface layer. Pflügers Arch 440: 653-666, 2000.*
205. ***Rabkin R, and Kitabchi AE***. *Factors influencing the handling of insulin by the isolated rat kidney. J Clin Invest 62: 169-175, 1978.*
206. ***Radermacher J, Klanke B, Kastner S, Haake G, Schurek HJ, Stolte HF, and Froelich JC***. *Effect of arginine depletion on glomerular and tubular kidney function: studies in isolated perfused rat kidneys. Am J Physiol 261: F779-F786, 1991.*
207. ***Radermacher J, Klanke B, Schurek HJ, Stolte HF, and Froelich JC***. *Importance of NO/EDRF for glomerular and tubular function: studies in the isolated perfused rat kidney. Kidney Int 41: 1549-1559, 1992.*
208. ***Rahbar E, Cardenas JC, Baimukanova G, Usadi B, Bruhn R, Pati S, Ostrowski SR, Johansson PI, Holcomb JB, and Wade CE***. *Endothelial glycocalyx shedding and vascular permeability in severely injured trauma patients. J Transl Med 13: 117, 2015.*
209. ***Rahgozar M, Guan Z, Matthias A, Gobe GC, and Endre ZH***. *Angiotensin II facilitates autoregulation in the perfused mouse kidney: An optimized in vitro model for assessment of renal vascular and tubular function. Nephrology (Carlton) 9: 288-296, 2004.*
210. ***Reale E, and Luciano L***. *The laminae rarae of the glomerular basement membrane. Their manifestation depends on the histochemical and histological techniques. Contrib Nephrol 80: 32-40, 1990.*

211. ***Reale E, Luciano L, and Kühn KW***. *Cationic dyes reveal proteoglycans on the surface of epithelial and endothelial kidney cells. Histochemistry 82: 513-518, 1985.*
212. ***Reale E, Luciano L, and Kühn KW***. *The fine structure of the laminae rarae of the glomerular basement membrane in the rat. Prog Clin Biol Res 295: 167-172, 1989.*
213. ***Reale E, Luciano L, and Kühn KW***. *Ultrastructural architecture of proteoglycans in the glomerular basement membrane. A cytochemical approach. J Histochem Cytochem 31: 662-668, 1983.*
214. ***Reale E, Luciano L, Kühn KW, and Stolte H***. *Morphological and functional aspects of the glomerular basement membrane. Basic Appl Histochem 23 Suppl: 5-11, 1979.*
215. ***Reale E, Luciano L, and Spitznas M***. *Histochemical demonstration of hyaluronic acid molecules by alcian blue. Histochem J 18: 306-316, 1986.*
216. ***Reinhardt HW***. *Die Rolle des Harnstoffs im Konzentrierungsprozess der Niere. Habilitation. LM Universität München, 1969. Bayerische Staatsbibliothek München.*
217. ***Reitsma S, Slaaf DW, Vink H, van Zandvoort MA, and Oude Egbrink MG***. *The endothelial glycocalyx: composition, functions, and visualization. Pflügers Arch 454: 345-359, 2007.*
218. ***Repp V***. *Untersuchungen zur "repaired defect" Hypothese der glomerulären Kapillarwand. Experimentelle und klinische Untersuchungen zu klinischen Analogien. Dissertation. Westfälische Wilhelms Universität Münster, 2016, p. 1-111.*
219. ***Roeckel A, Hertel J, Fiegel P, Abdelhamid S, Panitz N, and Walb D***. *Permeability and secondary membrane formation of a high flux polysulfone hemofilter. Kidney Int 30: 429-432, 1986.*
220. ***Rosenthal AM, Jones G, Kooh SW, and Fraser D***. *25-hydroxyvitamin D_3 metabolism by isolated perfused rat kidney. Am J Physiol 239: E12-E20, 1980.*
221. ***Röskenbleck H, Humann W, Gloy U, and Niesel W***. *Anwendung eines Dünnschicht-dialysators zur Gasäquilibrierung von Perfusionslösungen bei Durchströmungsversuchen an Organen. Pflügers Arch 294: 88-90, 1967.*
222. ***Ross B, Silva P, and Bullock S***. *Role of the malate-aspartate shuttle in renal sodium transport in the rat. Clin Sci (Lond) 60: 419-426, 1981.*
223. ***Ross BD***. *The isolated perfused rat kidney. Clin Sci Mol Med Suppl 55: 513-521, 1978.*
224. ***Ross BD***. *Perfusion Techniques in Biochemistry. Oxford: Clarendon Press, 1972.*
225. ***Ross BD, and Bullock S***. *Energy requirements for metabolic and excretory activities of perfused rat kidney. Curr Probl Clin Biochem 6: 86-98, 1976.*
226. ***Ross BD, Bullock S, Frega N, and Leaf A***. *Glucose as a fuel in kidney. Biochem Soc Trans 6: 524-526, 1978.*
227. ***Ross BD, Epstein FH, and Leaf A***. *Sodium reabsorption in the perfused rat kidney. Am J Physiol 225: 1165-1171, 1973.*
228. ***Sands JM***. *Mammalian urea transporters. Annu Rev Physiol 65: 543-566, 2003.*
229. ***Sands JM, and Layton HE***. *Advances in understanding the urine-concentrating mechanism. Annu Rev Physiol 76: 387-409, 2014.*
230. ***Sands JM, Timmer RT, and Gunn RB***. *Urea transporters in kidney and erythrocytes. Am J Physiol 273: F321-F339, 1997.*
231. ***Schafer AI***. *Vascular endothelium: in defense of blood fluidity. J Clin Invest 99: 1143-1144, 1997.*
232. ***Schimassek H***. *Perfusion of isolated rat liver with a semi-synthetic medium and control of liver function. Life Sci 1: 629-634, 1962.*
233. ***Schindhelm K, Schlatter E, Schurek HJ, and Stolte H***. *The isolated perfused rat kidney and uremic middle molecules. Contrib Nephrol 19: 191-200, 1980.*

234. ***Schindhelm K, Schlatter E, Schurek HJ, and Stolte H**. Renal handling of uremic middle molecules. a study with the isolated perfused rat kidney. Nephron 30: 166-172, 1982.*

235. ***Schlarmann J, Schurek HJ, Neumann KH, and Eckert G**. Chloride-induced increase of plasma potassium after transfusion of erythrocytes in dialysis patients. Nephron 37: 240-245, 1984.*

236. ***Schlatter E**. Metabolismus und Exkretion von Peptidhormonen in der Niere. Untersuchungen an der isoliert perfundierten Rattenniere. Dissertation. FB Biologie. Universität Hannover. , 1980.*

237. ***Schlatter E, Schurek HJ, and Zick R**. Renal handling of homologous and heterologous insulin in the isolated perfused rat kidney. Pflügers Arch 393: 227-231, 1982.*

238. ***Schmid U, Stopper H, Schweda F, Queisser N, and Schupp N**. Angiotensin II induces DNA damage in the kidney. Cancer Res 68: 9239-9246, 2008.*

239. ***Schmidt FH**. [Enzymatic determination of glucose and fructose simultaneously]. Klin Wochenschr 39: 1244-1247, 1961.*

240. ***Schnermann J, Stowe N, Yarimizu S, Magnsusson M, and Tingwald G**. Feedback control of glomerular filtration rate in isolated, blood-perfused dog kidneys. Am J Physiol 233: F217-F224, 1977.*

241. ***Scholz H, Schurek HJ, Eckardt KU, and Bauer C**. Role of erythropoietin in adaptation to hypoxia. Experientia 46: 1197-1201, 1990.*

242. ***Scholz H, Schurek HJ, Eckardt KU, Kurtz A, and Bauer C**. Oxygen-dependent erythro-poietin production by the isolated perfused rat kidney. Pflügers Arch 418: 228-233, 1991.*

243. ***Schurek H, Pagel H, and Kriz W**. Oxygen deficiency and lipid peroxidation in the isolated perfused rat kidney. In: Kidney Metabolism and Function, edited by Dzurik R, Lichardus B, and Guder WG. Martinus Nijhoff Publishing, 1985, p. 135-142.*

244. ***Schurek H, Pagel H, Thole H, Neumann K, Alt J, Bahlmann J, and Stolte H**. Die "repaired defect" Hypothese der glomerulären Kapillarwand. Untersuchungen an der isoliert perfundierten Rattenniere. Nieren- und Hochdruckkrankheiten 15: 368, 1986.*

245. ***Schurek H, Schwietzer G, Alt J, and Stolte H**. Albumin filtration and effective filtration pressure in cortical nephrons in the isolated perfused rat kidney. Proc. Int. Congr. Nephrol. 7th, Montreal, 1978, (Abstract px4).*

246. ***Schurek HJ**. Application of the isolated perfused rat kidney in nephrology. Contrib Nephrol 19: 176-190, 1980.*

247. ***Schurek HJ**. Discussion of paper "The glomerular permeability for water and albumin in the isolated perfused rat kidney". Int J Biochem 12: 195, 1980.*

248. ***Schurek HJ**. Mechanisms of glomerular proteinuria and hematuria. Kidney Int Suppl 47: S12-S16, 1994.*

249. ***Schurek HJ**. Physiologische und pathophysiologische Grundlagen der glomerulären Permeabilität für Plasmaproteine. Verh Dtsch Ges Inn Med 93: 466-472, 1987.*

250. ***Schurek HJ**. Untersuchungen zur Pathophysiologie der Niere bei Hypoproteinaemie. Habilitation. Medizinische Hochschule Hannover, 1981.*

251. ***Schurek HJ, and Alt JM**. Effect of albumin on the function of perfused rat kidney. Am J Physiol 240: F569-F576, 1981.*

252. ***Schurek HJ, Alt JM, and Stolte H**. Micropuncture experiments on albuminuria in the isolated perfused rat kidney. Kidney Int 13: 531-532, 1978.*

253. ***Schurek HJ, Aulbert E, and Ebel H**. The effect of Ca ion antagonist verapamil on ouabain inhibition of renal sodium reabsorption. Studies in the isolated perfused rat kidney. Curr Probl Clin Biochem 6: 281-290, 1976.*

254. ***Schurek HJ, Aulbert E, Ebel H, and Mueller-Suur C**. Influence of ouabain and ethacrynic acid on sodium transport and NaK-ATPase activity in the isolated perfused rat kidney. Curr Probl Clin Biochem 4: 162-168, 1975.*

255. ***Schurek HJ, Brecht JP, and Brandt P**. Na-Reabsorption und O_2-Verbrauch der isoliert perfundierten Rattenniere unter Einwirkung von Ethycrynsäure. Selbstverlag 1971.*

256. ***Schurek HJ, Brecht JP, Brandt P, Lange K, Kolbe H, and Keller K**. Substrate action on transport and metabolism of the isolated perfused rat kidney. Action of pyruvate, oxaloacetate, butyrate and succinate. In: Biochemical Aspects of Kidney Function, edited by Hohenegger M. München: Goldmann-Verlag, 1972, p. 110-126.*

257. ***Schurek HJ, Brecht JP, Lohfert H, and Hierholzer K**. The basic requirements for the function of the isolated cell free perfused rat kidney.
Pflügers Arch 354: 349-365, 1975.*

258. ***Schurek HJ, Ciarimboli G, and Helmchen U**. Orthostatische Proteinurie. Ist es ein intrarenaler Mechanismus?
Kidney & Blood Pressure Research 22: 228 Abstract A104, 1999.*

259. ***Schurek HJ, and Johns O**. Is tubuloglomerular feedback a tool to prevent nephron oxygen deficiency? Kidney Int 51: 386-392, 1997.*

260. ***Schurek HJ, Jost U, Baumgärtl H, Bertram H, and Heckmann U**. Evidence for a preglomerular oxygen diffusion shunt in rat renal cortex.
Am J Physiol 259: F910-F915, 1990.*

261. ***Schurek HJ, Jost U, Bertram H, and Baumgärtl H**. Preglomerular cortical oxygen diffusion shunt: a prerequisite for effective erythropoietin regulation?
Contrib Nephrol 76: 57-64, 1989.*

262. ***Schurek HJ, Klokkers J, Pavenstaedt H, Schlatter E, and Edemir B**. The analysis of aquaporin-2 regulation by means of the isolated perfused rat kidney.
Proceedings of the Deutsche Physiologische Gesellschaft P100: 232, 2011.*

263. ***Schurek HJ, and Kriz W**. Morphologic and functional evidence for oxygen deficiency in the isolated perfused rat kidney. Lab Invest 53: 145-155, 1985.*

264. ***Schurek HJ, Lohfert H, and Hierholzer K**. [Na-Reabsorption in the isolated perfused rat kidney. Dependency on substrates and Na-load].
Pflügers Arch, 1970, p. 1285 R1285.*

265. ***Schurek HJ, and Neumann KH**. Physiologie der Niere. In: Klinische Nephrologie, edited by Koch KM. Hannover: Urban & Fischer, München, Jena, 2000, p. 33-71.*

266. ***Schurek HJ, Neumann KH, Flohr H, Zeh M, and Stolte H**. The physiological and pathophysiological basis of glomerular permeability for plasma proteins and erythrocytes. Eur J Clin Chem Clin Biochem 30: 627-633, 1992.*

267. ***Schurek HJ, Neumann KH, Jesinghaus WP, Aeikens B, and Wonigeit K**. Influence of cyclosporine A on adaptive hypertrophy after unilateral nephrectomy in the rat.
Clin Nephrol 25 Suppl 1: S144-S147, 1986.*

268. ***Schurek HJ, Schlatter E, Meier W, Zick R, Dorn G, Hehrmann R, and Stolte H**. Renal handling of polypeptide hormones (insulin, C-peptide, h-PTH) as studied in the isolated perfused rat kidney. Int J Biochem 12: 237-242, 1980.*

269. ***Schweda F, Segerer F, Castrop H, Schnermann J, and Kurtz A**. Blood pressure-dependent inhibition of Renin secretion requires A1 adenosine receptors.
Hypertension 46: 780-786, 2005.*

270. ***Schweda F, Wagner C, Kramer BK, Schnermann J, and Kurtz A***. *Preserved macula densa-dependent renin secretion in A1 adenosine receptor knockout mice. Am J Physiol Renal Physiol 284: F770-F777, 2003.*
271. ***Schwietzer G, and Gertz KH***. *Changes of hemodynamics and glomerular ultrafiltration in renal hypertension of rats. Kidney Int 15: 134-143, 1979.*
272. ***Seeliger E, Wronski T, Ladwig M, Dobrowolski L, Vogel T, Godes M, Persson PB, and Flemming B***. *The renin-angiotensin system and the third mechanism of renal blood flow autoregulation. Am J Physiol Renal Physiol 296: F1334-F1345, 2009.*
273. ***Semenza GL***. *Hypoxia-inducible factor 1 and cardiovascular disease. Annu Rev Physiol 76: 39-56, 2014.*
274. ***Semenza GL***. *Hypoxia-inducible factor 1: regulator of mitochondrial metabolism and mediator of ischemic preconditioning. Biochim Biophys Acta 1813: 1263-1268, 2011.*
275. ***Semenza GL, Nejfelt MK, Chi SM, and Antonarakis SE***. *Hypoxia-inducible nuclear factors bind to an enhancer element located 3' to the human erythropoietin gene. Proc Natl Acad Sci U S A 88: 5680-5684, 1991.*
276. ***Silva P, Ross BD, Charney AN, Besarab A, and Epstein FH***. *Potassium transport by the isolated perfused kidney. J Clin Invest 56: 862-869, 1975.*
277. ***Skutul K***. *Über Durchströmungsapparate. Pflügers Arch 123: 249-273, 1908.*
278. ***Smyth DD, Umemura S, and Pettinger WA***. *Alpha 1-adrenoceptor blockade and altered renal α 2-adrenoceptors: a model(?) for the study of genetically altered α 2-adrenoceptors in hypertensive rats. J Hypertens Suppl 4: S205-S208, 1986.*
279. ***Smyth DD, Umemura S, and Pettinger WA***. *α 2-adrenoceptor antagonism of vaso-pressin-induced changes in sodium excretion. Am J Physiol 248: F767-F772, 1985.*
280. ***Smyth DD, Umemura S, and Pettinger WA***. *Alpha 2-adrenoceptors and sodium reabsorption in the isolated perfused rat kidney. Am J Physiol 247: F680-F685, 1984.*
281. ***Soldin SJ, Henderson L, and Hill JG***. *The effect of bilirubin and ketones on reaction rate methods for the measurement of creatinine. Clin Biochem 11: 82-86, 1978.*
282. ***Solomon R, Silva P, and Epstein FH***. *Aldosteron effects on renal function in the isolated perfused rat kidney. Ren Physiol 2: 1-11, 1979.*
283. ***Somers M, Piqueras AI, Strange K, Zeidel ML, Pfaller W, Gawryl M, and Harris HW***. *Interactions of ultrapure bovine hemoglobin with renal epithelial cells in vivo and in vitro. Am J Physiol 273: F38-F52, 1997.*
284. ***Sonnenburg-Hatzopoulos C, Assel E, Schurek HJ, and Stolte H***. *Glomerular albumin leakage and morphology after neutralization of polyanions. II. Discrepancy of protamine induced albuminuria and fine structure of the glomerular filtration barrier. J Submicrosc Cytol 16: 741-751, 1984.*
285. ***Sonnenburg C***. *Darstellung und Funktion von Polyanionen der glomerulären Filtrationsbarriere. Untersuchungen an der in vivo und isoliert perfundierten Rattenniere. Dissertation. FB Biologie. Universität Hannover, 1982.*
286. ***Staib W, Staib R, Herrmann J, and Meiers H.G.*** *Untersuchungen über die Cortisol-glykoneogenese in der isoliert perfundierten Rattenleber. In: Stoffwechsel der isoliert perfundierten Leber. Berlin: Springer-Verlag, Berlin, 1968, p. 155.*
287. ***Starling EH***. *On the absorption of fluids from the connective tissue spaces. J Physiol 19: 312-326, 1896.*
288. ***Stegbauer J, Friedrich S, Potthoff SA, Broekmans K, Cortese-Krott MM, Quack I, Rump LC, Koesling D, and Mergia E***. *Phosphodiesterase 5 attenuates the vasodilatory response in renovascular hypertension. PLoS One 8: e80674, 2013.*

289. ***Stegbauer J, Vonend O, Habbel S, Quack I, Sellin L, Gross V, and Rump LC***. *Angiotensin II modulates renal sympathetic neurotransmission through nitric oxide in AT2 receptor knockout mice. J Hypertens 23: 1691-1698, 2005.*

290. ***Stolte H, Alt JM, Baldamus CA, Galaske RG, and Schurek HJ***. *Direct assessment of the glomerular sieving coefficient for albumin in the rat kidney. Kidney Int 11: 220, 1977.*

291. ***Stolte H, Neumann KH, Reale E, Alt J, and Schurek HJ***. *Renal handling of serum proteins as studied by micropuncture techniques. Contrib Nephrol 26: 23-30, 1981.*

292. ***Stolte H, Schurek HJ, and Alt JM***. *Glomerular albumin filtration: a comparison of micropuncture studies in the isolated perfused rat kidney with in vivo experimental conditions. Kidney Int 16: 377-384, 1979.*

293. ***Swanson JW, Besarab A, Pomerantz PP, and DeGuzman A***. *Effect of erythrocytes and globulin on renal functions of the isolated rat kidney. Am J Physiol 241: F139-F150, 1981.*

294. ***Taft DR***. *The isolated perfused rat kidney model: a useful tool for drug discovery and development. Curr Drug Discov Technol 1: 97-111, 2004.*

295. ***Tay M, Comper WD, Vassiliou P, Glasgow EF, Baker MS, and Pratt L***. *The inhibitory action of oxygen radical scavengers on proteinuria and glomerular heparan sulphate loss in the isolated perfused kidney. Biochem Int 20: 767-778, 1990.*

296. ***Thole H***. *Zum Mechanismus der Angiotensin II induzierten Proteinurie. Dissertation. Medizinische Hochschule Hannover, 1988.*

296b. ***Thuillier R, Dutheil D, Trieu MTN, Mallat V, Allain G, Rousselot M, Denuzot M, Goujon J-M, Zal F, and Hauet T.*** *Supplementation with a new therapeutic oxygen carrier reduces chronic fibrosis and organ dysfunction in kidney static preservation. Am J Transplant 11: 1845-1860, 2011.*

296c. ***Trionfini P, and Benigni A.*** *MicroRNAs as master regulators of glomerular function in health and disease. J Am Soc Nephrol 28:…-…, 2017. doi: 10.1681/ASN.2016101117*

297. ***Timmer RT, Klein JD, Bagnasco SM, Doran JJ, Verlander JW, Gunn RB, and Sands JM***. *Localization of the urea transporter UT-B protein in human and rat erythrocytes and tissues. Am J Physiol Cell Physiol 281: C1318-C1325, 2001.*

298. ***Torelli G, Milla E, Kleinman LI, and Faelli A***. *Effect of hypothermia on renal sodium reabsorption. Pflügers Arch 342: 219-230, 1973.*

299. ***Ussing HH, and Zerahn K***. *Active transport of sodium as the source of electric current in the short-circuited isolated frog skin. Reprinted from Acta. Physiol. Scand. 23: 110-127, 1951. J Am Soc Nephrol 10: 2056-2065, 1999.*

300. ***Venkatachalam MA, Bernard DB, Donohoe JF, and Levinsky NG***. *Ischemic damage and repair in the rat proximal tubule: differences among the S1,S2, and S3 segments. Kidney Int 14: 31-49, 1978.*

301. ***Vink H, and Duling BR***. *Capillary endothelial surface layer selectively reduces plasma solute distribution volume. Am J Physiol Heart Circ Physiol 278: H285-H289, 2000.*

302. ***Vink H, and Duling BR***. *Identification of distinct luminal domains for macromolecules, erythrocytes, and leukocytes within mammalian capillaries. Circ Res 79: 581-589, 1996.*

303. ***Vonend O, Stegbauer J, Sojka J, Habbel S, Quack I, Robaye B, Boeynaems JM, and Rump LC***. *Noradrenaline and extracellular nucleotide cotransmission involves activation of vasoconstrictive P2X(1,3)- and P2Y6-like receptors in mouse perfused kidney. Br J Pharmacol 145: 66-74, 2005.*

304. ***Wagner C, de Wit C, Kurtz L, Grünberger C, Kurtz A, and Schweda F****. Connexin40 is essential for the pressure control of renin synthesis and secretion. Circ Res 100: 556-563, 2007.*

305. ***Walter R, and Bowman RH****. Mechanism of inactivation of vasopressin and oxytocin by the isolated perfused rat kidney. Endocrinology 92: 189-193, 1973.*

306. ***Weiss C****. Zur Frage der Sauerstoffversorgung der Säugetierniere. Habilitationsschrift. Physiologisches Institut der Universität Hamburg, 1962.*

307. ***Weiss C, Passow H, and Rothstein A****. Autoregulation of flow in isolated rat kidney in the absence of red cells. Am J Physiol 196: 1115-1118, 1959.*

308. ***Wesslau C, Jung K, and Schirrow R****. [Comparison of inulin and creatinine clearance determinations in anesthesized and conscious rats]. Z Urol Nephrol 81: 395-400, 1988.*

309. ***Wetzels JF, Huysmans FT, and Koene RA****. Creatinine as a marker of glomerular filtration rate. Neth J Med 33: 144-153, 1988.*

310. ***Willinger CC, Schramek H, Pfaller K, Joannidis M, Deetjen P, and Pfaller W****. Ultra-pure polymerized bovine hemoglobin improves structural and functional integrity of the isolated perfused rat kidney. Ren Physiol Biochem 18: 288-305, 1995.*

311. ***Willinger CC, Schramek H, Pfaller K, Pfaller W, and Deetjen P****. Ultrapure polymerized bovine hemoglobin (UPPBHb) improves integrity of the isolated perfused rat kidney (IPRK): effects on function and structure. Clin Nephrol 44: 32-43, 1995.*

312. ***Windhager EE, Lewy JE, and Spitzer A****. Intrarenal control of proximal tubular reabsorption of sodium and water. Nephron 6: 247-259, 1969.*

313. ***Wollenberger A, Ristau O, and Schoffa G****. [A simple technic for extremely rapid freezing of large pieces of tissue]. Pflügers Arch 270: 399-412, 1960.*

314. ***Wruck G****. Zur Konversion von Thyroxin zu Trijodthyronin an der isoliert perfundierten Rattenniere. Dissertation. Medizinische Hochschule Hannover, 1986, p. 1-44.*

315. ***Wusteman MC****. Comparison of colloids for use in isolated normothermic perfusion of rabbit kidneys. J Surg Res 25: 54-60, 1978.*

316. ***Yamamoto Y, Niki E, Kamiya Y, Miki M, Tamai H, and Mino M****. Free radical chain oxidation and hemolysis of erythrocytes by molecular oxygen and their inhibition by vitamin E. J Nutr Sci Vitaminol (Tokyo) 32: 475-479, 1986.*

317. ***Zeh M****. Zur glomerulären Permeabilität geladener und ungeladener Makromoleküle. Dissertation. Medizinische Hochschule Hannover, 1994, p. 1-90.*

318. ***Zimmerhackl B, Dussel R, and Steinhausen M****. Erythrocyte flow and dynamic hematocrit in the renal papilla of the rat. Am J Physiol 249: F898-902, 1985.*

319. ***Zimmerhackl B, Robertson CR, and Jamison RL****. Effect of arginine vasopressin on renal medullary blood flow. A videomicroscopic study in the rat. J Clin Invest 76: 770-778, 1985.*

Supplement:

320 ***Schurek HJ, Neumann KH, Schweda F and Czogalla J.*** *Laborhandbuch: Nieren-perfusion [Laboratory Manual: Kidney Perfusion]. Wissenschaftliche Schriften der WWU Münster, Reihe V, Band 5. Verlag Monsenstein & Vannerdat, Münster, 2015*

ISBN: 978-3-8405-0132-6, **online** URN: urn:nbn:de:hbz:6-88219516586
DOI: http://dx.doi.org/10.17879/67229530894

A Laboratory Manual of Kidney Perfusion Techniques

Hans-Joachim Schurek

An organ such as the kidney naturally functions best in a healthy organism. Once a kidney has been removed from its normal context, it is crucial to find the optimal compromise between the demands of the problem at issue and the experimental model to be adopted. An isolated kidney is, in effect, a “dying kidney”, although it may continue to function for between 1 and 4 hours, depending on one‘s definition of normal. The basic reason for the progressive deterioration in function can be found in the stresses set up by the transition from perfusion by whole blood to the use of a more or less artificial perfusing medium. Indeed, blood is a “liquid organ”, a highly complex cocktail that is steadily being reconditioned by the actions of other organs, and this complexity explains why all efforts to maintain kidney function in isolation are ultimately doomed to failure. If we want to approach its fantastic properties, then we should leave an organ as the kidney within the body. As Mephisto remarks in Goethe‘s drama “Faust”, Studierzimmer II: “Blut ist ein ganz besondrer Saft”: “blood is a quite special juice”.

ISBN 978-3-8405-0154-8 EUR 71,50